The Structure and Function of Cat Skull Bones in Relation to the Transmission of Biting Forces.

Buckland-Wright, J. C

THE STRUCTURE AND FUNCTION OF CAT SKULL BONES IN RELATION TO THE TRANSMISSION OF BITING FORCES

by

J.C. BUCKLAND-WRIGHT

Vol. I : Text Vol. II : Atlas

A thesis submitted for the Degree of

Doctor of Philosophy of the University

of London.

Department of Anatomy,

Kings College, London, WC2R 2LS

1975

THE STRUCTURE AND FUNCTION OF CAT SKULL BONES IN RELATION TO THE TRANSMISSION OF BITING FORCES

VOLUME I : TEXT

"Si l'on se perfectione dans une seule chose et qu'on la comprend bien, on acquiert par-dessus le marché la compréhension et la connaissance de bien d'autres choses."

Carnet. A. Camus.
Gallimard (1964).

THE STRUCTURE AND FUNCTION OF CAT SKULL BONES IN RELATION TO THE TRANSMISSION OF BITING FORCES

Abstract

An account is given of the histological organisation of the compact and cancellous bone of the cat skull. Stereo-projection microradiographs were made of five cat skulls. The identity of the shadow images of the trabeculae and large vascular canals was confirmed and their grade of structural organisation, orientation and frequency within the skulls were tabulated and described. Within specific areas of the skull a high degree of structural orientation and increased structural frequency was recorded, and both exhibited a contiguity between cranial elements such that a continuum of structural organisation was established between the attachment of the teeth, and that of the temporalis and masseter muscles. A statistical analysis of this pattern was applied to ten cats.

Having established the nature of the structural organisation of the bone, an attempt was then made to determine whether this orientation was related to the stress to which a skull is subjected during jaw closure, when a resistance is placed between the canines and carnassials respectively. An analysis was first carried out on dry skulls using colophonium resin to determine the direction of strain distribution and the areas of greatest bone deformation. The nature of the strain and the response of bone under increased stress was ascertained by replacing the resin with linear strain gauges. The dynamic recordings from the intra-vitally implanted strain gauges on ten anaesthetised cats largely confirmed the results of the experiments on the dry skulls, and showed that during jaw closure compressive

strain predominated in the facial bones. The results emphasis the importance, neglected hitherto, of experimental investigations in determining strain distribution in the skull and its relation to the detailed structural organisation of the bones.

These experiments enabled the hypothesis that the structural organisation of skull bones is related to the transmission of biting forces to be tested. The confirmation of this hypothesis has led to a revision of the "Trajectorial Theory".

ACKNOWLEDGEMENTS

I wish to express my gratitude to the late Professor Sir Francis Knowles, head of the Anatomy Department, and to the late Professor J.L. D'Silva, head of the Physiology Department for providing me with research facilities in their departments, to Dr. M.H. Hobdell and Dr. W.A.B. Brown for advice and encouragement throughout the preparation of the thesis, which was supported by a King's College Award of an S.R.C. studentship.

The X-ray work has only been possible through the kindness and personal generosity of Mr. R.V. Ely and the M.R. Research Trust, who together have provided all the X-ray equipment and which was made available through the kind permission of Mr. N.J.D. Smith of the King's College Hospital Dental School. Gratitude is also tended to Mr. P. Sullivan of the Department of Dental Anatomy, London Hospital Dental School for the use of the Bateman sectioning machine; to Mr. A.W. Blake and Mr. G.F. Adams of the Department of Civil Engineering of this college for the use of the Peekel strain measuring apparatus; to Dr. D.M. Band of the Physiology Department of this college for advice and use of the apparatus employed in the in vivo experiments; and to Dr. M.J. Laird for advice on the statistical methods employed in this thesis.

I wish to thank the following people for their generous help at various times during the preparation of this work: Professor R. Wheeler Haines, Dr. R.J. Whitney, Dr. G.D. Sales and Miss J.C. Smith. Thanks is also expressed to Miss A. Pitman for drafting, to Miss M. Lanyon for typing the thesis and to

Mr. P. Batten for the preparation of a number of the photographic plates.

CONTENTS

Chapter 1 Introduction.

Page No.

1.1. Introduction to the thesis.....17

1.2.1. Literature review of the work prior to the 20th century including an account of the Trajectorial Theory.....21

1.2.2. Summary and conclusion.....29

1.3. The present terms under which the architectural organisation of the skull is described.....30

1.3.1. The buttress theory.....30

1.3.2. The split-line phenomenon.....31

1.3.3. Summary and conclusion.....39

1.4. Methods of analysis of the stress and strain distribution in bones.....41

1.4.1. Mathematical analysis.....41

1.4.2. Analysis of stress and strain in bones using models.....44

1.4.3. Analysis of stress and strain in bones using engineering technique.....48

1.4.4. Summary and conclusion.....53

Chapter 2 Materials and Methods for the examination of the structural organisation of cat skull bones.

2.1. Introduction.....55

2.2. Materials.....56

2.2.1. Cat skull material.....56

2.2.2. Apparatus.....56

2.3. Histological examination of the structural

organisation of bone.....56
2.3.1. Ground polished sections.....57
2.3.2. Decalcified and stained sections.....58
2.4. Introduction to the radiographic examination of bone.....58
2.4.1. Projection microradiography.....60
2.4.2. Introduction.....60
2.4.3. Theoretical considerations.....62
2.4.3.1. Advantages of projection microradiography.....62
2.4.3.2. Limitations of projection microradiography.....62
2.4.3.3. Optimum conditions for projection microradiography.64
2.4.4. X-ray stereoscopy.....65
2.5. Method of preparation of projection radiographs....65
2.6. Examination of the structural orgainsation of bone and statement of aims.....66
2.6.1. Examination of the coronal sections.....67
2.6.2. Examination of the dissected bone.....68
2.6.3. Limitations in the examination of the coronal sections and dissected bone.....69
2.6.4. An assessment of the effect of the depth of bone and superimposition on the number of structures recorded in the projection radiographs.....70
2.7. Determination of the structural organisation of the skull bones.....71
2.7.1. Consistency of alignment between large vascular canals and trabeculae.....72
2.7.2. Description of the structural organisation of the cat skulls.....73

2.7.3. Statistical analysis of the consistency of the structural organisation.....73
2.7.4. Interdental and inter-radicular trabecular frequency.....74

Chapter 3 Results of the examination of the structural organisation of the cat skull bones.

3.1. Histology of the cat skull bones.....77
3.2.1. Examination of the structural orgainsation of the skull bones: coronal sections.....78
3.2.2. Examination of the structural organisation of the skull bones: dissected bone.....80
3.3. The assessment of the effects of the depth of bone and superimposition on the number of structures recorded in the projection radiographs.....82
3.4. The structural organisation of bone.....83
3.5. The consistency of alignment between the large vascular canals and trabeculae.....84
3.6. Description of the structural organisation of the cat skulls.....85
3.6.1. Skull viewed in norma lateralis.....85
3.6.2. Skull viewed in norma ventralis.....91
3.7. Description of the structural continua of the cat skull.....92
3.8. The statistical analysis of the consistency of structural orgainsation.....96

3.9. Interdental and inter-radicular trabecular frequency in the maxilla and mandible..... 97

3.10. Summary and conclusion..... 97

Chapter 4 Materials and methods for the in vitro determination of the transmission of biting forces in the cat skull.

4.1. Colophonium resin experiments..... 99

4.1.1. Introduction..... 99

4.1.2. Materials..... 101

4.1.2.1. Cat skull material..... 101

4.1.2.2. Testing frame for the skulls..... 101

4.1.3. Method of attachment of the substitute temporalis and masseter muscles..... 102

4.1.4. Procedure for coating and stressing the skulls..... 103

4.2. Strain gauge experiments..... 105

4.2.1. Introduction..... 105

4.2.2. Materials..... 106

4.2.3. Bonding of the strain gauges..... 107

4.2.4. The position of attachment of the strain gauges to the skulls..... 107

4.2.5. Experimental procedure..... 109

Chapter 5 Results of the in vitro determination of the transmission of biting forces in the cat skull.

5.1. Colophonium resin experiments..... 113

5.1.1. Introduction..... 113

5.1.2. The distribution of primary strain in the cat skull, with the support placed at either the canines or carnassials.....113
5.1.3. The distribution of secondary strain in the cat skull, with the support placed at either the canines or the carnassials.....114
5.1.4.1. The distribution of tertiary strain in the cat skull, with the support placed at the canines.....114
5.1.4.2. Summary and conclusion.....116
5.1.4.3. The distribution of tertiary strain in the cat skull, with the support placed at the carnassials....117
5.1.4.4. Summary and conclusion.....118
5.1.4.5. Experimental control in the colophonium resin experiments.....119
5.2. Strain gauge experiments.....119
5.2.1. Introduction.....119
5.2.2. Results of the in vitro strain gauge experiments.....119
5.2.2.1. Selective observations on the results of the strain gauge experiments.....120
5.2.2.2. Experimental control in the strain gauge experiments. 124
5.2.2.3. Summary and conclusion.....125

Chapter 6 Materials and methods for the dynamic strain gauge recordings from anaesthetised cats.

6.1. Introduction.....126
6.2.1. Materials.....127
6.2.2. Apparatus.....127

6.3. Position of attachment of strain gauges on the skull and the associated anatomy of the cats head..... 128
6.3.1. The design of the braces..... 129
6.3.2. Optimum conditions for the tetanic stimulation of the muscles..... 129
6.3.3. Results for the optimum conditions for the tetanic stimulation of the muscles..... 130
6.3.4. Modifications to the braces..... 131
6.4. Dynamic strain gauge recordings from anaesthetised cats, initial experiments..... 131
6.4.1. Dynamic strain gauge recordings from anaesthetised cats, final set of experiments..... 135
6.4.2. Calibration of the braces..... 136
6.4.3. The plotting of the results..... 137
6.4.4. Calculations..... 138
6.5. Limitations of the experimental technique..... 140

Chapter 7 Results of dynamic strain gauge recordings from anaesthetised cats.

7.1. Introduction..... 141
7.2. Results of the in vivo strain gauge experiments.... 141
7.3. Experimental variation..... 144
7.4. Experimental control in the in vivo strain gauge experiments..... 144
7.4. Summary and conclusion..... 145

Chapter 8 Discussion.

8.1. Introduction..... 146
8.2. Discussion of the structural and functional organisations of cat skull bones..... 146
8.2.1. Bone histology..... 146
8.2.2. Accuracy of projection microradiography as a method of examining the structural orgainsation of bone..... 148
8.2.3. The structural organisation of cat skull bones..... 149
8.2.4. Consistency of alignment between the large vascular canals and trabeculae..... 152
8.2.5. Discussion on the structural organisation of the cat skull..... 154
8.2.6. Statistical examination of the structural organisation of cat skull bones..... 157
8.2.7. Structural frequency within the skull bones..... 158
8.2.8. Trabecular frequency in the dental septae of the maxilla and mandible..... 160
8.2.9. Re-examination of the earlier methods of examining the structural organisation of skull bones..... 163
8.2.10. Conclusion..... 164
8.3.1.1.The relationship between the transmission of the biting forces in the cat skull and its structural organisation..... 165
8.3.1.2.Colophonium resin experiments..... 166
8.3.1.3.Strain gauge experiments on dry cat skulls..... 167
8.3.1.4.Strain gauge experiments on the anaesthetised cats. 169

8.3.1.5.Relation between the results obtained from the experiments and the underlying structural organisation of bone.....170
8.3.2. Primary stresses exerted by the temporalis.....175
8.3.3. Primary stresses exerted by the masseter.....175
8.3.4. Secondary stresses produced at the glenoid.....178
8.3.5.1.Tertiary stresses: with the support placed at the canines and the load applied to the cords representing the temporalis muscle..... 180
8.3.5.2.Tertiary stresses: with the support placed at the canines and the load applied to the cords representing the masseter muscle..... 182
8.3.5.3.Tertiary stresses: with the support placed at the canines and the load applied to the cords representing both the temporalis and masseter muscle..... 183
8.3.6.1.Tertiary stresses: with the support placed at the carnassials and the load applied to the cords representing the temporalis muscle..... 183
8.3.6.2.Tertiary stresses: with the support placed at the carnassials and the load applied to the cords representing the masseter muscle..... 185
8.3.6.3.Tertiary stresses: with the support placed at the carnassials and the load applied to the cords representing both the temporalis and masseter muscles..... 186
8.3.7. A discussion on some points arising from the configuration of the signal from the in vivo experiments..... 188

8.3.8. Force of bite at the canines and carnassials.....191

8.3.9. The transmission of force in the cat skull during phase I and II of biting.....192

8.3.10. Conclusion.....199

8.4.1. Re-examination of the Trajectorial Theory.....200

8.4.2. The structural continum theory.....202

References.....205

Publications.....218

CHAPTER 1

INTRODUCTION

1.1. Introduction to the thesis.

During a radiographic examination of frontal sinuses in early British populations (Buckland-Wright 1970b), the author's attention was drawn to the highly organised cancellous bone in the facial bones, and to the work of Walkhoff (1902) which demonstrated that more information on the detailed organisation of bone was obtainable from radiographs than by the split-line method. On examination of the literature this last method was shown to be inaccurate (section 1.3.2.). The skull was chosen as an organ of study as very little radiographic work appeared to have been done on it, except for instance Barth, 1919. Cat skulls were used because of the author's familiarity with them as well as their ready availability for both anatomical and experimental studies.

The majority of studies which have been carried out on the structural organisation of the skull in relation to the distribution of stress and strain in the bones during biting, have based their interpretations on the Trajectorial Theory. This states that the trabeculae are aligned within the cancellous bone in curves or straight lines along the lines of maximum internal stress; and that the compression resisting trajectories are set at right angle, to those of tension in accordance with the mathematical laws of stress distribution in solid homogeneous bodies. Which, in terms of their anatomical appearance the trabeculae should appear as calcified entities coursing as continuous lines within the spongiosa.

Examination of the stereo-projection microradiographs of the cat skulls in no way confirmed this description. This radiographic technique, which has a greater resolution than clinical X-ray machines, enabled a direct correspondence to be established between the large vascular canals within the compact bone and the trabeculae visible in the microradiographs and their histological appearance. The subsequent detailed examination of the organisation of the cranial bones revealed a high degree of orientation in the large vascular canals and the trabeculae,and an increase in their frequency in the regions around the teeth and within specific areas connecting the alveolar region to those of the muscle attachment and the glenoid fossae. This arrangement is described as a'structural continuum' to distinguish it from concepts held by the 'Trajectorial Theory'.

The fundamental disadvantage of the earlier workers on the skull is that their observations on the relation between the structural organisation within the skull bones and the transmission of biting forces are hypothetical as they are not supported by experimental evidence (section 1.3.2.). One known experiment has been carried out on the transmission of force in the human skull during simulated conditions of biting (Endo, 1965), but practically no attempt was made to relate the results obtained to the underlying structural organisation.

In reviewing the literature on the techniques that have been applied to studying the distribution of stress and strain in bone (sections 1.4. to 1.4.4.), it was found that the engineering technique of,(a) coating the bone with a brittle resin and,(b) bonding strain gauges to the bone surface,

gave the most reliable results. These two techniques have been used independently in the past to determine stress and strain distribution in bones, and are herein used in conjunction for the first time. The advantage was that the limitations of one technique were overcome by the results of the second. Namely, the brittle resin technique indicated the direction of strain in the cortical surface of the bone and only in a few situations was it possible to ascertain the nature of the deformation. As rosette strain gauges which give direction as well as the type of strain could not be used because of the sizes of the gauges relative to the skulls, linear gauges were employed. The linear gauges were bonded to the skull with their principal axis in the direction of the strain recorded from the resin experiments; the recordings gave the nature of the deformation in the bone. The linear strain gauges alone did not indicate the direction of strain.

Maynard Smith and Savage's (1959) subdivision of the carnivorous process of biting into phase I (force applied to the canine during the prehension and killing of the prey), and phase II (force applied to the carnassial during the slicing of the prey's flesh), was used to define the conditions under which stress was applied to the skulls in the <u>in vitro</u> and subsequent <u>in vivo</u> experiments.

The recently developed techniques of intravital implantation of strain gauges (Lanyon and Smith, 1969, 1970; Lanyon, 1971, 1972, 1973; Cochran, 1972) on limb bones was carried out for the first time on the skulls of ten anaesthetised cats in order to corroborate the results obtained from the artificial conditions of the <u>in vitro</u> experiments. The

results of the <u>in vitro</u> and <u>in vivo</u> experiments enabled the hypothesis that the structural organisation of the cranial bones is related to the transmission of biting forces to be confirmed.

The areas of increased structural organisation in the cranial bones were shown by the two engineering techniques to be zones of maximum force transmission, their direction being along the lines of orientation of the 'structural continuum'. The results obtained in the <u>in vitro</u> experiments were largely confirmed by the <u>in vivo</u> recordings, And the strain produced in the facial bones during phase I and II of biting was predominantly compressive and was transmitted along the 'structural continua' to regions in the skull where the strain was resisted or counter-acted upon by other strains in a manner so as to reduce the overall deformation of the bones.

These results emphasise the importance of carrying out a series of experiments to determine the direction and nature of strain in the bone under conditions approximately as close as possible to the living situation. Without experimental results the anatomical observations on bone organisation and its relation to the transmission of forces, are limited if not spurious.

The results presented in this thesis form the basis of a brief re-assessment of the Trajectorial Theory. In the absence of any relation between the anticipated organisation of bone as proposed by the Trajectorial Theory and the present observations, an alternative terminology is proposed and the term 'Trajectorial' is replaced by 'Structural Continuum'.

1.2.1. Literature review of the work prior to the 20th century including an account of the Trajectorial Theory.

Among the earliest recorded contributors to the study of bone was Galileo (1638) who mentioned in his mathematical treatise that a hollow cylinder was proportionally stronger than a solid rod for the same weight of material (Ascenzi, et al., 1972). Later, Clopton Havers in his "Osteologia Nova" of 1692 described the presence of bony strings in long bones, and these canular structures were subsequently named after him (Siepel, 1948).

Major contributions to the understanding of bone organisation were made from the middle of the 19th century onwards and these fall into two categories which have remained separate although not independent to this day. Firstly there is the description of the histology and microscopic structure of bone. This field was established with the recognition of the cellular nature of all living matter by Schwann (1838) and the improvements in light microscopy and its technique. Koellicker's manual of microscopic anatomy (1850) contained one of the earliest detailed descriptions of bone histology. The second category, with which this thesis is primarily concerned, is the relationship between the form and function of bone based largely on the macroscopic examination. The interpretation of osseus organisation throughout the decades has been in large part dependent on man's understanding of mechanics and the physical properties of materials.

The first contribution to the field of bone organisation appears to have been that of Ward (1838) who compared the trabecular arrangement seen in the frontal sections of the femur to that of a triangular bracket attaching a street lamp to an

upright pole, the oblique and horizontal bars were considered analogous to the trabecular arrangement.

Further observations on the cancellous nature of bone were made by Wyman (1857), who interpreted the trabecular arrangement seen in the femur, vertebrae, talus, and calcaneum in terms of "studs" (compression resisting bars) and "braces" (tension resisting bars) for withstanding the forces generated in the living body.

Humphrey (1858) noticed that in the frontal sections of the femur, the trabecular lines were perpendicular to the articular surface of the head and that they crossed each other at right angles. The significance of this observation was not appreciated until later when its importance was recognised in the mathematical analysis of the functional significance of trabecular orientation.

Meyer (1867), in collaboration with the mathematician Culmann, examined the trabecular organisation in the proximal end of the femur sectioned on different planes. Culmann computed the stress trajectories in the Fairbairn crane which he assumed to be a solid homogeneous structure approximating the femur in shape and loading. The coincidence between the arrangement of the trajectories and cancellous bone led Meyer and Culmann to conclude that the trabeculae were laid down along the lines of maximum internal stress, thereby enabling the femur to transmit a maximum load with a minimum of material.

This analysis of the stresses in a Fairbairn crane was the first attempt to use a model to study the stress and strain in bones. It is on this basis that the Trajectorial Theory of the functional arrangement of the trabeculae was established. This states that the trabeculae were aligned within the

cancellous bone in curves or straight lines along the lines of maximum internal stress, and that the compression-resisting trajectories were set at right angles to those of tension in accordance with the mathematical laws of stress distribution in solid homogeneous bodies.

The work of Meyer and Culmann on the neck of the femur was continued by Wolff, who suggested in a paper (1870) that tension stresses are primarily responsible for bone growth and the orientation of the trabeculae. Wagstaffe (1874), on the basis of his studies on the cancellous bone from sections taken at different planes of the appendicular skeleton and vertebral column, states that all cancellous bone has a "definite mechanical arrangement ensuring the greatest strength and elasticity along the line of greatest pressure." (Wagstaffe, 1874, p. 145). Contrary to Wolff (1870) he believed that compression forces provided the trophic stimulus for the deposition of bone during growth.

The Trajectorial Theory was tested experimentally by Roux (1885), when he applied a load to a wax-coated rubber model of an ankylosed knee joint. The cracks which appeared in the wax served as a basis for the trajectorial diagrams which Roux used to explain the functional significance of the trabeculae across the joint. Roux agreed with Wolff in believing that tensile stresses were the primary stimulus for the formation of bone.

Wolff's work from 1869 on the cancellous organisation of bone led in 1892 to the Trajectorial Theory of bone architecture receiving its best expression in the "Law of Bone Transformation.", This states that "every change in the form and function, or function alone, of a bone produces changes, in arrordance with mathematical laws, in its trabecular architecture

and external form.", (Wolff, 1892, cited Evans, 1957). Wolff's Law, as it has since been known, was based upon the orientation of the spongiosa of the neck of the femur and on Culmann's mathematical analysis.

Roux (1895) extended the work of Meyer (1867) in relating more freely both the internal architecture and gross outer form to functional stimulation and adaptation; and stated that a maximum of strength is reached with a minimum of construction material and that to this end functional adaptation means "adaptation of an organ to its function by practising the latter.",(Roux 1895, p. 157, cited Kummer 1972).

Research in functional cranial osteology, at the begining of the 20th century generally continued to be limited to macroscopic observations or radiographic examination of the cancellous bone.

Walkhoff (1901, 1902) carried out a morphological and radiographic examination of the relationship between the teeth and facial bones in man and the anthropoid apes. On the basis of the Trajectorial Theory, Walkhoff described the trabeculae in the mandible as following 'functional' lines, and he attempted a mathematical and mechanical interpretation of the structural conditions in order to co-ordinate the trajectoria of the mandible with its functional demands. He stated that the skeletal reinforcements visible in the external morphology as well as in the internal architecture were found in places where the largest forces were expected.

Woolard and Harpman (1938) later criticised Walkhoff for having exaggerated many of the architectural differences occuring in the mandibles.

The laws of physics were applied by Lewin (1913) to his description of the internal structural arrangement of the human mandible, which was not substantially different from the results obtained by Walkhoff (1902).

Davida (1915) examined the canal systems in the undecalcified mandibles by means of fine sections. His strict adherence to the mechanical interpretation of the trajectoria resulted in a two dimensional interpretation which disregarded the multiple forces operating in different directions in the jaws and facial bones.

Barth (1919) contributed to the trajectorial architecture of the facial bones by X-raying large numbers of New World monkeys. The radiographs gave a composite picture but did not permit a very detailed analysis of the organisation of the compact bone. She concluded that the "force from the gracile frame of the jaw was transmitted to the stronger bones of the cranial vault ", through "trajectories present in the whole of the facial skeleton ".

The importance of the cortical bone in the consideration of bone architecture was highlighted in Winkler's work (1921) in which he examined the pars compacta in long bones and in particular the mandible. He demonstrated the various trajectorial systems and the distribution of the compacta and spongiosa in the mandible.

It was not until around the 1920's that any concerted criticism was leveled at the Trajectorial Theory; although Culmann and Meyer's conclusions had been rejected by a number of workers at the time (Merkel, 1874; Bigelow, 1875; Dwight, 1875).

The most detailed criticism of Meyer's (1867) paper came from Koch (1917) who pointed out that only a small part of the femur had been analysed, its relation to the whole bone was not shown, the line of action of the assumed load was taken as parallel with the femoral shaft, and that the mathematical model was not applicable to the femur which had a different shape and was not a solid body of homogeneous material. Kuntcher in a number of papers (1934, 1935a, 1936) leveled similar criticisms and added that the model used by Culmann for the analysis was a simple curved rod; that the trabeculae only resembled tension lines when the femur was sectioned frontally and that a section taken slightly away from the midline presented an entirely different picture.

Of the Trajectorial Theory among the most ardent critics was Triepel (1922a), who provided over twenty objections of which the following are the most pertinent (cited Murray 1936): (a) within the trajectorial diagrams the stress lines are drawn from arbitrary selected points a certain distance apart. Should all the lines be drawn one would arise from every point on the periphery of the diagram with the result that the figure would be entirely blackened. If the trajectories were the only determining factor in the cancellous bone structure, by analogy, the latter would be replaced by solid compact bone. Conversely, should the trabeculae correspond to the calculated trajectories, then it must be accepted that the trajectories in them appear as calcified entities: (b) Engineers computing the stress trajectories in a body assume that it is homogeneous. But the inhomogeneity and anisotropy of bone recognised by Wolff (1870) would not justify the assumption that the course of the trajectories will be closely similar to that of a homogeneous body.

Petersen (1927) attempted to refute Triepel's last point by contending that cancellous bone is a conglomerate whose fragmentary components are of such a variety of form, size and orientation that the statistical result of chaotic anisotropies was equivalent to homogeneity. (c) The authors of the Trajectorial Theory regarded the trabeculae which do not cross each other at right angles as not being trajectorial. Triepel (1922a) and Jansen (1920) found frequently that the trabeculae were not "trajectorial" and suggested that an alternative principle should be proposed. The trabeculae, contrary to running in a regular curve or straight line as demanded by the theory, were irregular, with indentations and projections along the edges.

It is also assumed in the Trajectorial Theory that the secondary trabecular system crossing the recognised pressure trajectories are tension resisting. Triepel (1922a) and Jansen (1920) maintain that secondary trabeculae are not subjected to simple tension but to complicated bending moments.

Roux's (1885) experimental confirmation of the Trajectorial Theory was criticised by Jansen (1920) for the absence of a close correspondence between the trabecular arrangement of the specimen and the trajectorial diagram which showed that the trajectories did not behave as they should according to the theory.

Triepel's (1922a & b) alternative explanation to the Trajectorial Theory is based on the premise that the cancellous architecture harmonises with the external form of the bones. The relationship between the structure and form is geometrical so that bones of a similar form should have the same internal structure irrespective of whether the loading is similar or not.

The mechanical conditions remain secondary factors which modify the ideal structure. Triepel described the internal architecture as a system of plates which form domes and calyces, completed by other elements such as horizontal and radially arranged plates. Triepel's idealised scheme fits the structure of long bones, but a close comparison with that of the Trajectorial Theory revealed that they are not too dissimilar and that direct analogies can be drawn between the two. Murray (1936) points out two major objections to Triepel's hypothesis, namely that it does not take into account the facts of bone development, and that the ideal architecture of cancellous bone, which is presumably geometrically determined, does not appear until functional demands have been placed on the bone.

The Trajectorial Theory was also criticised by Jansen (1920) and Carey (1929) who found themselves in agreement with Triepel in denying the trajectorial nature of bone structure, but who differed in refusing to admit to tensile stresses playing any part. They believed that muscular pressure combined with gravity were the principal mechanical stimuli for bone formation; and Carey (1929) proposed that the cancellous architecture at the joints is determined by the back pressure vectors in those regions. In their view the cancellous bone is not a system of materialised trajectories, but a pressure resistant lattice, the primary elements of which represent the trajectories in an imaginary homogeneous body.

These criticisms appear to have had relatively little influence on subsequent investigations, possibly as a result of the absence of satisfactory alternative theories to describe the organisation of the cancellous bone.

1.2.2. Summary and conclusion.

The increased attention to detail in bone sections led to more accurate descriptions of the structural organisation of bone and in particular the spongiosa. The descriptions were extended by the recognition of the value of radiographic visualisation.

The interpretation of the cancellous organisation of bone has been based extensively on analogies drawn from mechanical models which embodied the principles best able to account for the structural arrangement. To this end von Meyer and Culmann (1867) established the 'Trajectorial Theory' on their mathematical analysis of the Fairbairn crane. The experimental justification of the theory was demonstrated in Roux's (1885) analysis of the distribution of strain in a rubber model of an ankylosed knee-joint.

This approach established the foundations for the biological theories of Wolff (1892) on bone function and of Roux (1895) on bone adaptation. The Trajectorial Theory was used, at the begining of the 20th century, to describe the areas of force transmission in the mandible (Walkhoff, 1901, 1902; Lewin, 1913; Davida, 1915; Winkler, 1921) and skull (Barth, 1919). These accounts are ill founded in view of the criticisms developed by Koch (1917), Jansen (1920), Thepel (1922a), Carey (1929) and Kuntscher (1934, 1935a, 1936). Although they followed different approaches they agreed that the assumption on which the theory was based, of bone being a homogeneous isotropic material, was untenable and consequently the stress trajectories would be impossible to compute. Furthermore, they did not find that the trabeculae conformed to the

expected patterns as described by the theory. These criticisms would appear to have removed any substantial support for the Trajectorial Theory. But by default of any alternative satisfactory theory it has continued to be used, as described in the successive sections.

1.3. The present terms under which the architectural organisation of the skull is described.

The following two sections give an account of the terms under which the architectural organisation of skulls is described today, and assesses the extent to which the methodologies can be applied to the present study of the detailed organisation of the cat skull.

1.3.1. The buttress theory.

Bluntschli (1926a & b, 1929) stressed the hypothetical nature of the trajectoria in his work on the functional morphology of the facial skeleton. He attempted to describe the co-ordination and interplay of forces between soft and hard tissues. From a gross morphological examination of the skull and cancellous bone he expressed the functional morphology of the face in terms of basal arches and pillars. Three vertical pillars arise from the basal arches of the left and right alveolar processes and anchor the processes to the neurocranium for the transmission of forces from the teeth to the solid bone of the cranial vault. This buttress theory has found its most recent expression in work by Weinmann & Sicher (1947) and Sicher and DuBrul (1970) who also describe the upper jaw and face as forming a biological and mechanical unit anchored at the base of the skull.

Tucker's (1954) work on the mammalian skull is based on the arrangement of 'nodes', thickened regions of the skull

of limited extent which are determined by local concentrations of stress. These are interconnected with one another as well as with the points at which stresses enter the skull by means of 'transmissive structures' such as 'arches and ridges'.

Tucker distinguishes three types of mammalian skull; the breviarcuate, longoarcuate and planoarcuate, which are characterised by the primary force transmitting structure termed the 'arcus principialis cranii'. These types broadly correspond with carnivores, rodents and primitive types of mammalian skull respectively.

The theories of 'buttresses' and 'nodes' offers a description of the gross architectural arrangement of the skull. It has little to offer this present study as the descriptions of the areas of stress within the skull are not intimately related to the internal architectural organisation.

1.3.2. <u>The split-line phenomenon</u>.

Emphasis has been placed on an examination of this theory as it offers a possible method of studying the detailed organisation of the cat skull.

The split-line technique was developed by Benninghoff (1925) to determine the structural organisation of decalcified long bones and flat bones of the human skull,which were then studied histologically under normal and polarised lighting. In long bones the split-lines coincided moderately well with the long axis of the bone, although quite complex patterns were obtained in the flat bones. These patterns were interpreted as indicating the orientation of the Haversian systems or osteones, which Benninghoff believed lay in the long axis of tension and compressive resistance, and were thus an indication of the greatest tensile and compressive strength of the bone.

On the basis of Meyer's (1867) contention that the pars compacta corresponded to a closely crowded spongiosa, Benninghoff assumed that the two types of bone represented different parts of the same stress system; consequently the orientation of the osteones is trajectorial in nature. Further, Benninghoff assumed that the interstitial lamellae between osteones resisted equally well forces impinging on them from any direction. He also believed (as did Petersen, 1927) that the apparent disordered arrangement of the lamellae absorbed stresses in such a manner as to render the bone functionally homogeneous. The latter was assumed to be a necessary feature of bone for it to exhibit relatively constant mechanical properties, and within the homogeneous bone definite trajectories were observed and maintained by a process of re-modelling.

Benninghoff's split-line technique was employed by many investigators. But the precise interpretation of what the split-lines represented varied with different authors i.e., what structural component of the bone the split-lines indicated and whether these lines were indicators of the bones response to mechanical forces or to the direction of growth. This last interpretation was upheld by Ahrens (1936), Pauwels (1950) and Evans and Goff (1957). Ahrens found that the split-lines in the human foetal and infant cranial vaults corresponded to the direction of growth of the original bone, radiating from the centres of ossification. Pauwels (1950) suggested that in long bones the split-lines represented growth trajectories arising from tensile strain generated in the periosteum by growth of the bone at the epiphyses.

However, the majority of investigators followed Benninghoff's (1925) interpretation of the split-lines. Olivo et al (1937) emphasised that although the decalcified bone had different properties, the predominant direction of split-lines in decalcified bone correlated with the direction of the greatest strength in the intact bone.

Siepel (1948) commented that quite divergent results had been obtained with the split-line method on the human facial skeleton and jaws, by different investigators, and that no attempt had been made to trace qualitative differences induced by different physiological and pathological conditions within the architectural frame. He suggested that in general, the architecture was considered as a pure mechanical problem which was solved once the architecture was shown to be present in a certain arrangement and in a certain number of skulls.

Siepel (1948) using the split-line method carried out an investigation on the jaws of individuals in various states of health and disease. His interpretation of the split-line phenomenon agreed with that of Benninghoff (1925). Siepel also considered the split-lines as stress trajectories, but was nonetheless aware both of the inadequacies of the technique and that the lines produced were a simplification and an exaggeration, for he states that these are "heavy lines signifying the directional arrangement of the minute structural elements which form the interior architecture" and the "the lines are by no means trajectories, only indicators of the main flow of lamellar and fibrous organisation in the bone", (Siepel's italics).

In contrast to Benninghoff, Siepel illustrated the crossing of split-lines which led him to emphasise that in bone

adaptation the biological aspect of bone reaction must be considered along with the mechanical stimulation. He also reported alterations in the trajectories of human mandibles as a result of variations in function arising from dentitional changes. The orientation of the mandibular trajectories were considered to be the result of muscle action, but he emphasised that from an anatomical point of view the tensile and compressive elements of a bone are not clearly differentiated, because the bone is constructed for multiple requirements. Siepel described a simple mechanical interpretation of the architecture of the mandible and as MacMillan (1928) had done, he compared it to a straight rod or long bone in which the upper trabecular systems represented the tensile, and the lower ones the compressive trajectories.

The contradictions between Siepel's description of bone histology and the inadequacies of the split-line technique on the one hand, and his reference to the split-lines as stress trajectories on the other, would tend to indicate that he was unable to relate the description of the bone histology to the mechanical interpretation provided by the split-lines. This could possibly be explained on the basis of the methodological limitations imposed by a combination of the split-line technique and the Trajectorial Theory.

The discrepancies highlighted in Siepel's (1948) work, although known to Tappen, did not deter the latter from extending Benninghoff's work in a series of papers (Tappen, 1953, 1954) in which he described the functional analysis of the orientation of the Haversian systems revealed in the split-line patterns of human and primate skulls. The split-lines were interpreted in terms of stresses and strains arising from

the musculat activity of chewing. In regions where the split-line patterns were not readily explained on a mechanical basis, Tappen suggested that they corresponded to the direction of growth of bone. He implied that this technique enabled an examination to be made of the primary genetic and secondary functional causes of form in the various parts of the skull.

As regards experimental confirmation of the mechanical forces interpretation of the split-line phenomenon, only Kuntscher (1935a) thought that this was provided by the deformation patterns obtained by the static vertical loading of colophonium-coated femora. It has, nonetheless, been emphasised by Evans (1957) that no experimental evidence has been provided to support the theory that the split-lines were indications of the greatest tensile and compressive strength of the bone.

Tappen (1954) admitted that the interpretations placed on the split-line patterns were largely theoretical, for there was no experimental evidence to support them and that any study of the organisation of the deep layers of bone must remain a matter of speculation.

Moss (1954) stated that the split-lines reflected a mean course of the osteones and that any deviation from an artificially smoothed pattern was not observed. He defined three postulates on which he felt the split-line technique was based, namely: 1) the patterns show the orientation of the osteones and lamellar bone, 2) the orientation is determined by functional demands and 3) the orientated bone is assumed to be homogeneous in morpholgy and constitution. These postulates were examined by Moss on the basis of the results obtained from his vital staining of bones which revealed the walls of intra-

osseus blood vessels and vascular channels of large diameter. Although Moss offered no evidence, he stated that the mean direction of osteones omitted much that is critical to correlate structure with the function of bone, and that an attempt to interpret the orientation of a system of osteones as being due primarily to the imposition of an external set of forces, is rejected as being an excessive oversimplification.

Although Moss does not make any reference to the matter, his observations infer a correspondence between the split-lines and the large vascular canals; the latter are referred to as osteones in his text.

Dempster and Enlow (1959) also demonstrated the complexity of vascular patterns in their study of the cortex of the mandible, using an ink injection and clearing technique which revealed the elaborate patterns of as many as eleven trajectories.

Evans and Goff (1957) compared the "stresscoat" patterns with those of the split-lines obtained from the same femora. Their argument against the split-line method as a means for interpreting mechanical forces was that that lines seldom crossed each other and therefore could not represent the theoretical stress trajectories which they believed the "stresscoat" patterns represented.

Evans (1957) criticised the split-line phenomenon and severely attacked the Trajectorial Theory. He found it difficult to accept the mechanical significance of the split-line patterns as their users did not understand the mechanical meaning of trajectories and stress, "They write and speak of trajectories and stress as if they are visible entities, which is not the case.", Evans states that a stress trajectory is

the curve along which the principal stress at any point would fall, and in order to draw such a curve the stress at the various points must be computed. Stress is the intermolecular resistance within an object to the deforming action of an outside force. Consequently stress cannot be seen but its magnitude can be computed, provided the magnitude of the load and the cross sectional area of the object to which it is applied are known. If the stresses in an object are known the trajectorial diagram of the object can be drawn and in so doing the engineers assume the object to be a solid homogeneous body. Evans emphasised (1957) that more experimental evidence was needed before the functional significance of the split-line patterns, especially with respect to stress and strain in bones, can be accepted.

In spite of the obvious absence of any experimental proof, Tappen defended his interpretation of the split-line patterns in two papers (1964, 1970). He answered the criticisms that the split-lines were an indication of the direction of growth of bone (Ahrens 1936; Evans & Goff 1957) by referring to the changes in the orientation of the split-lines during growth of human and primate skulls, as being an indication of the effect of mechanical factors. Tappen (1964) carried out experiments on long bones and demonstrated that the split-lines did not conform to the orientation of the vascular channels but to the orientation of the lamellae and cement lines.

Tappen's (1964) reply to Evans (1957) and Evans & Goff's (1957) criticism of the "Mechanical Forces" hypothesis that the split-lines seldom cross each other was that these lines represented a response to certain mechanical strains, although the nature of the response was probably more complex (cf. Tappen,

1954). Tappen further stated, without any experimental proof, that the clearest split-line patterns observed were in areas where the forces acting on the bone must have been principally tensile in nature.

Dempster (1967) in his paper describing the form-texture relationships to grain patterns and skull strength, discusses the split-line phenomenon in terms of "cortical trajectories" as defined by Benninghoff (1925), Siepel (1948), and Tappen (1953, 1954). Dempster suggests that the implication that tracts develop in the individual as a response to functional stresses must be speculative, since Dempster knew of no mechanism at the molecular level through which the process of bone organisation and growth might form pressure tracts or pillars under the influence of stress. Dempster suggested that the so called masticatory tracts or pillars could be genetically determined growth specialisations; the orientation of grain along them might or might not be a secondary mechanical adaptation. The implication of Dempster's hypothesis is that the shape of the bony structures in the human skull determines the orientation of the split-line patterns.

In an examination of Dempster's (1967) comments, Tappen (1970) illustrates his paper with photographs of baboon skulls with major variations in the split-line patterns, which, according to the author, show clearly that the shape of the cranial structures can not be a primary determinant of split-line orientation. Later, Tappen (1971) suggested that the grain of bone appears to be a feature of the periosteal attachment.

Tappen's explanation (1970) of the variations in the split-lines in the primate skulls is that they are due to a combination of influences of intrinsic and extrinsic factors (c.f. Tappen, 1954).

An examination of the photographs and text of Tappen's 1970 paper reveal that the split-lines are not generated in identical regions in the different skulls and that the technique appears too variable for the accuracy demanded by its exponents.

Tappen's position is further weakened by his recent paper (1971) in which he demonstrates that the split-lines are essentially identical to red-brown lines close to the freshly dissected bone surface, which represent resorption spaces and immature osteones containing blood vessels, as well as mature osteones. These observations support the work of Evans & Goff (1957), the inferred results of Moss (1954), and contradict Tappen's 1964 paper. Isotupa (1972) recently recorded the correspondence between split-line patterns and vascular spaces in the bones of growing mammalian skulls.

The recent development of the projection X-ray microscope (Ely, 1972) has provided a non-destructive method of examining, in three dimensions, the detailed organisation of bone. Hobdell (1970) used this technique to great advantage in his study of the structure and development of tooth supporting bone in the mandibles of a number of mammalian species. He found that the shape of the dental roots appeared to determine the organisation of the supporting trabeculae.

The technique of stereo-projection microradiography is used in the examination of the detailed organisation of the cat skull on the basis of the results obtained by Hobdell (1970), and because this method was devoid of the limitations present in the 'buttress' and 'split-line' methodologies.

1.3.3. Summary and conclusion.

At present there are two principal methods of describing

the architectural organisation of skull bones: The buttress theory and the split-line phenomenon. The former is founded on a gross morphological interpretation of the facial anatomy and cancellous bone, and was regarded as being too generalised a theory for use in the description of the detailed organisation of the cat skull. The second theory based on the split-line analysis of bone appears to provide a more detailed picture of its structural organisation. The protagonists, however, have difficulty in agreeing as to whether the split-lines represent the orientation of the Haversian system, osteones and lamellae (Benninghoff, 1925; Siepel, 1948; Tappen, 1953, 1954), or simply lamellae and cementing lines (Tappen, 1964), or vascular channels and immature osteones (Moss, 1954; Evans & Goff, 1957; Tappen, 1971; Isotupa, 1972). If these split-lines are to be accepted as indicators of stress trajectories then a contradiction exists at the histological level, as the lines are generally accepted as representing either vascular channels or osteones. This difficulty is obviated if the bone between the split-lines is taken as representing the trajectorial stress lines, this in turn leads to a marked decrease in the sensitivity of the technique.

Further disagreement also exists between authors as to the interpretation of the split-lines, either as indicators of the direction of mechanical forces (Benninghoff, 1925; Bruhnks, 1929; Henkel, 1931; Dowjallo, 1932; Kuntscher, 1935a; Siepel, 1948; Tappen, 1953, 1954, 1957, 1964, 1970), or direction of growth of bone (Ahrens, 1936; Pauwels, 1950; Evans & Goff, 1957; Isotupa, 1972). The interpretation of the split-line phenomenon must remain speculative particularly in view of the absence of any supporting experimental evidence. Because of these

dissadvantages the split-line technique was not considered viable for the present study. Instead the method of stereo-projection microscopy was used for examining the structural organisation of the cat skulls.

1.4. Methods of analysis of the stress and strain distribution in bones.

The use of mathematical and/or engineering methods for determining the stress and strain distribution in bones is reviewed in the remaining sections of this chapter. This enabled an assessment to be made of the relative value of each technique in determining as accurately as possible the response of bone to an applied force. The first two sections give an account of methods which are based on the principal of making a model of the bone in order to determine the distribution of strain in the bone. The third section describes techniques which use parts of, or whole bones in their examinations.

1.4.1. Mathematical analysis.

The mathematical analysis applied to the cross section of bones has played an important historical role particularly in the development of the theories of functional architecture of the spongiosa. The study has concentrated in general on the biomechanics of the human femur.

Koch, in his classical paper (1917), examined the sections of over thirty complete femora. He was an advocate of the theory that the trabeculae are produced by tension and pressure as demanded by the Trajectorial Theory. He proposed without a mensural assessment of the trabecular size that those

subjected to tensile stress were thinner than those subjected to compressive forces; that the thickness and closeness of the trabeculae was proportional to the stresses transmitted within them and that the quantity of the spongiosa in a region of vertical shear in the femur was directly proportional to the relative magnitude of the shear. Koch was at pains to point out the presence of orthogonality within the trabecular organisation. He said that observers could easily be deceived by the cursory examination of two intersecting curved lines, which may appear to lie at obtuse or acute angles to each other, but on closer examination are at right angles at the point of intersection. The stresses and strains were computed in the femur on the basis of a vertically applied load to the head of the femur.

Grunewald (1920) extended the mathematical analysis of the human femur and included the tibia. The stresses and strains were again resolved on the basis of a vertically applied load representing the body weight of the subject when standing.

Marique (1945) calculated the values for the magnitude of the various stresses in a femur under assumed conditions of loading. Further mathematical analyses have been executed to determine the stresses and strains within the human femur and in particular the coxa vara by Rydell (1966) and McLeish & Charnley (1970). The loading was directed at the centre of the femoral head combined with a second force at the greater trochanter.

The criticisms of this method by Kuntscher (1934) were largely disregarded. He pointed out that the formulae used in such analyses were based on the assumption of an even distribution of force in the cross sections of the bone, a condition which rarely occurs, That the formulae applied for the determination

of the strength of materials in simple bodies can not be applied to such a complex body as bone. This mathematical analysis is based on the theory of columns and beams which in turn is founded on the assumption that the body being analysed is of uniform shape throughout and composed of homogeneous material; an assumption which is not applicable to bone. Finally, Kuntscher states that the mathematical studies only deal with a two dimensional structure instead of a three dimensional one.

This last point was taken up by Toridis (1969) who retained the approximation of the beam theory, but modeled the femur as a three-dimensional space curve. This analysis included torsional as well as bending effects.

Mathematical models of portions of the femur such as the condylar structures have been used by Burstein et al (1970) to calculate the stresses and displacements for the variations in geometry and elastic properties.

Models for the behaviour of the human femur were used by Rybicki et al (1972) to examine the effects of muscle forces on the resulting stresses and strains during a one-legged stance. Their results show that tension in the tensor faciae latae very effectively served to counteract bending stresses in the femur, while also reducing strain energy.

Rybicki et al (1972) found that the choice of mathematical model was important, for their results showed that the beam theory is appropriate for the calculations of stresses in the shaft of the femur, whereas the finite element analysis was required for the proximal end and areas of muscular attachment.

Breckelmans et al (1972) supported the use of the finite element method, stating that it was suitable "par excellence" (their italics), for the analysis of complex constructions such as the femur. These authors, in their examination of the use of mathematical models, felt that the reality of bone could be schematised and considered in terms of mathematical equations. The beam theory method used by Koch (1917) and subsequent workers ran into complications through oversimplification; the causes lay in the difficulty of giving an analytical description of the geometry of the skeletal parts. The in vivo patterns of stress in bones were too complex to be calculated and the beam theory did not account for the physical properties of bone. All these problems were within the capabilities of the finite element method (Breckelmans et al, 1972) although the difficulty lies in the choice of data for the computer.

Nonetheless, both Rybicki, Brekelmans and their colleagues continue to ignore Kuntscher's criticism (1934) that mathematics can not describe satisfactorily a three dimensional, anisotropic, irregularly shaped hollow structure.

1.4.2. Analysis of stress and strain in bones using models.

The first person to use a model to study stress and strain in bones was Roux (1885) who used the cracks appearing in a paraffin coated rubber model of an ankylosed knee-joint as a basis for trajectorial diagrams. Kuntscher, however, suggested (1935a) that during Roux's tests the deformations in the rubber model were so great that the plane of application of force must have shifted, thus altering the direction and magnitude of the force, and hence the accuracy of the results.

The majority of the work in this field has concentrated on the photoelastic method based on the engineering technique. The initial examinations were carried out by Hallermann (1934), Milch (1940), and Pauwels (1948, 1951, 1954).

Hallermann (1934) constructed a simplified model of the leg bones and studied the stress distribution produced by an even axial pressure. He believed that the method was limited to resolving problems of general bone mechanics and could not be applied to dynamic studies as the velocity factor could not be demonstrated.

Milch (1940) carried out photoelastic studies on the models of the femur and calcaneus under compression loading. The stress lines seen in the femur were "markedly reminiscent of trabecular structures seen in the longitudinal section of the femur." Milch suggested that the stress patterns emphasised the importance of the mutual relation of the anatomical and mechanical axes as related to bone deposition. In contrast to the caution of Hallermann, Milch assumed that the stress lines of his models could be made to represent the actual conditions of loading of real bones. In consequence, he believed that the stress patterns were experimental confirmations of both Roux's and Wolff's hypotheses of bone growth and transformation as well as of the Trajectorial Theory.

Pauwels (1948, 1951) made an attempt to reproduce more closely the living situation, by applying forces to the plastic model in a manner similar to the action of the muscles and ligaments. The modifications had the effect of reducing the magnitude of stress in the femur and humerus respectively. Kummer (1972) stated that it was Pauwels' work of 1948 on the photoelastic patterns that firmly demonstrated the trajectorial

nature of the substantia spongiosa in normal and pathological bones.

Pauwels added further support (1954, 1965) when he compared directly the radiological density with the strain distribution in a plastic model of the upper end of the femur. In this and in his previous investigations he assumed the mechanical homogeneity of bone tissue as well as a constant relation between the mineral content and the strength of the bone. Kummer's (1956) use of a particular photographical method in his photoelastic experiments revealed not only an impression of the trajectorial diagram, but also the locally differing densities of bone within the proximal end of the femur.

The criticisms levelled at this method are similar to those applied to the mathematical analysis of stress and strain in bone. Principally, the plastic models are two dimensional and could not be representative since bone is a three dimensional body and a three dimensional stress pattern must differ widely from a two dimensional one (Knese, 1956). The method as used in engineering is for stress strain analysis of solid objects of homogeneous composition, and all models made from uniform resinous material are quite different from hollow bones of heterogeneous composition and complicated trabecular organisation; conditions which, Kuntscher (1934) pointed out, were impossible to duplicate on any model.

Kummer (1959, 1966) did not accept Knese's criticism for he considered (1972) that his geometrically constructed three dimensional trajectorial pattern of the proximal end of the femur was similar to the architecture of the spongiosa. However, this construction is a solid line projection into the three dimensions of the schematised mathematical trajectorial diagram. This construction does not account for the differences

in the organisation of the compacta and spongiosa. The construction bears no similarity to the sectioned bone illustrated by Kummer (1972).

The work of Pauwels was continued by Knief (1967a & b) who provided a quantitative comparison of X-ray densitometry with the results obtained from photoelastic experiments on the proximal end of the femur. These investigations revealed some minor differences between the distributions of bone minerals and strains which Knief was unable to explain fully. According to Konermann's (1970, 1971) recent results, using a photographic method for the determination of the density distribution in X-ray pictures, a still better harmony between mineral distribution and local stress appears highly probable. Konermann (1971) states that this good correspondence makes it highly probable that local stress and local quantity of material are inter-related and that the proximal end of the human femur is a "body of uniform strength". On the basis of his own investigations and those of Pauwels (1948, 1951, 1954, 1965), Knief (1967a & b), Konermann (1970, 1971), Kummer states (1972) that bone is a body of homogeneous strength.

This statement is not supported by all research workers for, as Brekelmans et al (1972) point out, the use of the photoelastic techniques, which has been moderately extensive in the biomechanical field, rests largely on a pronounced schematisation, in particular as regards the geometry and the material, for it does not account for the inhomogeniety and anisotropy of bone. This schematisation also extends to the interpretation of visible spongiosa architecture and radiographs of the femoral head. Calculations have provided quantitative results, from both the models and radiographs,

although these are often not accurate, particularly with three dimensional models.

1.4.3. Analysis of stress and strain in bones using engineering techniques.

As with the two previous methods of investigation the majority of work has been carried out on long bones, in particular the femur. The deformations generated under conditions of stress in bone are also set up in the mechanical material (brittle lacquers or strain gauges) applied to the surface of the bone. It is the alteration of the defined properties of these materials that enables the bone deformations to be monitored.

The orthopaedic surgeon Kuntscher (1934) was the first to study the stress-strain phenomena in human long bones by coating them with melted colophonium resin and studying the strain patterns produced by static and dynamic loading in various positions. Areas of tensile and compressive strain produced by tension, compression, bending and torsion loading of normal humeri, tibiae, femora, radii and clavicles were carried out by Kuntscher (1935a). He found that the areas of strain varied with the bone, its orientation during testing and the types and point of application of the forces.

Kuntscher (1935b) extended his studies to include dynamic loading of pathological bones and a discussion of fracture mechanisms. With the additional data he obtained on static loading, he concluded that tensile strain patterns produced by dynamic loading of normal femora was essentially similar to those obtained by static loading. Kuntscher (1935b) concluded from the uniformity of the deformation patterns obtained in his tests, that an intact bone is functionally a

homogeneous structure in spite of its morphological diversity (a conclusion reached by Messerer, 1880; Pauwels, 1954, 1965 and Kummer, 1972).

The strain patterns obtained in these experiments were taken as confirmation of Benninghoff's concept (1925) that the Haversian systems or osteones were functionally related to the stresses in bone. Kuntscher (1935a) suggested that in certain regions of the femur the osteones had a double function and transmitted both tensile and compressive forces, while in other parts of the bone they only resisted compressive forces.

The use of a brittle lacquer or the "Stresscoat" method was developed by Forest & Ellis (1940) as a refinement on the use of colophonium resin. Most of the studies of stress and strain in bones using this technique have been concerned with deformations and fractures in skulls (Gurdjian, Lissner and co-workers, 1945, 1946, 1947: 2 papers, 1950, 1953), and in femora (Evans et al 1948: 2 papers, 1951, 1952, 1953; Evans 1953). The tensile strain patterns obtained by Evans, Lissner, and their team (1948: 2 papers, 1951) in normal bones resembled those formed by Kuntscher under similar experimental conditions.

Few stresscoat studies have been carried out on deformation in the mandible and none on the skull, in relation to simulated forces generated during biting. Evans (1953) applied a load to the point of the chin and in a second experiment a load was applied to a brass rod laid across the body of the mandible near its angle. The deformation patterns from these experiments arose from the bone bending and causing cracks to appear in the convex tensile area.

An attempt at simulating the effect of the pull exerted by the external pterygoid muscles on a lacquered human mandible was carried out by DuBrul & Sicher (1954). They applied finger pressure lateral to the points of insertion of the muscles, squeezing the condyles together. The resulting deformation patterns revealed a tensile strain in the long axis of the mandible.

These experiments and those previously described on the femur, show that bone behaves like an elastic body whose deformations can be demonstrated with relatively small loads. The magnitude of the local deformation (strain) is slight and is proportional to the load, and so long as the elastic limit is not exceeded, the bone exhibits considerable powers of recovery (Evans, 1957). Marique (1945) has demonstrated the presence of hysteresis in the load deflection curves for increasing and decreasing loads applied to a femur, indicating that the energy relations between the two phases are not equal.

Many investigations involving strain gauge measurements on long bones in vitro have been accomplished by bonding them either to a piece of test bone (Frossblad, 1959; Frankel & Burstein, 1964), or to an isolated bone (Gurdjian & Lissner, 1944; Hirsch & Brodetti, 1956; Hirsch & Evans, 1965). The responses recorded from a dynamically applied load are very different from those of a static one, and the modulus of elasticity of bone as well as its ultimate yield strength are not constant (Sedlin, 1965).

The only in vitro strain gauge examination of a skull was made on a human crania by Endo (1965) who mounted the

skulls in a craniostat with supports placed at the glenoid fossae. He simulated the pull exerted by the masseter and temporalis by loading the free ends of canvas sheets which had been glued to the areas of muscle attachment. A force applied to the first molar produced a different pattern of strain from a force applied to the first incisor. Proportionally larger strains were recorded in the maxilla, zygoma and around the eyes, than in other parts of the skull. The greatest shearing stresses occurred under the orbits where they would have been greater still were it not for the lateral orbital walls which probably acted as stays for the zygomatic arch.

Direct strain measurements from bone in vivo are also required, for as Cochran (1972) points out, it is impractical to simulate static or dynamic loading by the interaction of forces generated by muscle action and gravity.

Gurdjian & Lissner (1944) bonded a wire resistance strain gauge to the exposed crania of a dog to analyse the mechanism of concussion. Strain gauges have been applied to bone in cadavers to evaluate the impact forces (Gurdjian & Webster, 1947; Lissner, 1964; Lissner & Roberts, 1966).

Evans (1953) successfully bonded gauges to a chronically exposed area of tibial bone in a living dog and recorded tibial tensile and compressive strains occuring in the bone while the dog walked. Recently, Lanyon (Lanyon & Smith, 1969, 1970; Lanyon, 1971, 1972, 1973) described the first successful biomechanical investigations using intravital strain measurements from bone. He analysed strains in sheep tibia which revealed a characteristic cyclical deformation during locomotion (Lanyon & Smith, 1969, 1970). Gauges bonded to thoracic vertebrae showed that the strain amplitude and rate increased with the

animal's speed during locomotion (Lanyon, 1971, 1972). Nevertheless, Lanyon stated that without making many assumptions it is impossible to quantify bone stress _in vivo_ and for complete specimens it is difficult to compute it realistically _in vitro_, although strain can be measured directly under both conditions.

The limitations of a single linear strain gauge were circumvented by using rosette strain gauges bonded onto the sheep's calcaneum (Lanyon, 1973). This had the advantage not only of providing a reading of the principal strains but also of recording the change in direction throughout the deformation cycle.

Even so, one of the major difficulties with strain gauge attachment to bone _in vivo_ is that the inherent level of inaccuracy in the technique cannot be demonstrated until satisfactory calibration procedures are evolved. Lanyon's (1973) quantitative post mortem calibration method suggested that the gauges have a linear response to bone deformation, over the range recorded during life.

The complexity of the cycles of bone deformation during locomotion recorded by Lanyon (1973) prompted him to state that considerably more work has to be done before an understanding can be obtained of the deformation pattern which occurs even in the shaft of the calcaneum. As the strain amplitude and rate of change were comparable to values obtained from other regions in the same species, Lanyon suggested that this agreement tended to support the hypothesis that bone deformation _per se_ may be at least one of the governing stimuli for the remodelling necessary to the maintenance of the bone's structure and mechanical strength.

1.4.4. Summary and conclusion.

Mathematical models founded on the beam theory were initially employed to define the trajectoral theory; beyond this description the model was unable to handle the complex data of stress analysis of bone in spite of many attempts. Recent use of computers, however, has made some authors optimistic.

Photoelastic models have been extensively used in biomechanical examinations because of the adaptability of the technique to different loading situations and the apparent parallelism between the lines of stress in the model and the diagrammatized trajectional arrangement in limb bones. Recently, the method has been extended to demonstrate the relationship between the mineral content of the proximal end of the femur, determined from roentgenograms, and the strength of bone assessed from the photoelastic models. In their correlations a number of authors (Pauwels, 1954, 1965; Kummer, 1972) have suggested that a bone is a body of homogeneous strength.

The mathematical analysis and use of models to describe the stress-strain relationships in bone have been heavily criticised for being founded on an extensive schematisation of the shape and material composition of bone. Analyses are generally applied to two dimensional models and no account is taken of the inhomogeneities and anisotropy of bone. In particular, this diagramatisation extends to the interpretation of the cancellous architecture, the structural organisation of the compact bone and the information visible in the radiographs is disregarded.

The coating of bones with brittle resins, such as 'colophony' and 'stresscoat' have proved successful in providing strain patterns of bone deformations in static and dynamic loading of limb bones and in simulated conditions of concussion

and fracture in human calvaria.

Based on the results of his resin experiments, Kuntscher (1936b) suggested that bone was functionally a homogeneous structure. This was not upheld by Sedlin (1965) who demonstrated, be means of strain gauges bonded to bone that its modulus of elasticity and yield strength were not constant during dynamic loading.

Numerous strain gauge experiments have been carried out on prepared bone to examine its physical properties and the response of limb bones and skulls to static and dynamically applied loads. Only one *in vitro* strain gauge examination has been carried out on the human skull under simulated conditions of biting. Endo (1965) demonstrated that a relatively greater deformation occurred in the antero-inferior facial bones relative to those of the rest of the face.

The recently developed intravital implantation of strain gauges has enabled recordings to be made of deformation cycles, strain amplitude and rate of change of strain taking place in limb bones and vertebrae.

In view of the limitations listed above for the mathematical analysis and the use of models in describing stress-strain relationships in bone, these methods were rejected for use in the present study. The engineering technique of coating the bone with a brittle resin and the *in vitro* and *in vivo* bonding of gauges to bone, were deamed more efficacious and all three methods are employed in conjunction for the first time in this thesis.

CHAPTER 2

MATERIALS AND METHODS FOR THE EXAMINATION OF THE STRUCTURAL ORGANISATION OF THE CAT SKULL BONES.

CHAPTER 2

MATERIALS AND METHODS FOR THE EXAMINATION OF THE STRUCTURAL ORGANISATION OF CAT SKULL BONES

2.1. Introduction.

Frequently in functional-morphological studies, the structure alone is described and the functional interpretation is inferred from these observations. Conversely, experiments have been performed on material without relating the results of the functional studies to the underlying structure.

This thesis is concerned with the structure and function of the cranial bones of the cat and the text is divided accordingly into a description of the structural organisation and the experimental procedures carried out to determine the functional characteristics of the cranial bone.

Bone is a specialised form of connective tissue characterised by the deposition within a soft organic matrix of a complex mineralised substance. Emphasis has, therefore, been given to those techniques which would provide the most information concerning the structural organisation.

Projection microradiography was regarded as an important technique as it provided a method of studying one of the essential features of bone, namely the distribution of the mineralised tissue in the whole skull and at a greatly increased resolution than that obtained from conventional X-ray machines.

Recognised histological techniques were used to identify the structures within the mineralised tissue of the skulls which were radiographed. The histology of the bone is described and is then followed by the radiographic examination.

2.2. Materials

2.2.1. Cat skull material.

A total of seventeen fresh skulls were obtained from adult female cadavers at the termination of acute experiments carried out in the Department of Physiology, King's College, London. The skin was removed and the heads stored in 10% formol-saline solution. Adult female cat skulls were used for the investigations in order to obviate any possible variation due to sexual dimorphism. The skulls were prepared by stripping the flesh off the bone.

2.2.2. Apparatus.

Radiographic investigations were carried out on the XX 50 Modified Intercol projection X-ray microscope fitted with a variable solid target unit. This equipment was used by the kind permission of Mr. N.J.D. Smith and was made available to King's College Hospital Dental School through the generosity of R.V. Ely, and the Trustees of the M.R. Research Trust.

A Hilger and Watts folding mirror stereoscope was used for the examination of stereo-pair radiographs.

Ward's Bioplastic (Rochester U.S.A.) cold setting resin was used for embedding the skulls for serial coronal sectioning. The skulls were cut on a Bateman sectioning machine, made available by the kind permission of Patrick Sullivan of the Department of Dental Anatomy, London Hospital Dental School.

An Olivetti desk calculator type 'Programmar 101' was used for calculating the statistics associated with the trabecular frequency in the alveolar processes of the maxilla and mandible.

2.3. Histological examination of the structural organisation of bone.

2.3.1. Ground polished sections.

Five sagittaly sectioned cat skulls numbered from A to E were selected for detailed structural and histological examination of polished ground sections. The right halves of the skulls were placed in rectangular perspex moulds with the mid-sagittal plane on the base of the mould. The skull was aligned so that the palate was parallel to the wall of the mould. The skulls were encased in Ward's cold setting 'Bio-Plastic' resin which was cured at room temperature. The casts were released from the moulds. Coronal sections 3 mm. thick were cut perpendicular to the palate commencing at the anterior tip of the premaxilla on a Bateman Sectioning machine with a water-cooled circular diamond blade (28 μm width). The sections used for histological examination were ground and polished on both sides using graded alumina powders of 1 μm to 0.03 μm with ethylene glycol as a lubricant.

The slabs were examined under a binocular dissecting microscope with incident light and under a Zeis Ultraphot Mark III microscope using light and dark background reflected lighting conditions. Photographs of pertinent regions of the ground and polished sections were taken on the Ultraphot III using dark background reflected lighting conditions.

The advantages of this method were that the histology of a whole section of a skull could be examined. The relative position and relation to one another of the compact and cancellous bone could be compared to the successive coronal sections in the skull as well as within the five different cat skulls.

The principal drawback was the large amount of time required for the preparation of the polished sections. The method of preparation of these calcified slabs did not permit

the examination of the cellular nature of certain histological structures such as the osteones and lacunae.

2.3.2. Decalcified and stained sections.

Confirmation of the histological interpretations and identification of the cellular nature was carried out on decalcified and stained sections.

Two cat skulls were stripped of flesh and approximately 5 mm. square blocks were cut from the maxillae, frontals, parietals, temporals, jugals and palatal bones using a small circular saw fitted to a dental drill. The blocks of tissue were demineralised in phosphate buffered ethylene diamine tetra acetic acid (E.D.T.A., pH 7.4) and prepared for routine histology. Serial sections were cut off these blocks at between 5 and 7 microns and alternate slides stained with haematoxylin and eosin, Van Gieson and Mallory (Figs 3.1., 3.2.).

The limitations were that this method enabled only a very localised region of the skull to be examined, and that both the techniques used provided only a two dimensional interpretation. The nomenclature employed in the account of the bone histology was based on terms used by Pritchard (1972).

2.4. Introduction to the radiographic examination of bone.

The value of X-rays is their short wavelength compared with that of visible radiation which is characterised by the ability of the X-rays to penetrate optically opaque objects. This provides a non-destructive method of investigating internal structures of biological speciments. Its importance as an investigative and mensural tool for bone was soon recognised (Walkoff, 1898; Wolff, 1900). Pacini (1922) in his anthropological

studies attempted to show that more accurate measurements could be made from radiographs of the skull than from the skull itself. Broadbent (1931) described techniques for improving the accuracy of radiographic cephalometry.

Most radiographic studies on the structural organisation of jaws and skulls using clinical X-ray machines do not appear to have taken account of the histology of the structures recorded. However, Becks and Grimm (1945) did attempt to define the accuracy of the X-ray machines in terms of the histological structures recorded on radiographs of human mandibles. Siepel (1948) argued that the use of X-rays for the study of the trabeculation within the mandibular medullary bone provided no information that could not be obtained by the dissection of demineralised specimens. The relatively gross level of Becks and Grimm's examination validates Siepel's criticism. Siepel was further supported by the investigations of Chasin (1928) on the trabecular nature of human vertebrae in which he observed that X-rays of various vertebrae often revealed little indication of the bone rarefaction that was present. This has been confirmed by Bohming and Prévôt (1931) and Borak (1942). The latter found that bone defects as large as 2.5 cm. were often not noticeable on clinical radiographs unless the beam passed directly down the lesion. Goldman & Millsap (1957) removed the buccal and lingual plates of bone from mandibles with no effect on the X-ray appearance of the cancellous bone associated with the teeth. Conversely, Bender & Seltzer (1961) removed all the cancellous bone of the mandibles and observed that its absence was not detectable.

The above are examples of the limitations of the clinical X-ray machines which are the result of three factors. The first

is the characteristics of the radiation; the radiographs are produced at relatively high kilo-voltages (80 - 110 KV), the component of "white" radiation in the spectrum of the X-ray beam is consequently large and the contrast in biological speciments is therefore limited. Second, the resolution of an object is a function of the source size which in commercial tubes is frequently about 1 mm^2 and at best 0.3 mm^2. This introduces considerable penumbral blurring unless the distance between the tube and specimen is large. Third, resolution is reduced through the use of relatively fast, coarse-grained films.

These limitations have been overcome with the development of the projection X-ray microscope which has been successfully used by Hobdell (1970) to describe the structure and development of the tooth supporting bone of the mandible of a number of mammals.

2.4.1. Projection microradiography.

2.4.2. Introduction

A simple way of forming enlarged images with X-rays is to place the object close to a small source. Direct image enlargement is obtained by positioning the specimen between the source and photographic emulsion, magnification being the ratio of the source image to source object distance.

One method of obtaining a point source is to place a pin-hole in front of a macroscopic focal spot. Early attempts were disappointing (Czermak, 1897; Uspenski, 1914) on account of the low intensity of the X-ray tubes then available. More recently Sievert (1936) and Rovinsky and Lutsan (1957) have applied the method with greater success.

The use of a fine focal spot, instead of a pin-hole was first proposed by Malsch (1939). The principles of the projection

X-ray microscope were formulated in 1939 (Ardenne, 1939; Marton, 1939) when it was suggested that the newly developed electron optical techniques would make it possible to concentrate an electron beam into a focus of 1 μm. or less in diameter. Subsequent developments in Cambridge (Cosslett & Taylor, 1948) led to the construction of a machine for high magnification with a resolution approaching that of the ultra-violet microscope (Cosslett & Nixon, 1951, 1952a, b, 1953). The fine beam of electrons was focused by means of electro-magnetic lenses onto a thin foil target which also acted as the end window of the electron beam column and from which X-rays were emitted.

One of the major disadvantages of this machine is that under conditions of increased electron beam intensity the foil target overheats and perforates. This limitation has been overcome through modifications by Ely (1957) to produce a high definition machine for ultimate use in medical radiography. The foil target is replaced by a solid oil or water cooled target which does not act as the end window of the vacuum tube. The rod lies over the pole piece of the objective lens in a position which allows the electron beam to strike the side of the rod at a slight angle. The X-rays are emitted at right angles to the electron beam through a thin aluminium or beryllium window (Figs 2.1., 2.2.).

The focal spot size has been estimated to be about 10-20 μm. in diameter, the spot itself is eliptical instead of circular because of the characteristics of the electromagnetic focussing system. And therefore high resolution microradiography (0.5 μm) suffers at the expense of high kilovoltage projection microradiography.

2.4.3. Theoretical considerations.

2.4.3.1. Advantages of projection microradiography.

Primary magnification of the object in the photographic emulsion is one of the principal advantages of the technique. Under the conditions of a very small X-ray source the magnification (M) is given by:

$$M = \frac{I}{O} = \frac{a}{b} = \frac{b + c}{c} \qquad -(2-1)$$

Where (O) is the lateral separation between two points in the specimen at a specimen distance (b) from the source, (I) is the distance between the corresponding points in the plane of the emulsion at a distance (a) from the source and (c) from the specimen (Fig 2.3.).

As a result of the primary magnification, the need to use fine-grained emulsions is not as critical as in contact microradiography.

Areas of special interest in a specimen can be selected before the exposure is made by viewing the magnified image on a fluorescent screen.

2.4.3.2. Limitations of projection microradiography.

The geometric distortion which sets in with divergent X-rays arising from a point source limits the field of view and distorts the image in comparison with orthogonal projections obtained with parallel X-rays. Bellman (1953) states that the lateral displacement of the image due to this distortion (D) is given by:

$$D = \frac{c}{b} \cdot \frac{1}{2} W \qquad -(2-2)$$

where (c) is the object to image distance, (b) the source to object distance and (W) the width of the object (Fig 2.3.). The lateral displacement of the image depends upon the distance from the object to the photographic emulsion and upon the displacement of the structure from the beam.

Nixon (1961) later stated that the useful cone of X-rays fills an angle of about 60°. The diameter (F) of the field of view is then

$$F \doteq 2b \tan (60^{\circ}/2) \doteq b \qquad -(2-3)$$

Where (b) is the source to object distance (Fig 2.3.) i.e. the field of view is approximately equal to the distance from the window to the object.

Limitations in resolution are twofold, that of penumbra and diffraction.

The intensity of the image and the limit of the detail resolvable in it are primarily determined by the geometric relations of the X-ray source (s), object (0) and image (I). The definition in the image is described in terms of the penumbra width (p) which is related to the diameter of the source (s) and the specimen spacings (b) and (c) (Fig 2.3.).

$$p = s (a - b) / a \qquad -(2 - 4)$$

Where (a) is the source to image distance. The theoretical resolution is given by Hall et al (1972) as effectively the size of the source.

The image may also be blurred by Fresnel diffraction, which results in edge effects which may obscure detail and limit the resolving power of the X-ray microscope. Cosslett and Nixon (1960) show, that under condition of projection radiography the limit is defined by specimen thickness and position.

Hobdell (1970) in examining the Fresnel effect with a solid target system, instead of the transmission target used by Cosslett & Nixon, suggests that the number of fringes is lower in the former. But because of the elliptically focussed electron beam on the solid target (Ely, 1957) the fringe is not symmetrical in the horizontal and vertical planes.

2.4.3.3. Optimum conditions for projection microradiography.

The limitations of having to operate within a useful cone of X-rays of 60° and with specimens as large as cat skulls necessitated operating at a moderately large source to object distance.

It was found that optimum conditions of magnification and contrast could be obtained at a primary magnification of X2 as has been advocated by Le Poole & Ong (1957) and evaluated by Cossett (1957) who also put forward a number of reservations on the claims of Le Poole & Ong.

With a magnification of two, the cat skull midway between the source and the emulsion, the penumbra (p) is equal to the source size (s) from equation (2 - 4) and according to Cosslett (1957) the resolving power (d) is then one-half of the value of (s). From equation (2-1) the magnification (M) is given as M = (b+c)/b and by geometry

$$p = s \cdot \frac{c}{b} = s\ (M - 1) \qquad (2\text{-}5)$$

Assuming that $p \gg g$, where (g) is the grain size of the photographic emulsion, the resolution referred to the object plane is

$$d = g/M = s \cdot g/s+g \qquad (2\text{-}6)$$

$$\text{therefore, } d = \tfrac{1}{2}\, s = \tfrac{1}{2}\, g \qquad (2\text{-}7)$$

The source size for the modified Cosslett & Nixon

machine has been estimated at approximately 10 μm diameter. The penumbra width can be calculated from equation (2-4) and is equal to the size of the source. The photographic film used in the present study was 'Dupont's' fine-grain industrial film NDT 55 with a grain size of less than 1 μm. (Manufacturers information). As the grain size is smaller than the source, from equation (2-14), the resolution (d) will tend to approach 5 μm.

2.4.4. X-ray stereoscopy.

The depth of focus obtained in projection microradiography is virtually unlimited and for this reason is outstanding as a method of ascertaining non-destructively the relative positions of the structural elements of an optically opaque object.

The increase in the geometric blurring with separation of the object planes from the emulsion emphasises the importance of structural displacements and variations in magnification which occur when a thick specimen is placed close to the point source. Cosslett & Nixon (1960) conclude that this fact may be of value in stereoscopic viewing since a perspective as in normal vision is produced.

A more detailed description of X-ray stereoscopy and its limitations has been described by Bellman (1953) and Hobdell (1970), a comprehensive review of three dimensional techniques has been given by Latham (1966, 1968).

2.5. Method of preparation of projection radiographs.

Stereo - projection radiographs were prepared at a tilt angle of 10^{o} of the lateral and ventro - dorsal views of all the cranial material and non-stereo radiographs of antero-posterior views of the serial coronal sections of the skulls A to E, using the modified Intercol X-ray microscope (XX 50). The skulls were

placed in a stereotaxic frame which ensured a standardised position. The Intercol was set to operate at 50 KV, a tube current from 0.5 to 1 mA, with a tungsten target. The radiographs were recorded on Cronex NDT 55 fine-grain industrial X-ray film. These were developed in Phenisol at approximately 69°F. for four minutes, the slight increase in development time enhances the photographic contrast.

The stereopairs obtained were examined in a Hilger and Watts folding mirror stereoscope.

2.6.1. Examination of the structural organisation of bone, and statement of aims.

The advantages of radiography as a non-destructive method of examining bone was well established and the greater power of resolution of the projection X-ray microscope has been described in the earlier sections of this chapter. It nonetheless remains that the limitations of this technique are that (1) the structures recorded in the emulsion are not defined, they appear as shadow images; and (2) according to the workers on the trajectorial organisation of bone the structures within certain areas course in nearly uniform straight and/or curved lines and are intersected at right angles by tension bearing structures.

It is therefore necessary to relate the radiographic images to the actual osseous structures in the skull and assess their relative orientation to one another.

Two techniques were used in which (1) serial coronal sections were prepared from the right halves of sagittally sectioned cat skulls, (Figs 3.3. and 3.4.), and (2) the cortical bone was dissected off the left halves of the same skulls (Figs 3.5 and 3.6.).

2.6.1. Examination of the coronal sections.

One ground and polished coronal section was chosen from different areas in the five cat skulls; these were the jugal (skull A), the palate (skull B), the perpendicular plate of the maxilla (skull C), the horizontal plate of the maxilla (skull D) and the supra-orbital region of the frontal (Skull E). The sections were viewed under a binocular dissecting microscope with incident lighting, and with a micrometer graticule fitted into one of the eye pieces. The medial and ventral margins of the bone section were used as base lines. The X and Y co-ordinates were measured by means of the graticule for all the histological structures visible on the section. The diameter of each structure was measured and recorded. Photographs were then taken of the sections with a single lens reflex and attached bellows unit.

Detailed histological confirmation of the structures recorded were obtained by viewing the specimen with the Zeis Ultraphot III, using light and dark back-ground reflected lighting conditions (Figs 3.1., 3.2.). The position of the structures were established by means of the X and Y co-ordinates. Photographic records were made of some of the histological structures using the Ultraphot photographic apparatus.

The identification of the structures as radiographic images was initially ascertained from the antero-posterior radiographs of the bone slabs. The radiographs were set up under the binocular microscope in an identical manner to that used in examining the coronal sections with the lighting altered so as to be transmitted through the radiograph. The position of the structures was established on the radiograph by means of the X and Y co-ordinates.

From a mensural assessment of the thickness of the sections, the position of each slab was demarcated on one of the stereopair radiographs of the whole skull. The position of the section was marked out with two cotton threads drawn across the radiograph and afixed with sellotape. The stereopair radiographs were examined in the stereoscope with the binocular viewer. A graticule was placed on the radiograph alongside the cotton thread marking the position of the surface of the serial section previously examined (Figs 3.3., 3.4.).

The position and dimensions of each shadow image was recorded from the same base lines as that used in the examination of the coronal sections. These measurements were compared with the observations made from the coronal sections and their antero-posterior radiographs. This provided (1) the confirmation that the structures recorded in the projection radiographs of the whole skull were the same as those observed in the coronal sections, and (2) the minimum size of the different structures that were recorded in the projection radiographs of the skull.

2.6.2. Examination of the dissected bone.

The left sides of the cat skulls were treated with industrial bleach ($Ca(OCl)_2$) to remove a large proportion of the organic content of the bone. This procedure also rendered the structural organisation more readily visible under normal lighting conditions (Figs 3.5., 3.6.).

The undecalcified bone was set up under a binocular microscope and the bone gradually pared down using a dental drill and bit, until the underlying structures were exposed. The dissected regions were then photographed (Figs 3.5., 3.6.). The longitudinal correspondence between the structures in the dissected bone and projection radiographs of the left half of

the skulls was established by a comparative examination of the angle of orientation of the osseous structures and their radiographic images. For the different areas in each of the skull, the position of the base line on the photograph of the dissected bone and the radiograph was established by precise comparative mensural assessment between points of reference on the whole skull, the area of bone photographed and the radiograph. The base line was drawn on the photographs and radiographs (Figs 3.5., 3.6.), the 0^{o} - 180^{o} line of the graticule for measuring angles was aligned with the base line and viewed under a low magnification travelling microscope. The protractor graticule measured the orientation, to within $\pm 5^{o}$, of the trabeculae and large vascular canals present. Mensural accuracy was limited by the method employed and by the effect of the angle of tilt in the stereopair radiographs.

2.6.3. Limitations in the examination of the coronal sections and dissected bone.

A limitation common to both methods was that the structures could only be examined in two dimensions and the superimposition of the overlying structures masked the underlying organisation. The method of dissecting the bone had a number of further disadvantages: (1) the preparation in bleach damaged the finer structures of the bone; (2) the paring down of the bone can also destroy structures when care is not taken; (3) the technique is tedious and time consuming.

The advantages of the large depth of focus in stereo-projection radiography overcomes many of the limitations of these two methods in providing a three dimensional image of the organisation of the cranial bones. There was, however, a reduction in the detail and number of structures recorded in

the radiographs with increasing depth of bone and number of superimposed structures. A more detailed examination of this phenomenon was carried out.

2.6.4. <u>An assessment of the effect of the depth of bone and superimposition on the number of structures recorded in the projection radiographs</u>.

The apparatus used for this examination was the same as that used in the study of the serial coronal sections of the skulls.

The coronal sections selected were those immediately posterior to the first molar comprising the thick cortical and cancellous bone of the jugal and part of the supra-orbital process of the frontal. On the basis of the results obtained in section (3.2.1.) only those structures larger than the minimum size recorded in the projection radiographs were noted. A graticule was placed along the norma lateralis of the jugal and the norma verticalis of the frontal, The sections were viewed under the binocular microscope and the number of large vascular canals and trabeculae per half millimeter were recorded as well as the depth of bone at each division. This gave a count of the number of structures and their type for the different depths of bone.

The position of the coronal sections on the radiograph was demarcated by cotton thread drawn across one of the pair of stereo-projection radiographs and affixed with cellotape. Taking into account the proportional increase in magnification of the projection radiographs, the transects were divided into the equivalent half millimeter divisions. The number and type of structure were recorded per division starting at the same base line as that of the coronal section. The difference in the

numbers of large vascular canals and trabeculae recorded on the coronal sections and in the projection radiographs were expressed in terms of the percentage number of canals or trabeculae absent. Histograms were drawn up of the relationship of the numbers of large vascular canals and trabeculae absent to (1) the increase in depth of bone, and (2) the increase in the number of underlying structures. The disadvantages in the method of using a percentage as a means of indicating the presence or absence of structures was that in the regions where few structures were present the percentage of structures absent would appear greater than in reality.

2.7. Determination of the structural organisation of the skull bones.

The description of the cranial structural organisation was based on a preliminary examination of the projection radiographs in order to ascertain the different grades of the structural organisation, and the relative orders of frequency present in the skull of the trabeculae and large vascular canals per unit millimeter.

The grades of organisation were determined by assessing the number of groups of structures, of either large canals or trabeculae, orientated in any one particular direction. Photographs were taken of regions of the skull representative of the different grades recognised on the dissected skulls and of the coronal sections in the same regions (Figs 3.9., 3.10., 3.11)

The determination of the average frequency per millimeter was obtained by a count of the number of structures crossing a line drawn with a fine pointed 'Chinagraph' pencil on the radiograph.

2.7.1. Consistency of alignment between large vascular canals and trabeculae.

The difference in the organisation between cancellous and compact bone required a statistical examination of the probability that these different structures were similarly aligned in an area where they gave that appearance. The area selected was that above the canine as it was the most readily visible and apparently consistent in organisation. The examination was carried out on ten cat skulls.

On one of the stereopair radiographs two transects were drawn parallel to each other and to the palatal process of the maxilla, across the zones of cancellous and compact bone respectively (Fig 2.4.a). The stereopair radiographs were placed under the stereoscope and the graticule for measuring angles placed on the radiograph not marked with the transect lines. When viewing through the stereoscope the graticule was moved along the line of the transect and the angle and the number of structures per millimeter recorded. The probability "P" that the structural orientation was dissimilar within the cancellous and compact bone was calculated by applying the Mann-Whitney U test (Siegel, 1956). The advantages of this test were that it is the most powerful of the nonparametric tests and that the method of algebraic ranking of the scores rendered the test independent of any anatomical base line.

The repeatability of this method of counting was established by recording ten times the readings from one transect on a skull chosen at random from the sample of ten cats. The probability "P" that there was a significant difference in the orientation of the structures recorded was computed using

the Mann-Whitney U test. The percentage error of measurement was obtained from the frequency of structures recorded at each count. The recordings were spread over a period of three weeks in order to avoid similarity of results as a result of memory recall.

2.7.2. Description of the structural organisation of the cat skulls.

The lateral and dorso-ventral stereo projection radiographs were examined in the folding mirror stereoscope. Each cranial element was subdivided into a number of regions corresponding to changes in the grade and frequency of organisation (Fig 2.5.). The frequency, ~~and~~ the mean and standard deviation of the angle of orientation of the structures in each region were ascertained as previously described and tabulated along with the grades of organisation. This was repeated for the different regions in the five cat skulls.

2.7.3. Statistical analysis of the consistency of the structural organisation.

Statistical confirmation that the cranial structural patterns described were consistent within the five cats and for a total sample of ten skulls was established by measuring the angle of the structures of the cancellous and compact bone bisecting transects drawn at four different regions on the lateral projection radiographs of the skulls.

The base line (A in fig 2.4.b.) for the transects was taken as the image cast by the palatal process of the maxilla between the canine and the fourth premolar. From the antero-medial point of the nasal bone a reference line (B) was projected posteriorly and parallel to the base line and along which transects (2) and (4) were located. Two further reference lines were drawn in order to define transects (1) and (3). Both

lines were at right angles to the base line, the first (C) bisected the skull immediately posterior to the apex of the canine and the second (D) posterior to the distal surface of the first molar and parallel to (C).

Transects (1) to (4) were as follows:

Transect (1): extended along the reference line (C) from a point immediately posterior to the apex of the canine, dorsally to the ventral margin of the nasal bone.

Transect (2): started from the vertical projection of the posterior margin of the lacrimal foramen onto the reference line (B), and posteriorly along that line to the point of intersection with the image cast by the zygomatic arch.

Transect (3): extended from the horizontal projection of the antero-ventral surface of the temporal component of the zygoma onto the reference line (C) and along the latter to the dorsal surface of the jugal.

Transect (4): extended for 5 mm on either side of the intersection between the reference line (B) and the orbito-temporal line.

The orientation of the trabeculae and large canals bisecting the transects was recorded in the manner described previously. Rose histograms were drawn up for the percentage number of structures in each 10° angle division. The Mann-Whitney U test was used to establish the consistency of structural orientation between the ten cat skulls for transects (1) to (4) and between transects (1) to (4) for one cat skull selected at random.

2.7.4. Interdental and interradicular trabecular frequency.

Walkoff (1902), D'Arcy Thompson (1942), Scott and Symons (1964) and Johnson (1966) have stated that the density of trabeculae within a dental septum is proportional to the relative

loading of each tooth.

The lateral stereo-radiographs of the ten skulls and fifteen mandibles were examined to determine the number of trabeculae per square millimeter within the interdental and interradicular septae. The following method was devised, which was found later to be a modification of a method employed by Moss, et al (1967) to compare the alveolar process trabecular bone density between American whites and negroes. Measurements were carried out on the alveolar process posterior to the third incisor in the maxilla and the canine in the mandible (Fig 2.6.a). The base line for each septum was defined as a line drawn tangential to the apices of the roots of the teeth and parallel to the alveolar margin (Fig 2.6.b). In those instances where the roots were of unequal length, the apex of the shorter root was taken for the base line. Each septum was then divided by three equally spaced horizontal and vertical lines. A measure of the frequency of the vertical trabeculae was obtained by counting the number of trabecular bars that crossed the horizontal lines. The process was repeated for the vertical lines thus giving a measure of the number of horizontal trabeculae. The two dimensional mean was obtained by summating the counts from the horizontal and vertical lines. The area of each septum was obtained by counting on a graticule, the number of millimeter squares enclosed by the area of the septum and dividing the figure by the magnification of the radiograph.

For each septum of the maxilla and mandible, the frequency of horizontal and vertical trabeculae per square millimeter and the two dimensional mean per square millimeter was calculated. An Olivetti desk computer was used to compute

the mean, variance, standard deviation and standard error for each dental septum from formulae given in Sokal and Rohlf, (1969). The null hypothesis was set up and the t test (Sokal & Rohlf, 1969) was applied to compare the horizontal vertical and two dimensional frequency of trabeculae between all the septae in the maxilla and then in the mandible. The results indicated the relationships in the frequency of horizontal and vertical trabeculae and the two dimensional mean of trabeculae between the different septae along the length of the alveolar process of the maxilla and mandible.

CHAPTER 3

RESULTS OF THE EXAMINATION OF THE STRUCTURAL ORGANISATION OF THE CAT SKULL BONES.

CHAPTER 3

RESULTS OF THE EXAMINATION OF THE STRUCTURAL ORGANISATION OF OF CAT SKULL BONES

3.1. Histology of the cat skull bone.

This examination established the identity at the histological level of the structures visible in the projection radiographs.

Bone is a complex mineralised connective tissue, comprising cells separated by a variable amount of intercellular matrix which has been formed by the cells. The matrix consists of an intricate system of collagen fibres embedded in an amorphous ground substance consisting of protein polysaccharides, and of crystals of calcium hydroxyapatite.

From the polished ground sections of the cat skulls the compact bone was identified as that of a primary vascular bone (Enlow, 1968) (Fig 3.1). Within the compact bone the lacunae are relatively numerous and are arranged in a random fashion. The bone was composed primarily of circumferential lamellae and within certain areas of interstitial lamellae.

Two categories of vascular canals were identified (a) those of the primary and secondary osteones and (b) the large intra-osseus vascular canals. Of the canals mentioned in category (a) those of the primary osteones were observed to be the most frequent of the two types of osteone, and they exhibited a close conformity with the surrounding compacta. The mean and standard deviation of the diameter of the canals was 38 ± 13 μm.

The large intra-osseus vascular canals is the term employed herein for narrow medullary spaces, resorptive spaces and immature osteones. The canals are bounded by a number of

concentric lamellae and restricted to the inner medulla of regions of thick compact bone. The mean and standard deviation of the diameter of the canals is 0.35 ± 0.36 mm. In areas of thin compact bone, such as the orbital plate of the frontal, which is composed entirely of narrow circumferential lamellae, the large vascular canals are absent or very infrequent as are the primary osteones.

The histology of the course cancellous organisation of the membrane bone is illustrated in Fig 3.2. It comprises a network of interconnecting trabeculae with a lamellar organisation similar to interstitial bone.

The stained histological sections confirmed the organisation seen in the polished ground sections and further showed that the compacta was a fine fibred lamellate structure with an extensive canalicular system connecting the lacunae and vascular canals (Figs 3.1., 3.2.).

This section established the histology of the principal osseous structures, i.e., the trabeculae of the spongiosa and the type of canal present in the compacta. The following sections show that the structures recorded in the projection radiographs were the trabeculae and large vascular canals, and that the osteones and lacunae were not recorded.

3.2.1. <u>Examination of the structural organisation of the skull bones: coronal sections.</u>

The determination of the structural organisation of bone from coronal sections provided a method of assessing the changes in organisation along the transverse section of cat skulls. The direct comparison between the structures seen in the coronal sections and their radiographic image enabled the nature of the latter to be established. Figures 3.3. and 3.4.

illustrate two methods used to relate the structures seen in the coronal section with those of the radiograph. In Fig 3.3. (top left) is the antero-posterior photograph of the coronal section through the region of the frontal process of the maxilla containing the apex of the canine, (x) indicated the latter's supero-lateral margin. Superior to the root of the canines are a number of structural features lettered (b) to (f): (b) small trabecula situated within a small vascular space, (c) trabecula, (d) small vascular space, (e) trabecula and (f) a vascular space with a number of trabeculae inferiorly. The superior part of the frontal process of the maxilla comprises compact bone containing very small vascular canals. A few of these canals are seen above structure (b) in the ground polished section (Fig 3.3., bottom left), in the region delineated by the quadrangle (A) on the coronal section. The clarity of detail of the structures described above is reduced in the antero-posterior radiograph of the coronal section (Fig 3.3. top right). This is due to the superimposition in the radiographic plate of the underlying structures in the coronal section as well as the limitations of the preparation of the photographic plate from the projection radiograph. This last disadvantage also applies to the latero-medial projection radiograph of the anterior region of the skull (Fig 3.3. bottom right). The parallel vertical lines indicate the position of the anterior and posterior surfaces of the coronal section. In the latero-medial radiograph (Fig 3.3. bottom right) the position of the quadrangle (A) is indicated by the broken line, the positions of the structures (b) to (f) are represented by a continuous line. With this method of examining bone it is possible to relate the histological organisation and position of a structure within

the bone to its position in the stereo-projection radiograph of the whole skull.

Figure 3.4 illustrates the position of large vascular canal(s) (a) on the anterior surface of the coronal section (A and B Fig 3.4) and (b) to (f) on the posterior surface of the section (C and D Fig 3.4) in the frontal process of the maxilla of skull (C). The position and appearance of these canals is seen in the latero-medial and dorso-ventral projection radiographs (1 and 2, Fig 3.4).

The comparative mensural examination of the relative sizes of the smallest vascular canals recorded was 0.06 mm. and for the smallest trabeculae 0.14 mm.

3.2.2. Examination of the structural organisation of the skull bones: dissected bone.

This method of examining the bone provided a longitudinal assessment of the arrangement of structure in the cranial bones. Five different areas are illustrated (Figs 3.5 and 3.6), one from each of the cat skulls examined. The photographs of the dissected regions of the skulls are not aligned identically to the same area in the radiograph because of the proximity of the camera lens attached to the bellows unit of the camera resulted in recording a restricted field of view of the skull. The position of the structures, i.e. trabeculae or large vascular canals, whose angle of orientation relative to the base line was measured, are indicated by arrow points in both the photographs and radiographs.

Skull A: figure 3.5.a illustrates the dorsal surface of the temporal component of the zygomatic arch, superior to the glenoid fossa. The orientation of the trabeculae indicated in the photographs is given as follows, from left to right:

Dissected Bone	Projection Radiograph
135°	140°
140°	140°
140°	140°
110°	120°
140°	140°
140°	140°

Skull B: figure 3.5.b illustrates the lateral surface of the temporal component of the zygomatic arch. The orientation of the trabeculae is as follows, from above down:

Dissected Bone	Projection Radiograph
90°	90°
90°	100°
90°	90°
80°	80°
90°	95°
100°	100°

Skull C: figure 3.5.c shows the posterior region of the pterygoid process of the palatine bone. Only two vascular canals were revealed after dissecting off the cortical bone. Their position was recorded photographically using transmitted illumination. The orientation of the canals, which appear in the dissected bone as light bars, is from above down:

Dissected Bone	Projection Radiograph
140°	140°
100°	100°

Skull D: figure 3.6.a illustrates the inferior margin of the orbital plate of the frontal bone. The orientation of the large vascular canals from above down is:

Dissected Bone	Projection Radiograph
80°	80°
85°	85°
90°	90°
100°	95°
100°	95°

Skull E: figure 3.6.b illustrates the squamous part of the temporal bone. The orientation of the trabeculae from above down is:

Dissected Bone	Projection Radiograph
0°	5°
10°	10°
150°	160°

With this method of examining bone the correspondence can be established between the orientation of the trabeculae and large vascular canals in the dissected whole bone and their radiographic appearance.

3.3. <u>The assessment of the effects of the depth of bone and superimposition on the number of structures recorded in the projection radiographs</u>.

In general the cranial bones of the cat are not very thick, the average is approximately 2 mm. This is confirmed by the result that 80% of trabeculae recorded from the coronal sections were within a bone thickness from 0 to 2.5 mm., and 75% of all vascular canals within a bone thickness up to 2 mm.

The results of the investigation into the percentage number of trabeculae and canals not detectable in the radiographs due to the increasing thickness of bone is presented in the histograms in figure 3.7.a. The histogram indicates that from a bone thickness of 3 mm. and over the number of trabeculae not

detected increased markedly. For the large vascular canals, over 50% were no longer detected above a bone thickness of 1.5. mm.

The results were rearranged to give an indication of the effect of superimposition of structures upon the number of trabeculae or canals detected. Although the sample number is not large enough to provide an accurate assessment, the histograms in figure 3.7.b. show a gradual decrease in the number of trabeculae detected with increasing superimposition. Whereas approximately 50% of the vascular canals are not recorded as a result of the superimposition of a single structure. This marked decrease in the detection of vascular canals as a result of superimposition of structures is also responsible for the marked drop in canals recorded with increased depth of bone (Fig 3.7.a.).

3.4. <u>The structural organisation of bone</u>.

Three grades of structural organisation i.e. trabeculae and large vascular canals, were distinguished from the examination of the stereo-projection radiographs of the cat skulls (Figs 3.8.a. and b).

Grade I: The structures are orientated in the same principal direction. In general the alignment of the cross-connecting structure is close to that of the principal structures and within a mean angular standard deviation of $\pm$ 5° 15' (Fig 3.9.)

Grade II: The structures are orientated in two principal directions and can be regarded as a region in which two grade I of different orientation are present (Fig 3.10.).

Grade III: The structures are orientated in three or more principal directions. In the majority of the latter cases, the structural organisation demonstrates no clear pattern of

orientation as seen in Fig 3.11. It was not possible to photograph structures orientated in three principal directions as in general only grade II structures were visible in any one plane.

The assessments of the frequency per millimetre of the number of structures crossing four transects drawn on the cat skulls (Fig 2.4.b) are presented as the solid columns in the histograms of figure 3.12. The frequency of structures present per millimetre in a skull varied with the individual. As the structural frequency along transect 2 was the lowest compared to the rest of the skull, it was decided to use that value as the common denominator on which the frequencies of the structures for the rest of the skull were based (open columns in figure 3.12.). This provided a basis whereby the structural frequencies within the different skulls could be compared.

3.5. <u>The consistency of alignment between the large vascular canals and trabeculae</u>.

The null hypothesis was set up to establish whether there was a significant difference between the orientation of the large vascular canals and trabeculae with the significance level set at 0.02.

The results from the ten cats gave a probability of $P \geqslant 0.1$ for a two-tailed test. The data provided evidence which justified the rejection of the null hypothesis. The conclusion is that the large vascular canals and trabeculae are similarly aligned.

The consistency of this method of mensural examination was tested by setting up the null hypothesis to test whether there was a significant difference in the orientation of the

structures recorded from the same transect in the ten cat skulls. The significance level was set at 0.05.

The results gave a probability P which approached 1.0 for a two tailed test. The data justify the rejection of the null hypothesis. The conclusion drawn is that within successive readings there is no significant difference in the orientation of the structures recorded.

From an examination of the number of structures recorded at each of the ten counts, the percentage error of measurement was 4%.

3.6. Description of the structural organisation of the cat skulls.

A brief description of the results of the detailed examination of the latero-medial and dorso-ventral radiographs is given below. The grade, orientation and frequency of structures in the different regions of the skull are recorded in Table 3.1. and illustrated in figures 3.13., 3.14. and 3.15. The numbers associated with the different areas of the skull refer to the same areas depicted in figure 2.5.

3.6.1. Skull viewed in norma lateralis.

1. Nasal bone. The perpendicular plate of the nasal bone is thin and exhibits very few structures. The supero-medial surface is thicker and comprises a greater number of structures. A few trabeculae are present at the anterior tip of the bone and are arranged at right angles to the dorsal surface.

2. Premaxilla, alveolar region. Compact bone is present at the anterior and ventral margins. Trabeculae are orientated horizontally and vertically.

3. Premaxilla, nasal process. Structures tend to be more frequent at the posterior margin of the bone.

4. Maxilla, alveolar region. Grade II organisation was seen in two skulls at the antero-dorsal surface of the canine and postero-dorsally to the apex of the canine, where a few trabeculae were orientated at right angles to the principal trabeculae. The infra-jugal region consists of compact bone as well as several large trabeculae passing vertically. The jugal process of the maxilla is comprised of compact bone.

5. Maxilla, frontal process. The central region of the process comprises fewer large canals than the anterior and posterior margins. The trabeculae and canals of the circumorbital bar or posterior margin are relatively more numerous, they are continuous dorsally with those of the maxillary process of the frontal and inferio-laterally with those of the jugal.

6. Frontal, anterior region or pars nasalis. The maxillary process comprises a large number of trabeculae and canals that are contiguous ventrally with those of the maxilla and postero-dorsally with the structures of the rest of the norma verticalis of the frontal. The region posterior to the maxillary incisure comprises slightly fewer structures than the maxillary process, a number of which are contiguous with those of the frontal process of the maxilla. A trend towards grade II was observed in four of the skulls in which cross-connecting structures were present in the anterior region. In the medial part of the pars nasalis canals are more numerous than trabeculae.

7. Frontal, post-orbital process. The canals and trabeculae at the antero-dorsal region are concentrated at the lateral margin and extend posteriorly. A grade II organisation occurs in the posterior part of the central area dorsal to the tip of the process, the vertically orientated structures course towards the posterior part of the process. The tip of the process consists

of thick trabeculae and compact bone. Four of the skulls exhibited a grade II organisation at the anterior margin of the process.

8. Lacrimal bone; 9. Frontal, anterior part of orbital plate. These two areas are comprised of thin cortical bone containing a few large vascular canals with no recognisable pattern of organisation.

10. Frontal, posterior part of the orbital plate. The anterior region, immediately posterior to the ethmoid bone and anterior to the frontal sinus exhibits the same structural organisation at the anterior part of the orbital plate (9). In the posterior part of the orbital plate, the trabeculae and canals pass from the pars temporalis of the frontal inferiorly along the posterior margin of the frontal sinus. They are joined at the inferior margin of the sinus, by a number of structures from the anterior surface of the sinus. The region immediately inferior to the frontal sinus is demarcated anteriorly and posteriorly by areas of grade III organisation and a frequency of 1. In the region inferior to the sinus, the trabeculae are replaced by canals which continue postero-inferiorly to the fronto-presphenoid suture and the sutural junction between the temporal, frontal and alisphenoid.

11. Frontal, orbito-temporal ridge. At the superior part of the orbito-temporal ridge, medial to the post orbital process of the frontal, the structures are arranged in a fan like manner which narrows inferiorly towards the orbito-temporal ridge. The grade III organisation resulted from the overlap of the structures from the anterior and posterior regions of the bone. Anterior to the orbito-temporal ridge is a narrow zone of thin cortical bone with few large canals. The trabeculae and

canals within the orbito-temporal ridge pass initially antero-inferiorly from the region medial to the post-orbital process, curve posteriorly and continue inferiorly to the sutural junction between the frontal, temporal and alisphenoid where the grade I organisation changes to grade III.

12. Frontal, pars temporalis. This comprises a central zone of thin cortical bone of few or no structures which when present have an organisation of grade III. The trabeculae and canals course around this zone and are bounded posteriorly by the parietal and temporal bones. In the dorsal region the trabeculae and canals exhibit a grade III organisation of which a number of trabeculae pass postero-inferiorly from the superior region of the post-orbital process, through the pars temporalis of the frontal into the parietal bone. At the inferior region of the pars temporalis a number of trabeculae and canals run parallel to those of the orbito-temporal ridge and are cross-connected with structures extending towards the fronto-temporal suture.

13. Parietal bone. The large canals in the antero-dorsal region of the parietal are contiguous with the structures of the frontal bone. The rest of the parietal, apart from the tentorium osseum, exhibits no clear structural organisation common to all the cat skulls. However, towards the ventral margin of the bone the structures tend to run horizontally and approximately parallel to the parieto-temporal suture. In the posterior region a large number of the structures course antero-inferiorly.

14. Parietal, tentorium osseum. A grade II structural organisation occurs at the junction between the antero-medial and infero-lateral laminae of the tentorium which grades into I in the infero-lateral lamina.

15. Temporal, squama. Two areas with a structural organisation of III and unit frequency are situated on either side of the groove for the middle meningeal vessels. In the latter region and those of the anterior, dorsal and posterior margins, the bone is thick and exhibits a tendency towards a grade III organisation except in that part immediately dorsal to the junction with the zygoma where grade II is present.

16. Jugal, orbital margin. The trabeculae and large canals in the lacrimal process are contiguous with those of the circumorbital bar of the maxilla. Inferiorly the structures pass laterally and then postero-dorsally along the orbital margin. The junction at which the structures alter their orientation is an area of grade III organisation where a number of the trabeculae at the anterior margin of the jugal extend approximately vertically to become contiguous with those of the lacrimal process. Perpendicular to the near vertical trabeculae of the infero-anterior region are a number of relatively large trabeculae orientated medio-laterally and aligned postero-dorsally.

17. Jugal, orbital process. At the anterior margin, the structures are aligned parallel to the border. In the central region the general pattern of the structures is that they radiate out to the anterior, posterior margins and dorsal tip of the process. In the latter area there are numerous small cross-connecting trabeculae. A number of trabeculae pass medio-laterally in the central area. At the posterior margin the general pattern is similar to that of the anterior margin.

18. Jugal, antero-central region and masseteric margin. In the anterior part of the central region the structures show a grade II organisation with their orientation approximately at right angles to one another. Posteriorly the vertical

structures are replaced by trabeculae orientated medio-laterally within the large vascular space of the jugal.

The masseteric margin consists of compact bone in which the large vascular canals parallel the inferior margin of the jugal with the exception of three of the skulls where a few structures are orientated approximately vertically at the anterior region of the masseteric margin.

19. Temporal, zygoma. The structures extend posteriorly following the outline of the bone.

20. Sphenoid, body and alar major. The temporal and tentorial processes of the sphenoid appear as dense compact bone within which the structures appear to extend into the body of the sphenoid. The latter generally consists of compact bone, the few trabeculae that are visible are orientated in a general vertical direction. The alar major presents a complex structural pattern in which structures contiguous with those of the frontal, temporal and parietal course inferiorly through the alisphenoid into the body of the sphenoid bone. Within this arrangement there are a number of structures set at right angles to those passing approximately vertically.

21. Presphenoid. The structures at the superior margin of the bone extend posteriorly to unite with those structures coursing inferiorly, posterior to the optic foramen, into the alisphenoid. The rest of the perpendicular plate of the presphenoid has a structural frequency of one and less, and a grade III organisation.

The body of the presphenoid comprises either compact bone or that of a complex structural organisation.

22. Pterygoid plate. The lateral lamina comprises a few canals directed postero-dorsally. The structures in the process of the medial lamina follow the outline of the bone and cross-

connect within the tip of the process. Within the posterior margin the structures extend postero-dorsally into the sphenoid process where they are cross-connected by nearly vertical trabeculae closely associated with the body of the sphenoid.

23. Palatine, perpendicular plate. Apart from its inferior margin, the perpendicular plate comprises thin cortical bone with a structural frequency of one and less and a grade III organisation. The large canals within the inferior margin pass posteriorly towards the pterygoid.

3.6.2. Skull viewed in norma ventralis.

24. Premaxilla, palatine process. Trabeculae run medio-laterally at the interpremaxillary suture and in the alveolar process. From the apex of the incisors trabeculae pass posteriorly and postero-dorsally to the dorsal surface of the premaxilla alveolar process.

25. Maxilla, palatine process. In the alveolar region a large number of thick trabeculae pass medio-laterally, in the region posterior to the incisive foramen, and in the lateral margin of the horizontal process of the palatine, trabeculae also run latero-dorsally towards the jugal. The region medial to the third premolar comprises few structures within the thin compact bone.

26. Palatine, horizontal process. Trabeculae and canals run posteriorly, parallel to the lateral margin of the bone, towards the pterygoid plate. The medial region has few structures which show no clear structural organisation.

27. Temporal, root of zygoma superior to the glenoid. At both the anterior and posterior margins the trabeculae and canals parallel the margins of the bone, these are cross-connected by

Text cut off in original

structures extending into the central region of the bone. Proximal to the squama are a number of vertically orientated trabeculae.

Within the glenoid process the structures are orientated dorso-medially; these are cross-connected by trabeculae set at approximately right angles to the former.

3.7. Description of the structural continua of the cat skull.

The description in this section is based on the results presented in chapter three ~~and~~ which are disucssed in sections 8.2 to 8.2.10. of the Discussion.

In describing the structural organisation within the cat skull, the terms 'trajectorial' or 'tract' are omitted as by definition they describe one or a series of continuous uninterrupted lines, a description not applicable to either the large vascular canals or trabeculae. The use of these terms would also suggest a direct association with the principals of the Trajectorial Theory and the descriptions based on the split-line method. For this reason the term 'structural continuum' has been devised in order to describe the continuation of structures with a relatively high frequency within the compacta and spongiosa from one region of the skull to another and, as figure 3.16. illustrates, is independent of the boundaries drawn on the skulls.

Structural continuum of the anterior facial region.

Within the premaxilla the structural continuum (1, Fig 3.16.) extends dorsally to the superior part of the nasal process where it becomes continuous with the continuum of the anterior margin of the frontal process of the maxilla.

Canino-frontal continuum (2, Fig 3.16): Dorsal to the apex of the canine structures extend approximately vertically up the frontal process

of the maxilla into the anterior region of the frontal. The frequency of structures in the continuum is highest at the antero-superior region of the canine apex and along the anterior margin of the frontal process of the maxilla, and from the postero-superior aspect of the canine along the circumorbital bar of the maxilla. From the anterior region of the frontal the structural continuum extends posteriorly within the frontal to the region superior to the post-orbital process, where the continuum divides into three. The lateral branch continues into the tip of the post-orbital process (3, Fig 3.16.). The middle branch passes postero-ventrally, medial to the post-orbital process (4, Fig 3.16.), to unite with the trabeculae of the orbito-temporal line. The medial branch extends posteriorly and slightly ventrally within the temporal component of the frontal, into the anterior region of the parietal bone (5, Fig 3.16.). The three branches are termed the fronto-post-orbital (3), the superior part of the fronto-orbito-temporal (4) and the fronto-parietal continua (5) respectively.

Alveolar-canino-frontal continuum (6, Fig 3.16.): in the alveolar region immediately posterior to the canine, the trabeculae extend from the alveolar margin superiorly to the posterior surface and apex of the canine. Anterior to the infra-orbital foramen the structures run dorsally to unite with the central region of the canino-frontal continuum. Posterior to the infra-orbital foramen the vertical and antero-vertically orientated structures are continuous with those in the anterior margin of the jugal which in turn extend into the canino-frontal continuum.

Alveolar-jugal continuum (7, Fig 3.16.): the postero-dorsally directed structures course from the alveolar region of the premaxilla and maxilla into the central and inferior regions of the jugal. A number of trabeculae in the postero-central region of the jugal are contiguous with those in the temporal component of the zygoma.

Jugo-temporal continuum (8, Fig 3.16.): In the temporal component of the zygoma the structures run posteriorly and then medially to unite with the structural organisation of the temporal squama and the body of the sphenoid. The structures of the glenoid fossa and process are aligned antero-medially and postero-laterally and unite the structures of the horizontal bar with the squama.

Alveolar continuum seen in norma ventralis: At the medial surface of the premaxilla the structural continuum of the alveolar process is contiguous medially with the continuum on the opposite side of the skull (9, Fig 3.16.). The continuum extends laterally to the canine, then posteriorly within the alveolar process to the first molar. The continuum is strengthened by trabeculae approximately perpendicular to the lateral margin of the alveolar process. In the region of the fourth premolar and first molar the latero-medial trabeculae extend laterally to join the alveolar-jugal continuum (7, Fig 3.16.); and medially to form the anterior part of the palato-sphenoid continuum (14, Fig 3.16) running posteriorly in the inferior margin of the vertical process of the palatine bone.

Circumorbital continuum (10, Fig 3.16): The structures of the orbital margin form an almost complete loop extending from the tip of the orbital process of the jugal, anteriorly along the inferior orbital margin, dorsally in the circumorbital bar of

the maxilla, posteriorly in the orbital margin of the frontal and inferiorly into the post-orbital process of the frontal. In the living cat the loop is completed by the thick band of collagen fibres in the post-orbital ligament. As can be seen in figure 3.16. the anterior part of the loop is closely associated with the canino-frontal continuum.

Masseteric continuum (11, Fig 3.16.): The structures associated with the attachment of the masseter muscle course superiorly from the infero-posterior margin of the alveolar process, and posteriorly along the inferior margin of the jugal. At the anterior region of the jugal the horizontal structures are cross-connected by approximately vertical trabeculae coursing towards the lacrimal process of the jugal. These structures are aligned in approximately the same direction as the principal line of action of the masseter muscle. However, the majority of the structures within the masseteric continuum lie normal to the direction of the masseter's muscle fibres.

Structural continua associated with the attachment of the temporalis muscle: These are not as clearly defined as those of the masseter. The complex trabecular organisation at the dorsal surface of the parietal revealed no clear structural pattern associated with the origin of the temporalis. On the other hand, at the base of the temporal squama, the bone comprises vertically orientated structures which are united with those from the zygoma. At the anterior margin of the muscle attachment the fronto-orbito-temporal continuum (12, Fig 3.16.) extends, from the region of the frontal medial to the post-orbital process, inferiorly along the orbito-temporal line of the frontal and alisphenoid bones into the body of the sphenoid. Along the length of the inferior region of the fronto-orbito- temporal

continuum its trabeculae are cross-connected by structures which are contiguous with those in the bordering temporal component of the frontal, the parietal and temporal bones. Passing also into the body of the sphenoid are the structures in the lateral lamina of the tentorium osseum which are probably associated with the transmission of stress from the temporalis.

Fronto-sphenoid continuum (13, Fig 3.16.): This structure is closely associated with that of the fronto-orbito-temporal continuum but differs in that it has a lower structural frequency and is more medial in position. The fronto-sphenoid continuum passes from the superior region of the temporal component of the frontal, antero-inferiorly to the posterior wall of the frontal finus, thence inferiorly to the ventral margin of the sinus and infero-posteriorly in the perpendicular plate of the frontal and presphenoid to unite with the fronto-orbito-temporal continuum in the region of the alisphenoid.

The area of attachment of the pterygoid muscles, unlike those of the masseter and temporalis, comprises an area of thin compact bone devoid of a structural continuum except at its margins. One of these continua is the fronto-sphenoid which borders on the superior and posterior margins of the area of the muscle attachment. Its inferior margin is bordered by the palato-sphenoid continuum (14, Fig 3.16.) in the palatine and pterygoid bones.

3.8. The statistical analysis of the consistency of structural organisation.

The rose histograms representing the results of the investigation into the angle at which the structures bisect the four transects in the ten cat skulls are given in figures 3.17 and 3.18.

The null hypothesis was set up to establish whether there was a significant difference in the orientation of structures bisecting transect (1) between any of the individual cat skulls at a significance level set at 0.02. The test was repeated for transects (2), (3) and (4); the results for transect two are given in table 3.2. The results of the test for transects (1), (3) and (4) gave in all cases a probability $P \geqslant 0.1$, for a two tailed test. The data justified the rejection of the null hypothesis for these three transects. The conclusion is that the orientation of the structures bisecting transects (1), (3) and (4) is similar within the ten cat skulls.

Table 3.3. presents the results of the null hypothesis set up to determine whether there is a significant difference between the orientation of the structures bisecting transects (1), (2), (3) and (4) in skull (F) at a significance level set at 0.02.

3.9. Interdental and inter-radicular trabecular frequency in the maxilla and mandible.

The mean, standard error and the result of the 't' test applied to determine whether there *are* a significant difference in the trabecular frequency between the dental septae at a significance level of 0.05, is given in tables 3.4 and 3.7. for the two dimensional mean of trabeculae per square millimetre in the maxilla and mandible respectively (Fig 3.19); for the frequency of horizontal and vertical trabeculae per square millimetre in the maxilla and mandible refer to tables 3.5, 3.6, 3.8 and 3.9 respectively.

3.10. Summary and conclusion

The comparative examination of the position and orientation of structures seen in the coronal sections and

dissected bone with their appearance in the stereo-projection radiographs established the accuracy of projection radiography as a technique for examining the structural organisation of bones. The histological organisation of trabeculae and large vascular canals was correlated directly with their radiographic appearance in the whole skull.

Within the cranial bones three grades of structural organisation were recognised, which along with the assessment of the frequency and orientation of the structures, established the detailed organisation within the bones. The skull exhibited a high degree of organisation and a structural contiguity between the cranial elements. The statistical analysis confirmed the consistency of the structural orientation within ten cats, as well as established the differences in structural frequency between the dental septae of the maxilla and mandible respectively.

CHAPTER 4

MATERIALS AND METHODS FOR THE IN VITRO DETERMINATION OF THE TRANSMISSION OF BITING FORCES IN THE CAT SKULL.

CHAPTER 4

MATERIAL AND METHODS FOR THE *IN VITRO* DETERMINATION OF THE TRANSMISSION OF BITING FORCES IN THE CAT SKULL.

4.1. Colophonium resin experiments.

4.1.1. Introduction

This chapter describes the materials and methods used to determine the distribution of strain in the skull bones under simulated conditions of biting with the support placed at the canines (phase I) and at the carnassials (Phase II).

Crude attempts have been carried out to stimulate stresses set up during biting, on the 'stresscoated' human mandible (Evans, 1953; Du Brul and Sicker, 1954). To date only one reference has been found describing a method of simulating biting stresses in a skull. Endo (1965) glued canvas sheets representing the massete and temporalis muscles to the superior margin of the muscle insertions on human skulls. The other end of the canvas sheets were attached to a frame and the skull suspended upside down; tensile forces were thus produced in the canvas sheets. Compressive forces were produced by supports in the glenoid fossae and by a loaded lever arm applied to a selected tooth. The fundamental disadvantage of this method was that the forces generated in the canvas sheets applied to the skulls was present only at the inferior margin of the area glued to the cranium, immediately below the superior border of the muscle insertion. This is not representative of the action of the muscle.

Although this apparatus was used for *in vitro* strain gauge measurements, it could have been employed for brittle

lacquer experiments. However, from the diagram of the apparatus (Endo, 1965, Fig 1) the removal of the skull from the frame for examination would have proved difficult without damaging the lacquer coating.

The apparatus designed for use in the present experiments followed the same basic principles. The frame enabled isometric conditions of jaw closure to be simulated during experimentation and was constructed for easy visualisation of the resin coating.

Kuntscher (1934, 1935a, b) as mentioned previously, was the first to use a strain sensitive lacquer on bones. These were coated with melted colophonium resin, his best results being obtained at a coating thickness of one millimeter. After drying, the resin cracked in a direction transverse to that of the tensile strain. Because of its low tensile strength, the colophonium cracked at a stress or load far less than the elastic limit of the bone. The sensitivity of the colophonium is approximately 0.001 inches per inch (Evans, 1957). Cracks also appeared in areas formerly under compression from the tension or stretching of bone as the load was removed. The method gave a fairly good indication of the strain distribution in a bone subject to tensile and compressive loading.

The application of the 'stresscoat' method, initially developed by Forest and Ellis (1940), for the study of the tensile distribution in whole bones has proved successful. The principals of the method are almost identical to that of the colophonium except that the former has a greater sensitivity (0.0005 inches per inch). However, the lacquer's sensitivity is markedly influenced by ambient changes in termperature and humidity.

Colophonium was used in the present experiments as 'stresscoat' was not readily available in this country. The colophonium has the disadvantages of a reduced sensitivity, and as a result of its homogeneity, a tendency for cracks to propagate in their initial direction without regard to the stress conditions in the underlying bone (Evans, 1957). However, it has the advantage that the cracks are readily visible without having to resort to special preparatory procedures as with 'Stresscoat'.

4.1.2. Materials

4.1.2.1. Cat skull material.

Five adult female cat skulls were obtained from the Physiology Department, King's College. They were prepared by having the flesh stripped off the bone and then macerated for the complete removal of soft tissue.

4.1.2.2. Testing frame for the skulls.

The frame (Fig 4.1.a) comprised a wooden platform to which were fixed two vertical brass rods at the tops of which brackets had been attached (A, Fig 4.1.a). The brackets were sheathed in a soft polythene tubing to provide a better surface for articulation with the glenoid cavities of the skull. In front of the vertical rods and in the midline was a T-shaped rod, adjustable in height, and fixed at its base to a metal plate whose distance from the two rods could be varied. The top surface of the T piece was grooved for receiving the canines or carnassials. The whole platform was supported by two planks above the base board. To the latter, a shaft and handle with supports was fixed to the board in the position illustrated in Fig 4.1.b. At the opposite end of the shaft to that of the handle a ratchet and pin was attached. A rectangular sheet of

canvas was bound to the main body of the shaft. Two buttonholes were cut, sewn and reinforced with a metal loop at the corner of the free ends of the canvas sheet. The canvas sheet was connected to the Salter spring balance by a metal rod passing over the hook of the balance and through the buttonholes of the canvas.

4.1.3. Method of attachment of the substitute temporalis and masseter muscles.

Thin canvas sheets were cut to the size of the origins of the left and right temporalis muscles. A strong wire mesh was applied to the surface of each canvas sheet and cut to just under the same size. A loop of the wire mesh was pulled through the canvas sheet at one centimetre intervals. The canvas and wire mesh were moulded to the shape of the cranium and bonded to the latter with 'Araldite' and cured in an oven at 60°C. Lengths of strong cotton thread were passed through each wire loop and tied into position. All the threads from the origin of the temporalis were drawn together along the line of action of the muscle, and twisted together so that they followed the alignment of the muscle fibres. The cord of threads was held together by plaiting the cord with wire.

Over the origin of the masseter muscle, small holes (less than 1 mm) were drilled into the bone approximately 5 millimetres apart. Lengths of cotton thread were passed through the holes and tied into position. The threads were drawn together along the line of action of the muscle, in a manner similar to that of the temporalis and held together by plaiting the cord with wire.

This procedure was repeated for the left and right sides of the five cat skulls. The pterygoid muscles were omitted as

they are weak and appear more phasic than tonic in action.

4.1.4. Procedure for coating and stressing the skulls.

The colophonium resin was melted to just above its melting point in a small and moderately deep enamel developing dish. To avoid undue blistering of the resin on the bone, the skulls were preheated in an oven at 60°C. They were then dipped into the molten resin. The whole of the anatomical face of the skull (frontals, nasals, maxillae, premaxillae, palatals, jugals, the zygoma of the temporal bones and the bones of the orbits), were coated with a resin thickness of approximately one millimetre. The skull was returned to the oven at 60°C, subsequently brought to room temperature (18°C) after having been passed through a second oven at 30°C. Leaving the skulls to cool at room temperature after coating resulted in the resin shattering through the differential cooling rates of the skull and resin.

The skull was placed in the frame with the horizontal bars (A in Fig 4.1.a) supporting the skull at the glenoid fossae. The bolt and nut (B in Fig 4.1.a) on the tooth supporting bar were adjusted so that the palate was horizontal when the support was placed at either the canines or carnassials. These two positions were selected as they represent the points at which the principal load was likely to be applied in the upper jaw during biting. Firstly, the force imposed on the canines by the seizing of its prey and secondly, by the pressure applied to the carnassials when slicing its food.

Prior to the coating of the skulls with resin, the cords representing the masseter and temporalis muscles were plaited and bound together with wire to prevent separation, in the following sequences for the different experiments.

(1) Left masseter to right masseter.

(2) Left temporalis to right temporalis.

(3) Left masseter to left temporalis and right masseter to right temporalis.

The skull having been set in the frame, a rectangular bar was placed within the loop formed by the uniting of the threads as in (1) or (2). The bar was gradually depressed along the line of action of the masseter or temporalis respectively. With the masseter and temporalis united on each side (condition 3) each loop was twisted so that the cord representing the two major muscles crossed each other at an angle of approximately 80°, the angle at which the principal fibres of the masseter subtended those of the temporalis. The rectangular bar was passed through the two loops thus formed, the latter were adjusted so that the bar lay horizontally. The two groups of threads were loaded equally by the application of pressure to the midpoint of the bar.

The pattern of cracks formed in the resin was observed with the aid of a magnifying lens and with proper adjustment of the direction of light illuminating the skull. The patterns were recorded on duplicated drawings of the lateral, dorsal and ventral views of the skull. From the orientation of the cracks and the direction at which stress was applied to the skull, it was possible to determine the direction of strain in the bone, and in a number of cases the type of strain produced in the resin. At the end of the test, the resin was removed with acetone.

The experiments were repeated three times for each of the above muscle combinations with the support placed initially at the canines, then at the carnassials; making a total of eighteen recordings for each of the five cat skulls and a total of 90 recordings. A control was provided by a comparative examination

of the results obtained from the different experiments performed.

A summarised illustration of the repeated recordings is presented in the text for each of the five skulls for the different combinations of force applied to the muscles and teeth (Figs 5.2 to 5.19.). A further diagram summarising the results of the five cat skulls is illustrated and described (Figs. 5.4., 5.7., 5.10., 5.13., 5.16., 5.19).

The direction of force within the bone and areas of high stress concentration are demonstrated by the colophonium technique. However, the limitations are that it is impossible to determine with any confidence the type of strain deforming the bone. Further, the experiments were carried out on dry skulls, which reduced their flexibility and hence the extent of the patterns produced.

4.2. Strain gauge experiments.

4.2.1. Introduction.

Wire resistance strain gauges operate on the principal that the electrical resistance in the wire alters in proportion to the increase or decrease in the length of the wire and therefore to similar changes occurring in bone to which the gauge is bonded. A form of balance system is employed for this sort of measurement and is provided by a bridge or half bridge network. This raises the sensitivity and enables refinements to be introduced for eliminating drift. When stress is applied to the bone and transducer the resistance changes and the bridge is unbalanced. The resulting output voltage will be a measure of this change and with the calibration factor of the transducer (change in resistance/ change in length) known, the actual strain can be determined immediately.

The application of foil strain gauges to the surface of the cat and dog skulls (Buckland-Wright, 1970a) after the removal of the colpphonium resin proved to be a successful means of determining the nature of the strain in the underlying bone. This had been carried out without the knowledge of Evans' (1957) remark "... if one wishes to take very accurate measurements of the magnitude of the strain produced in an object under given experimental conditions, the strain pattern produced in the lacquer indicates the site where extensiometers or strain gauges should be.".

No reference has been found in which an investigator has used both techniques on the same bone although there are a number who have used both methods at different times but not on the same material.

Endo's (1965) work on the distribution of stress and strain in the human facial skeleton appears to be the only work in which strain gauges have been applied to the dry skull. In his experiments rosette strain gauges were cemented onto the facial bones. The gauges gave the nature, direction and magnitude of the strain. Rosette gauges were not used in the present investigation on cat skulls because the size of the gauges relative to the skulls was too large and their cost was prohibitive.

4.2.2. Materials.

Fifty foil strain gauges (type 4/120/E/C, Tinsley Telcon Ltd., London) with one centimetre leads were obtained for bounding onto the cat skulls. The strain gauge recording apparatus consisted of a Peekel Extension box type 4UD and a Peekel Strain Indicator type T200. This apparatus was made available by the kind courtesy of the Department of Civil Engineering, King's College.

4.2.3. Bonding of the strain gauges.

Prior to bonding the gauges to the right side of the skull, the bone surfaces were thoroughly cleaned with acetone and prepared by scoring with a file. The bonding surface of the strain gauges and surfaces of the bone were coated with a film of 'Araldite'. The gauges were affixed to the selected areas and their position maintained by strips of cellotape during the curing process in an oven at 60°C.

4.2.4. The position of attachment of the strain gauges to the skulls

Ten strain gauges were allocated to each of the five skulls. The areas to which these gauges were bonded was determined by the results of the colophonium resin experiments and were in general those of high stress concentration (Figs. 4.2., 4.3., 4.4., table 4.1.).

The relationship between the structural organisation and the position of the strain gauges bonded to the cat skulls is given in table 8.1. and is discussed in section 8.3.1.3.

(1) The lateral surface of the temporal bar of the zygomatic arch; skulls I, II, III, IV, and V.

(2) The lateral surface of the jugal close to its superior margin and above the attachment of the main body of the masseter muscle; skulls I, II, III, IV, and V.

(3) The lateral surface of the alveolar process of the maxilla dorsal to the fourth premolar and posterior one third of the third premolar; skulls I, II, III, IV, and V.

(4) The central area of the frontal process of the Maxilla; skulls I, II, III, IV, and V.

(5) The dorsal surface of the frontal, posterior to the maxillo-frontal suture and close to the supra-orbital margin. Although this position appears to be one of low stress

concentration the gauge was placed in the line of the direction of force indicated by the resin; skulls I, II, III, IV, and V.

(6) The ventral surface of the palatine bone, at the lateral border of the horizontal plate. In this position the gauge was not under the direct influence of any one tooth and could record the effects on the hard palate from the load being applied to either the canine or carnassial; skulls I, II, IV and V.

The stress patterns in a number of the above areas were examined in greater detail.

(7) A strain gauge was attached to the medial surface of the jugal; in a position comparable to that on the lateral surface of the bone; skull I.

Particular attention was paid to the direction and relative deformation of the bone in the anterior facial region. Strain gauges were cemented to the following areas:

(8) The lateral surface of the canine; skull IV. When the support was placed at the carnassials, the recordings from this gauge acted as a control in determining the extent of zero drift during the experiments.

(9) The lateral surface of the premaxilla; skull IV.

(10) The circumorbital bar of the maxilla dorsal to the superior margin of the maxillo-jugal suture; skulls II and IV.

(11) The anterior margin of the frontal process of the maxilla, proximal to the nasal bone and parallel to (10); skull II.

(12) Strain gauges were arranged on the frontal process of the maxilla, one in the vertical plane in the centre, and two on either side at 15° to the horizontal in positions (10) and (11) respectively. This was in order to ascertain the principal direction of strain being transmitted through the bone during the

experimental procedure; skull V.

(13) The orbital plate of the frontal; skulls I and V.

(14) The internasal suture; skulls I and II.

(15) In the parasagittal plane, medial to the gauge bonded to the frontal and immediately posterior to the naso-frontal suture; skull V.

(16) The orbito-temporal line, an area difficult to coat with resin; skulls I and II.

An experimental control was set up, whereby gauges were cemented to positions (1) to (5) on the left as well as on the right side of skull III. The skull was then stressed with the support at the canine on the left side having been removed during all the experiments. A further control was provided by a comparative examination of the results obtained from the different experiments performed.

4.2.5. Experimental procedure.

Two wire leads (80 centimetres long) were wound together and stripped at their ends of their insulation. The wires of one end were soldered to the 1 cm. connecting leads of the strain gauges. This procedure was carried out for each strain gauge. The other end of the wire leads were later attached to the terminals of Peekel Extension Box.

The skulls were placed in succession in the frame for stressing in the manner described for the colophonium experiments. The same combination of the cords representing the masseter and temporalis muscles was employed, with the supports placed initially at the canines then at the carnassials.

Two metal flanges were passed through slots cut in the wooden base of the frame immediately below the position of the cords representing the muscles. At the upper end of each flange

large notches were cut to accommodate the cords of the masseter and temporalis respectively. The loop formed by the uniting of the cords of the left and right temporalis or left and right masseter, was slotted into the anterior or posterior notches respectively (Fig 4.5.a) so that the line of action of the muscle was maintained during the process of applying the load to the skull. The loop was prevented from approximating the two metal flanges and altering the direction of pull, by a long brass bolt spanning the gap between the flanges, and maintained in position by means of nuts. The flanges, themselves, were kept in their vertical position by the neat fit of the slots in the base of the frame.

When the masseter and temporalis from each side were plaited and wired together, the brass bolt was removed and the flanges acted independently. The loop formed was slotted into the anterior and posterior notches of each flange. The height of the latter was altered by means of bolts of adjustable length attached to the Salter spring balance, so that the balance hung vertically and the pull in the two flanges was equal.

The skulls were placed under stress simulating the conditions of jaw closure in the same sequences as described for the colophonium resin experiment (section 4.1.4.). The load was applied by turning the winch handle attached to the base board supporting the cranial frame. The winch consisted of a canvas sheet and rod which was secured to the hook at the end of the Salter spring balance. The different loads applied by the winch to the spring balance and hence the skull, could be maintained by means of a ratchet and pin locking the winch handle.

The ten leads from the strain gauges of a skull under test were connected to the terminals of the Peekel Extension Box,

as well as the leads from a passive strain gauge on a skull not under test. The Extension Box was connected by its leads to the Peekel Strain Indicator (Fig 4.5.b). The half bridge circuit, formed by an active and the passive strain gauge , was balanced by altering the reference switch and the continuously adjustable scale on the Peekel Strain Indicator until the null point was obtained. The position in microstrains on the scale was noted. Each of the active gauges was in turn balanced against the passive gauge by turning the selector switch on the Extension Box and the balance point obtained on the continuously adjustable scale.

With the load applied to the skull, the active gauges changed in resistance and a potential difference was set up across the bridge. The potential difference was balanced by altering the scale on the Peekel Strain Indicator for each of the active gauges. The new position on the scale indicated directly in microstrain the change in length of the gauge and hence that of the bone.

The scale on the Salter spring balance indicated the load applied to the cords attached to the skull. The load was applied in 2 kilogram steps from 0 to 10 kgm. During unloading, the load was removed in 2 kilogram steps from 9 to 1 kgm, the zero or initial balance point was then re-recorded. The experiments were repeated to ascertain the degree of experimental variation.

The change in microstrain during loading and unloading was obtained by computing the difference between the successive readings and the first zero balance point. Tensile strain was indicated by positive results and compressive strain by negative ones (table 5.1.). Graphs were compiled for results

obtained from each strain gauge. The results from each gauge for the load applied to the masseter, temporalis and combined masseter and temporalis respectively were added to one graph for when the support was at the canines and then at the carnassials (Figs. 5.20 to 5.25, table 5.1).

The advantages of the Peekel Strain Indicator and Wheatstone bridge circuit is that it is relatively very sensitive, and is particularly useful for measuring static strain as the circuit resistance variations in the connecting leads has practically no influence upon the results.

The limitations of this technique was zero drift caused by ambient temperature changes shifting the readings on the Strain Indicator. This was overcome by operating in a large room of constant temperature and isolating the skull from draughts by covering it with gauze sheets. The fundamental limitation of this experiment was that the recordings were carried out on dry prepared skulls. The removal of the fluid phase of bone through drying resulted in an increase in the average ultimate strength of the bone and a decrease in the strain or percentage elongation (Evans and Lebow, 1951). Drying destroyed a large percentage of the elastic component of bone provided by collagen and the contents of the cranial sutures (Le Gros Clark, 1971). The schematisation of the simulation of the forces generated during biting in the prepared cat skulls can only provide an approximation to the real situation.

CHAPTER 5

RESULTS OF THE IN VITRO DETERMINATION OF THE TRANSMISSION OF BITING FORCES IN THE CAT SKULL.

CHAPTER 5

RESULTS OF THE IN VITRO DETERMINATION OF THE TRANSMISSION OF BITING FORCES IN THE CAT SKULL

This chapter describes the results of the distribution of strain in the skull bones under simulated conditions of biting at the canines (Phase I) and carnassials (phase II). The relationship between the structural organisation and the position of the strain gauges bonded to the cat skulls is given in table 8.1. and discussed in section 8.3.1.3.

5.1. Colophonium resin experiments.

5.1.1. Introduction.

Tucker's (1954) recognition of three types of stress exerted on the skull during biting are used here in the description of the direction of stress passing in the skulls during the experiments. Primary stresses are those produced by the muscles at their attachment, secondary stresses are those exerted at the glenoid cavity and tertiary stresses are those that develop in the jaw bones during biting.

The direction of force transmitted in the bone is described on the basis that the cracks lie at right angles to that of tension and compression. In general, individual cracks within the resin are not described; however, their frequency in any particular region is an approximate indication of the degree of bone deformation (Fig 5.1.).

5.1.2. The distribution of primary strain in the cat skull, with the support placed at either the canines or carnassials.

(a) With the load applied to the cords representing the temporalis muscle. (Figs 5.2., 5.3., 5.4., 5.11., 5.12., 5.13)

The strain ran medially in the superior region of the parietal bone and medially and antero-medially in the frontal bone posterior to the post-orbital process.

(b) With the load applied to the cords representing the masseter muscle. (Figs. 5.5., 5.6., 5.7., 5.14., 5.15., 5.16.).

In norma lateralis the strain passes along the inferior margin of the jugal and inferiorly in the alveolar process of the maxilla above the fourth premolar. In norma medialis the strain passes antero-inferiorly from the orbital margin of the jugal into the dorsal surface of the palatine process of the maxilla. The application of a load to the masseter cords results in the separation of the posterior two-thirds of the jugal and temporal components of the zygomatic suture, and an increase in strain at the anterior one-third of the suture, inferior to the orbital process of the jugal.

(c) With the load applied to the cords representing the temporalis and masseter muscles. (Figs 5.8., 5.9., 5.10., 5.17., 5.18., 5.19.).

The pattern of strain distribution represented a combination of those observed under condition (a) and (b); although the degree of bone deformation was not as great as in the former two instances.

5.1.3. <u>The distribution of secondary strain in the cat skull, with the support placed at either the canines or the carnassials. (Figs 5.2 to 5.19).</u>

The strain passes anteriorly along the temporal component of the zygomatic arch when the load was applied separately or jointly to the cords representing the temporalis and masseter muscles.

5.1.4.1. <u>The distribution of tertiary strain in the cat skull with the support placed at the canines.</u>

(d) With the load applied to the cords representing the temporalis muscle. (Figs 5.2., 5.3., 5.4.).

The compressive force applied to the canines resulted in strain passing vertically up the canines, the canine eminence and frontal process of the maxilla. This produced a dorsal rotation of the anterior region of the face relative to the neurocranium, exerting strain in the circumorbital bar of the maxilla, the orbital margin and post-orbital process of the jugal, also along the inferior margin of the jugal, the alveolar and palatal processes of the maxilla and premaxilla. From the premaxilla, the strain runs postero-dorsally into the frontal process of the maxilla. The strain in the dorsal surface of the palatine process of the maxilla and horizontal process of the palatine bone passes medio-laterally.

The dorsal rotation of the anterior part of the skull also resulted in the ventral displacement of the jugal relative to the temporal bar of the zygoma on the right sides of skulls III and V. Deformation of the bones of the hard palate was greatest in skulls II, III and V.

(e) With the load applied to the cords representing the masseter muscle. (Figs 5.5., 5.6., 5.7.).

The differences in the distribution of strain in the skull compared with (d) are due to the effect of the primary stress. The strain in the alveolar process extends from just above the third premolar to the alveolar process of the premaxilla, and from the former region strain passes antero-superiorly, anterior to the infra-orbital foramen, to above the canine eminence. The strain in the circumorbital bar of the maxilla extends further dorsally around the orbit and is paralleled by a strain in the anterior region of the orbital plate of the frontal bone. Strain in the hard palate extended posteriorly from the palatal process of the premaxilla to the posterior region of the horizontal process of the palatine.

Shear strain was recorded in the region immediately superior to the canine eminence where one or more cracks ran horizontally across the maxilla from the lateral margin of the nasal bone to the orbital margin of the maxilla separating cracks with slightly different orientations inferiorly and superiorly.

(f) With the load applied to the cords representing the temporalis and masseter muscles (Figs 5.8., 5.9., 5.10.).

The tertiary stresses at the canine pass vertically into the frontal process of the maxilla, this is particularly marked in skull V. In general the cracks do not extend vertically to the extent that they do under the experimental conditions of (d) and (e). This is also the case with the strain in the orbital margin of the jugal and maxilla and would suggest that the overall strain in the skulls is not as great as in (d) or (e).

The strain in the alveolar process extended anteriorly from the posterior region of the maxilla, dorsal to the fourth premolar, to the alveolar process of the premaxilla. As in (e) strain runs antero-superiorly from the alveolar process into the frontal process of the maxilla passing anteriorly to the infra-orbital foramen. In the hard palate the strain was generally low for cracks were recorded only in skulls I and V and were absent from the dorsal surface of the palatine process of the maxilla.

5.1.4.2. Summary and conclusion.

The deformation of the skulls was greatest with the load applied to the cords representing the masseter and least with it applied to the temporalis. The degree of deformation lay approximately between the two former states rather than when the load was applied to the cords representing both muscles. This was

demonstrated by the relative degree of deformation in the skulls as registered by the number of cracks in the resin and the reduction of shear strain generated by the load applied to the masseter in the regions of the zygomatic arch and the frontal process of the maxilla.

In general the regions of high strain concentration occurred in the zygomatic arch, the circumorbital bar of the maxilla, and in the areas proximal to the canine.

5.1.4.3. <u>The distribution of tertiary strain in the cat skull with the support placed at the carnassials.</u>

(g) With the load applied to the cords representing the temporalis muscle. (Figs 5.11., 5.12., 5.13).

The strain at the carnassial passes vertically into the alveolar process of the maxilla and along its inferior margin to the premaxilla and thence dorsally within the premaxilla and canine eminence of the maxilla. Strain was transmitted along the orbital margin of the jugal from the inferior region of the circumorbital bar of the maxilla to immediately anterior to the orbital process of the jugal. At the inferior margin of the jugal strain passes directly into the alveolar process of the maxilla. A high concentration of strain was recorded on the ventral surface of the hard palate, and on the dorsal surface of the palatal process of the maxilla.

(h) With the load applied to the cords representing the masseter muscle. (Figs 5.14., 5.15., 5.16.).

The stress applied to the carnassial passed vertically up the alveolar process. The left and right sides of the skulls in figure 5.16. (bottom set) illustrate minor variations in the distribution of the vertical strain resulting from differences in the posterior extension of the horizontal stress in the alveolar

process of the maxilla. Strain orientated vertically in the premaxilla and maxilla has an arrangement similar to that when the support is placed at the canines (section 5.1.4.1.(e)). In the circumorbital bar of the maxilla the strain extends vertically as far as the maxillo-frontal suture (skulls III, IV and V) and is paralleled by strain in the anterior region of the orbital plate of the frontal (skulls I, II and III). In all skulls but one, strain ran posteriorly in the anterior two thirds of the frontal bone, and in a couple of experiments postero-laterally into the post-orbital process (skull III).

(i) With the load applied to the cords representing the temporalis and masseter muscles. (Figs 5.17., 5.18., 5.19.).

The applied stress at the carnassial passed vertically up the alveolar process and posterior region of the maxilla, and antero-medially on the dorsal surface of the palatal process of the maxilla. The horizontal strain at the inferior margin of the alveolar process did not extend anteriorly much beyond the level of the infraorbital foramen. Strain in the superior margin of the jugal ran from the orbital process of the jugal to the inferior region of the circumorbital bar of the maxilla. Skull III provided the only record of strain on the ventral surface of the hard palate which ran antero-posteriorly along its length.

5.1.4.4. Summary and conclusion.

As in the case with the support placed at the canines, the extent of cranial deformation is not as great with the load applied jointly to the cords representing the temporalis and masseter as it is when applied to those muscles separately.

The tertiary stresses are here largely confined to the infraorbital region. The greatest deformation occurred in the zygomatic arch and posterior half of the maxilla.

5.1.4.5. Experimental control in the colophonium resin experiments.

Experimental control was obtained from the examination of the individual results of the colophonium resin experiment. For identical conditions of stress applied to the skull the results were similar for successive recordings on the same skull and for the five cat skulls. Alterations in the conditions of stress applied to the skull resulted in changes in the arrangement of the cracks. These observations indicate that the pattern of cracks depends primarily on the stresses applied to the skull and is not a property of the colophonium resin alone.

5.2 Strain gauge experiments.

5.2.1. Introduction

The mechanism for applying the load simultaneously to the cords representing the temporalis and masseter muscles was subject to a certain amount of variation due to the limitations imposed by the design of the loading apparatus; namely, it was not possible to ascertain whether the load was equally distributed between the cords of the temporalis and masseter. For this reason greater attention was paid in the analysis of the graphs to the results of when the load was applied separately to the masseter and temporalis.

5.2.2. Results of the in vitro strain gauge experiments.

The following strain gauges were found not to work during the experiments: at position (1) on the zygoma of the temporal bone on skull II and at position (3) on the maxilla above the fourth premolar on the right side of skull III. The strain gauge at position (7) on the medial side of the jugal on skull I responded slightly abnormally as a result of a kink produced in the gauge during the bonding process of the gauge to the bone.

The results of the experiments are presented graphically in figures 5.20 to 5.25. Each figure comprises a number of composite graphs, each composite graph represents the results for one cat skull from the gauges bonded to the area of bone listed on the illustration. The number of the cat is indicated in roman numerals to the left of each graph. The ordinate is the deformation of bone in microstrain, where each division represents 50 microstrain. The recordings with a positive signal indicate tensile strain, those with negative signals indicate compressive strain. The abscissa is the load applied to the threads representing the muscles. The change in load between each recording was in 2 kg steps from 0 to 10 kg during loading and unloading, of which the former are represented by the even numbers. In each composite graph the squares, circles and crosses represent the results of the load applied to the cords representing the masseter, temporalis and combined masseter and temporalis respectively. Table 5.1. presents the recordings for each strain gauge when an 8 kilogram load was applied by the spring balance to the cords representing the temporalis, masseter and combined temporalis and masseter muscles respectively, with the support placed initially at the canines and then at the carnassials. The percentage distribution of strain within the cat skull is given in Tables 5.2 and 5.3.

5.2.2.1. <u>Selective observations on the results of the strain gauge experiments.</u>

The following observations are concerned with the results of the control strain gauges on the left side of skull III and the variations in recordings from the other gauges.

Strain gauge at position (1): the zygoma of the temporal bone (Fig 5.20). The control gauge demonstrated no difference

from the recordings on the other skulls.

Strain gauge at position (2): the lateral surface of the jugal (Fig 5.2 1.). Support placed at the canines and load applied to the cords representing the masseter and temporalis muscles: a moderately low tensile strain was recorded on skull IV and the right and left sides of skull III. In these two skulls the strain is similar to that produced when the load was applied only to the cords representing the temporalis muscles. The strain in skulls I, II and V is closer to the anticipated result.

The control gauge does not show any great difference in strain pattern from the results of the gauge on the right side of skull III or from that on skull IV but does differ markedly from those on skulls I, II and V. With the load applied to the cords representing the masseter and temporalis muscles respectively, there was no marked dissimilarity between the strain recorded from the control gauge and from the gauges on the other skulls.

Support placed at the carnassials and load applied to the cords representing the masseter and temporalis muscles: the pattern is approximately the same as for the support placed at the canines. The tensile strain on the right side of skull III is extremely low.

Strain gauges at position (3) on the maxilla above the fourth premolar (Fig 5.22). The control gauge exhibited no marked difference from the results recorded from the other skulls. Support placed at the carnassials and load applied to the cords representing the masseter and temporalis muscles: the compressive strain on skull IV may be associated with the effects of a large compressive strain exerted by the load applied to the cords

representing the masseter muscles.

Strain gauges at position (4) on the frontal process of the maxilla (Fig 5.23.). Support placed at the canines and load applied to the cords representing the temporalis muscle: a low compressive strain is absent in skull IV.

The pattern of strain at the control gauge differed markedly from that of the other skulls and probably resulted from the effects produced in the bone by the action of the muscles when no support was present at the left canine.

Support placed at the carnassials: the pattern of strain between individuals is relatively more variable in this area.

Strain gauge at position (5) frontal (Fig 5.23). Support placed at the carnassials: as with the gauges at position (4) the strain pattern between individuals was variable.

The strain pattern from the control gauge bore a close parallel to that produced at position (4) except that the magnitude of the strain was not as large.

Strain gauge at position (6) palatine (Fig 5.25): Support placed at the carnassials and load applied to the cords representing the masseter and temporalis muscles: this arrangement resulted in an enhancement of the strain produced when the load was applied to the cords representing the temporalis muscle.

Strain gauge at position (8) lateral surface of the canine (Fig 5.25). Support placed at the canine and load applied to the cords representing the temporalis muscles. The application of loads greater than 4 kilograms resulted in a reduction in the magnitude of the strain due to the alteration in the direction of stress in the canine and hence along the line of the gauge.

Strain gauge at position (12) on the frontal process of the maxilla, one in the vertical plane in the centre and one on either side at 15° to the horizontal in position (10) and (11) respectively on skull V.

The results of the vertically placed strain gauge are given along with those from the other skulls with the gauge at position (4) (Fig 5.23). In comparison the former exhibits no difference in strain pattern from those of the other skulls.

Strain gauge at 15° to the horizontal on the circumorbital bar of the maxilla (Fig 5.24). With the support placed at the canines, the results were similar to those from the gauges at position (10) on skulls II and IV.

Support placed at the carnassials and load applied to the cords representing the masseter and temporalis muscles. A large compressive strain passes postero-dorsally into the frontal and does not resemble the strain at position (10) on skulls II and IV. Although tables 5.1. and 5.3. record the compressive strain from skull V it is rejected as being anomalous in the subsequent descriptions. This result is rejected on the basis that it does not lie between the readings for the load applied separately to the cords representing the masseter and temporalis which is a general feature of all the graphs. As stated in section 5.2.1. importance is laid on the results obtained from when the load was applied separately to the cords representing the masseter and temporalis in assessing the results obtained when the load was applied to both muscles simultaneously. The results for the latter situation in skull V indicate that the load on the cord representing the temporalis is proportionately greater for that region of bone. A corrected recording would be a low tensile strain, not very dissimilar from that recorded on skull II.

Strain gauge at 15° to the horizontal near the anterior margin of the maxilla proximal to the nasal bones (Fig 5.24). The support placed at either the canines or carnassials. Compared with the strain pattern recorded from the gauge at position (11) on skull II, the near absence of strain during the experiment would indicate that stress was not orientated in the direction in which the strain gauge was aligned.

Strain gauge at position (13): orbital plate of the frontal (Fig 5.25). With the support at the canines or carnassials, the strain patterns recorded from skulls I and V bore very little similarity to one another.

The standard deviation in microstrain of the deformation of bone at the strain gauge positions (1) to (5) is given in tables 7.6 and 7.7 for the brace at the canines and carnassials respectively. The variation in strain between successive experiments can be attributed to three principal factors. One, due to zero-drift which has been estimated at ± 5 microstrain from the strain gauge at position (8) on the canine when the support was placed at the carnassial. Second, and most important, that resulting from the variations in the degree of bone deformation between the cat skulls and third, in the method in which stress was applied to the skulls.

5.2.2.2. Experimental control in the strain gauge experiments.

Experimental control was obtained from an examination of the individual results of the experiments which followed similar lines to that carried out for the colophonium resin experiment. The results obtained from the control experiment carried out on skull III when the support was removed from the left canine demonstrated that the strain pattern was different at the left anterior facial region compared to that on the right. This

confirms that the strain pattern in the skull depended on the applied stress.

5.2.2.3. Summary and conclusion

The strain gauge experiments provided the type and the magnitude of strain passing in the bone directly under the gauges bonded to the skulls. The results confirmed quantitatively the observations of the colophonium resin experiments. The deformation of the cranial bones was not as great with the load applied jointly to the cords representing the masseter and temporalis as it was when applied separately to those muscles. In general the action of the masseter generated a strain in the bone of opposite sign to that produced when the load was applied to the cords representing the temporalis. With the application of stress to both muscles the magnitude of the strain produced tended to lie between the values for when the muscles were stressed independently.

With the load applied to the cords representing the masseter and temporalis muscles the areas of greatest bone deformation, when the support was placed at the canines, were the zygomatic arch, and maxilla and premaxilla; when the support was placed at the carnassials, these areas were the zygomatic arch, the orbito-temporal line, the circumorbital bar of the maxilla, the premaxilla and palatine bone.

CHAPTER 6

MATERIALS AND METHODS FOR THE DYNAMIC STRAIN GAUGE RECORDINGS FROM ANAESTHETISED CATS.

CHAPTER 6

MATERIALS AND METHODS FOR THE DYNAMIC STRAIN GAUGE RECORDINGS FROM ANAESTHETISED CATS.

6.1. Introduction.

This chapter describes the materials and methods of the in vivo determination of the strain distribution in the cat skull.

The experiments were perfromed to compare the results with those obtained in the in vitro experiments and to assess the relative accuracy of the latter. As far as could be ascertained from the literature, no reference has been found describing experiments in which the results obtained from tests on dry specimens were directly compared with the in vivo condition or vice versa, apart from those on skull deformation. Gurdjian & Lissner (1947) carried out experiments with a strain gauge bonded to the skull of an anaesthetised dog; the results were similar to tests performed on cadaver heads with the skull contents intact. They showed also that the frequency response of bone from a blow to the skull of a human cadaver was from 1/5000 to 1/2000 of a second; this confirmed previous work of Gurdjian & Lissner (1944) on the dog skull. The frequency response was also independent of the intensity of the blow.

Investigations into the physical properties of wet and dry samples of bone from the femora of embalmed cadavers was carried out by Evans and Lebow (1951). The stress-strain curves of dry and wet samples of standardised size from the same region of a bone demonstrated the greater absorbing capacity of wet bone. The authors considered the results obtained for tensile stress and strain from the wet samples were a closer approximation of the true values of living bone than the dry samples. Further

tensile tests on wet and dry samples of bone were carried out by Dempster and Liddicoat (1952) confirming the findings of the former.

These references would suggest that the differences in bone behaviour in the in vitro situation are not markedly different from that found in vivo. However, in view of the limitations described for the in vitro strain gauge experiments this present series of experiments were designed to provide a broad quantitative assessment of the similarities and differences between the two conditions and hence the relative accuracy of the in vitro experiments.

6.2.1. Materials

Ten female cats were obtained for experimentation. Each cat was weighed in order to determine the volume of Nembutal needed for narcortisation.

No.	Weight in in kgm	No.	Weight in kgm
1	3.8.	6	2.6
2	3.5	7	2.5
3	2.3	8	2.2
4	2.97	9	2.0
5	2.575	10	1.7

Cats (1) to (8) were adult, whereas cats (9) and (10) were adolescent animals as at this period there were no adults available from the animal suppliers. The results presented in chapter 7 show that there is no significant difference in the recordings obtained from the adult and young cats.

6.2.2. Apparatus.

The experiments were carried out in the Department of Physiology, King's College, using the following apparatus made available by the kind permission of Dr. D.M. Band: Dual Beam Oscilloscope type 502A (Tektronics Ltd); AC Carrier Amplifier

and Demodulator and an Ultra-Violet Recorder (S.E. Laboratories); Biomac 1000 with punch paper tape facilities (Data Laboratories); Philips Data Tape Recorder type Ana-Log 7; Bryan's X-Y/T Autoplotter Series 22000; Devices Digitimer, Gated Pulse Generator and Stimulator and a Zeiss Binocular Dissecting Microscope.

6.3. Position of attachment of strain guages on the skull and the associated anatomy of the cats head.

Five areas had been selected for the implantation of the encapsulated strain gauges on the anaesthetised cat skulls (Fig 4.4.b). These corresponded to the principal areas used in the in vitro strain gauge experiments: (1) the zygomatic component of the temporal bone, (2) the superio-lateral border of the jugal, (3) the alveolar process of the maxilla dorsal to the fourth premolar, (4) the central region of the frontal process of the maxilla, and (5) the dorsal surface of the frontal, posterior to the maxilla-frontal suture (table 7.1). A control strain gauge was bonded on one of the cat skulls (6) in position (4) at right angles to the direction of the gauge in the remaining experiments. From Poisson's ratio the sign of the signal from this gauge should be reversed.

In order to bond the gauges to the cranial bones a knowledge of the associated anatomical structures was necessary. Fresh post-mortem cat heads were obtained for dissection. Particular attention was paid to the distribution of supra-orbital infra-orbital and superior labial vessels. The branches of the trigeminal nerve innervating the temporalis and masseter muscles were traced. From the configuration of the above structures the incisions necessary for reflecting the skin were determined as

well as the sites for the insertion of the stimulating electrodes, and those vessels that would require ligaturing in order to maintain a dry field for operation.

6.3.1. The design of the braces.

Isometric conditions of muscular stimulation were considered the most appropriate for this experiment. Braces were designed, one to be inserted between the upper and lower canines (phase I of biting) and one between the carnassials (phase II of biting). The braces were milled out of brass and are I shape in design (Fig 6.1., 6.2). The cusps of the teeth inserted into grooves cut into the outer surfaces of the upper and lower horizontal bars. A strain gauge was cemented with 'Araldite' to the front surface of the vertical bar of each brace for recording the force of bite generated by the electrical stimulation of the muscles.

As only one brace was in use at any one time, the strain gauge on the one not in use acted as the passive gauge. The two gauges were wired up as a half wave bridge and connected to a carrier amplifier and demodulator box.

6.3.2. Optimum conditions for the tetanic stimulation of the muscles.

Experiments were carried out on three adult female anaesthetised cats, obtained from elsewhere they had been used for respiratory experiments, to determine the optimum settings on the Devices Gated Pulse Generator and Stimulator for the maximum contractions of temporalis and masseter muscles. Eight insulated thin silver wires were used as stimulating electrodes, two wires were inserted into each muscle close to the position of the branch of the fifth cranial nerve. A two millimetre stripped end of the wire was bent and passed into the tip of an

hyperdermic needle. The needle and wire were inserted into the muscle and the needle then withdrawn leaving the wire electrode in place. The wires from the left and right temporalis and masseter muscles were collected together and connected to the positive and negative terminals of the stimulator. The brace was placed between the cat's teeth and held in position by a clamp attached to the operating table. The cat and brace were then earthed.

The Carrier Amplifier box was connected to an Ultra-Violet Recorder. The apparatus was switched on and the Carrier Amplifier adjusted for full scale deflection on the U-V Recorder for the maximum possible stress applied to the strain gauge during the experiment. The frequency in cycles per second and the voltage applied to the electrodes were altered during the experiment to obtain the conditions of maximum contraction of the masseter and temporalis.

The force of contraction deformed the brace between the cat's jaws. The potential difference set up through the change in resistance in the active strain gauge was amplified by the Carrier Amplifier and recorded on the U-V paper trace. Direct mensural examination of the U-V trace indicated the relative force of contraction. The settings on the Gated Pulse Stimulator for maximum contraction of the muscles obtained in the first experiment were confirmed on two successive cats.

6.3.3. <u>Results for the optimum conditions for the tetanic stimulation of the muscles.</u>

The results of the experiments performed on the three cats indicated the optimum setting on the Gated Pulse Generator and Stimulator for maximum contraction to be at an applied voltage of 3, a frequency of 60 per second and a pulse width of

5 milliseconds. Although increased frequency of stimulation produced slightly greater levels of contraction, the muscles rapidly became fatigued; for this reason the lower setting was used.

Stimulation of the muscles of mastication in this manner has the disadvantage that the muscles are probably not in maximal contraction through proprioceptive feedback from the muscle and antidromic stimulation causing the antagonist muscles to come into play.

6.3.4. Modifications to the braces.

Subsequent to these experiments the sensitivity of the braces was increased by boring a 7 mm hole through the centre of the vertical bar parallel to the horizontal bars of the canine brace and a 4 mm hole in the same area in the carnassial brace. Grooves 1 by 1 mm were cut into the front and back of the vertical bars thus increasing the radius of the hole at its midpoint (Fig 6.1.d., 6.2). A second strain gauge was cemented onto the braces on the opposite surface of the vertical bar to that of the first. The two gauges were connected as a half bridge. Under stress the sensitivity of the brace was doubled by the differential action due to the increase in resistance of one gauge being accompanied by a decrease in resistance of the other.

6.4. Dynamic strain gauge recording from anaesthetised cats, initial experiments.

The direct recording from encapsulated strain gauges bonded to the cranial bones of anaesthetised cats was carried out initially on three adult female cats.

Five half wave bridges were prepared by soldering the leads from five canon plugs to five active and passive strain gauges. The canon plugs were connected to the inputs of three Carrier

Amplifier boxes. The first of the six channels available on the Carrier Amplifier boxes was for the input plug for the strain gauges on the braces. All the passive strain gauges were bonded onto a short thin aluminium strip. The insulation surrounding each of the active gauges was pared down leaving a margin approximately 1.5 mm in width around the foil gauge. The gauges were then cleaned in acetone. As the experiment was acute, it was not deemed necessary to sterilise the gauges.

The apparatus was set up as follows (Figs. 6.3., 6.4). The output leads from the Carrier Amplifiers were inserted into the Tape Recorder inputs <u>via</u> the connecting panel. The signals from any one of the seven Tape Recorder outputs could be monitored by a jump-lead connecting one of the outputs to the input channel of the Oscilloscope. The Digitimer was set to operate the Gate Pulse Generator and Stimulator for a cycle time of two seconds by connecting the output of the digitimer into the Gated Pulse input. The Gated Pulse Stimulator was set to provide a train of pulses at a frequency of 60 per sec at 3 volts and a pulse width of 5 milliseconds. The positive and negative outputs of the Stimulator were connected to the A and B terminals of the second input channel of the Oscilloscope. The cathode ray tube beam was switched to A-B, and the beam gain was adjusted and the beam sweep positioned to give a suitable signal on the Tape Recorder channel 7 for recording.

The cats were weighed and narcotised with a volume in cubic centimeters of Nembutal (sodium pentabarbitone) equivalent to two-thirds of the cat's body weight, which was injected intraperitoneally. On anaesthetisation a catheter was inserted into the right femoral vein for introducing dilute Nembutal (two volumes of Nembutal to eight of saline) for maintaining

anaesthesia. Urine was removed from the cat's bladder from time to time by means of an hypodermic syringe to maintain the comfort of the cat and prevent flooding of the operating table.

All the fur was shaved off the cat's face and throat with electric clippers. A tracheotomy was performed and a polythene tube inserted into the trachea to facilitate the cat's breathing and to avoid the air currents from breathing causing zero drift in the strain guages on the braces. Incisions 1, 2 and 3 (Fig 6.5) were made in the skin above the temporal component of the zygomatic arch. Retractors were applied and with the use of a Zeiss binocular dissecting microscope the fascia and periosteum were reflected from the surface of the bone. A fine pointed cautery was used to seal the fine blood vessels at the surface of the bone. Incisions 4, 5 and 6 were made and the superior surface of the jugal prepared; care was taken not to damage the attachment of the masseter. The superior one-third of incision 7 was made and the superior labial vessels secured and ligated. Incision 7 was completed and 8 performed. At this juncture the infraorbital vessels were secured and ligated to provide a dry field of operation in the infraorbital region and that of the frontal process of the maxilla. Incisions 9, 10, 11 and 12 were performed and the bone surfaces prepared as before.

A modified method based on the techniques of Lanyon and Smith (1970) and Lanyon (1971) and Cochran (1972) was used for preparing the bone surface for the bonding of strain gauges. The bone surfaces were degreased and then dried with solutions of chloroform and methanol respectively applied with a small paint brush. A thin coat of surface activator (Activator 272, Ciba-Geigy, U.K.) was applied to the bone surface and the excess allowed to evaporate. The back of the encapsulated strain gauge

was coated with a film of adhesive (IBC2, Buerylate Tissue Adhesive, Ethicon Ltd.) and applied to the bone surface and maintained in position for approximately half a minute. The activator polymerised the adhesive which bonded the gauge to the bone. To prevent any stress being placed on the gauge from the leads, the latter was also bonded to the bone five millimetres away from the gauge. The skin flaps were replaced and held in position by a suture or adhesive tape. This process was repeated for the five separate sites (Fig 6.6). To avoid undue movement of the leads, these were taped to the surface of the skull. Incisions 13 and 14 were made and the stimulating electrodes inserted into the left and right temporalis and masseter, as described previously. The electrodes were connected to the terminals of the stimulator. A small incision was made in the skin at the nape of the neck and the metal strip supporting the passive strain gauges were inserted to simulate the recording conditions of the active gauges.

The canine brace was put into position. The apparatus was switched on. The balance point between the active and passive gauges was obtained on the Carrier Amplifier boxes. During short bursts of tetanic stimulation of the muscles, the attenuator dials on the Carrier Amplifier boxes and the separate Tape Recorder channels were adjusted to give the maximum frequency response from each of the transducers.

The Tape Recorder was switched to run at 15 inches per second. The muscles were stimulated into tetanic contraction by pressing the starter button on the Digitimer. After stimulation the Tape Recorder was switched off and three minutes delay was given for the re-establishment of biological equilibrium before the experiment was repeated. Ten recordings were made with the

brace at the canines, the second brace was then placed at the carnassials and a further ten recordings made.

At the end of the experiment each active gauge was calibrated by connecting a shunt of known resistance (3.3 megaohms) across the gauge. The shunt produced a deflection which was recorded on the Tape Recorder.

The results of the experiment were played out through the Ultra-Voilet Recorder onto the U-V paper trace. Direct mensural examination of the U-V traces was carried out to determine the deformation of the bone at the points to which the gauges were bonded.

The limitations of this method of playing out the results was the time involved in analysing and summating the results from one series of the experiments.

6.4.1. Dynamic strain gauge recordings from anaesthetised cats, final set of experiments.

The above method of playing out results was improved upon by having a 12 volt negative signal recorded on the tape 1.5 seconds prior to the stimulation of the muscles. The 12 volt signal was used to trigger the sweep on the cathode ray tube of the Biomac, which in turn was used to plot out the results graphically on the X-Y plotter as well as in making permanent record of the signals on punch paper tape.

The 12 volt initiating impulse was produced by the Digitimer which was connected to the input channel of the variable resistance R1 (Fig 6.3) on the connecting panel. The output of R1 was connected to the Tape Recorder input channel 7. The initiating impulse was isolated from the Gated Pulse Stimulator and cat by the Oscilloscope amplifiers. The circuit remains as described previously except that the output

from the second Oscilloscope channel was connected *via* the variable resistance R2 to the Tape Recorder input channel 7.

The Digitimer was set to provide a delay of 1.5 seconds after the initiating impulse and then to produce a pulse for two seconds operating the Gated Pulse Stimulator.

Seven further cat experiments were carried out following the procedures described for the initial experiments.

6.4.2. Calibration of the braces.

In calibrating the braces, the conditions of their loading was simulated as closely as possible. Two screw holes were cut into a steel platform, 2.3 cm apart. The platform was mounted and fixed firmly into the moveable arm of a Dale-Schuster myograph stand. The brace being tested was placed with its grooved surface for the maxillary teeth on the stand (Fig 6.7). A screw was passed through each of the holes until its tip just lifted the brace off the stand. A steel bar cut to fit the groove of the braces for the mandibular teeth, was put into position on the brace. The ends of the bar extended beyond the brace and stand; these ends were fashioned to accept metal flanges. The latter were attached to a Salter spring balance at their lower ends, the spring balance in turn was fixed to the base of the myograph stand.

The recording apparatus was set up with the same settings on the attenuator dials of the Carrier Amplifier box and Tape Recorder as during the experiments. As the attenuator dials did not have the same settings for all the experiments, the following procedure was repeated for the different attenuator readings.

The load was applied in 2 kgm steps from 0 to 10 kgms to the brace by turning the handle to raise the moveable arm of the Dale-Schuster myograph stand. The recording apparatus was turned

on and the load was applied to the brace and then released. This was repeated three times for each 2 kgm rise in the scale division.

6.4.3. The plotting of the results.

The apparatus was connected in the following manner for the plotting of the results. Channel 7 of the Tape Recorder output was connected via the Oscilloscope Channel 1 to the Sweep Trigger input on the Biomac. The Sweep Trigger was set to receive a negative incoming signal. The beam level on the Oscilloscope was adjusted so that the initiating impulse from Channel 7 triggered the sweep on the cathode ray tube (C.R.T.) of the Biomac. The remaining six Tape Recorder Channels were connected in succession to the input of the Biomac Channel 1. The Biomac programme was set to Average, the sweeptime of the C.R.T. to 5.12 seconds equivalent to the recording period, and with an after delay of 5.12 seconds so that the on-off impulse from the Tape Recorder did not trigger a second sweep on the Biomac.

A permanent record was made of all the signals from each of the strain gauges on punch paper tape. This enabled the recordings from each experiment with the brace placed at either the canines or carnassials to be summated. The information on the paper tapes for each series of experiments was played into the Biomac and summated. The resulting signal was averaged by setting the Normaliser scale of the Biomac to a figure nearest the number of recordings. The summated and averaged result was punched out on paper tape. A moving pen Autoplotter was connected to the Biomac and the information stored in the Biomac of a summated series of results or of an individual recording was then mapped out by the X-Y Autoplotter (Figs 7.1 to 7.12).

Observations were carried out on the variation between single recordings during the experiments. The degree of experimental variation was estimated in one experiment by calculating the mean and standard deviation for ten successive recordings when the brace was placed at the canines and carnassials respectively (Table 7.10).

The individual results of the calibrations performed on the strain gauges bonded to the skulls and braces were plotted out in the manner described above.

6.4.4. Calculations.

The deflections recorded by the shunt being placed across the strain gauges were measured from the output on the Autoplotter. The strain equivalent to that produced by the shunt was calculated from basic principles and the results used to plot the ordinate scale for each signal (Figs 7.1 to 7.12).

The gauge factor (K) for the strain gauge is defined as

$$K = \frac{r}{R} \div \frac{1}{L} = \frac{r}{R.s} \qquad - (6\text{-}1)$$

where (r) is the change in gauge resistance as a result of change in strain, $\frac{1}{L} = s$ is the change in strain applied to the gauge, and (R) is the initial resistance of the gauge.

Thus the change in strain is,

$$s = \frac{r}{K.R} \qquad - (6\text{-}2)$$

The calibration of the gauge was achieved through a resistance being placed in parallel with the system. With a parallel resistance (P) the apparent change in resistance is (r) where,

$$\frac{1}{R-r} = \frac{1}{R} + \frac{1}{P} \qquad - (6-3)$$

$$r = -\frac{R \cdot P}{R+P} + R$$

$$= -\frac{R \cdot P}{R+P} + \frac{R^2+RP}{R+P}$$

$$= \frac{R^2}{R+P} \qquad - (6-4)$$

The strain corresponding to this change is given by,

$$s = \frac{r}{K \cdot R} \qquad - (6-2)$$

$$= \frac{R}{K \cdot (R+P)}$$

For $P \gg R$, as for instance in these experiments

$$s = \frac{R}{K \cdot P} \qquad - (6-5)$$

If (a) is the deflection produced as a result of the strain in the bone during the experiment, and (b) is the deflection produced by the shunt. The apparent strain produced by the shunt is

$$sb = \frac{R}{K \cdot P}$$

then the strain recorded on the bone is

$$sa = \frac{a}{b} \cdot sb$$

$$sa = \frac{a}{b} \cdot \frac{R}{K \cdot P} \qquad - (6-6)$$

The autoplot out-put of the results from the calibration of the braces were measured and plotted out on graph paper for the different settings of the attenuator dials used during the experiments. The approximate force of bite at the canines and

carnassials was then determined for each experiment (table 7.8., 7.9).

6.5. Limitations of the experimental technique.

The principal shortcoming of these experiments was the abnormal method of stimulating the muscles into tetanic contraction and the attendant effects of proprioceptive feedback and antidromic stimulation. The limitation of the strain gauge technique was that the information obtained was relevant only to the piece of the structure to which the gauges were directly adherent.

The results presented in this thesis were interpreted qualitatively for as yet no satisfactory demonstration has been given that strain gauge bonded to bone *in vivo* gives an absolute indication of bone strain (Lanyon, 1973); and further, the absence of a satisfactory calibration procedure of a gauge's response to a known deformation and the inability to test the degree of bonding of the gauge to the bone.

The canine and carnassial braces had the disadvantage of being unalterable and therefore unable to accommodate to the different jaw gapes of the cats. This would result in a number of muscle fibres of the masseter and temporalis being over-stretched in the smaller sized cats with an associated reduction in the force of bite.

CHAPTER 7

RESULTS OF THE DYNAMIC STRAIN GAUGE

RECORDINGS FROM ANAESTHETISED CATS.

CHAPTER 7

RESULTS OF THE DYNAMIC STRAIN GAUGE RECORDINGS FROM ANAESTHETISED CATS.

7.1. Introduction.

The informational content of the signals recorded from the strain gauge during the *in vivo* experiments was high, principally becauss of the time based nature of the record. For the purposes of comparing the *in vivo* results with those of the *in vitro* strain gauge experiments, all measurements were made at one second after the initiation of the tetanic stimulation to the masseter and temporalis muscles. This point had been chosen as it was after the bone had responded to the onset of muscular contraction and, in the majority of the cases, the tetanic contraction of the muscles and the response of the bone had reached an equilibrium.

The braces placed between the teeth recorded the force of bite as well as monitoring the contractile action of the muscles. These results have not been examined in great detail as they are peripheral to the main hypothesis of this thesis.

7.2. Results of the *in vivo* strain gauge experiments.

The results from the following gauges had to be discarded as the gauges had become detached from the bone during the experiment or before the gauges had been calibrated (table 7.1.).

Strain gauge at the temporal of the zygoma on cats (1) and (2) with the brace placed at the canines and carnassials.

Strain gauge at the jugal on cat (1) with the brace placed at the canines.

Strain gauge at the maxilla above the fourth premolar on cats (1) and (2) with the braces placed at the canines and carnassials.

Strain gauge at the frontal process of the maxilla and at the

frontal on cat (1) with the brace placed at the canines.

The separation of the gauge from the bone surface was largely due to inexperience in the bonding technique of the gauges to the surface of the cat skull.

Examination of the gauges under the Zeiss binocular dissecting microscope revealed the following gauges to be incompletely bonded to the bone surface: temporal of the zygoma on cats (6) and (8); maxilla above the fourth premolar on cats (3), (4) and (9), the gauge on cat (4) exhibited extremely poor bonding; maxilla, frontal process on cat (7); and frontal on cat (8). Inspection of the canine brace at the termination of the experiment on cat (8) revealed that the brace had been incorrectly placed between the canines. At the maxilla above the fourth premolar on the cat skulls (8) and (9), one half of the surface of the gauge had been bonded onto the exposed root of the fourth premolar. The very thin cortical bone overlying the lateral surface of the root had been inadvertently removed during the preparation of the bone surface prior to the bonding of the gauge. As stated by Lanyon (1973, see section 6.5) the fundamental limitations of the intravital bonding of strain gauges is the present impossibility of satisfactorily calibrating the gauges and the assessment of their degree of bonding to the bone. Therefore, those gauges which showed signs of not being completely bonded to the bone were included in the calculations, for these gauges would give a relative reduced magnitude of strain. A sample on ten cats was thus used in order to reduce these differences in strain magnitude as well as those resulting from the difference in bone thickness below the gauges in the different skulls.

The results recorded on the U-V paper trace are not

presented here graphically nor the summated results for cats (1) and (2). The latter is due to the absence of an initiating impulse on the record, which meant that the Biomac could not summate the results for the different gauges. The recordings for the experiments on cats 3 to 10 are presented in figures 7.1 to 7.12. The signs of the signals from the carnassial brace in figure 7.7 have been reversed from their initial positive sign to a negative sign to indicate a compressive force in the brace. This was necessary as the circuit arrangement of the carnassial brace which formed the opposite side of the Wheatstone bridge to the canine brace, inverted the sign of the signal. Each figure (Figs 7.1 to 7.12) represents the results from cats (3) to (10) of gauges bonded to the brace (Figs 7.1, 7.7) or area of bone listed on the illustration. The number of each cat is indicated on the graph. The abscissa is indicated by a series of crosses set at $\frac{1}{2}$ second intervals, The tetanic stimulation of the muscles commenced $1\frac{1}{2}$ seconds from the beginning of the run and lasts for 2 seconds. The ordinate is the deformation of the bone in microstrain, the scale for each graph having been calculated from equation (6-6), the negative signal represents a compressive strain in the bone, a positive signal a tensile strain. The strain after one second of tetanic stimulation was calculated from equation (6-6) and is given in tables 7.2 and 7.3.

The majority of the strain gauge recordings showed that compressive strain predominated in the facial bones during biting with the brace placed at the canines or carnassials. A few signals showed the strain altering from an initial tensile to a final compressive deformation (Figs 7.2., 7.3., 7.4., 7.8., 7.11.) indicating that the bone was bending in the area immediately below the gauge.

The force of bite in kilograms and the deformation of bone in microstrain is presented in table 7.2 with the brace at the canines and in table 7.3 with the brace placed at the carnassials. The percentage deformation of the cranial bones recorded for each skull is given in tables 7.4 and 7.5. Table 7.6. and 7.7 compares the mean percentage deformation of the skull in the in vivo with the in vitro experiments. The force of bite per kilogram cat body weight at the canines and carnassials is given in tables 7.8 and 7.9 respectively.

7.3. Experimental variation

In general the variation between successive recordings from the gauges during the experiments was very low. This is emphasised by the degree of standard deviation between ten successive recordings from the gauges bonded to the skull (table 7.10).

Variation in the force of contraction of the masseter and temporalis muscles resulting from muscular fatigue and the variable effects of proprioceptive feedback and antidromic stimulation are principally responsible for the differences between individual recordings. Although the effect may be small, account must be taken of the fact that bone is an anisotropic and heterogeneous material and it cannot be assumed that the bone response is identical for a given load applied successively.

7.4. Experimental control in the in vivo strain gauge experiments.

Examination of the differences in strain patterns in the skulls with the different conditions of applied stress confirm, as in the in vitro experiments, that the former is related directly to the latter.

The performance of the control gauge on the frontal process of the maxilla on cat skull (6) established the normal behaviour of

the strain gauges in the <u>in vivo</u> experimental situation. The reversal of the sign from the gauge confirmed the equation for Poisson's ratio, viz: $E_2 = -U.E_1$, where E_1 and E_2 is the strain from two gauges set at right angles to one another at the same point and U is Poisson's ratio.

7.5. <u>Summary and conclusion</u>.

The measurements of bone deformation in the bone were carried out one second after the commencement of the tetanic stimulation, therefore the numerical information employed in the comparison with the <u>in vitro</u> strain gauge results is restricted.

The results of the <u>in vivo</u> strain gauge experiment confirm the viability of the method of intra-vital implantation of gauges onto cat skulls for determining the strain pattern at different regions.

The deformation of the cranial bones, in microstrain, was greater in the <u>in vivo</u> than in the <u>in vitro</u> experiments. Although the relatively greater flexibility is related to the properties of living bone, it would indicate that the <u>in vitro</u> experiments were carried out within the physiological limits of stress applied to the skull <u>in vivo</u>.

With the brace placed at the canines the greatest deformation of the cranial bones occurred at the temporal component of the zygoma, the frontal process of the maxilla and at the frontal bone. When the brace was placed between the carnassials, strain was concentrated in the region of the zygomatic arch and at the maxilla above the fourth premolar. The results are not markedly dissimilar to those from the <u>in vitro</u> experiment; the differences are discussed in the following chapter.

CHAPTER 8

DISCUSSION.

CHAPTER 8

DISCUSSION

8.1. Introduction.

This chapter is divided into three sections. The first is a discussion of the results obtained from the examination of the skull bones in relation to that of previous workers. The second relates to the structural organisation of cat skull bones with the transmission of biting forces during phase I of biting, when the canines are used to apprehend prey, and phase II when food is cut at the carnassials. The third section is a re-examination of the 'Trajectorial Theory' in the light of the results presented in this thesis.

8.2. Discussion of the structural and functional organisation of cat skull bones.

8.2.1. Bone histology.

The histological examination of bone established the structural units of bone described in this thesis. These are the trabeculae of the coarse cancellous bone (Fig 3.2) and the large vascular canals seen in the compact bone (Fig 3.1). The latter are those structures that are readily visible in the projection microradiographs of the compacta and correspond to the alignment of the areas of compact bone between parallel canals. Both the trabeculae and the bone between the canals are concerned with the transmission of biting forces as discussed in the second section of this chapter.

One of the principal difficulties in examining the radiographs, was the variation in mineral density seen in regions of the compact bone which had the effect of confusing the assessment of the frequency of bony bars present. For this reason, greater importance was placed on the large vascular canals for

measuring the orientation and frequency of the areas of bone between parallel canals. In this thesis the term large vascular canal encompasses narrow medullary spaces, resorptive spaces and immature osteones. These spaces are not readily identifiable in the radiographs. This can only satisfactorily be done by means of a histological examination of each of the canals so as to determine the cellular contents and the nature of the vessels within the spaces. The term large vascular canals does not apply to primary and secondary osteones which although present in the compact bone, had vascular canals which were too small to be recorded in the projection microradiographs.

In the histological examination of the bone primary osteones were seen more frequently than Haversian ~~canals~~ systems, this may be a feature of the cat skull bones as well as being due to the Haversian ~~canals~~ systems occurring in mature bone and bone which is continually subject to large stresses (Enlow, 1968). With reference to thq observations of the split-line investigators Moss (1954), Evans and Goff (1957), the recent work of Tappen (1971), and Isotupa (1972), show that it is the large vascular canals which are associated with the production of the split-lines, and not the Haversian canals. This agrees with the present interpretation of the principal structural unit observed in the compact bone, and demonstrates that it has been the tendency of investigators to accept too readily the findings of earlier workers which has led to the Haversian system being accepted as the structural unit within the compact bone of the skulls of higher mammals. As a consequence doubt must fall on the interpretation of the split-line phenomenon by such workers as Benninghoff (1925), Siepel (1948) and Tappen (1953, 1954, 1964, 1970).

8.2.2. Accuracy of projection microradiography as a method of examining the structural organisation of bone.

As described previously (Chapter 2, section 4) the use of X-rays as a method of examining the trabeculation within medullary bone has been rejected by a number of workers. Even Becks and Grimm (1945) in their work on the correlation between the roentgenographic image and the histological appearance of gross changes within human mandibles, state that the roentgenograms confirmed the histological aspect and that "to bring out the differences in structural designs ..... the highest type of roentgenographic techniques ..... must be employed.". In the present study it has been possible, using the projection microradiographic techniques to define the radiographic appearances of the histological organisation of bone.

Although the theoretical limit of resolution of the X-ray microscope has been estimated at 10-20 µm., the actual limit recorded on the photographic emulsion is greater, due to the effect of absorption by the cortical bone on the X-rays. The relatively large figures for the smallest canals (0.06 mm.) and trabeculae (0.14 mm.) recorded is due to this effect as well as that produced by the superimposition of ~~neighbouring~~ structures.

Comparison between the coronal sections and dissected bones with their projection microradiographs showed that the bone structure can be recognised in the radiographs. Hence the position and orientation of structures within the bone can be determined with an accuracy hitherto not possible with other radiographic techniques. However, one difficulty in carrying out the observations on bone was in the regions of the skull where there were well defined separate cortical plates. It was occasionally difficult to distinguish between an area of bone which

lay between two parallel large vascular canals and a single trabeculum lying within a medullary cavity. The distinction was only possible when the stereoscopic pairs of radiographs were examined.

The accuracy of the method of projection microradiography is further demonstrated by the mensural assessment of the effects of bone thickness and superimposition on the number of structures recorded, a test not formerly feasible with structures of this size (Fig 3.7). The results show that within the range of thickness of the cat skull bones, the majority of trabeculae and large vascular canals were recorded on the photographic emulsion.

8.2.3. Structural organisation of the cat skull bones.

The examination of the dissected cat skull bones showed that the trabeculae and large vascular canals are curvilinear structures. In measuring their angular orientation as great a length of the structure as possible was taken into account. The figure recorded was the principal orientation of the structure which avoided recording the minor variations in the course of the trabeculum or canal. This approach is at variance with Moss (1954) who laid great emphasis on the detailed arrangement of the osteones and vascular canals in the surface of the compact bone. Moss's attention to minor variation in the course of structures, if applied to the present study, would produce an enormous amount of data which would render more difficult the determination of the principal orientation of a structure within the bone.

As described in section 5.4. three grades of organisation were recognised in the skull bones. In grade I (Fig 3.9.) the trabeculae and/or canals are orientated in one principal direction and it is therefore possible to assess the mean orientat-

ion of the structures. As seen in transects (1)(Figs 3.17., 3.18) the orientation of a group of structures such as a 'structural continuum' has a mean direction from which it is possible to estimate the angular deviation. Although the measurements of the orientation of the trabeculae and canals were made in the plane of the radiographs it was possible to assess while viewing the stereo-radiographs, under the stereoscope whether the structures were following the conformation of the bone or had altered their grade of organisation. The observations were confirmed by an examination of the stereo-projection radiographs of the skull taken at right angles to the former (Fig 3.8.a and b).

Grade II organisation (Fig 3.10) ~~also~~ represented in transect (4) (Figs 3.17 and 3.18), is the convergence of two grade I's in which the angular divergence between the two is large and in general outside the limits of the angular deviation of each mean structural orientation. This description also applied to grade III (table 3.1.) in those areas in which three grade I's intersected. It is difficult to illustrate a grade III in the dissected bone as the structures were rarely in a single plane. For this reason it was easier to photograph the extreme condition of grade III, which is a complex multidimensional arrangement of trabeculae and canals (Fig 3.11). The defining of the structural organisation of bone in terms of angular orientation and frequency of structures is a method which has apparently not been carried out by previous investigators, as they have employed only one of these criteria in their studies on bone organisation. Moss et al. (1967) used a count of the trabecular frequency in an attempt to compare the dental septae within the alveolar processes of American whites and negroes. Quantitative evaluations of trabecular frequency is employed in the understanding of different

systemic bone diseases (see review in Merz and Schenk, 1970). The supporters of the 'Trajectorial Theory' (Meyer, 1867; Koch, 1917; and others) stated that the angle of intersection between cross-connecting structures was at 90°. Those investigators employing the split-line method were not concerned with the detailed orientation of the underlying structures in the skull bones but more so with the discrete linear arrangement produced by this method. However, Tappen (1969) does describe the split-lines as having an angular divergence of approximately 5° in seven out of nine specimens, the remaining two had an average divergence of 13° and 14° respectively. Siepel (1948) describes, but does not measure, the angles at which a number of his split-lines cross. More recently Sicker and Weinmann (1966) and Hobdell (1970) recognise two types of trabecular organisation within the dental septae of different mammals, which the latter author relates to the degree of divergence of the dental roots.

The method described here of assessing the grade, orientation and frequency of structures within bone can be used to establish a more accurate characterisation of the structural organisation than hitherto of skull and flat bones. With modification the techniques could be applied to long bones.

The stereo-projection microradiographs of the cat skulls enabled the grade of structural organisation within the bones to be readily assessed by the measurement of the angles of orientation of the structures. This method of determining the grade and angle of orientation of the structures showed that there is a consistency of organisation between the skull bones of the cats examined. The greater degree of consistency occurred in the areas of high stress concentration in the facial bones.

This method of recording the structural organisation of

bone overcomes the limitations imposed on the examination of the osseous organisation by the Trajectorial Theory and the split-line method, and on the other hand incorporates the classifications suggested by Sicker and Weinmann (1966) and Hobdell (1970).

The projection radiographs of the cat skulls revealed a variation in the frequency of structures in the same area in the different skulls. These differences were probably due to age and varying nutritional and hormonal conditions within the cats. Thus in order to establish a correspondence between the structural frequency between the different skull bones a reference area was chosen. The orbital plate of the frontal was selected as it was a large area of bone not closely associated with the principal stress bearing zones, and with a structural frequency which was consistently low among the skulls (Fig 3.12). The frequency of structures per millimetre in the orbital plate of each skull was used as the common denominator in order to standardise the frequency of structures in the rest of the skull which provided the means of determining, for purposes of comparison, those areas of greatest structural density.

8.2.4. Consistency of alignment between the large vascular canals and trabecula.

The statistical confirmation of the similarity in the alignment between the large vascular canals and trabeculae is important as it demonstrates a direct association between the structural units of the compact and cancellous bone.

An account of this structural conformity was given by Von Meyer (1867) and Wolff (1870) for the head of the femur. The compact bone of the shaft was described as a condensation of the cancellous bone in the head of the femur. However, this aspect of bone organisation was not included in the Trajectorial

Theory. In the field of functional craniology Benninghoff (1925) was the first to describe the functional unity of the compacta and spongiosa stating that the split-lines produced in the compact bone overlying the spongiosa indicated its underlying trabecular organisation. This observation was extended to describe a contiguity of structural organisation between adjacent areas of compact and cancellous bone. This interpretation of the correspondence between the cortical bone and underlying cancellous organisation has been accepted in general by the investigators using the split-line method. Biepel's (1948) interpretation of the "grain" or direction of the Haversian system in the cortical bone of the jaws is confused, as he freely relates his split-line work with the radiographic appearance of the trabeculae in the mandible described by Walkhoff (1902). Although Benninghoff (1925) was correct in ascribing a contiguity between the compact and cancellous bone, he did not describe the histology of that region to establish its nature. This omission has led to a great deal of inaccuracy in the split-line method.

The structural contiguity between cancellous and compact bone is familiar to histologists and anatomists (Enlow, 1968; Gray, 1973; Fig 3.10., page 217). The statistical confirmation of this correspondence is therefore to a great extent a corroboration of the technique of measuring the orientation of the large vascular canals and trabeculae recorded in the projection microradiographs.

In the compacta, the area of bone between two parallel canals extends as trabeculae in the spongiosa thus forming the unit of a structural continuum which is associated with the transmission of force (section 8.3.1.1. to 8.3.1.5.). The structural continuum

is a region of bone in which the trabeculae and/or large vascular canals exhibit an increased frequency and a higher degree of structural orientation characterised in general by a grade I organisation, e.g. canino-frontal, circumorbital and jugo-temporal continua (Figs. 3.13., 3.16., and table 3.1). The intersection of two structural continua produces a grade II organisation e.g. in the region of the alveolar process of the maxilla with the alveolar-jugal continuum crossing the alveolar-canino-frontal continuum (Figs. 3.13., 3.16. and table 3.1). This also applied to grade III organisation produced by the intersection of three continua, e.g. the region of the alar major of the sphenoid (Figs 3.14., 3.16 and table 3.1).

8.2.5. <u>Discussion on the structural organisation of the cat skull.</u>

This section discusses observations not reported in section 3.7. and their relation to the structural continua described in the results section (Chapter 3).

In figure 3.16. the structural continuum, seen in norma ventralis, running antero-posteriorly in the alveolar process was not readily visible in norma lateralis due to the dense nature of the dental roots absorbing the X-rays.

In approximately half the skulls examined a few large vascular canals were observed lying parallel to the sutural margin. For instance at the superior margin of the frontal process of the maxilla, at the anterior tip of the temporal component of the zygoma immediately below the orbital process, and at the sutural margins between the parietal, temporal and frontal bones. These large vascular canals paralleling the sutural margins were not observed at the remaining sutures. A possible explanation for the presence of these canals is that they are associated with the final stages of growth of the skull bones at their margins

and have no relation to the structural continua in terms of force transmission.

The following structural continua exhibit a grade II pattern within their organisation of the continuum: the alveolar continuum seen in norma ventralis, where there are short cross-connecting trabeculae running medio-laterally at the interdental regions, these are associated with the transmission of the various forces exerted on the teeth. The circumorbital continuum exhibits a grade II,and occasionally a grade III,organisation at the orbital process of the jugal and frontal. Here, as described in greater detail later in section 8.3.1., the complex arrangement of trabeculae recorded is associated with the transmission of tensile strain from the jugal to the frontal. During biting the action of the masseter muscle displaces the posterior part of the jugal inferiorly thus exerting a tensile strain in the post-orbital ligament. The principal direction of this strain is probably altered as the contraction of the fibres in the masseter muscle increases. This variation in force transmission in the post-orbital ligament could account for the detailed arrangement of trabeculae at the tip of the orbital processes of the jugal and frontal (Figs 3.8 and 3.13). Further the trabeculae in the orbital process of the jugal are also closely associated with the compressive strain produced during biting at the anterior one third of the jugo-temporal suture (see chapers 5 and 7, and Fig 8.1).

The structural organisation in the nasal bones does not appear to be directly related with the structural continua of the anterior facial region, except possibly via the structures cross-connecting the canino-frontal continuum in the anterior region of the nasal process of the frontal. Alternatively, these cross-

connecting structures may be associated with complex stresses generated in the antero-superior region of the face at the maxilla-frontal suture.

In the central region and orbital process of the jugal, horizontal trabeculae span the medial and lateral surfaces of the bone. In the temporal component of the zygoma above the glenoid, trabeculae run vertically between the ventral and dorsal surfaces. This trabecular arrangement in areas of high trabecular frequency emphasises the close anatomical and mechanical connection between the two surfaces of the bone.

Within the skull there are areas of complex structural organisation associated with regions where a number of structural continua are confluent. These are defined by grade II and III. Among the most complex type is the basisphenoid into which course structures from the fronto-orbito-temporal, the palato-sphenoid, the jugo-temporal continua and the structures from the temporal squame and tentorium osseum. For this reason the organisation of the basisphenoid was not easily decipherable.

The complex pattern of trabecula and large vascular canals seen in the parietal, temporal squame and the temporal component of the frontal is probably due to the variable deveolpment of the cancellous bone between the exocranial and endocranial surfaces. The former is associated with the functional activity and growth of the temporalis muscle and the latter with the closely adapted brain (Scott, 1967). The structural patterns visible in the temporal component of the frontal bone and the inferior margin of the temporal squame, are orientated in approximately the same direction as the muscle fibres of the temporalis, suggesting that these regions are not under as great a control from the brain as the rest of the calvaria.

8.2.6. Statistical examination of the structural organisation of cat skull bones.

Confidence in the account of the structural continua was confirmed as a result of the statistical analysis of the orientation and frequency of structures bisecting the four transects drawn on the radiographs of the skulls (Fig 2.4.b). There was no statistical difference in the orientation of the structures bisecting transect (1) within the ten cats examined, this applied also to transects (3) and (4). However, the use of statistics did not reveal the minor variations in structural orientation depicted in the rose histograms (Figs 3.17 and 3.18). These histograms showed that transects (1) and (3) were drawn across an area largely comprising a grade I organisation, whereas transect (4) was in the region of a grade II organisation. In transect (4) the majority of the structures were orientated postero-inferiorly along the fronto-orbito-temporal continuum, the lower frequency of structures orientated antero-inferiorly and superio-inferiorly were those of the inferior region of the temporal component of the frontal bone. Within the four transects approximately 5 to 10% of the structures were normal to the principal direction of the structures.

The difference in the results between transect (2) and those of (1), (3) and (4) is the very low structural frequency in (2) (Fig 3.12) and an absence of consistent orientation of the structures bisecting the transect (Fig 3.17 and 3.18). The results of the statistical examination showed that there was no significant difference in the orientation of the structures bisecting the transect between a number of the skulls within the ten examined. The group of skulls showing a similar orientation was slightly greater, in a ratio of four to three, to those which

exhibited no similarity. The differences occurred where the majority of structures bisecting the transect were arranged in a separate quadrant. It would be reasonable to conclude that within the normal variation of structural orientation present in the skulls, that the structural organisation in the orbital plate of the frontal bears no correspondence with that present in the frontal process of the maxilla, the jugal and the orbito-temporal region of the frontal bone, The structural variation observed in the orbital plate could wall account for the differences recorded from the strain gauges bonded to this bone (Fig 5.25 and table 5.1).

Comparison between the transects in skull (F) (Fig 3.18) showed no significant difference in the orientation of the structures in the frontal process of the maxilla (1) and jugal (3) but that these two areas differed significantly with the alignment of the structures in the orbito-temporal region (4). The absence of any significant difference between transect (2) and those of (1), (3) and (4) is due to the very low frequency of structures in the former being beyond the limits for a satisfactory statistical correlation with the recordings from the other three transects which have a relatively higher frequency. This would tend to confirm the adoption of the orbital plate of the frontal as a standard for defining those areas of the skull which exhibit a high degree of structural orientation and increased frequency characteristic of the 'structural continua'.

8.2.7. <u>Structural frequency within the skull bones</u>.

The disadvantage of the method shown in figures 3.13., 3.14., and 3.15 of illustrating the mean frequency of structures within the different areas drawn on the skull is the inability to represent graphically the gradation in the structural frequencies

between adjacent areas. The results show that the greatest number of structures per millimetre occurs in the zygomatic arch and in particular along the orbital margin of the jugal and the temporal component of the zygoma; these are also areas of grade I organisation. The structural frequency is high in the alveolar process of the maxilla, and a brief examination of the latero-medial radiograph of the cat skull (Fig 3.8.a) shows that the alteration in frequency between the alveolar and frontal processes of the maxilla is not as marked as illustrated in figure 3.13. The majority of the structures in the frontal process of the maxilla are concentrated in the circumorbital bar of the maxilla and at a frequency approaching that of the alveolar region, thus presenting a greater continuity of structural frequency in the circumorbital continuum from the jugal to the frontal. The frequency of structures in the anterior region of the frontal bone is continued within the superior and temporal regions of the frontal and parietal bones.

The principal influence of the temporalis on the calvaria is the production of tensile force over its area of attachment. If Oxnard's (1971) hypothesis is correct this force could account for the presence of the thin cortical bone in the temporal component of the frontal and on either side of the groove for the middle meningeal vessels in the temporal bone. Oxnard's (1971) hypothesis states that where net tension exists in bone the latter is either very thin or is replaced by a fibrous sheet. The thin cortical bone of the area of attachment of the pterygoid muscles would tend to support this hypothesis, although, the same conclusion cannot readily be drawn for the area of origin of the masseter.

Here the structures present may be associated with the attachment of the muscle and/or complex mechanical demands imposed on the zygomatic arch. However, Oxnard's hypothesis (1971) does not explain the very low frequency of structures within the bones of the orbital fossa which are areas of practically no stress and where the bone is acting as a supporting role for the tissues of the orbit.

8.2.8. Trabecular frequency in the dental septae of the maxilla and mandible.

In the statistical examination of trabecular bone the frequency of structures is emphasised rather than orientation. The two dimensional mean frequency of interradicular and interdental septae per square millimetre showed an antero-posterior gradient of increasing trabecular density in the maxilla with a maximum at the interradicular septae of P^4 (Fig 3.19 and table 3.4). There is also a small increase in frequency anterior to the canine. The relative number of horizontal to vertical trabeculae within the maxilla is approximately the same although there is a trend towards a slight increase in vertical trabeculae in the interdental septae of $I^3 - C$ and $C - P^2$ (tables 3.5 and 3.6). Although the antero-posterior gradient is a reflection of the combined values for the frequencies of horizontal and vertical trabeculae, there is within the distribution of horizontal trabeculae along the length of the alveolar process a slight increase, although not statistically significant, in their number on the interdental septae of $P^2 - P^3$ and $P^3 - P^4$ (table 3.5). Within the distribution of vertical trabeculae there is a slight increase in the interdental septum of $P^3 - P^4$ relative to the other septae in the alveolar process (table 3.6). These results would suggest that the interdental septum $P^3 - P^4$ should have the highest two-dimensional mean

frequency; the fact that it is slightly smaller than the inter-radicular septum P^4 demonstrates that there is a variation in trabecular organisation in the P^3 - P^4 septum, i.e. different skulls have either a greater number of horizontal or vertical trabeculae , and accounts for the relatively large standard error of the mean for this septum (Fig 3.19).

The results from the mandible exhibit a different pattern from that of the maxilla in that there is no recognisable antero-posterior gradient, the only similarity being a reduction in trabecular frequency at C - P_3 which corresponds to C - P^2 in the maxilla. As in the maxilla, the number of horizontal and vertical trabeculae within the septae is approximately the same. (table 3.7). In comparing the relative trabecular frequency between the maxilla and mandible, the former exceeds that of the latter which agrees with Moss's (1967) findings on the alveolar process of adult American whites and negroes. The results, nonetheless, differ from those of Moss, for his study showed that the vertical trabecular frequency exceeding that of the horizontal trabeculae.

A possible explanation for the antero-posterior gradient of increased trabecular frequency in the post canine region of the maxilla is that the gradient corresponds to the ralative size of the maxillary teeth. The mandibular teeth, compared with those of the maxilla, are approximately the same size which is reflected in the trabecular frequency in the alveolar process of the mandible. The apparent absence of an association between trabecular frequency and the canine, apart from the slight increase in the interdental septum of I^3 - C, is due to a different arrangement of trabecular support for the long root of the canine, where a lower frequency of trabeculae appears to be distributed throughout

the length of the canine root.

An alternative suggestion for the presence of the frequency gradient in the maxilla is that it is related to an increased structural frequency associated with the root the zygomatic arch. This hypothesis is not supported by the work of Moss et al. (1967) as he records a gradient in the mandible, and the root of the zygomatic arch does not bear the same close relationship with the maxillary teeth as it does in the cat. It would appear that Moss's (1967) results support the first hypothesis as the frequency gradient in the alveolar process of man would correspond to the alteration in size of the post-canine teeth.

In the cat the size of the tooth is also proportional to the relative loading of the tooth during biting (Ewer, 1973). The larger post-canine teeth receive a relatively greater proportion of the loading during biting, as well as being those which are specialised for slicing flesh. Therefore, by extension, the trabecular density within the dental septae is proportional to the loading of the teeth and thus agrees with the findings of Walkhoff (1902), D'Arcy Thompson (1942), Scott and Symons (1964) and Johnson (1966).

Under the circumstances just described, the trabecula frequency in the mandible should reflect that recorded in the maxilla. The absence of an antero-posterior gradient in the mandible may be due to the marked divergence of the roots of M_1 which could result in fewer interradicular septae. A large proportion of the support for that tooth appears to come from the attachment of the periodontal ligament to the anterior region of the vertical ramus of the mandible, which would transmit a large proportion of the strain during biting. The absence of an antero-

posterior gradient in the trabecula frequency may also be associated with the configuration of the mandible and may account for the relatively lower frequency of trabeculae in the dental septae compared with the maxilla. An attempt is planned, in the near future, to resolve these difficulties by extending the study to include a variety of mammals.

8.2.9. Re-examination of the earlier methods of examining the structural organisation of skull bones.

Within the organisation of the structural continua described in chapter 3 (section 3.7, Fig 3.16) it is possible to recognise the broad arrangement of buttresses which were originally described in the human skull by Bluntschli (1926, 1929), Weinmann and Sicher (1947) and Sicher and Du Brul (1970). In the cat skull three pillars arise from the basal arch of the alveolar process to anchor it to the neurocranium. They extend up the maxillary process to the frontal, along the zygomatic arch and along the inferior margin of the palatal and pterygoid bones.

The buttress hypothesis is a reflection of the gross morphological organisation of the skull and only in the broadest of terms an indication of the underlying structural organisatin.

Tucker's (1954) description of the arrangement of pressure nodes in the skull is not supported by the present study. However, Tucker's classification of the carnivores skull as 'breviarcuate' agrees with the structural pattern of the canino-frontal and fronto-orbito-temporal continua, which links two areas of high stress concentration, i.e. the canine and glenoid.

An appraisal of the split-line method of examining the organisation of skull bones (Benninghoff, 1925; Siepel, 1948; Tappen, 1953, 1954, 1964, 1970, 1971) has already been made in the

introductory chapter. This method has been fairly extensively used for examining the organisation of skull bones. In my opinion it has been over-rated, for the split-lines are more a reflection of the mechanical response of bone to the puncturing awl, as the vascular spaces and the decalcified inter-lamellar spaces in the compacta act as crack stoppers (Gordon, 1968). The crack stopping behaviour of the compact bone renders it impossible to examine the underlying organisation of bone in order to establish the grade of osseous organisation. The very nature of the technique makes it impossible to ascertain the frequency of structures within the bone. As previously mentioned by Evans (1957) the interpretation of stress and strain in skulls based on the split-line method is entirely theoretical and without any experimental basis. For instance Tappen (1953, 1954) describes a tensile strain being produced in the zygomatic arch as a result of the action of the masseter. This description is in no way confirmed by the present experiments described in section 8.3.

The method of stereo-projection microradiographic examination of the skulls provides means whereby qualitative and quantitative methods can be applied to the assessment of bone organisation. In combination with the experimental techniques it is possible to determine the direction, nature and approximate magnitude of bone deformation under different conditions of stress.

8.2.10. Conclusion.

Within the cat skull there are three types of structural organisation. Type A is a thin compact bone in which course a few large vascular canals and whose orientation bears little or no similarity to that observed in other cat skulls. This type is exemplified by the orbital plate of the frontal. Type B is composed of compact and cancellous bone exhibiting a high degree

of structural orientation and increased frequency ranging from grade I to III. Type B is present in the facial and majority of cranial bones where it exhibits a contiguity between the skull bones such that a structural continuum is established between the attachment of the teeth and that of the masseter and temporalis muscles. Type C is composed of cancellous and compact bone with a complex grade III organisation with a relatively high structural frequency. This type is seen in the parietal and squame of the temporal which are under the morphogenic influence of the brain and the forces exerted by the temporalis.

Within the range of osseous organisation of the cat skull, the structures therein are arranged into continua which unite the facial bones with those of the neurocranium forming a highly integrated functional unit.

8.3.1.1. <u>The relation between the transmission of biting forces in the cat skull and its structural organisation.</u>

With the establishment of the pattern of structural organisation within the cat skull described in the results section 3.7. (Fig 3.16), experiments were then carried out to determine the transmission of force within the cat skull. The results of the latter are presented in chapters 5 and 7.

Any experimental procedure that attempts to determine the deformation of bone, resulting from applied stress, can only ascertain the effect of the latter on the cortical bone. The deformation of structures within the bone, such as the trabeculae can only be inferred; for it is not possible to bond transducers to trabeculae within the bone. Should the cortical bone be removed in order to examine the effect of stress on the cancellous bone, this method could only destroy the system and it would not be possible to perform any meaningful experimental measurements.

Therefore, those techniques which have proved most efficacious in the past for the determination of the deformation of the cortical bone were used in this study. The principal advantage of using a brittle resin followed by the strain gauge technique, as Evans (1957) pointed out, is that the disadvantages of one technique are overcome by the advantages of the other. Thus a maximum amount of information was obtained from the combined use of these methods which is discussed in the following sections.

8.3.1.2. Colophonium resin experiments.

These experiments indicate the areas of strain and its direction in the bone. The resin shows those regions of bone close together which are undergoing similar types of deformation as exemplified by the cracks in one area continuing into those of the next, e.g. a similar strain is present in the superior and inferior margins of the jugal bone (Figs 5.1 to 5.19.). The resin also indicates areas on the skull close together where the orientation of strain is different. This is demonstrated by the resin shattering within itself (Figs. 5.8., 5.9., 5.14., 5.15., 5.17., 5.18., 5.19) or by a marked change in the alignment of the cracks in adjacent areas e.g. the frontal process of the maxilla when the support is placed at the carnassial and the load is applied to the cords representing the masseter muscle (Figs. 5.14 to 5.16). Other examples are seen in the region of the canine eminence of the maxilla (Figs 5.7., 5.16) and on the bones of the hard palate (Figs 5.2., 5.3 and 5.4). In comparing figures 5.10. and 5.19, which represent phase I and II of biting, with the figure 3.16 depicting the alignment of the large vascular canals and trabecula within the cat skull, it can be seen that when a line is drawn normal to the cracks in figures 5.10 and 5.19 that it [redacted] corresponds to the alignment of the underlying structural

organisation. This correspondence between the line drawn normal to the cracks and the underlying structures is seen in all the recordings of the resin experiment although there were a number of situations where there was not a direct correspondence. This occurred when the cords representing only one muscle was being loaded e.g. with the support placed at the canines and the load applied to the cords representing the masseter, a line drawn normal to the direction of the cracks produced by shear strain in the frontal process of the maxilla does not correspond to the underlying structural organisation (compare fig 5.7 with fig 3.16).

As a result of the method of preparation of the cat skulls, the sutures are rigid and the strain is thus transmitted into areas of bone which in the living cat may be mechanically isolated by the soft tissues at the suture, e.g. Figs 5.7., 5.10., 5.16.; the strain in the anterior margin of the orbital plate of the frontal runs parallel to that in the circumorbital bar of the maxilla. The strain in the former zone bears no relation to the underlying large vascular canals within the bone.

8.3.1.3. Strain gauge experiments on dry cat skulls.

Whereas the colophonium resin experiments gave the direction of strain in the bone, the strain gauges recorded the nature of bone deformation. The strain gauges have a linear response along the axis of the gauge; the gauge was thus bonded along the line of strain indicated by the resin experiments which has an orientation corresponding to that of the underlying organisation of the structural continua i.e. the large vascular canals and/or trabeculae. The position of each strain gauge placed on the skulls is tabulated and the positions of some are discussed in relation to the results of the colophonium resin experiments during

phase I and II of biting, and the underlying structural organisation seen in Fig 3.16. (Refer to figures 4.2., 4.3., 4.4.a and table 4.1 for the disposition of the strain gauges on the skulls). Table 8.1. describes the arrangement of the gauges in relation to the direction of the strain recorded in the colophonium resin experiments and to the alignment of the structural continua within the skull. The following strain gauge positions are discussed in more detail.

Gauge at position (3) was bonded so that its axis lay parallel to that of the alveolar margin. This gauge recorded the response of the cortical bone to the stress applied to the carnassial tooth. The horizontal position of the gauge presented the largest recording surface, whereas, the alternative position of a vertically placed gauge would reduce the effective recording area for the tooth as well as record strains associated with the circumorbital region.

Gauge at position (7), the principal axis of the gauge was bonded in a direction similar to that of the gauge on the lateral surface of the jugal and hence along the line of the circumorbital continuum of the jugal. The direction of strain on the medial surface recorded in the resin experiments is at right angles to the alignment of the gauge and continuum, this is due to the mechanical response of bone producing cracks in the resin resulting from tensile strain which is at right angles to the compressive strain in the circumorbital continuum.

Gauge at positions (10) and (11) were at the anterior and posterior margins of the canino-frontal continuum on the maxilla, which recorded the extent of deformation in these regions.

Gauge at position (12), section 4.2.4 described the fan like arrangement of the strain gauges on skull V. The orientation

of the gauge bonded at position (10) on this skull corresponds to both the direction of strain in this region recorded in the resin experiments and to the alignment of the circumorbital continuum of the maxilla. Whereas, the orientation of the gauge at position (11) lay diagonally across the alignment of the anterior margin of the canino-frontal continuum and bore no relationship to the direction of strain recorded in the resin experiments. The vertical alignment of the gauge at position (4) ment that the gauge was slightly out of alignment with the direction of strain in the bone and the underlying canino-frontal continuum.

The gauge at position (13) was bonded normal to the direction of strain recorded in the resin experiments. Both the gauge and the results of the resin experiments bore no relation to the organisation of the orbital bone of the frontal which exhibited a grade III organisation.

The gauge at position (14) bore no relation to underlying structural organisation of bone or to the results of the resin experiments as its purpose was to determine the degree of vertical displacement of the facial bones during biting.

8.3.1.4. Strain gauge experiments on the anaesthetised cats.

The disadvantage of the in vitro strain gauge measurements was that the gauges recorded the response of dry cortical bone which has a greater resistance to strain than the living bone (Evans & Lebow, 1951). Ideally, in order to determine more accurately the response of bone to the stresses exerted during biting, one would have liked to bond many more gauges to the skulls of the living cats. As this was not experimentally feasable, the in vivo experiments were performed to corrobarate the nature and degree of bone deformation recorded in the in vitro experiments, the results presented in tables 7.6 and 7.7

show that this is the case.

Five areas were selected for bonding the gauges on the skulls of anaesthetised cats, which were common to five areas on the dry cat skulls and provided the maximum amount of information on the deformation of the skull bones. The areas chosen were those at positions (1) to (5) in the in vitro experiments, and as shown in the previous section (see table 8.1) the alignment of these gauges corresponds to the underlying strucutral continuum in those regions and to the direction of strain recorded from the colophonium resin experiments.

8.3.1.5. Relation between the results obtained from the experiments and the underlying structural organisation of bone.

Although the resin and strain gauges only recorded the deformation of the cortical bone, it also follows that the surface deformations are not isolated from the internal bone structures. The bone surrounding the large vascular canals in the compact bone and the trabeculae would tend to reflect the overall strain in the bone generated by the forces exerted on the skull. However, within this system local variations in strain are produced in the structures which can not be recorded.

The response of the underlying structures to strain recorded on the surface is illustrated by the following two examples.

(1) The large vascular canals in the frontal process of the maxilla indicate the alignment of the canino-frontal continuum (Fig 3.16). The results of the resin and both the strain gauge experiments show that a compressive strain is transmitted in the same direction as the underlying continuum in phase I and II of biting (Figs 5.10., 5.19., 5.23., 7.5 and 7.11). The frontal process of the maxilla is relatively thin and any strain recorded at the surface must also be transmitted to the bone between the

large vascular canals within the continuum.

(2) The jugal component of the zygomatic arch comprises at its superior margin a grade I organisation of the circumorbital continuum (Fig 3.16) aligned antero-posteriorly. The action of the masseter muscle on the zygoma is to pull the latter inferomedially along the principal line of action of the muscle. The results of the resin and strain gauge experiments show that the entire surface of the arch undergoes compression, (particularly in view of the non-circular cross section of the jugal) (Figs 5.1., 5.5 to 5.10., 5.14. to 5.19., 5.21., 5.25., 7.3., 7.9 and table 5.1). It would be reasonable to infer that the structures in the circumorbital continuum of the jugal are undergoing compression.

A more accurate assessment of the response of the different skull bones to applied stress would have been obtained if gauges had been bonded to both surfaces of the flat bones without damage to the skull, as for instance in the case of the jugal bone (Strain gauge positions (2) and (7) section 4.2.4., Fig 4.2. and table 4.1)

Prior to describing the transmission of force in the cat skull it is necessary to emphasise the relationship between the direction of force in the bone and the alignment of the structures therein.

This study has been concerned primarily with the transmission of force in the anterior facial region. The antero-superior region of the face was chosen for a more detailed examination as the structural organisation in the frontal process of the maxilla exhibited a grade I organisation which did not course simply in a straight vertical line to unite with the structures from the canine on the opposite side, at the anterior region of the frontal; but extended superiorly from the canine

to the frontal process where the structures curved supero-posteriorly into the frontal bone (Fig 3.13) to continue posteriorly in the dorsal region of the frontal (fronto-parietal continuum) and postero-laterally along the orbital margin of the frontal (fronto-post-orbital continuum) (Fig 3.16). The results of the experiments were to establish whether the force generated at the canine during biting was dissipated radially from the area of pressure and if not, in which direction was the strain aligned.

The results of the colophonium resin experiments, with the support at the canine, show that the force from the canine is transmitted superiorly into the frontal process of the maxilla (Figs 5.2 to 5.10). Although when the load was applied only to the cords representing the masseter there is an indication that the strain in the anterior margin of the process is orientated antero-superiorly (Figs 5.5 to 5.7). This was not confirmed by the strain gauge examination, the pattern in the resin resulting from the effect of shear strain in that region.

The results of the strain gauges at position (12) on skull V (Figs 5.23 and 5.24) demonstrate that the compressive strain across the antero-posterior width of the frontal process of the maxilla runs dorsally and then postero-dorsally into the anterior region of the frontal where the compressive strain is recorded by the gauge near the orbital margin of the frontal. The in vivo experimental results confirm the findings of the in vitro experiments (table 7.5) and show that in living bone there is a 2-3% drop in the mean compressive strain between the recordings from the gauges on the frontal process of the maxilla and on the dorsal surface of the frontal (table 7.5). This small change in bone deformation is probably due to the absorptive

action of bone and of the soft tissues in the maxilla-frontal suture.

These results show that the force exerted on the canine does not radiate outwards in the frontal process for practically no strain was recorded passing anteriorly at the anterior margin of the process. That the force does not extend vertically to be cancelled out in the anterior region of the frontal by an equal force from the opposite side of the skull, is demonstrated by the presence of strain in the anterior margin of the frontal process of the maxilla passing postero-superiorly instead of superiorly, and by the existence of the compressive strain in the frontal close to the orbital margin, which also exhibits a close correspondence with the degree of bone deformation in the frontal process of the maxilla. The absence of this close agreement in the degree of bone deformation in the i. vitro experiments is discussed later in this chapter. The transmission of force is in the same direction as the underlying structural organisation, and is further supported by the direction of the compressive strain generated by the support at the carnassial, as it has a similar pattern in the antero-superior facial bones to when the brace is placed at the canines (compare figs 5.4 and 5.13., 5.7 and 5.16., 5.10 and 5.19., see figs 5.23., 5.24., 7.5., 7.11., and table 5.1.).

The results of the gauges bonded to the orbital plate of the frontal corroborate the above findings in that there is no correspondence between the strain transmitted in the posterior margin of the frontal process of the maxilla and that in the orbital plate (Figs 5.24., 5.25. and table 5.1). The pattern of strain recorded in the orbital plate bears no similarity between the skulls or to any correspondence to the different patterns of stress applied to the skulls. This response of the

bone is uncharacteristic when compared with the results of the gauges from other parts of the skull (table 5.1), and is related to the orbital plate being an area of little or no stress. Although strain was recorded from the gauges on the orbital plate in the in vitro experiments, there may well have been even less strain in the in vivo situation due to the effect of the sutures mechanically isolating this bone from the surrounding region of high stress concentration. It is suggested that the pattern of strain in the orbital plate is probably a reflection of the underlying structural organisation of the bone (section 8.2.6.).

These examples demonstrate that it is reasonable to assume that the structures underlying the cortical bone are undergoing a deformation similar to that recorded on the surface of the bone by the resin and strain gauge techniques. Where there are probable differences in the nature of strain is on the surface of a flat bone opposite to that to which the gauge has been cemented, and in the trabecula which would undergo small local deformations.

The results from the experiments carried out are used for describing the transmission of force in the cat skull during biting. Bearing in mind that it is a description which does not take into account the nature of the strain on the endocranial surface, the surface of the facial bones in the nasal cavity and of the small undetectable changes in strain in the trabeculae.

An account of the transmission of force in the cat skull during biting is given in the following sections which are subdivided according to Tucker's (1954) classification of primary, secondary and tertiary stresses in the skull.

8.3.2. Primary stresses exerted by the temporalis

When the support was placed separately at the canines and carnassials. The action of the temporalis muscle is to exert a tensile strain in the postero-superior region ~~of the frontal~~ and antero-superior region of the frontal and antero-superior region of the parietal bones (Figs 5.1 to 5.4., 5.8 to 5.13). The direction of strain, as indicated by the resin experiments, is medial in the parietal and antero-medial and medial in the frontal. In the latter area this direction corresponds with the trabeculae of a similar alignment in the temporal component of the frontal (Fig 3.16).

The strain recorded along the orbito-temporal line (gauge position 16, Fig 5.21, table 5.1) indicates that under the conditions in which the load is applied to the cords representing the temporalis and combined temporalis and masseter, a tensile strain passes in the fronto-orbital-temporal continuum (Fig 3.16) which is approximately parallel to the anterior fibres of the temporalis. The tensile strain generated under the action of the combined temporalis and masseter is in general not as large as with the temporalis alone (Fig 5.21), this is due to the influence of the action of the masseter tending to produce in the fronto-orbito-temporal continuum a low compressive strain when the support is placed at the canine and low tensile with the support at the carnassials. These results indicate that the continuum within the orbito-temporal line is closely associated with the transmission of tensile strain exerted by the action of the temporalis muscle.

8.3.3. Primary stresses exerted by the masseter.

When the support was placed separately at the canines and carnassials. The strain produced by the masseter is located in

the posterior margin of the alveolar process of the maxilla and the jugal. The strain in the inferior orbital margin is also closely associated with tertiary stresses and is thus described in the two sections.

The action of the masseter is to exert a postero-inferior pull on the inferior margin of the jugal which results in the jugal rotating slightly inferiorly relative to its fulcrum at the middle of the jugo-maxillary suture. The zygomatic suture separates along the posterior two thirds of its length causing the jugal to be compressed against the anterior surface of the temporal component of the zygoma (Figs 5.1., 5.5 to 5.10., 5.14 to 5.19). With the load applied to the cords representing the masseter and the support at the canines, the <u>in vitro</u> strain gauge experiments show that the jugal tends to reduce its lateral curvature, becoming flatter as a large compressive strain and a small tensile strain were recorded from the lateral and medial surfaces respectively (Figs 5.21., 5.25 and table 5.1). A condition which is produced in the jugal by a slight medial pull to the principal action of the masseter muscle.

Under the remaining conditions in which stress is applied to the skull, a compressive strain was recorded on the lateral and medial surfaces of the jugal, indicating that the jugal was being pulled vertically downwards. The recordings from the gauges (position 2) attached to skulls III and IV (table 5.1) gave anomalous results for when the load was applied to the cords representing the combined temporalis and masseter muscles. This was probably due to an error in the method of load application to the cords for the same error is present when the support was placed at the canines and carnassials (Fig 5.21). The presence of a compressive strain on the lateral surface of the jugal is

confirmed by the in vivo experiments (Figs 7.3 and 7.9). These experiments also showed the jugal undergoing an initial lateral bending, represented by a tensile strain (Fig 7.3), in cats (3) and (4) prior to establishing the compressive strain associated with the downward movement of the jugal. With the rejection of the recordings from gauge (position 2) on skulls III and IV under the combined action of the temporalis and masseter, the results in Tables 5.2 and 7.6 are altered to give a compressive strain. The results in Table 7.6 then show a close agreement between the in vitro and in vivo experiments for the percentage strain present in the jugal in phase I and II of biting.

The area of attachment of the masseter muscle on the jugal and posterior margin of the maxilla can be regarded as part of a narrow round arch with a single pillar. Its apex is at the maxillo-jugal suture and a support is fitted to the pillar half way down its length at the jugo-temporal suture immediately posterior to the prbital process of the jugal. The action of the masseter produces a compressive strain in the alveolar-jugal continuum and in the circumorbital continuum of the jugal. With an increase in stress applied by the masseter to the jugal, the temporal process of the jugal rotates inferiorly causing the posterior two thirds of the jugo-temporal suture to separate (Figs 5.5 to 5.10., 5.14 to 5.19), compressive strain is transmitted across the anterior third of the jugo-temporal suture from the jugal to the temporal bone (Fig 8.1). The area immediately inferior to the orbital process of the jugal and anterior to the suture, is a region in which a large compressive strain runs antero-posteriorly and in a number of skulls shear strain present is represented by an internal shattering of the colophonium resin (Figs 5.6., 5.8., 5.14 to 5.19). However, in the majority of the skulls the cracks

in the resin occur at right angles to those on the rest of the body of the jugal indicating that the dominant horizontal compressive strain is expressed as a vertical tensile strain which continues into the orbital process of the jugal (Figs 5.2 to 5.19).

In the living cat the post-orbital ligament would prevent too large an inferior rotation of the jugal during biting by transmitting some of the stress as a tensile strain in the ligament to the post-orbital process of the frontal thus reducing the shear strain in the jugal. The transmission of force in the area around the orbital process of the jugal and its attendant structures is complex and requires a more detailed study to reveal a precise account of their interactions.

8.3.4. Secondary stresses produced at the glenoid.

When the support was placed separately at the canines and carnassials. With the load applied to the cords representing the temporalis muscle, the compressive stress produced in the glenoid fossa by the supports appears to be transmitted to the basisphenoid and would account for the tensile strain recorded in the temporal component of the zygomatic arch (gauge position 1) (Fig 5.20 table 5.1). This tensile strain in the zygoma is also associated with a similar strain in the jugal (Fig 5.21., table 5.1) indicating that under these conditions the secondary stress is continuous with those in the jugal. Thus with the load applied to the temporalis along the zygomatic arch tends to bow laterally.

With the load applied to the cords representing either the masseter or combined masseter and temporalis, the compressive stress exerted by the supports at the glenoid fossae is transmitted as a large compressive strain in jugo-temporal continuum (Fig 5.20 table 5.1). The concentration of strain at

the anterior region of the jugo-temporal suture (Figs 5.5 to 5.7, 5.14 to 5.16), when the load was applied to the cords representing the masseter, confirms that the compressive strain is running anteriorly in the jugo-temporal continuum and posteriorly in the alveolar-jugal continuum. This pattern of strain is similar for when the load was applied to the cords representing the combined temporalis and masseter, although in the latter case the degree of bone deformation was not as large. The in vivo experiments corroborate the presence of the compressive strain in the jugo-temporal continuum and that it is larger than that recorded in the jugal under phase I and II of biting (tables 7.5., 7.7). The moderately larger compressive strain recorded on the lateral surface of the temporal component of the zygoma in the in vitro experiments relative to that recorded in the in vivo situation is probably due to the eccentric support of the brackets placed in the glenoid fossae (Fig 4.1.a). With an increase in the load applied to the skull via the cords representing the muscles, the brackets would tend to bend under the load and a greater proportion of the stress would be applied by them to the lateral region of the glenoid fossa and thus be transmitted along the zygoma.

The presence of a compressive strain in the jugo-temporal continuum indicates that the articular condyles of the mandibles exerts a compressive force in the glenoid fossa during biting. This agrees with the theoretical conclusions of Scapino (1965) and Badoux (1971) for the pressures generated in the glenoid fossa by the mandibular condyle during jaw closure in the dog; and Davis (1955) conclusion that the combined action of the muscles tends to reduce the force at the glenoid is confirmed experimentally. However, the results of my experiments and the

conclusions of Scapino (1965) and Badoux (1971) leads to the rejection of Maynard Smith and Savages (1959) conclusion that when both muscles are in contraction the resultant moment of force acting at the temporo-mandibular joint is small or absent.

8.3.5.1. Tertiary stresses: with the support placed at the canines and the load applied to the cords representing the temporalis muscle.

In phase I of biting the role of the canine is in the catching of the prey and the piercing of its skin. The force exerted on the canine is not vertical but directed antero-superiorly at the tip of canine (Maynard Smith and Savage 1959). The stress results in the antero-superior rotation of the canine about an axis immediately proximal to its cervical line, which can be resolved into two components: (1) vertical, in which the stress is transmitted vertically up the canine and to the bone at its antero-superior surface, and producing a vertical tensile strain via the periodontal ligament in the premaxilla at the anterior surface of the canine, and in the region immediately posterior to the canine; (2) anterior rotation, produces an anterior compressive strain in the alveolar process of the premaxilla, and a posterior compression proximal to the apex of the canine which would pass along the postero-superiorly orientated structures to the circum-orbital continuum.

As the load is applied to the temporalis, the compressive strain in the canine increases initially (Fig 5.25), the subsequent decrease in strain is due to the marked anterior rotation of the canine which results from the length of the lever arm between the canine and the fulcrum at the glenoid. The resin experiments indicate an anterior compressive strain in the alveolar process of the premaxilla and an infered tensile strain in the

nasal process of the premaxilla (Figs 5.2 to 5.4). The latter tensile strain is not recorded by the strain gauge in skull IV and may be due to the overall strain in this region being relatively low particularly in skull IV. In the canino-frontal continuum a low compressive strain is transmitted vertically. The strain recorded at the anterior region of the maxilla and internasal region (table 5.1) is absent or within experimental variation. The compressive strain in the frontal process is concentrated close to the orbital margin and extends along the canino-frontal continuum into the frontal bone.

The stresses exerted on the skull under the present conditions causes the zygomatic arch to bow outwards resulting in (1) tensile strain in the circumorbital continuum of the jugal, the alveolar-jugal and jugo-temporal continua, and (2) a compressive strain in the circumorbital continuum of the maxilla. The tensile strain in the alveolar jugal continuum above the fourth premolar is not only related to the lateral bowing of the zygomatic arch, but also to the tensile strain produced along the alveolar process of the maxilla resulting from the stress applied to the canine. The tensile strain in the alveolar process is also seen in the cracks in the resin on the horizontal process of the maxilla (Figs 5.2 to 5.4). The strain in the palatine bone is approximately normal to that in the horizontal process of the maxilla and is produced probably by the strain in the zygomatic arch. The absence of strain recorded from the gauge on the palate is due to its position which is at the junction between the two sets of strain in the hard palate (Fig 5.4), their combined effect tending to cancel one another which suggests that the strain in the palatine bone is compressive.

8.3.5.2. Tertiary stresses: with the support placed at the canine and the load applied to the cords representing the masseter muscle.

The compressive force exerted at the canines extends vertically in the canine, producing an anterior compressive strain in the alveolar process of the premaxilla and a tensile strain in the nasal process of the premaxilla. The compressive strain passes vertically up the canino-frontal continuum in its central region and anterior margin, to pass into the frontal bone (Figs 5.5 to 5.7., table 5.1). The postero-superior compressive strain recorded at the internasal region indicated the superior rotation of the anterior facial bones (Figs 5.24., table 5.1). This is corroborated by the inferior rotation of the jugal through the action of the masseter which produces a compressive strain on the lateral surface of the jugal, and a tensile strain on its medial surface, which results in the medial bowing or flattening of the zygomatic arch (Figs 5.21., 5.25. table 5.1). Directly associated with this movement is the tensile strain in the circumorbital continuum of the maxilla (Fig 5.24) and the continuation of the compressive strain from the jugal part of the alveolar-jugal continuum into alveolar process of the maxilla above the fourth premolar (Fig 5.22). The presence of tensile strain recorded on the palate (Fig 5.25) supports the superior rotation of the anterior facial bones and indicates that the strain immediately posterior to the canine and anterior to the fourth premolar is tensile.

The result of the superior rotation of the anterior facial bones and the inferior rotation of the jugal is that a shear strain is produced in the frontal process of the maxilla by the tensile strain in the circumorbital continuum of the maxilla and the compressive strain in the canino-frontal continuum, a

phenomenon clearly demonstrated by the results from the resin experiments (Figs 5.5 to 5.7).

8.3.5.3. Tertiary stresses: with the support placed at the canines and stress exerted by both the temporalis and masseter muscles.

In general the strain produced by this system is less than that produced by the effects of the temporalis and masseter separately and in magnitude between those values produced by the two systems (table 5.1).

The pattern of the strain is similar to that described, for when the load was applied to the cords representing the masseter muscle (compare figs 5.7 and 5.10). The stresses applied to the skull result in a superior rotation of the anterior facial bones through the effect of the large vertical compressive strain exerted on the canine. The jugal rotates inferiorly through the action of the masseter. The movement is restricted to the sagittal plane through the contra-acting effects of both muscles. The extremely low tensile strain in the circumorbital continuum of the maxilla means that there is little or no shear strain in the frontal process of the maxilla. The results of the two in vitro experiments is confirmed by the recordings from the in vivo strain gauge experiments (table 7.5).

8.3.6.1. Tertiary stresses: with the support at the carnassials and the load applied to the cords representing the temporalis muscle.

In phase II of biting the role of the carnassial is in the slicing of flesh, the compressive strain exerted on the tooth is transmitted via the periodontal ligament as a tensile strain along the inferior margin of the alveolar process and a resulting vertical compressive strain in the posterior region of the alveolar process of the maxilla.

Under the present conditions of stress applied to the skull, the results of the resin and strain gauge experiments show that the tensile strain from the carnassial is transmitted horizontally along the alveolar process of the maxilla,and as a low compressive strain in the premaxilla and canine eminence (Figs 5.13., 5.22). A shear strain is present in the frontal process of the maxilla, as a tensile strain was recorded from the gauges at the internasal region and anterior margin of the frontal process, and a compressive strain at the circumorbital bar of the maxilla (Fig 5.24). Apart from skull IV the tensile strain at the anterior margin of the frontal process of the maxilla continues into the frontal bone at a reduced magnitude.

The strain pattern in the structural continua of the jugal is similar to that described in section 8.3.5.1. with the support at the canine. This accounts for the compressive strain in the circumorbital continuum of the maxilla, and the tensile strain in the alveolar region of the alveolar-jugal continuum, which combines with the tensile strain from the carnassial to produce a resulting magnitude in strain greater than that exerted in this region, when the support was placed at the canines.

The alignment of resin cracks on the hard palate show that the principal direction of strain passes medially, at right angles to the position of the strain gauge (Figs 5.12., 5.13). The latter recorded a compressive strain indicating that a tensile strain is passing medio-laterally (Fig 5.25. table 5.1). The cracks in the resin on the dorsal surface of the maxilla (Fig 5.13) may be either tensile related to the lateral bowing of the zygomatic arch, or compressive associated with the tensile strain on the ventral surface of the palatal process of the maxilla.

The overall pattern of strain in the skull shows that the zygomatic arch bows laterally and that there is a tendency for the carnassials to move laterally resulting in the tension in the palate and a medial compression of the antero-superior region of the maxilla and internasal accounts for the tensile strain recorded from the gauges in that region.

8.3.6.2. Tertiary stresses: with the support at the carnassials and the load applied to the cords representing the masseter muscle.

The proximity of the primary and tertiary stresses results in the production of very large strains in the infra-orbital region (Figs 5.14 to 5.16., table 5.1).

The strains produced by the masseter have been described in earlier sections, suffice it to say that the tensile strain produced in the circumorbital continuum of the maxilla under these conditions is much greater and extends as far as the post-orbital process of the frontal (Fig 5.16). The large compressive strain in the alveolar-jugal continuum appears to over-ride the tensile strain produced in the posterior alveolar region by the pressure on the carnassial (Fig 5.22). The compressive strain from the latter passes antero-superiorly, anterior to the infra-orbital foramen and up the anterior margin of the frontal process of the maxilla which produced a resulting tensile strain in the premaxilla (Fig 5.16). The low compressive strain recorded at the internasal region (Fig 5.24., table 5.1) indicates that as a result of the stresses there is a slight superior rotation of the anterior facial bones which causes a large shearing strain in the frontal process of the maxilla. The superior displacement of the anterior facial bones is corroborated by the presence of an antero-posterior tensile strain in the posterior part of the ventral surface of the palate (Fig 5.25., table 5.1) and a compressive strain at right angles to the latter on the dorsal surface of the maxilla.

8.3.6.3. Tertiary stresses: with the support at the carnassial and stress exerted by both the temporalis and masseter muscles.

The counteracting effects of the temporalis and masseter muscles on the strain produced in the skull is described in section 8.3.5.3. when the support was placed at the canine. With the inferior rotation of the jugal in the sagittal plane there is only a low tensile strain in the circumorbital continuum of the maxilla (table 5.1). The compressive strain in the jugal region of the alveolar-jugal continuum is replaced by the low horizontal tensile strain in the alveolar region of the continuum produced by the stress at the carnassial, except in skull IV where a very large compressive strain in the alveolar-jugal continuum produced by the masseter over-rides the strain generated at the carnassial (Fig 5.22). The compressive strain from the carnassial extends antero-superiorly, anterior to the infra-orbital foramen along the alveolar-canino-frontal continuum. There is no superior rotation of the anterior facial bones for no strain was recorded from the internasal regions. As a consequence the shear strain in the frontal process of the maxilla is very low. The strain recorded in the frontal is very low and is of a variable pattern (Fig 5.23) and would indicate that the strain has been largely absorbed by the facial bones. This applies also to the results when stress was applied separately to the temporalis and masseter. The compressive strain in the posterior region of the hard palate is at an angle of between 30° - 40° to the direction of strain directly medial to the alveolar process of the maxilla (Fig 5.19). The latter is probably tensile as it is associated with the tensile strain in the premaxilla which results from the transmission of the compressive strain from the carnassial antero-superiorly to the

frontal process of the maxilla. The latero-medially directed strain on the dorsal surface of the maxilla is approximately normal to that on the ventral surface indicating a compressive strain.

Comparison between the results from the <u>in vivo</u> and <u>in vitro</u> experiments (table 7.7.) shows that although there is a large degree of agreement, the results from the latter experiments demonstrate a greater variation in the magnitude of the percentage strain recorded from the dry skulls as well as between the same areas on the skull in the two experimental conditions, viz: the temporal region of the zygoma, the maxilla above the fourth premolar and the frontal bone.

The larger compressive strain in the temporal component of the zygomatic arch recorded in the <u>in vitro</u> experiment (table 5.1 and 7.7) is very probably due to the differences between the mechanical arrangement of the support at the glenoid and the direction of pressure exerted by the mandibular condyle. The results from the gauge bonded to the maxilla above the fourth premolar (table 7.7) indicate that in the anaesthetised cats the compressive strain in the alveolar-jugal continuum is greater than the horizontal tensile strain produced by the pressure at the carnassial. This suggests that the effect of the pull of the masseter on the alveolar-jugal continuum is greater than that produced by the brace at the carnassial, except on cat (4) where a very low tensile strain was recorded (Fig 7.10, table 7.5). Either the mechanical arrangement in the <u>in vitro</u> experiments or the relative pull exerted on the cords representing the masseter is probably such as to account for the slight dominance of the horizontal tensile strain produced by the carnassial in the alveolar process. The <u>in vivo</u> recordings from the gauges on

the frontal bone shows that compressive strain is more effectively transmitted along the canino-frontal continuum of the frontal process of the maxilla into the frontal bone than in the *in vitro* experiments, this is discussed more fully in section 8.3.9.

The percentage strain recorded from the jugal and frontal process of the maxilla is of the same order of magnitude in the *in vivo* and *in vitro* experiments (table 7.7). The overall results of the *in vivo* experiments confirm the general findings of the *in vitro* experiments but also show that inaccuracies are present in the latter under conditions in which large strains are produced in dry bone close to one another.

8.3.7. A discussion on some points arising from the configuration of the signal from the *in vivo* gauge experiments.

As stated in the results of the *in vivo* strain gauge experiments (chapter 7), the region of the signal examined was one second after the initiation of the tetanic stimulation to the muscles. However, an examination of the traces from the experiments raises two points which are briefly discussed in the context of the information at present available.

Approximately three quarters of all the *in vivo* signals showed an initial rapid peak response to the initiation of the tetanic stimulus. A few of these signals depicted the strain altering from an initial tensile to a final compressive deformation (Figs 7.2.,7.3.,7.4.,7.8.,7.11) indicating that the bone was bending in the area immediately below the gauge. In the majority of the signals, however, an initial peak compressive strain was recorded which declined to a lower compressive strain within approximately quarter of a second. It is suggested that the configuration of these signals is related to the performance of

the soft tissues within the facial sutures, and in particular to that of the zygoma between the temporal and jugal. The following interpretation is based on results obtained from a pilot study (Buckland-Wright, 1972) which demonstrated in the anaesthetised cat that on tetanic stimulation of the temporalis and masseter muscles the jugal and temporal bones on either side of the zygomatic suture separated by as much as 40 μm. It is suggested that the initial peak response is due to the deformation of bone resulting from the stress exerted on the bone from the contraction of the masseter and temporalis muscles. That this peak strain is not maintained is probably due to the opening of the zygomatic suture with the attendant stretching of the sutural collagen fibres which results along with other minor movements in the remaining facial sutures, in the superior rotation of the anterior facial bones. This alteration in the relationship between the facial bones during the bite, effects a more efficatious transmission of force from the antero-inferior region of the face to the cranium and reduces the maximum amount of strain initially produced by the muscles. The fall in strain recorded by the gauges represents the changes taking place at the sutures. This mechanism has the advantage of reducing the potential amount of strain in the skull and maintaining it at a level below that produced initially by the muscles.

With the termination of the stimulation, the area between the base line and the initial rapid drop in strain is probably associated with the relaxation of the muscles and the energy released in the reorganisation of the collagen fibres within the facial sutures. Close to the base line the curve of decreasing strain shows a second point of deflection where the curve depicts a more gradual reduction in the strain. This feature is probably

associated with the phenomenon of creep in bone and is the gradual release of energy in the bone following its deformation. The absence of initial peak responses in a few of the signals may be due to the sutures opening and/or reorganising prior to the onset of the maximum strain produced by the contraction of the muscles.

This description of the generalised shape of the signal recorded during biting in the anaesthetised cat is probably an oversimplification as it is likely that there are other phenomena present which have not been accounted for. In order to elucidate the role of sutures during biting further work is to be carried out on the anatomy of the sutural tissues and their relation to the type of strain being transmitted across the syndesmoses.

The second point arising from the configuration of the signal recorded from the <u>in vivo</u> gauge experiments concerns the piezoelectric effect of bone. This hypothesis states that in "whole bones, cortical bone strips and component parts of the tooth .... osseus accretion is the result of compressive loads and resorption the result of tensile loads", (Bassett, 1972). If this statement is to be upheld in the <u>in vivo</u> situation then any bone of the skull from which compressive strain has been recorded during biting must subsequently undergo a tensile deformation of approximately equal magnitude if the skull bone is to remain a constant shape. The results of the <u>in vivo</u> experiments (Figs 7.1 to 7.12) show that this is clearly not the case except with the possible exception of cat (10) Fig 7.5, and that compressive strain predominates in the facial bones. The fact that the cat skull does not increase in bone thickness nor alter its configuration during its life would tend to contradict the

piezoelectric hypothesis of bone and an alternative statement of the hypothesis will have to be found to describe the phenomena observed by the investigators in this field. An alternative explanation is that the anticipated tensile strain, subsequent to the removal of stimulation, is present but not recorded by the gauge. This could be due to the effects of hysteresis in the bone and the alterations in the sutures masking the tensile strain. The latter would be contained within the curve of the signal depicting the return of the deformed bone to zero. This explanation can not be tested with the equipment described in this thesis and it remains that the present experiments contradict the hypothesis of piezoelectricity when applied to whole bones.

8.3.8. Force of bite at the canines and carnassials.

The maximum mean force of bite per kilogram body weight recorded at the canines (table 7.8) corresponds closely to that found by Khodorov (1970) for the power of the jaw muscles in the dog which he quotes as 8.3 times its own body weight. This is not far from the results obtained by Robins (personal communication 1974) for the inter-incisal force produced in rats which is just under ten times their body weight.

The low results of the force of bite exerted at the carnassials (table 7.9) is probably due to the masticatory muscles being stretched beyond their normal physiological length by the brace. In view of the mechanical design of the jaws for exerting a larger force at the carnassials than at the canines (Maynard Smith and Savage, 1959) I suggest that the recordings from cats (7) and (9) may be closer to the maximum force of bite exerted at the carnassials; viz: 11 kilogram force per kilogram body weight.

A precise examination of the force of bite is out of the scope of this thesis but a more detailed examination is intended. In this connection it would be possible to determine the force of bite at the carnassials by calculating the degree to which the mean sarcomere length of the masseter and temporalis has been stretched from a mensural knowledge of the specimens and the dimensions of the carnassial brace. And on the basis of the work of Bishop et al. (1973) and Nordstrom and Yemm (1973) to estimate the correction factor which would have to be applied to the results of the force of bite recorded at the carnassials.

8.3.9. The transmission of force in the cat skull during phase I and II of biting.

Under conditions of phase I of biting the greatest percentage deformation of bone occurred as a compressive strain along the canino-frontal and jugo-temporal continua (table 7.6). The compressive strain in the jugal part of the circumorbital continuum and in the alveolar part of the alveolar-jugal continuum is relatively lower and is due to the superior rotation of the anterior facial bones producing a tensile strain in alveolar continuum (section 8.3.5.3).

In phase II of biting the areas of greatest percentage bone deformation, apart from that in the jugo-temporal continuum, is the reverse from that in phase I. The largest compressive strain occurs in the circumorbital continuum of the jugal and the alveolar part of the alveolar-jugal continuum above the fourth premolar (table 7.7). The compressive strain in the canino-frontal continuum of the maxilla and frontal is relatively lower (table 7.7). A proportion of the stress from the carnassial would appear to be transmitted postero-laterally in the palato-sphenoid continuum (Figs 5.19., 5.25., tables 5.1., 5.3., section 8.3.6.3). The

results show that during jaw closure in phase I and II of biting, compressive strain predominates in the facial bones. From the mechanical point of view bone is particularly well adapted to resist compression rather than tension (Dempster and Liddicoat, 1952; Evans, 1957; Gordon, 1968). The largest apparent tensile strain in the skull is transmitted by the collagen fibres of the post-orbital ligament (section 8.3.3). In comparing the strain generated in phase I and II of biting it is proportionally greater in the former (tables 7.6 and 7.7) as the moment of load about the glenoid is relatively larger, a conclusion reached by Endo (1965) for the human skull.

Examination of the gross morphology of the cat skull without a knowledge of the internal structure would tend to lead to the suggestion that the compressive strain produced at the carnassial is transmitted posteriorly along the zygomatic arch and superiorly in the circumorbital via the maxilla. This speculation is based on patterns suggested by the investigators using the split-line method and in particular Tappen (1953), 1954). The above pattern of strain is disproved by the present experiments which demonstrate the transmission of compressive strain in phase I and II of biting from the region of the alveolar process into the frontal process of the maxilla and in particular the superior part of the canino-frontal continuum (sections 8.3.5.3 and 8.3.6.3.). The broad similarity in the overall strain pattern in phase I and II of biting is attributed to the structural organisation of the facial bones (Figs 3.16 and 8.1).

The distribution of strain around the orbit is in general similar to that in the human skull described by Endo (1965). Large compressive strains are present at the superior and inferior margins of the orbital ring and tensile strains at the anterior

and posterior margins. Endo (1965) draws a direct comparison between the strain observed on the human skull to the distribution of stresses along the contour line of a circular hole within an infinite plate which is subject to a shearing force acting upwards in the anterior region and downwards in the posterior part. Examination of figure 8.1. shows that this is an over-simplificatior of the situation, for under phase I of biting in the cat, where the above analogy would appear to operate, this is not the case, as a low compressive strain is present instead of the tensile strain at the anterior margin of the orbit (tables 5.2 and 7.6). The compressive strain is associated with the extension superiorly of the compressive strain exerted on the canine, which is transmitted to the circumorbital continuum of the maxilla as a result of the antero-superior rotation of the cusp of the canine. That the compressive strain in the anterior orbital margin is of a relatively low magnitude may be due to the influence of the tensile strain produced by the shearing strain around the orbit.

The shear strain around the orbit is present in phase II of biting, where the compressive strain from the carnassial has been transmitted to the antero-superior part of the facial bones (section 8.3.6.3). The tensile strain in the circumorbital continuum of the maxilla is very low, and is not proportional to the compressive strains in the superior and inferior regions of the circumorbital continuum, a necessary feature of the elasticity theory when applied to the hole in a plate of infinite size. The analogy, although applicable in general terms, is an over-simplification principally because it assumes that bone is an homogeneous material and it does not take into account the role of the highly organised internal structure.

The pattern of strain depicted in figure 8.1. demonstrates that as a result of biting, the principal mechanical response in the facial skeleton is a vertical bending moment relative to the neurocranium about an axis in the region of the jugal. This bending moment is greatest in phase I of biting. Endo's work (1965) showed that the greatest deformation resulting from this moment occurred at the antero-inferior facial bones and the area of bone about the tooth to which the load was applied. The results of the in vitro experiments (chapter 5) described in this thesis exhibit a similar pattern, but in addition the zygomatic arch shows a greater magnitude of strain compared with Endo's results for the same region on the human skull. The present in vivo experiments show a similar pattern although the extent of bone deformation is considerably greater throughout the facial bones (table 7.6 and 7.7), indicating that in living bone compressive strain is transmitted rapidly along the structural continua within the skull with relatively little absorption of strain. Whereas in the dry skull compressive strain does not extend so far in the skull, demonstrating that dry bone is stronger in compression than in the living bone. The second factor associated with the absorption of strain in bone is the presence of hysteresis which was recorded from the strain gauges on the skull bones under conditions of compressive and tensile strain in the in vitro experiments (Figs 5.20 to5.25). The difference between the curves for increasing and decreasing loads represents the extent to which energy was absorbed by the bone, this feature was described in dry limb bones by Marique (1945). Hysteresis is seen for the first time in the recordings from the in vivo experiments where the deformation produced in the bone does not return to zero immediately after the removal of the stimulus to

the muscles, there is instead a gradual drop in strain. The area below the line of declining strain from the point at which the stress is removed until zero strain is reached is partly an indication of the energy absorbed by the bone during the action of biting (section 8.3.1.5).

The results of the <u>in vitro</u> experiments clearly demonstrate that the magnitude of the strain in the skull bones was less under the combined action of the temporalis and masseter than when the load was applied separately to the cords representing either muscle (tables 5.2 and 5.3). In general the action of the temporalis was to produce a tensile strain, whereas a compressive strain resulted from the stress exerted by the masseter (tables 5.2 and 5.3). Of the two muscles the magnitude of strain produced by the action of the masseter was slightly greater than that of the temporalis. The contra-acting role of the muscles of mastication on the deformation of the facial bones was described as early as 1922 by Wetzel in his experiments on decalcified skulls. More recently, this feature of muscles reducing the loading strain in bones has been recorded by Pauwels (1948, 1951) and Rybicki <u>et al</u> (1972) in their respective photo-elastic and mathematical analysis of stress in limb bones. The investigators using photo-elastic models (section 1.4.2) were the only people to carry out some form of experimental work to relate the observed structural organisation of bone with the experimental results. The findings presented in this thesis emphasise the importance of carrying out a variety of experiments to determine the strain pattern transmitted in bone; and that no confidence can be placed on the strain patterns based on the beam theory and its application to the Trajectorial Theory (Benninghoff, 1925; Siepel, 1948; Tappen, 1953, 1954; and others).

Examination of the figures 3.16 and 8.1 shows that there is an arrangement of loops which demonstrates the contiguity of structural and functional organisation between the skull bones and the presence of the structural continua connecting the attachment of the teeth with that of the temporalis and masseter muscles. The structural organisation of the alveolar process is such as to transmit the strain produced at the canine or carnassials to the canino-frontal continuum. This continuum forms the anterior part of the anterior facial loop which extends from the temporal bone along jugo-temporal, alveolar-jugal and alveolar continua into the canino-frontal continuum and posteriorly into the parietal via the fronto-parietal continuum. This anterior facial loop is closely associated with the smaller orbital loop of which the canino-frontal continuum forms a part. In norma ventralis the teeth are placed within the alveolar continuum which forms a maxillary loop, the latter extends posteriorly along the palato-sphenoid continuum to the basisphenoid where it is interconnected with the structures associated with the stresses exerted by the temporalis. At the postero-lateral margin of the maxilla the maxillary loop is connected to the attachment of the masseter via the alveolar-jugal continuum.

The structural organisation of the cat skull is such that the strain produced during biting is not only resisted by the inherent mechanical property of bone, but is also transmitted along the structural continua to a region where it can be more effectively resisted: (1) in using the property of incompressibility of bone to resist compressive strains within the skull. This is most effectively achieved by transmitting the strain to a region of thick bone of which the following are the most obvious examples: (a) compression in the canino-frontal continuum is resisted by

the large area of cancellous bone in the superior region of the frontal and parietal bones (Fig 3.8); (b) the basisphenoid is a region which is a complex structural organisation resisting in large part the compressive strain resulting from the action of the temporalis muscle and transmitted across the temporo-sphenoid suture, the inferior continuation of the fronto-orbito-temporal continuum and of any stresses produced in the tentorium osseum. The basisphenoid also receives stresses from other parts of the skull, such as those exerted by the pterygoid muscle in the fronto-sphenoid continuum, those stresses that are present in the palato-sphenoid continuum and probably secondary stresses from the glenoid (Fig 8.1). It is conceivable that these stresses reaching the basisphenoid may contra-act to reduce the overall level of strain within the bone.

(2) in which strain is resisted through the effect of soft tissues. (a) The role of the post-orbital ligament (section 8.3.3.). The action of the masseter exerts a downward pull on the jugal producing a large compressive strain in the circumorbital continuum of the jugal and alveolar-jugal continuum, this in turn generates a large compressive strain at the anterior third of the jugo-temporal suture. These compressive strains are prevented from increasing through the post-orbital ligament resisting the downward movement of the jugal and transmitting the resulting tensile strain into the post-orbital process of the frontal, where the latter strain may assist in reducing the compressive strain in the superior part of the canino-frontal continuum (Fig 8.1). (b) The compressive strain in the superior region of the canino-frontal continuum may be reduced through the tensile strain produced approximately normal to the continuum by the action of the temporalis muscle. (c) The contraction of the masseter muscle exerts a large compressive strain in the alveolar-

jugal continuum which over-rides the horizontal tensile strain produced in the alveolar region by pressure on the carnassial.

8.3.10. Conclusion.

The cat skull consists of a series of plates within which the structural continua are continuous and form a series of loops which functionally unite the facial bones to the neurocranium. Primary, secondary and tertiary stresses generated in the skull during biting are transmitted along the structural continua to regions in the skull where the strain is more effectively resisted or counteracted by other strains in a manner to reduce the overall deformation of bone.

Knowledge of the magnitude and direction of strain within the structural continua reveals more information on the organisation of the 'structural continua', and confirms the observations of D'Arcy Thompson (1943), Frost (1964), Johnson (1966), and Bassett (1966, 1971a, b). Namely the frequency of structures appears to correspond directly to the magnitude of strain transmitted therein, for example, the zygomatic arch (Fig 3.13, tables 7.6 and 7.7) and dental septae of the maxilla (section 8.2.8). In those regions of the skull where the magnitude of strain is large, as in the zygomatic arch and frontal process of the maxilla (tables 7.6 and 7.7) the structures exhibit a uniformity of alignment (Fig 3.16). Where there is one principal strain present a grade I organisation exists (jugo-temporal continuum). In a grade II organisation there are two principal stresses orientated in different directions, for example the alveolar region around the fourth premolar (Figs 3.13 and 3.16). The grade of organisation is therefore an indication of the complexity of the strain pattern (section 8.2.4). There appears to be no correspondence between the size of the trabeculae in the

cat skull and the nature of the strain transmitted within the structures as suggested by Koch (1917). This is corroborated by the fact that during the various phases of biting the nature of the strains in different parts of the skull is reversed (Figs 7.2., 7.3., 7.4).

The mammalian skull is traditionally regarded as a rigid box and is described so by Endo (1965). However, the presence of a moderately flexible post-orbital ligament and the separation of the posterior two thirds of the zygomatic suture indicated by the results of the resin experiment (section 8.3.3.) and an initial pilot study (Buckland-Wright, 1972) demonstrated the presence of a flexible component within the cat skull. The advantages of such a system within the cat skull is that very large forces can be exerted during biting without the danger of over stressing the facial bones which could potentially be the case in a rigid system.

8.4.1. Re-examination of the Trajectorial Theory.

The Trajectorial Theory is founded principally on the mathematical interpretation of a two dimensional model (section 1.2.1 and 1.4.1) and supported by the experimental work of the photo-elastic studies (section 1.4.2). These two methods are corroborative as they are based on their common assumption of the characteristics of bone behaviour. Inspite of recent attempts at expanding the methodology in order to overcome the limitations (Kummer, 1972; Breckelmans et al, 1972; Rybicki, et al 1972), it nevertheless remains that their interpretation of bone behaviour is limited, for the assumptions are fundamentally incorrect (Kuntscher, 1934; Goodman, 1971). This applies also to the efforts of the split-line workers to describe the distribution of force within bone for their interpretation is based on the Trajectorial Theory and without any experimental support (sections 1.3.2., 8.3.9)

The results presented in this thesis add to the criticism of the Trajectorial Theory. The stereo-projection microradiographs showed that no individual structure was orientated in a straight line or curve (sections 3.2., 3.4., 8.2.3., figs 3.3 to 3.11) which agrees with Tdepel's (1922a) rejection of the theory on the grounds that the 'trajectories' did not appear in the bones as calcified entities.

The theory also states that 'the compression resisting trajectories are set at right angles to those of tension in accordance with the mathematical laws of stress distribution in solid homogeneous bodies'. The second part of this definition has already been examined and is established as being invalid (sections 1.2.1 and 1.3.2). However, it is necessary to examine the aspect of the orthogonal arrangement of bone, particularly as it is this feature that has characterised the Trajectorial Theory and to which its exponents have strongly adhered.

In the present study few structures were observed to have an orthogonal arrangement, the rose histograms (transect (1), figs 3.17., 3.18) showed that within a single structural continuum approximately 5 to 10% of the structures were at right angles to the principal orientation of the structures within the continuum. Where a grade II organisation was present the angle of intersection between the structures was infrequently orthogonal (transect (4), figs 3.17, 3.18). The mean angle of intersection indicated the angular separation between the two forces being transmitted within the structures of the grade II organisation (section 8.2.4). By extension this also applied to a grade III organisation where structures were aligned in three principal directions.

Contrary to the principles of orthogonality defined by the Trajectorial Theory, structures parallel to one another in the skull transmitted strains of an opposite nature (sections 8.3.5.3. and 8.3.6.3). For instance in the circumorbital and canino-frontal continua in the maxilla under phase II of biting (Fig 8.1). This example, along with others, described in the text demonstrates that Koch's (1917) concept of the tensile bearing trabeculae being relatively thinner than those of compression is not tenable as it is not supported by the observational and experimental evidence.

The situation remains that although the Trajectorial Theory has been discredited since the 1920's (Jansen, 1920; Thepel, 1922a; Carrey, 1929) no successful alternative theory has been suggested. This may be due to the investigators tending to concentrate on the problem of analysing the extremely complex stresses in the head and neck of the femur. The investigations presented in this thesis adds to the accumulating evidence against the Trajectorial Theory, and in particular the unacceptability of the orthogonal arrangement of trabeculae. The emphasis on the orientation and relative frequency of large vascular canals and trabeculae in relation to the results obtained from the experiments laid the foundation for proposing the 'Structural Continuum Theory'.

8.4.2. <u>The structural continuum theory</u>.

As the beam theory has been shown to be inadequate in describing bone behaviour (Goodman, 1971; Breckelmans <u>et al</u>., 1972; Rybicki <u>et al</u>., 1972) emphasis was placed, in the present study, on the detailed organisation of the structures within the bones and their relation to the regions of stress in the skull (section 8.3.1.). These observations form the basis of the 'structural continuum theory' which states:

(1) The structural continuum is a zone in the bone which exhibits a relatively higher degree of structural orientation and increased structural frequency (sections 3.4., 3.6., 3.7., 8.2.6., 8.2.7) and consists, in the compacta, of areas of bone delineated by parallel vascular canals which are contiguous with the trabeculae of the spongiosa (sections 3.5., 8.2.4.).

(2) A structural continuum is aligned along the direction of one internal strain whether tensile or compressive in nature (sections 8.3.1.5., 8.3.9). Where strain is orientated in two or more directions it is transmitted by similar numbers of continua (section 8.3.9).

(3) Structural continua transmitting tensile or compressive strain do not necessarily have an orthogonal arrangement (sections 3.6., 3.7., 8.2.3., 8.3.9), but are aligned in the optimum direction for the transmission of strain (section 8.3.1.5) to a region in the bone where it is resisted by (a) an equal and opposite strain generated within the system, and/or (b) the large energy absorbing capacity of a thicker region of bone (section 8.3.9).

The structural continuum theory can be summarised as follows:

'The structural continuum is the common structural unit of the compact and cancellous bone, which transmits stress in the direction of the maximum internal strain to a region in the bone where it is effectively resisted'.

This definition does not alter the concepts stated in the theories of Wolff (1892) on bone transformation and of Roux (1895) on bone adaptation as they are understood in the literature today (e.g. Hoyte and Enlow, 1966) as the mathematical basis of the theories is no longer taken into consideration. One of Trdpel's (1922a) principal criticisms of the Trajectorial Theory is that should all the lines be drawn from every point on the periphery of

the trajectorial diagram, the resulting figure would be entirely blackened, and by analogy the spongiosa should be composed of compact bone. This criticism does not apply to the 'structural continuum theory' as the maximum size a single structure can reach is defined by the distance between the osteocytes at its centre and the nearest capillary at the periphery (Ham, 1952). The minimum distance from one structure to the next is related to the diameter of the capillaries in the bone. This condition agrees with Evans' (1957) statement that the size of the structures is not dependent on mechanical stimulation.

The 'structural continuum theory' is based on results obtained from the examination of flat bones. The theory would appear to be applicable to the structural organisation within limb bones but that this can be confirmed by further research along lines similar to those described in this thesis.

REFERENCES

Ahrens, H.J. (1936) Die Entwicklung der Spaltlinienarchitektur des Knochernen menschlichen Schadels. Morph. Jahrb., 77 : 357-371.

Ardenne, M. von (1939) Zur Leistungsfähigkeit des Elektronen-Schatten-microskopes und uber ein Röntgenstrahlen-Schattenmikroskop. Naturwissenschaften, 27 : 485-486.

Ascenzi, A. and Bell, G.H. (1972) Bone as a mechanical engineering problem. In 'The Biochemistry and Physiology of Bone.' Vol 1. Bourne, G.H. (ed.) Academic Press : London.

Badoux, D.M. (1971) Some notes on the stress in the caudal part of the lower jaw in domesticated dog. Proc. Kon. Nederl. Akad. Wetenschappen, Sieries C, 75 : 34-43.

Barth, M. (1919) Ueber die funktionelle Struktur des Oberkieferapparates bei Neuweltaffen. Anatomische Hefte I, 56 : 171-242.

Bassett, C.A.L. (1966) Electromechanical fadors regulating bone architecture. Calc. Tissue 1965, Proc. 3rd. Eur. Symp., 78-89.

Bassett, C.A.L. (1971a) Effect of force on skeletal tissues. In Physical Basis for Rehabilitation. Downey, J. and Darling, R.E. (eds.). Saunders : Philadelphia.

Bassett, C.A.L. (1971b) Biophysical principles affecting bone structure. In Biochemistry and Physiology of Bone. Vol 3. Bourne, G.H. (ed.) Academic Press : London.

Bassett, C.A.L. (1972) A biophysical approach to craniofacial morphogenesis. Acta Morph. Neerl. Scand., 10 : 71-86.

Becks, H. and Grimm, D.H. (1945) Comparative X-ray and histological study of the human mandible. Am. J. Orthodont., Oral Surg., 31 : 383-406.

Bellman, S. (1953) Microangiography. Acta Radiol. Suppl. 102. pp 104.

Bender, I. and Seltzer, S. (1961) Roentgenographic and direct observation of experimental lesions in bone. J. Amer. dent. Ass., 62 : 152-160.

Benninghoff, A. (1925) Spaltlinien am Knochen, eine Methode zur Ermittlung der Architekture platter Knochen. Verh. Anat. Gesellsch., Anat Anz., 60 : 189-206.

Bigelow, H.T. (1875) The true neck of the femur : its structure and pathology. Bost. Med. Surg. J., 92 : 1-5, 29-33.

Bishop, M.A., Nordstrom, S.H. and Yemm, R. (1973) The relationship between the sarcomere length and jaw position in the masseter muscle of the rat. J. Dent. Res., 52 : 933.

Bluntschli, H. (1926a) Rückwirkungen des Kieferapparatus auf den Gesamtschädel. Z. zahnarzt. Orthop., 18 : 3. Cited Siepel, 1948.

Bluntschli, H. (1926b) Die menschlichen Kieferwerkzeuge in verschiedenen Alterszustanden. Verh. anat. ges. Anat. Anz., 61 : 163-174.

Bluntschli, H. (1929) Von den Kräften, welche den Kiefer bewegen und Gestalten. Paradentium, 1929 : 3.

Böhmig, R and Prévôt, R. (1931) Verleichende Untersuchengen zur Pathologie und Rontgenologie der Wirbelsaule. Fortschr. Rontgenstr., 43 : 541-575.

Borak, J. (1942) Relationship between the clinical and roentgenological findings in bone metastases. Surg. Gynaec. Obstet., 75 : 599-604.

Brekelmans, W.A.M., Poort, H.W. and Slooff, T.J.J.H. (1972) A new model to analyse the mechanical behaviour of skeletal parts. Acta orthop. scand., 43 : 301-317.

Broadhent, B.H. (1931) A new X-ray technique and its application to orthodontia. Angle orthodont., 1 : 45-66.

Bruhnke, J. (1929) Ein Beitrag zur Struktur der Knochencompakta bei Quadrupen. Morph. Jahrb., 61 : 555-588.

Buckland-Wright, J.C. (1970a) The distribution of masticatory forces in the breviarcuate skull, as represented by Canis familiaris and Felis catus. B.Sc. Dissertation. London University.

Buckland-Wright, J.C. (1970b) A radiographic examination of frontal sinuses in early British populations. Man, (Proc. Roy. Anthrop. Soc., N.S.) 5 : 512-517.

Buckland-Wright, J.C. (1972) The shock-absorbing effect of cranial sutures in certain mammals. J. Dent. Res., 51 : 1241.

Burstein, A.H., Schaffer, B.W. and Frankel, V.H. (1970) Elastic analysis of condylar structures. Presented at A.S.M.E. Winter Annual Meeting. December 1970, New York. Cited Rybicki et al 1972.

Carey, E.J. (1929) Studies in the dynamics of histogenesis. Experimental, surgical and roentgenographic studies in the architecture of human cancellous bone, the resultant of back pressure vectors of muscle action. Radiol., 13 : 127-168.

Chasin, A. (1928) Die Dimensionen destruktiven Veränderungen in den roentgenographisch bestimunt werden Konnen. Fortsch. Roentgenstrhl., 37 : 529-535.

Cochran, G. van B. (1972) Implantation of strain gauges on bone in vivo. J. Biomechanics, 5 : 119-123.

Cosslet, V.E. (1957) Optimum conditions of magnification and contrast in projection X-ray microscopy. In X-ray Microscopy and Microradiography. Cosslett, V.E., Engstrom, A. and Pattee, H. (eds.). Academic Press : New York.

Cosslett, V.E. and Nixon, W.C. (1951) X-ray shadow microscope. Nature, 168 : 24-25.

Cosslett, V.E. and Nixon, W.C. (1952a) X-ray shadow microscope. Nature, 170 : 436-438.

Cosslett, V.E. and Nixon, W.C. (1952b) An experimental X-ray shadow microscope. Proc. roy. Soc., B., 140 : 422-431.

Cosslett, V.E. and Nixon, W.C., (1953) X-ray shadow microscope. J. Appl. Phys., 24 : 616-623

Cosslett, V.E. and Nixon, W.C. (1960) X-ray Microscopy. Cambridge University Press.

Cosslett, V.E. and Taylor, [illegible]. (1948) Progress report, Cavendish Laboratory, Cambridge. Cited Cosslett and Nixon, 1960.

Czermak, P. (1897) Ann. Phys., Lpz., 60 : 760. cited Cosslett and Nixon (1960).

D'Arcy Thompson, W. (1942) On Growth and Form. U.P. Cambridge.

Davida, L. von (1915) Die Struktur des unterkiefers. Festchrift zum Prof. K. Lechner. Klausenburg. 1915.

Davis, D.D. (1955) Masticatory apparatus in the spectacled bear, Tremarctos ornatus. Fieldiana, Zool., 37 : 25-45.

Dempster, W.T. (1967) Correlation of types of cortical grain structure with architectural features of the human skull. Am. J. Anat., 120 : 7-32.

Dempster, W.T. and Enlow, D.H. (1959) Patterns of vascular channels in the cortex of the human mandible. Anat. Rec., 135 : 185-205.

Dempster, W.T. and Liddicoat, R.T. (1952) Compact bone as a non-isotropic material. Am. J. Anat., 91 : 331-362.

Dowgjallo, N.D. (1932) Die Struktur der Compacta des Unterkiefers bei normalen und reduzietem Alveolarfortsatz. Z. Anat. Ent. gesch., 97 : 55-67.

DuBrul, E.L. and Sicher, H. (1954) The Adaptive Chin. Thomas : Springfield.

Dwight, T. (1875) Remarks on the position of the femur and its so-called neck. J. Anat. Physiol., 9 : 311-314.

Ely, R.V. (1957) Fine focue X-ray tube with turret window and rotatable target. In X-ray Microscopy and Microradiography. Cosslett, V.E., Engstrom, A. and Pattee, H.H. (eds.) Academic Press : New York.

Ely, R.V. (1972) X-ray microscopy. In Physical Methods of Chemistry Part III. Weissberger, A. and Rossiter, B.W. (eds.). Wiley and Sons.

Endo, B. (1965) Distribution of stress and strain produced in the human facial skeleton by the masticatory force. J. Anthrop. soc. Jappan, 73 : 123-136.

Enlow, D.H. (1968) The Human Face. Hoeber : New York.

Evans, F.G. (1953) Methods of studying the biomechanical significance of bone form. Am. J. Phys. Anthrop., 11 : 414-436.

Evans, F.G. (1957) Stress and train in Bones. Their Relation to Fracture and Osteogenesis. Thomas : Springfield.

Evans, F.G., and Goff, C.W. (1957) A comparative study of the primate femur by means of the stresscoat and split-line techniques. Am. J. Phys. Anthrop., 15 : 59-77.

Evans, F.G., Hayes, J.F. and Powers, J.E. (1953) "Stresscoat" deformation studies of the human femur under transverse loading. Anat. Rec., 116 : 171-188.

Evans, F.G and Lebow, M. (1951) Regional differences in some of the physical properties of the human femur. J. Appl. Physiol., 3 : 563-572.

Evans, F.G. and Lebow, M. (1952) The strength of the human compact bone as revealed by engineering techniques. Am. J. Surg., 83 : 326-331.

Evans, F.G. and Lissner, H.R. (1948) "Stresscoat" deformation studies of the femur under static vertical loading. Anat. Rec., 100 : 159-190.

Evans, F.G. and Lissner, H.R. and Pedersen, H.E. (1948) Deformation studies of the femur under dynamic vertical loading. Anat. Rec., 101 : 225-241.

Evans, F.G. Pendersen, H.E. and Lissner, H.R. (1951) The role of tensile stress in the mechanism of femoral fractures. J. Bone Int. Surg., 33A : 485-501.

Ewer, R.F. (1973) The Carnivores. Weidenfeld & Nicholson : London.

Forest, A.V. de and Ellis, G. (1940) Brittle lacquer as an aid to stress analysis. J. Aeronaut. Sc., 7 : 205-208.

Frankel, V.H. and Burstein, A.H. (1964) Load capacity of tabular bone. In Biomechanics and Related Bio-Engineering Topics. Kenedi, R.M. (ed.) Proceedings of a symposium held in Glasgow. Sept. 1964.

Frossblad, P. (1959) Determination of elastic modulus of bone. Acta. orthop. scand., 28 : 262-268.

Frost, H.M. (1964) The Laws of Bone Structure. Thomas : Springfield.

Galilei, G. (1638) "Discorsi e Demostrazioni Matematiche Intorno a Due Nuove Scienze." Leida : Elsevirii. English translation by H. Crew & A. de Salvio. Constable : London. 1914.

Goldman, H., Millsap, J. and Brenman, H.S. (1957) Origin of registration of the architectural pattern, the lamina dura and the alveolar crest in the dental radiograph. Oral Surg., Oral Med., Oral Path., 10 : 749-758.

Goodman, T. (1971) The Internal Architecture of the Head and Neck of the Femur. M.Sc. Dissertation, Surrey University.

Gordon, J.E. (1968) The New Science of Strong Material. Penguin : London.

Gray, H. (1973) Anatomy. Descriptive and Applied. 35th Ed. Warwick, R. and Williams, P.L. (eds.). Longmans : London.

Grunewald, J. (1920) Die Beanspruchung der langen Röhrenknochen des Meschen. Z. Orthop. Chir., 39 : 27-49; 129-147; 257-286.

Gurdjian, E.S. and Lissner, H.R. (1944) Mechanism of head injury as studied by cathode ray oscilloscope. Preliminary report. J. Neurosurg., 1 : 393-399.

Gurdjian, E.S. and Lissner, H.R. (1945) Deformation of the skull in head injury. A study with the "stresscoat" technique. Surg. gynec., Obst., 81 : 679-687.

Gurdjian, E.S. and Lissner, H.R. (1946) Deformations of the skull in head injury studied by the "stresscoat" technique, quantitative determinations. Surg. Gynec. Obst., 83 : 219-233.

Gurdjian, E.S. and Lissner, H.R.(1947) Deformations of the skull in head injury as studies by the "stresscoat" technique. Am. J. Surg., 73 : 269-281.

Gurdjian, E.S. and Lissner, H.R. and Webster, J.E. (1947) The mechanism of production of linear skull fracture. Further studies on the deformation of the skull by "stresscoat" technique. Surg. gynec., Obst., 85 : 195-210.

Gurdjian, E.S. and Webster, J.E. (1947) The mechanism and management of injuries of the head. J. Am. Med. Assoc., 134 : 1072-1076.

Gurdjian, E.S. and Webster, J.E. and Lissner, H.R. (1950) The mechanism of skull fracture. J. Neurosurg., 7 : 106-114.

Gurdjian, E.S. and Webster, J.E. and Lissner, H.R. (1953) Observations on prediction of fracture site in head injury. Radiol., 60 : 226-235.

Hall, T.A., Rockert, H.O.E. and Saunders, R.L. de C.H. (1972) X-ray Microscopy in Clinical and Experimental Medicine. Thomas : Springfield.

Hallermann. (1934) Die Beziehungen der Werkstoffmechanik und Werstofforschung zur allgemeinen Knochen-Mechanik. Verh. Deutsch. orthop. Gesch., 62 : 347-360.

Ham, A. (1952) Some histophysiological problems peculiar to calcified tissues. J. Bone, Int. Surg., 34A : 701-728.

Havers, C. (1692) Osteologia Nova or some new observations of the bones, and parts belonging to them; with the manner of their accretion and nutrition. Innys : London 1729 (2nd Ed.).

Henkel, K.O. (1931) Vergleishend-anatomische Untersuchungen über die Struktur der Knochencompakta nach der Spaltlinien-methode. Morph. Jahrb., 66 : 22-45.

Hirsch, C. and Brodetti, A. (1956) The weight bearing capacity of structural elements in femoral necks. Acta. orthop. Scand., 26 : 15-24.

Hirsch, C. and Evans, F.G. (1965) Studies on some physical properties of infant compact bone. Acta. orthop. Scand., 35 : 300-313.

Hobdell, M.H. (1970) The relationship between the function and structural organisation of bone in the jaws of mammals. Ph.D. Thesis. London University.

Hoyte, D.A.N. and Enlow, D.H. (1966) Wolff's law and the problem of muscle attachment on resprptive surfaces of bone. Am. J. Phys. Anthrop., 24 : 205-214.

Humphrey, G.M. (1858) A Treatise of the Human Skeleton. Cambridge.

Isotupa, K. (1972) Alizarin trajectories in experimental studies of skull growth. Proc. Finnish Dent. Soc., 68 : 1-49. Suppl II.

Jansen, M. (1920) On Bone Formation. Manchester U.P.

Johnson, L.C. (1966) The principles of structural analysis. In Human Palaeopathology, Proceedings of a Symposium on Human Palaeopathology. Jarcho, J. (ed.). Yale U.P.

Khodorov, B. (1970) Muscular contraction. In Human Physiology Vol 2. Babsky, E.B. (ed.), Shirokov, Y. (translator). Mir Publishers : Moscow.

Knese, K-H. (1956) Belastungsuntersuchungen des oberschenkels unter des Annahme des Knichens. Morph. Jarb., 97 : 405-452.

Knief, J.J. (1967a) Quantitative Untersuchung der Verteilung der Hartsubstanzen im Knochen in ihre Beziehung zur lokalen mechanischen Beanspruchung. Methodik und Biomechanische Problematik, dargestelt am Beispiel des coxalen Femurendes. Z. Anat., 126 : 55-80.

Knief, J.J. (1967b) Materialverteilung und Beanspruchungsverteilungim coxalen Femurende. Densitometrische und spaunungsoptische Untersuchungen. Z. Anat., 126 : 81-116.

Koch, J.C. (1917) The laws of bone architecture. Am. J. Anat., 21 177-298.

Koellicker, A.V. (1850) A manual of human microscopic anatomy. Translated : Busk, G. and Huxley, T. Parker : London.

Konermann, H. (1970) Dichteverteilung im Röntgenbilde des Skeletts. Naturwisschaften, 5 : 255.

Konermann, H. (1971) Quantitative Bestimmung der Materialverteilung nach Rontgenbildern des Knochens mit einer neuer fotografischer Methode. Z. Anat., 134 : 13-48.

Kummer, B.K.F. (1956) Eine Vereinfachte Methode zur Darstellung von spannungstrajektorien gleichzeitig ein Modellversuch fur die Ansrichtung und Dichteverteilung der spongiosa in den Gelenkenden der Röhrenknochen. Achter Beitrag zur funktionellen Anatomie und kausslen Morphologie des Stützapporates von Friedrich Pauwels. Z. Anat., 119 : 223-234.

Kummer, B.K.F. (1959) Bauprinzipien des Saugerskeletes. Thieme : Stuttgart.

Kummer, B.K.F. (1966) Photoelastic studies on the functional structure of bone. Fol. biotheoret., 6 : 31-40.

Kummer, B.K.F. (1972) Biomechanics of bone. In Biomechanics. Its Foundations and objectives. Fung, Y.C., Perrone, N. and Annliker, M. (eds.). Prentice Hall : New Jersey.

Kuntscher, G. (1934) Die Darstellung des Kraftfusses im Knochen. Zentralbi. Chir., 61 : 2130-2136.

Kuntscher, G. (1935a) Die Bedentung der Darstellung des Kraftflusses im Knochen fur die Chirurgie. Arch. Klin. Chir., 182 : 489-551.

Kuntscher, G. (1935b) Uber den Nachweis von Spannungspitzen am menschlichen Knochengrut, Morph. Jahrb., 75 : 427-444.

Kuntscher, G. (1936) Die Spannungsverteilung am Schenkelhals. Arch. Klim. Chir., 185 : 308-321.

Lanyon, L.E. (1971) Strain in sheep lumbar vertebrae recorded during life. Acta orthop. scand., 42 : 102-112.

Lanyon, L.E. (1972) In vivo bone strain recorded from thorasic vertebrae of sheep. J. Biomechanics, 5 : 277-281.

Lanyon, L.E. (1973) Analysis of surface bone strain in the calcaneus of sheep during normal locomotion. J. Biomechanics, 6 : 41-19.

Lanyon, L.E. and Smith, R.N. (1969) Measurements of bone strain in the walking animal. Res. Vet. Sci., 10 : 93-94.

Lanyon, L.E. and Smith, R.N. (1970) Bone strain in the tibia during normal quadrupedal locomotion. Acta orthop. scand., 41 : 238-248.

Latham, R.V. (1966) A review of 3-dimensional techniques in micro X-radiography. J. roy. microsc. soc., 85 : 255-282.

Latham, R.V. (1968) A theoretical assessment of a proposed technique of stereo-tomography. J. roy. microsc. Soc., 88 : 183-187.

Le Gros Clark, W.E. (1971) The Tissues of the Body. 6th Ed. Clarendon : Oxford.

Le Poole, J.B. and Ong, S.P. (1957) Description of the Deft X-ray microscope. In X-Ray Microscopy and Microradiography. Cosslett, V.E., Engstrom, A. and Pattee, H. (eds.). Academic Press : New York.

Lewin (1913) Die innere Struktur der Mandibula der Anthropinen und Anthropoiden in mechanischer Belenchtung. Diss. Bonn 1913. Cited Siepel. 1948.

Lissner, H.R. (1964 The response of the human body to impact. In Biomechanics and Related Bio-Engineering Topics. Kenedi, R.M. (ed.) Proceedings of a symposium held in Glasgow, Sept. 1964.

Lissner, H.R. and Roberts, V.L. (1966) Evaluation of skeletal impacts of human cadavers. In studies on the Anatomy and Function of B nes and Joints. Evans, F.G. (ed.) Springer : Berlin.

MacMillan, H.W. (1928) Radiographic and histological evidence of the functional adaption of the alveolar process. J. Am. Dent. Ass., 15 : 316-321.

Malsch, von F. (1939) Erzengung stark vergröberter Röntgen Schattenbilder. Naturwissenschaften, 27 : 854-855.

Marique, P. (1945) Études sur le Fémur. Librairie des Sciences : Bruxelles.

Marton, L. (1939) Internal Report, R.C.A. Laboratories, Princetown. Cited Cosslett and Nixon, 1960.

Maynard Smith, J. and Savage R.J.C. (1959) The mechanics of the mammalian jaws. Sch. Sci. Rev., 141 : 289-301.

McLeisch, R.D. and Charnley, J. (1970) Abduction forces in the one legged stance. J. Biomechanics, 3 : 191-209.

Merkel, F. van (1874) Betrachtungen über das Os femoris. Virchows Arch., 59 : 237-256.

Merz, W.A. and Schenk, R.K. (1970) Quantitatove structural analysis of human cancellous bone. Acta anat., 75 : 54-66.

Messerer, O. (1880) Über Elasticität und Festigkeit der menschlichen Knochen. Cotta : Stuttgart.

Meyer, H. von (1867) Die Architektur des Spongiosa. Arch. Anat. Physiol., 34 : 615-628.

Milch, H. (1940) Photoelastic studies of bone form. J. Bone Jnt. Surg., 22 : 621-626.

Moss, M.L. (1954) Demonstration of the intrinsic vascular pattern of compact bone. Am. J. Phys. Anthrop., 12 : 373-380.

Moss, M.L., Chase, P. and Kameros, J. (1967) Trabecular bone structure of post canine alveolar processes in adult American whites and negroes. Acta anat., 67 : 399-423.

Murray, P.D.F. (1936) Bones. Cambridge UP.

Nixon, W.C. (1961) X-ray microscopy. Contemp. Phys., 2 : 183-197.

Nordstrom, S.H. and Yemm, R. (1973) The effect of length changes on the isometric active tension produced by direct stimulation of the rat masseter muscle, J. Dent. Res., 52 : 933.

Olivo,, O.M., Maj, G. and Toajari, E. (1937) Sul significato della minuta struttura del tessuto osseo compatto. Bull. delle Sci. Med., 109 : 369-394.

Oxnard, C.E. (1971) Tensile forces in skeletal structures. J. Morph., 134 : 425-436.

Pacini, A.J. (1922) Roentgenray anthropometry of the skull. J. Rad., 3 : 230-237; 322-331; 418-426.

Pauwels, F. (1948) Die Bedentung der Bauprinzipien des Stütz und Bewegungsapparates fur die Beanspruchung der Röhrenknochen. Beitrag zur funktionellen Anatomie und Kausalen Morphologie des Stútzapparates. Z. Anat. Entwickl., 114 : 129-166.

Pauwels, F. (1950) Uber die mechanische Bedeutung der Gröberen Kortikalisstruktur beim normalen und pathologischen verbogenen Röhrenknochen. Anat. Nachrichten., 1 : 53-67.

Pauwels, F. (1951) Über die Bedeutung der Bauprinzipien des Stütz und Bewegungsapparates fur die Beanspruchung des Röhrenknochen. Acta. anat., 12 : 207-227.

Pauwels, F. (1954) Uber die Verteilung der Spongiosadichte im coxalen Femurende und ihre Bedeutung fur die Lehre vom funktionellen Bau des Knochens. Siebenter Beitrag zur funktionellen Anatomie und kausalen Morphologie des Stütz apparates. Morph. Jb., 95 : 35-54.

Pauwels, F. (1965) Gesammelte Abhandlungen zur funktionellen Anatomie des Bewegungsappates. Springer Verlag : Berlin.

Petersen, H. (1927) Über den Feinban den menschlichen Skeletteile. Wilhelm Roux Arch. Entw Mech. Org., 112 : 112-141.

Pritchard, J.J. (1972) General histology of bone. In Biochemistry and Physiology of Bone. Vol. 1. Bourne, G.H. (ed.) Academic Press : London.

Roux, W. (1885) Beitrage zur morphologie der funktionellen Anpassung. 3. Beschreibung und Erlanterung einer Knochen Kniegelenksaukylose. Arch. Anat. Physiol., Anat. Abt., 9 : 120-158.

Roux, W. (1895) Gesammette Abhandlungen uber die Entwicklungsmechanik der Organismen. Bd. 1. Funktionelle Anpassung. Engelmann : Leipzig.

Rovinski, B.M. and Lutsan, V.G. (1957) X-Ray Microscopy and Microradiography. Academic Press : New York.

Rybicki, E.F., Simonen, F.A. and Weis, E.B. (1972) On the mathematical analysis of stress in the human femur. J. Biomechanics, 5 : 203-215.

Rydell, M. (1966) Forces acting on the femoral head. Acta. orthop. scand., 37 : 88-96.

Scapino, R.P. (1965) The third joint of the canine jaw. J. Morph., 116 : 23-50.

Schwann, C.T. (1838) Microscopical investigation on the accordance in the structure and growth of plants and animals. Berlin.

Scott, J.H. (1967) Dento-Facial Development and Growth. Pergamon Press : London.

Scott, J.H. and Symons, N.B.B. (1964) Introduction to Dental Anatomy. 4th Ed. Livingston ; London.

Sedlin, E.D.(1965) A rheologic model for cortical bone. Acta orthop. scand., suppl.83.

Sicher, H. and DuBrul, E.L. (1970) Oral Anatomy. 5th Ed. Mosby : St. Louis.

Sicher, H. and Weinmann, J.P. (1966) Maxilla and mandible (alveolar process). In Orban's Oral Histology and Embryology. Sicher, H. (ed.). Mosby : St Louis.

Siegel, S. (1956) Nonparametric Statistics. McGraw-Hill : New York.

Siepel, C.M. (1948) Trajectories of the jaws. Acta odont. scand., 8 : 81-191.

Sievert, H.A. (1936) Two methods of Roentgen microphotography. Acta Radiol. Stockh., 17 : 299-309.

Sokal, R.R. and Rohlf, F.J. (1969) Biometry. Freeman & Co. : San Francisco.

Tappen, N.C. (1953) A functional analysis of the facial skeleton with split-line technique. Am. J. Phys. Anthrop., 11 ; 503-532.

Tappen, N.C. (1954) A comparative functional analysis of primate skulls by the split-line technique. Hum. Biol., 26 : 220-238.

Tappen, N.C. (1957) A comparison of split-line patterns in the skulls of juvenile and adult male gorillas. Am. J. Phys. Anthrop., 15 : 49-57.

Tappen, N.C. (1964) An examination of the alternative explanations of split-line orientation in compact bone. Am. J. Phys. Anthrop., 22 : 423-442.

Tappen, N.C. (1969) Relationships of split-line patterns to underlying microscopic structures in skulls of infant, juvenile and adult gorillas. Proc. 2nd Int. Congr. Primat., Atlanta. G.A. 1968, Vol 2 : 181-186.

Tappen, N.C. (1970) Main patterns and individual differences in baboon split-lines and theories of causes of split-line orientation in bone. Am. J. Phys. Anthrop., 33 : 61-72.

Tappen, N.C. (1971) Two orientational features of compact bone as predictors of split-line patterns. Am. J. Phys. Anthrop., 35 : 129-140.

Toridis, T.G. (1969) Stress analysis of the femur. J. Biomechanics, 2 : 163-174.

Triepel, H. (1922a) Die Architektur der Knochenspongiosa in neuer Auffasung. Z. Konstit Lehre., 18 : 269-311.

Triepel, H. (1922b) Uber gestaltliche Beziehungen zwischen Struktur und Organform. Z. Anta. Entw Gesch., 63 : 608-623.

Tucker, R. (1954) Studies in functional and analytical craniology Aust. J. Zool., 2 : 381-430.

Uspenski, N. (1914) Lochkamera fur vontgenstrahlen. Physik. Z., 15 : 717-718.

Wagstaffe, W.W. (1874) On the mechanical structure of the cancellous tissue of bone. St. Thomas's Hosp. Rep., 5 (N.S.) : 192-214.

Walkhoff, O. (1898) Aufnachmen der Gesichtsknochen mit Roentgenstrahlen. Korresp Bl. Zahnärzte., 27 : 97-99.

Walkhoff, O. (1900-01) Der menschliche Unterkiefer im lichte der Entwicklungsmechanik. Dtsche. Mtschrift. Zhkde., 1900-01. Cited Siepel, 1948.

Walkhoff, O. (1902) Der Unterkiefer der Anthropomorphen und des Menschen in seiner funktionellen Entwicklung und Gestalt. Menschen-Affenstudien über Entwicklung und Schädelbau. Selenka : Wiesbaden.

Ward. F.O. (1838) Outlines of Human Osteology. Renshaw : London.

Weinmann, J.P. and Sicher, H. (1955) Bone and Bones. Foundations of Bone Biology. 2nd Ed. Mosby : St. Louis.

Wetzel, G. (1922) Studien zur Schädelstatik. Verh. Anat. Ges. Anat. Anz., 55 : 216-226.

Winkler, R. (1921) Ueber den funktionellen Bau des Unterkiefers. Z. Stomat., 19 : 403-427.

Wolff, J. (1870) Ueber die innere Architecture der Knochen und ihre Bedeutung fur die Frage vom Knochenwachstum. Virchow's Arch. path. anat., 50 : 389-453.

Wolff, J. (1892) Das Gestz der Transformation der Knochen. Berlin.

Wolff, J. (1900) Bemerkungen zur Demonstration vom Röntgenbilden der Knochen-Architektur. Berl. klin. Wschr., 37 : 381-384; 414-417.

Woollard, H.H. and Harpman, A. (1938) Note on the internal architecture of the mandible. J. Anat., 72 : 575-578.

Wyman, J. (1857) On the cancellate structure of the bones of the human body. Boston. J. Nat. Hist.. 6 : 125-140.

PUBLICATIONS.

Reprint from J. Dent. Res. (1971) 50 : 1168-1169

11. THE DISTRIBUTION OF BITING FORCES IN THE SKULLS OF DOGS AND CATS.—*J. C. Buckland-Wright, Anatomy Department, King's College, London.* The distribution of the bony trajectoria in the skull and mandible of dogs and cats was determined by radiographic examination. Simulation of the biting forces at the canines (phase 1) and at the carnassials (phase 2) in defleshed skulls was done by fixing silk threads to the regions of muscular attachment of the temporalis and masseter muscles. Strain distribution was determined by coating the skulls with colophonium resin, setting them in a frame that gave support at the glenoid fossae and at the canines or carnassials, and pulling the threads in the line of contraction of the muscles. The resin cracked at right angles to the direction of strain passing in the trajectoria. The compressive or tensile nature of the strains was ascertained by replacing the resin with linear strain gauges fixed to the cortical bone overlying the trajectoria. The trajectorial density above the canine and carnassial of the maxilla was found to correlate with the density of the trabeculae in the interdental and interradicular septae of the mandible in the same regions. The results indicated that the forces generated in the skull and mandible of the dog and cat were resisted because the trajectorial organization formed a closed system. The foreshortening of the face in the cat resulted in a rearrangement of the trajectoria.

12. THE SPLIT LINE PHENOMENON IN BONE.—*M. H. Hobdell and J. C. Buckland-Wright, Anatomy Department, King's College, London.* Little attention has been given to the method of preparation of bone before its examination by use of the split line technique. This study was carried out to determine (1) the effect of boiling on this pattern before split line formation and (2) the relationship between bone structure and split line formation in cat and monkey skulls. One side of the skull was defleshed by boiling, the other side by stripping. Stereopair radiographs were made and the skulls decalcified in 5% nitric acid, rinsed in sodium sulfate, and stored in 70% alcohol. The cortical bone was pierced by use of a mounted needle dipped in India ink to a depth of 1 to 2 mm, and the orientation of the splits was compared with the radiographs. The skulls were cut into blocks, paraffin embedded, sectioned, and stained for routine histology. Wax reconstructions were made of specific regions. The results showed that, on decalcification of the boiled skulls, the sutures separated and the cortical bone was distorted and stained irregularly. The split lines were deranged and often diverged from the direction of the Haversian canals, unboiled material stained more regularly, and the splits diverged less. In all instances, the splits were superficial, and often their orientation did not reflect that of the underlying trabeculae. It is suggested that the direction of the split lines reflects both the direction of growth and mechanical forces.

Reprint from J. Dent. Res. (1972) 51 : 1241

24. THE SHOCK-ABSORBING EFFECT OF CRANIAL SUTURES IN CERTAIN MAMMALS.—*J. C. Buckland-Wright, Anatomy Department, King's College, London.* Sutural morphology and its relation to function in the adult mammalian skull generally has been ignored. Sutures in adult cats and dogs, irrespective of their type of development, were classified as fused or open. Gross morphologic and histologic examinations were carried out on the sutures. Experiments were performed on a number of anesthetized cats to determine the relative movement of the sutures. Pins were implanted on either side of all the maxillofacial sutures, braces were placed initially at the canines and then at the carnassials, and the masticatory muscles were stimulated into tetany. The changes in the relative positions of the pins were recorded photographically. Where the tensile forces crossed the sutures, there was a relatively greater displacement of the bones than at the points where compressive forces acted. This difference was reflected in the length and organization of the collagen fibers and in the type of intersutural intercuspation. In general, fused sutures were associated with muscle attachments and improved cranial rigidity. The greater flexibility of the open sutures enabled larger forces to be exerted during mastication by assisting in absorption.

J.C. BUCKLAND-WRIGHT

Ph.D. Thesis. 1974

J. Zool., Lond. (1969) **159**, 17–29

Craniological observations on *Hyaena* and *Crocuta* (Mammalia)

J. C. BUCKLAND-WRIGHT*

National Museum, Centre for Prehistory and Palaeontology, Nairobi

(*Accepted 11 March 1969*)

(With 3 plates and 7 figures in the text)

The results are presented of a comparative study of certain features of the cranial osteology of *Hyaena hyaena* (Brisson) and *Crocuta crocuta* (Erxleben), of the atlas and axis vertebrae and of the associated cranial and nuchal musculature. Observable osteological differences between the two forms are shown to be correlated with the degree of development of particular muscles and thus with the functional activity of the jaws in the seizing and carrying of prey. Secondary sexual characters are more pronounced in the male than in the female of either form.

Contents

	Page
Introduction	17
Materials and methods	17
Observations	18
(a) Craniological	18
(b) Vertebral	26
(c) Myological	27
Discussion	28
References	29

Introduction

At present the determination of fossil hyaena forms is based principally upon dentitional characters rather than upon the general cranial osteology. It was therefore considered desirable to provide the palaeontologist with a broader basis for diagnosis by establishing a more informative account than generally available of the differences in cranial structure characterizing the extant genera *Hyaena* and *Crocuta*. A detailed study was therefore made of 20 *Hyaena* and 26 *Crocuta* skulls, and of five *Hyaena* and six *Crocuta* atlas and axis vertebrae in the Nairobi National Museum, later supplemented by observations made upon similar material in the British Museum (Natural History).

Attention was given to osteological features likely to prove of diagnostic value, e.g. the sagittal and occipital crests, the configuration of the periotic region, the planum occipital and the zygomatic arch.

Materials and methods

The range of material examined is set forth in Table I. Direct observation was confirmed by radiography and/or by mensural checking of life-size drawings made with the dioptograph.

* Present address: 50, Beechwood Avenue, Kew Gardens, Surrey, England.

J. Zool., Lond. (1969) **159**, 17–29

Craniological observations on *Hyaena* and *Crocuta* (Mammalia)

J. C. BUCKLAND-WRIGHT*

National Museum, Centre for Prehistory and Palaeontology, Nairobi

(*Accepted 11 March 1969*)

(With 3 plates and 7 figures in the text)

The results are presented of a comparative study of certain features of the cranial osteology of *Hyaena hyaena* (Brisson) and *Crocuta crocuta* (Erxleben), of the atlas and axis vertebrae and of the associated cranial and nuchal musculature. Observable osteological differences between the two forms are shown to be correlated with the degree of development of particular muscles and thus with the functional activity of the jaws in the seizing and carrying of prey. Secondary sexual characters are more pronounced in the male than in the female of either form.

Contents

	Page
Introduction	17
Materials and methods	17
Observations	18
(a) Craniological	18
(b) Vertebral	26
(c) Myological	27
Discussion	28
References	29

Introduction

At present the determination of fossil hyaena forms is based principally upon dentitional characters rather than upon the general cranial osteology. It was therefore considered desirable to provide the palaeontologist with a broader basis for diagnosis by establishing a more informative account than generally available of the differences in cranial structure characterizing the extant genera *Hyaena* and *Crocuta*. A detailed study was therefore made of 20 *Hyaena* and 26 *Crocuta* skulls, and of five *Hyaena* and six *Crocuta* atlas and axis vertebrae in the Nairobi National Museum, later supplemented by observations made upon similar material in the British Museum (Natural History).

Attention was given to osteological features likely to prove of diagnostic value, e.g. the sagittal and occipital crests, the configuration of the periotic region, the planum occipital and the zygomatic arch.

Materials and methods

The range of material examined is set forth in Table I. Direct observation was confirmed by radiography and/or by mensural checking of life-size drawings made with the dioptograph.

* Present address: 50, Beechwood Avenue, Kew Gardens, Surrey, England.

Where deemed useful, simple indexes were established and calculated to express metrically the findings of naked-eye observations, and these appear in the descriptive text. The variance or mean of the squares of deviation was calculated from the formula in Bishop (1966: 133). A

TABLE I

Osteological material examined

Species	Skulls		Atlas Vertebrae		Axis Vertebrae	
	Nairobi	B.M. (N.H.)	Nairobi	B.M. (N.H.)	Nairobi	B.M. (N.H.)
Hyaena hyaena	16 ad. 4 imm.	10 ad.	5	2	5	2
Crocuta crocuta	20 ad. 6 imm.	14 ad.	6	3	6	3

study of the sexual differences in hyaena skulls was conducted upon 14 male and 12 female *Hyaena* skulls and upon 14 male and 20 female *Crocuta* skulls. A thorough dissection was made of the cranial and nuchal musculature in one adult and one young male *Hyaena* and in one adult male and one female *Crocuta*: the nuchal musculature alone was studied in one additional young female *Crocuta*, but only such myological findings are referred to herein as have relevance to the configurations of the hyaena skull.

Observations

(a) *Craniological*

(1) *Sagittal and supraoccipital region.* Probably the greatest craniological difference between *Hyaena* and *Crocuta* lies in the relative size and shape of the sagittal crest and supraoccipital region. In both genera the tall sagittal crest passes posteriorly over the cranial vault on to the supraoccipital bone, which forms the hindmost region of the skull. Radiographic examination of the skulls of both genera demonstrates the frontal sinuses to extend backwards from the post-orbital region into the anterior portion of the supra-occipital bone. Without such sinuses the massive sagittal crest would significantly increase the weight of the skull. Reynolds (1902) comments that such sinuses often have irregular surface openings: in the present material damaged specimens only showed such openings, and it seems unlikely that, normally, the floor of the temporal fossa should suffer weakening from the presence of any such openings.

In *Hyaena* the sagittal crest is relatively more massive posteriorly than in *Crocuta* and overlies the lambda: in *Crocuta* the crest is maximally developed in its middle region and extends less far ventrally before meeting the lambda. (Plate I, Fig. 1.) Dissection showed that the temporalis muscle origin was more posteriorly situate in *Hyaena* than in *Crocuta*.

The outlines of the sagittal crest were dioptographically traced onto millimetre squared paper and the surface area of the crest calculated in each genus: an index for each was then obtained by dividing the condylobasal cranial length by the surface area: the mean for *Hyaena* is 1·52 (variance 0·13), for *Crocuta* 2·12 (variance 0·65), thus demonstrating that the posterior part of the crest has the greater surface area in *Hyaena*.

The greater convexity of the supraoccipital in *Hyaena* is reflected by the angle subtended between the nuchal crest and the paramastoid ridge, estimated in norma lateralis (Fig. 3): the mean for *Hyaena* is 121° (variance 12°), for *Crocuta* 130° (variance 7·3°). The difference shows the lambda to be relatively more superiorly situate in *Crocuta* and

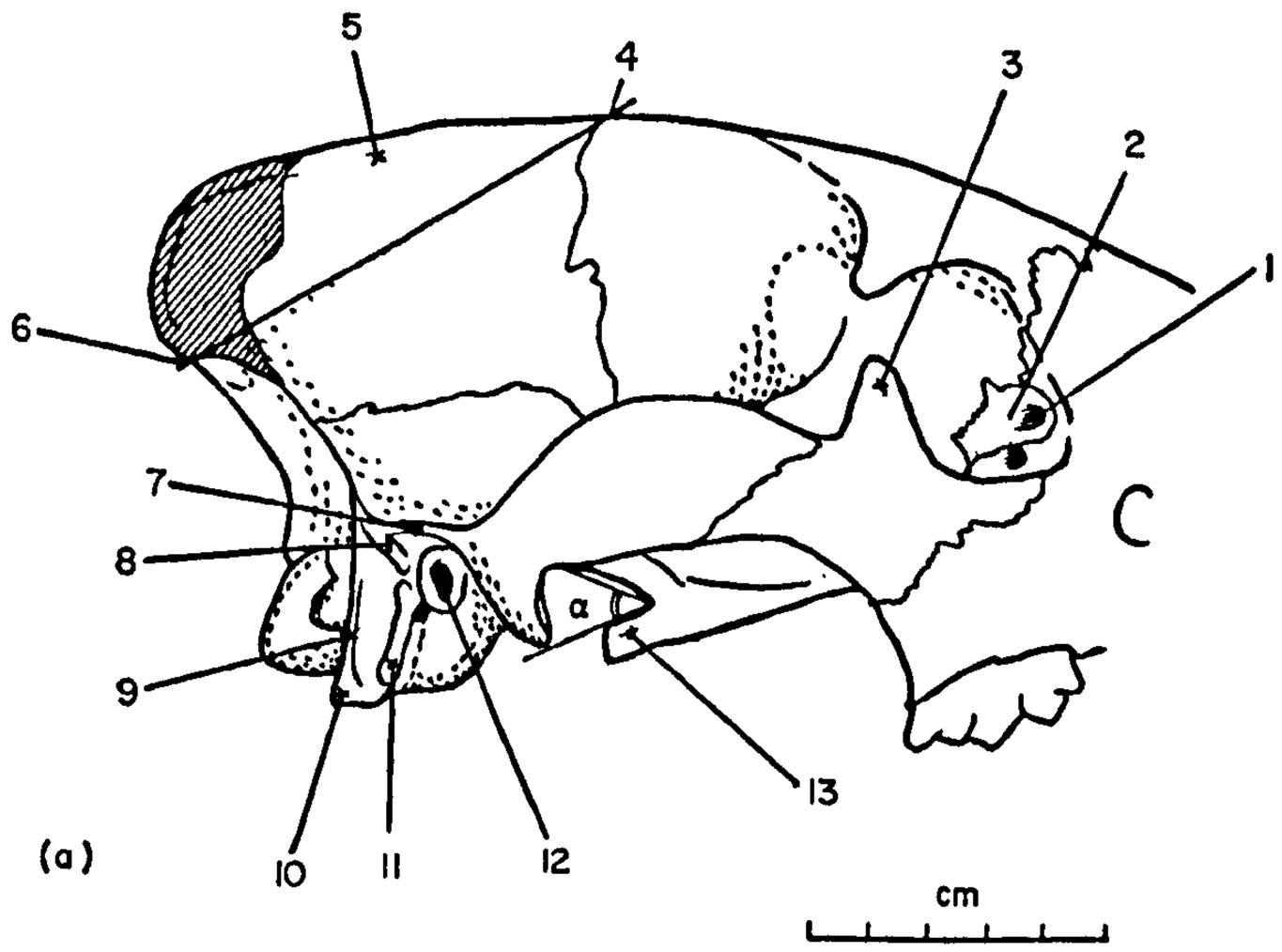

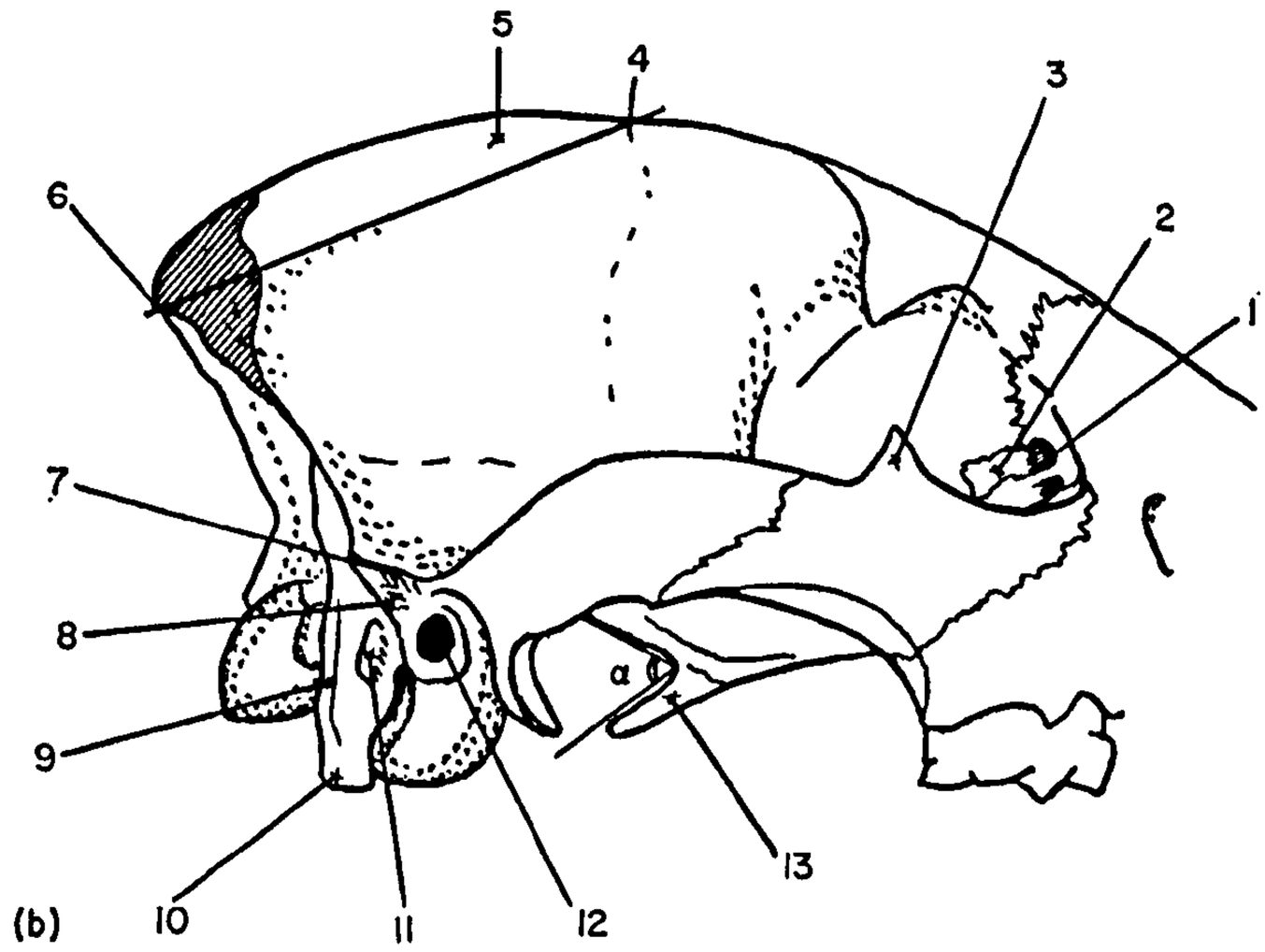

FIG. 1. (a) Norma lateralis of *Hyaena* and (b) of *Crocuta*. The shaded area is the region of the supraoccipital which forms the posterior part of the sagittal crest. The area above the line from the bregma to the lambda was calculated in order to find the relative size of the posterior part of the sagittal crest in *Hyaena* and *Crocuta*, α shows the angle measured between the basis cranii and the dorsal border of the medial pterygoid lamina.

1, Lachrymal foramen; 2, lachrymal bone; 3, frontal process of the jugal; 4, bregma; 5, sagittal crest; 6, lambda; 7, supramastoid crest; 8, mastoid crest; 9, paramastoid ridge; 10, paramastoid process; 11, mastoid process; 12, external auditory meatus; 13, medial pterygoid lamina.

the paramastoid region and process to project downwards in that form, but slightly backwards in *Hyaena*.

(2) *Occipital region.* In *Hyaena* the planum occipitale is low, in *Crocuta* relatively high owing to the more dorsal situation therein of the lambda. The nuchal crest in *Hyaena* passes to the mastoid in virtually a straight line, seldom broadening after the lambda, and only curving outwards at its base to join the mastoid. The crest in *Crocuta* is more sinuous, and curves outwards below the lambda before proceeding downwards to the mastoid. In both genera the external occipital crest arises from a slight eminence (external occipital protruberance) directly below the lambda and is low in *Hyaena* but well raised in *Crocuta*; it ends above the dorsal rim of the foramen magnum at a distance of some 5 mm in *Hyaena*, 5 to 10 mm in *Crocuta*. Some 13 to 20 mm distant from the lambda a ridge (crista occipitalis obliqua) arises from the nuchal crest and passes diagonally medialwards towards or into the external occipital crest, at a distance of 10 to 20 mm above the foramen magnum. The degree of development of this crista occipitalis obliqua varies according to the age and sex of the specimen. (Fig. 2.) Between the dorsal part of the nuchal crest and the oblique crest are depressions for the insertion of the complexus muscle: these depressions are more emphatically concave in *Crocuta*, wherein the complexus muscle is more powerfully developed than in *Hyaena*.

(3) *Squamosal region.* In both genera a very marked fossa occurs in the hinder region of the squamosal, directly above the supramastoid crest. In *Crocuta* this fossa extends from the dorsal root of the zygomatic arch to the anterior border of the nuchal crest and as a slight groove a little way dorsally in front of that crest: in *Hyaena* the fossa is neither so deep nor so extensive, but is otherwise similar. Dissection shows this fossa to give origin to the pars horizontalis of the temporalis muscle.

(4) *Condylar region.* In *Hyaena* and *Crocuta* the occipital condyle is trochlear, with dorsal and ventral surfaces demarcated by a blunt ridge. In *Hyaena* the dorsal rim of the foramen magnum meets the condyle about half way along the medio-dorsal border, but in *Crocuta* about two-thirds of the way. The condylar ventral moieties curve medially in mutual approach and obscure the ventral rim of the foramen. In *Hyaena* the condyles establish contiguity mid-ventrally (or are very narrowly separated) whereas in most *Crocuta* skulls they remain separated by a distance of 1 to 7 mm. In norma basalis, therefore, the condylo-magnum region differs in outline, being V-shaped in *Hyaena* and U-shaped (even semicircular) in *Crocuta*. (Fig. 4.) In *Hyaena* the spinal aspect of the condylar ventral moiety displays, immediately dorsal to the medial articular surface, a depression or fossa for the attachment of the odonto-occipital ligaments. In *Crocuta* this fossa is mainly, or even wholly, wanting and its rather shallow posterior end alone is preserved.

(5) *Nuchal crest.* In both genera an emphatic nuchal crest is compounded of the confluent temporal and nuchal ridges, closely associated with the development of the temporalis muscle and the nuchal musculature respectively: it extends from lambda to mastoid process. Superiorly and along the upper third of the crest, the temporal and nuchal ridges are inseparable, but thereafter they diverge, the former continuing inferiorly into the supramastoid ridge, the latter forming the paramastoid ridge. (Plate II, Fig. 2.)

In *Hyaena* the nuchal crest is well developed in its entirety. In *Crocuta* the crest is well developed superiorly and inferiorly but is much reduced in its intermediate portion: indeed in female and in immature skulls it may thereabouts be only faintly discernible.

In norma occipitalis the planum occipitale is of differing outline in *Hyaena* and *Crocuta*.

PLATE I. (a) Norma lateralis of the skull of *Hyaena* and (b) of *Crocuta*.

[*To face page* 20

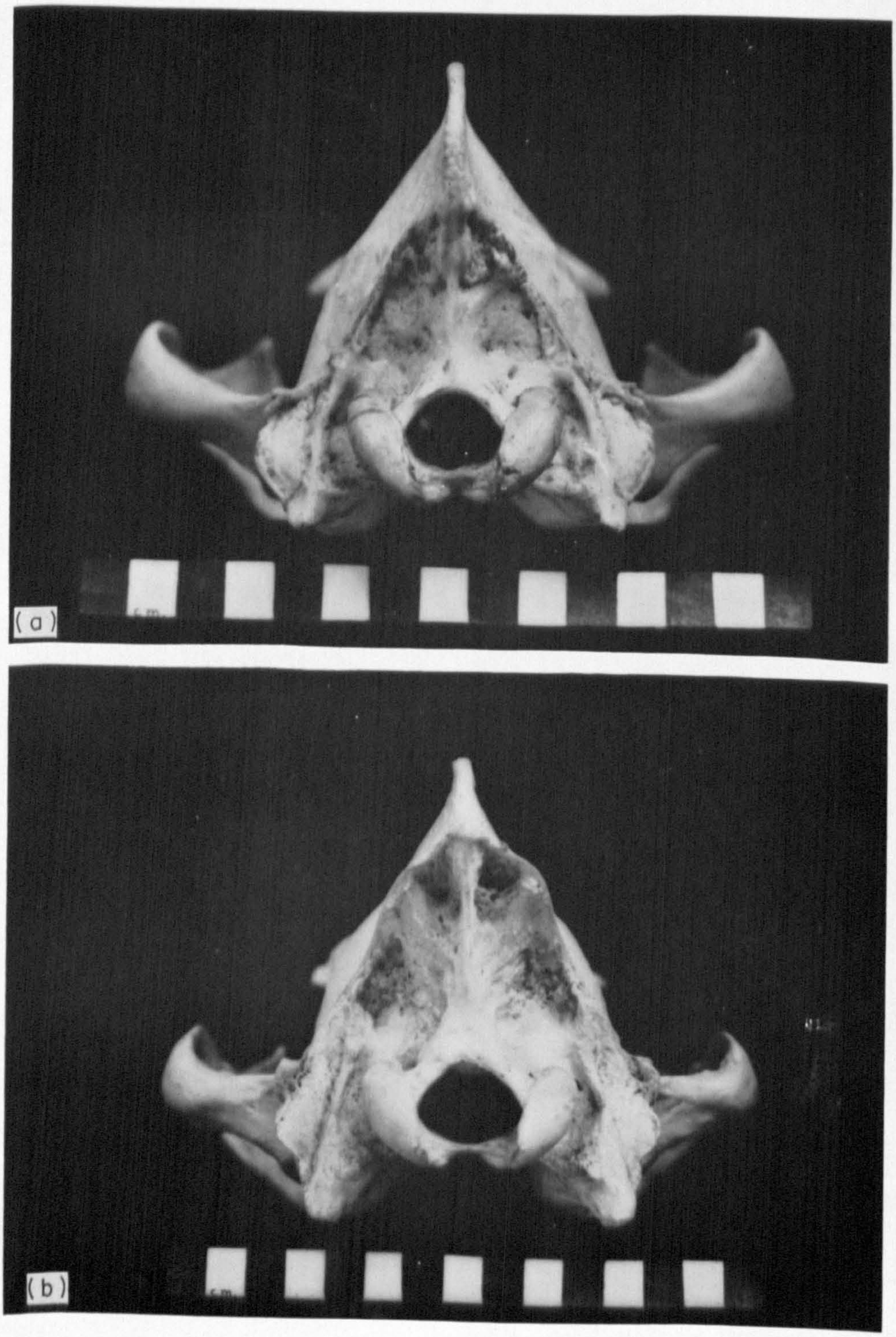

PLATE II. (a) Norma occipitalis of the skull of *Hyaena* and (b) of *Crocuta*.

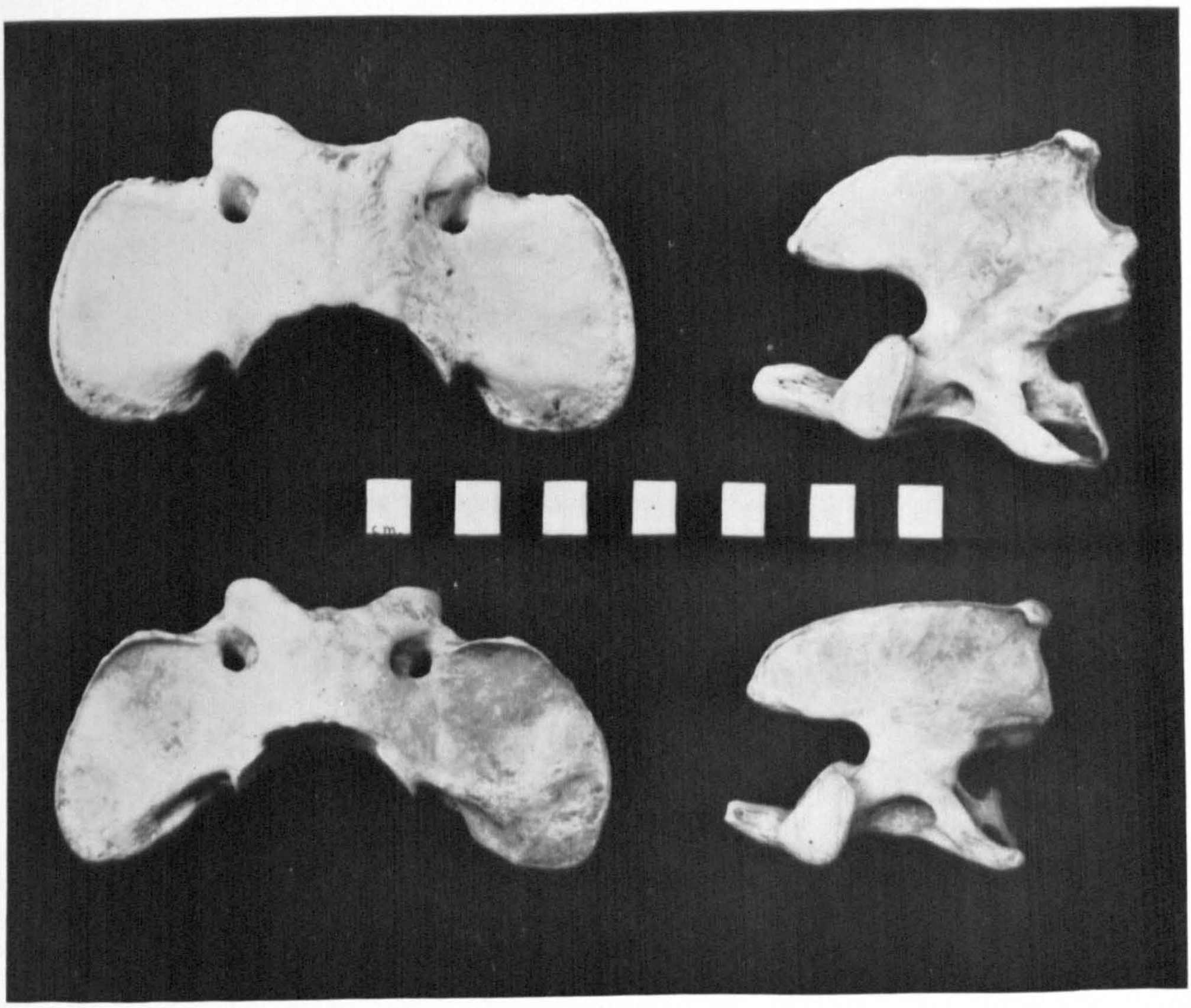

PLATE III. Norma dorsalis of the atlas and norma lateralis of the axis of *Crocuta* (above) and *Hyaena* (below).

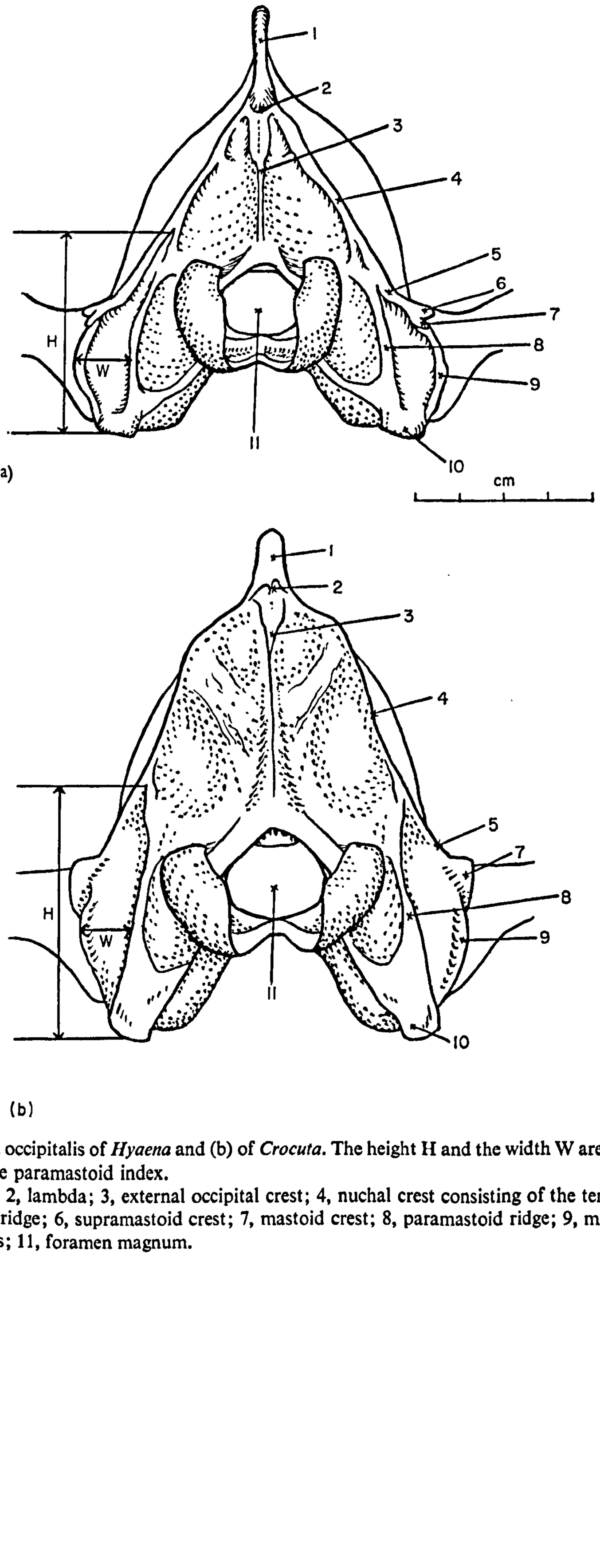

FIG. 2. (a) Norma occipitalis of *Hyaena* and (b) of *Crocuta*. The height H and the width W are the measurements used to calculate the paramastoid index.

1, Saggittal crest; 2, lambda; 3, external occipital crest; 4, nuchal crest consisting of the temporal and nuchal ridges; 5, temporal ridge; 6, supramastoid crest; 7, mastoid crest; 8, paramastoid ridge; 9, mastoid process; 10, paramastoid process; 11, foramen magnum.

(Plate II, Fig. 2.) In *Hyaena* it is triangular and straight sided, in *Crocuta* more polygonal and irregularly sided.

(6) *Otic region.* The triangular paramastoid region is bounded dorsally by the nuchal crest, antero-laterally by the mastoid process and postero-medially by the paramastoid ridge: its inferior free tip is the paramastoid process. In *Hyaena* the paramastoid ridge descends on the medial aspect of the paramastoid process, in *Crocuta* it terminates on the lateral aspect of that process. In *Hyaena* the paramastoid process is wide, moderately long and backwardly directed: its free tip is antero-posteriorly compressed and directly

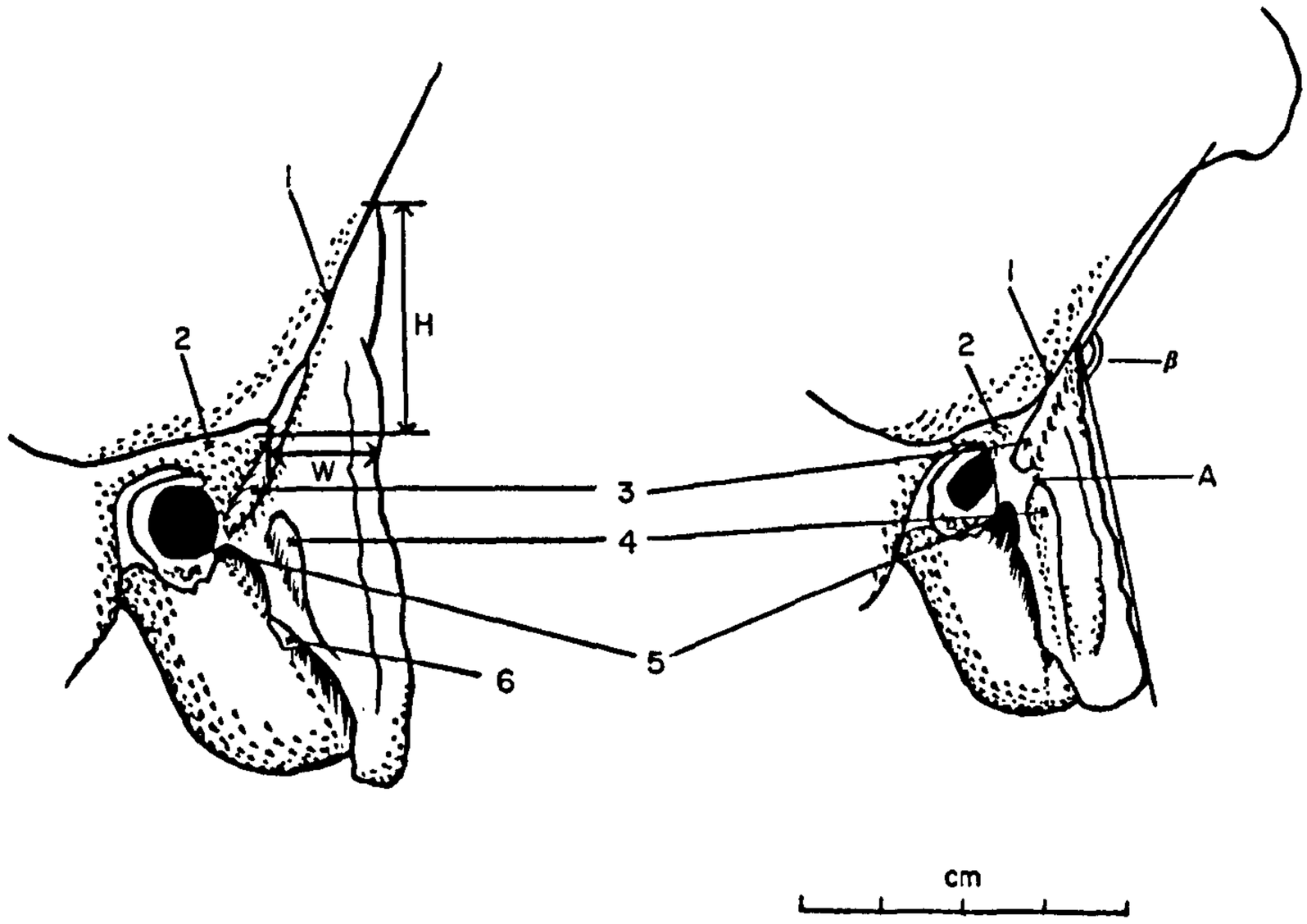

FIG. 3. Norma lateralis of the left otic region in *Hyaena* (right) and *Crocuta* (left).

1, Temporal ridge of the nuchal crest; 2, supramastoid crest; 3, mastoid crest; 4, mastoid process; 5, stylomastoid foramen; 6, origin of the styloid process. The height H and the width W are the measurements used to calculate the second paramastoid index. β shows the angle measured between the nuchal crest and the paramastoid ridge.

anterior thereto is a small, shallow depression: the crest of the paramastoid process makes an angle of 45° to 50° with the median sagittal plane (Fig. 4). In *Crocuta* the paramastoid process is larger, longer and more robust: directed downwards, not backwards, it presents a large and rounded free tip, devoid of any depression. The greater vertical extent of the *Crocuta* paramastoid region is confirmed by osteometry (Fig. 2). Vertical extent (height) divided by anterio-posterior extent (width) gives a mean for *Hyaena* of 2·88 (variance 0·13) and for *Crocuta* of 3·75 (variance 0·92). A second height-index is obtainable by measurement (*in norma lateralis*) of the paramastoid vertical extent from a line projected backwards from the junction of supramastoid and mastoid crests to the point of union of paramastoid with nuchal crest and of paramastoid width along the projection line to the posterior border of the paramastoid (Fig. 3). This index gives a mean for *Hyaena* of 1·49 (variance 0·16) and for *Crocuta* of 3·42 (variance 0·90).

The mastoid region is of diagnostic significance. In both *Hyaena* and *Crocuta* the temporal ridge component of the nuchal crest divides postero-inferiorly into supramastoid crest and mastoid crest, disposed respectively above and obliquely towards, the external auditory meatus. In some *Hyaena* crania the mastoid crest blends with the mastoid process, but usually a short gap intervenes (Fig. 3, A). The *Hyaena* mastoid process is relatively larger than that of *Crocuta*; it extends laterally beyond the mastoid crest and inferiorly some 16 mm beyond the anterior end thereof. In *Crocuta* supramastoid and mastoid crests are more emphatically developed as laterally projecting flanges: the mastoid crest runs from temporal ridge to the postero-inferior aspect of the bony meatus: the mastoid process is but moderately developed and shows a lateral ridge extending some 14 mm below the middle of the mastoid crest: in many (though not all) male crania, the process projects laterally beyond the crest.

In both *Hyaena* and *Crocuta* the stylo-mastoid foramen is situate between tympanic plate and mastoid. The tympano-hyal element of the styloid process is, in *Hyaena*, accommodated within a narrow, ventro-medial extension of the foramen: in *Crocuta* the process is separated from the foramen by a short bony bar extending from the mastoid process to the auditory bulla. The process is never completely ossified and is usually lost from the prepared skull. In *Hyaena* the process faintly grooves the bulla antero-inferiorly to the mastoid process: in *Crocuta* the corresponding groove is more emphatic and much closer to the paramastoid process.

A curvilinear recess intervenes between the anterior aspect of the tympanic plate and the posterior aspect of the post-glenoid process. In *Hyaena* the curvilinear recess is restricted to the antero-superior rim of the bony auditory meatus as it widens markedly below. In *Crocuta* the recess (1·5 to 2·0 mm wide throughout) is narrower below and is therefore longer and distinctly crescentic. The degree of development of this recess reflects the configuration of the external auditory meatus, which tends to the oval or irregular in *Hyaena* but to the circular in *Crocuta* (Fig. 3).

The bony auditory meatus projects laterally more obtrusively in *Hyaena* than in *Crocuta*, being less overhung by the more feebly developed supramastoid crest. An index of relative meatus size, obtained by dividing the meatal vertical diameter by the horizontal, gives a mean for *Hyaena* of 1·25 (variance 0·07) and for *Crocuta* of 0·97 (variance 0·03).

The large, ovoid, convex auditory bulla is synostosed to the basioccipital posteriorly and to the basisphenoid anteriorly. It is not more inflated in *Crocuta* than in *Hyaena* as Reynolds (1902) supposed, the degree of bullar inflation appearing to vary equally in either genus.

(7) *Basis cranii.* The basioccipital is of diagnostic importance, especially when only the hind region of the cranium is available for identification. In *Hyaena* the generally flat inferior surface of the basioccipital is divided medianly by a narrow, low ridge, extending from the anterior intercondylar region to the spheno-occipital synchondrosis, which lies on the same level as the ostia of the osseus Eustachian tubes. About its midpoint this ridge is crossed by a faint transverse ridge, which ends bilaterally in a low eminence synostosed with the tympanic bulla. Both anterior and posterior to this transverse ridge is situate a pair of shallow muscle impressions, for the insertion of rectus capitis ventralis and longus capitis.

In *Crocuta* the basioccipital displays descriptively obtrusive posterior and anterior moieties. The posterior much resembles that of *Hyaena*, having a median ridge (beginning

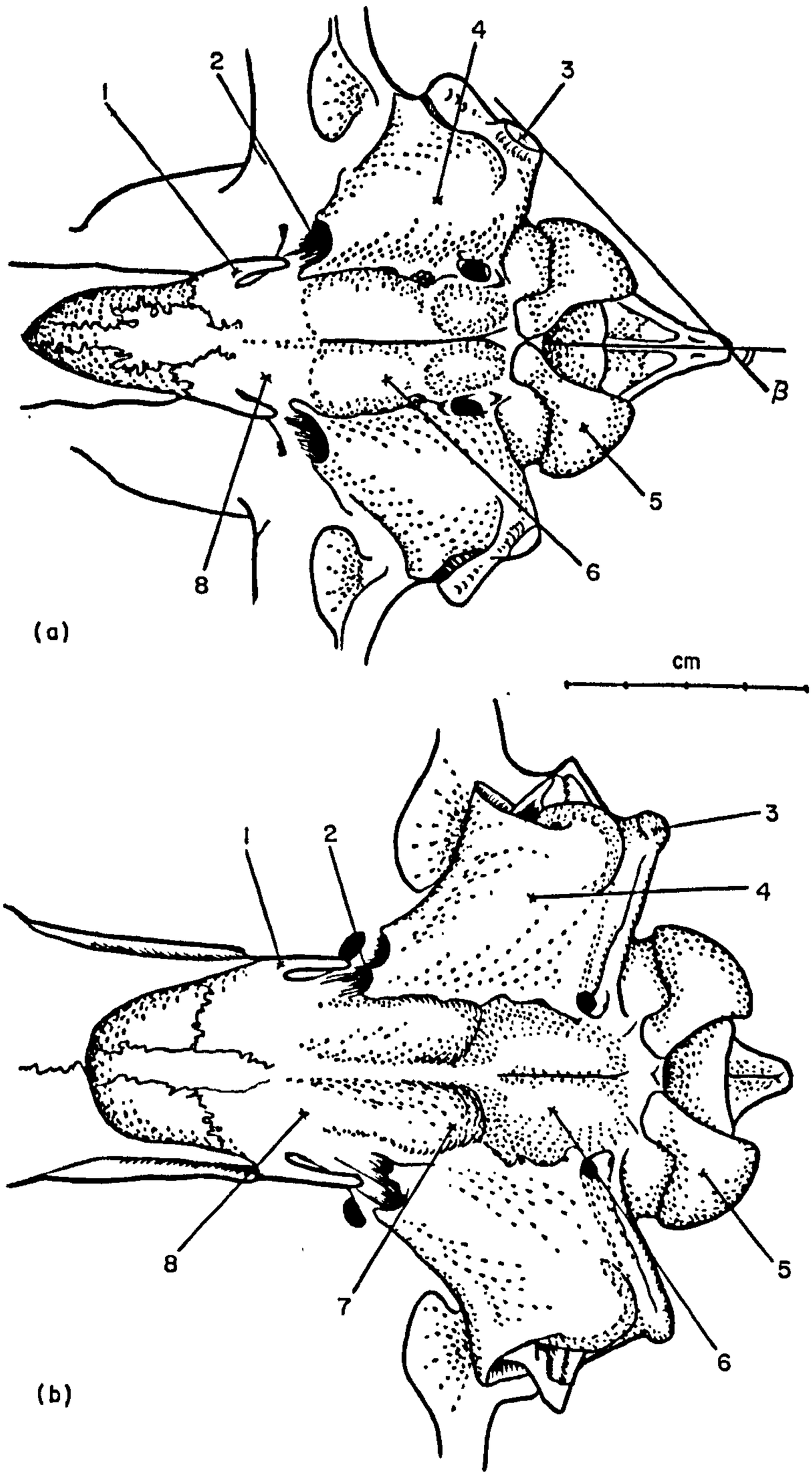

FIG. 4. (a) Basis cranii of *Hyaena* and (b) of *Crocuta*. β is the angle measured between the paramastoid process and the median sagittal plane.

1, Medial pterygoid lamina; 2, eustachian foramen; 3, paramastoid process; 4, tympanic bulla; 5, occipital condyle; 6, basioccipital; 7, tuberosity; 8, basisphenoid.

some 10 to 14 mm anterior to the foramen magnum) separating two impressions for rectus capitis ventralis muscle insertions. The anterior moiety shows a median groove, separating two prominent tuberosities, each of which slopes anteriorly on to the basi-sphenoid.

In both *Hyaena* and *Crocuta* the pterygoid process is, for practical purposes, continued inferiorly into a single, well developed (medial) pterygoid lamina: the lateral pterygoid lamina is reduced to a mere tuberosity and the pterygoid fossa (floored by a narrow process from the palatine bone) to a shallow groove between the two. The thin (medial) pterygoid lamina sends backwards a somewhat triangular recurved portion, whose inferior border lies, in *Hyaena* on the palatal level, but in *Crocuta* tends to fall below that level. The laminar dorsal border makes with the basis cranii an angle of 45 to 50° in *Hyaena*, of 70 to 80° in *Crocuta* (Fig. 1).

(8) *Zygomatic arch.* The zygomatic arch shows differences of configuration between the two genera. In *Hyaena* its temporal component has a relatively more convex border, and extends laterally to a greater extent. In *Hyaena* the jugo-maxillary suture is the shorter (Ehrenberg, 1938). Both the frontal processes of the jugal and the post-orbital wall are relatively larger in *Hyaena* than in *Crocuta*.

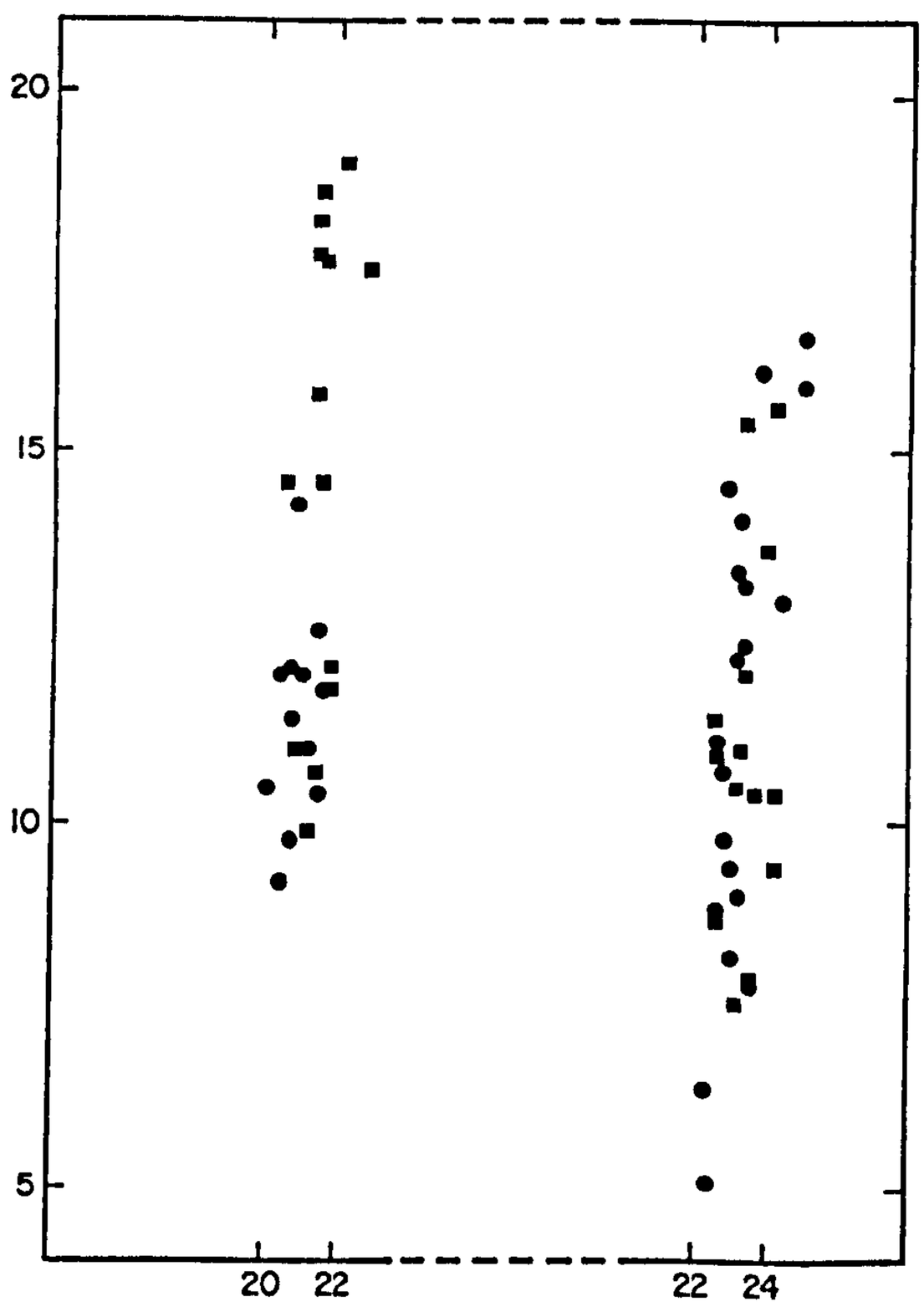

FIG. 5. Graph showing the relative size of the posterior region of the sagittal crest in the two sexes of *Hyaena* (left) and *Crocuta* (right). The abscissa is the condylo-basal length of the skull in centimetres; the ordinate is the surface area of the posterior region of the crest in square centimetres. ■, Male; ●, female.

(9) *Orbit.* The inferior border of the relatively smaller *Hyaena* orbit is distinctly concave: the corresponding *Crocuta* border is fairly straight and tends to meet the medial border at a perceptible angle. In *Hyaena* the lachrymal bone is the relatively larger and completely encloses the lachrymal foramen: in *Crocuta* this foramen lies between lachrymal and maxilla.

(10) *Secondary sexual characters.* The material examined, particularly that of *Hyaena*, revealed a certain sexual dimorphism, but many further specimens require examination before anything beyond an indication of these is possible. The posterior region of the *Hyaena* sagittal crest is generally larger in males than in females, but considerable overlap between the sexes occurs. In Fig. 5, wherein the surface area of the posterior crest region is plotted against the condylo-basal length, the upper region of the graph is occupied by the male specimens, the lower by the female specimens, and the sex overlap is obvious. The graph also shows that in *Crocuta* the size of the posterior crest region is without sexual significance, since the females are as large as, or even larger than, the males. Visually, the parietal region of the crest appears to be slightly higher in male than in female *Crocuta* skulls, but the difference eludes osteometrical expression by any satisfactory index.

The planum occipital of the male *Hyaena* skull shows an expectedly more vigorous development of secondary markings than does the female. In *Crocuta* the same is true, the crista occipitalis obliqua being relatively well preserved in male specimens, but less pronounced in female and immature specimens. In both genera the compound structure of the nuchal crest is more apparent in the male than in the female skull.

(b) *Vertebral*

In *Hyaena* the atlas vertebra is relatively gracile compared with the more robust *Crocuta* bone: the ala atlantis is relatively narrow and more prolonged posteriorly, though its surface area is much the same in the two forms. The spinal canal outline is oval in *Hyaena*, round to oval in *Crocuta*. The tuberculum dorsalis atlantis is a median tubercle in *Hyaena*, but is subdivided into two paramedian tubercles in *Crocuta*. The arcus dorsalis atlantis is relatively stouter in *Crocuta*. In *Hyaena* the anterior (occipital) articular facet

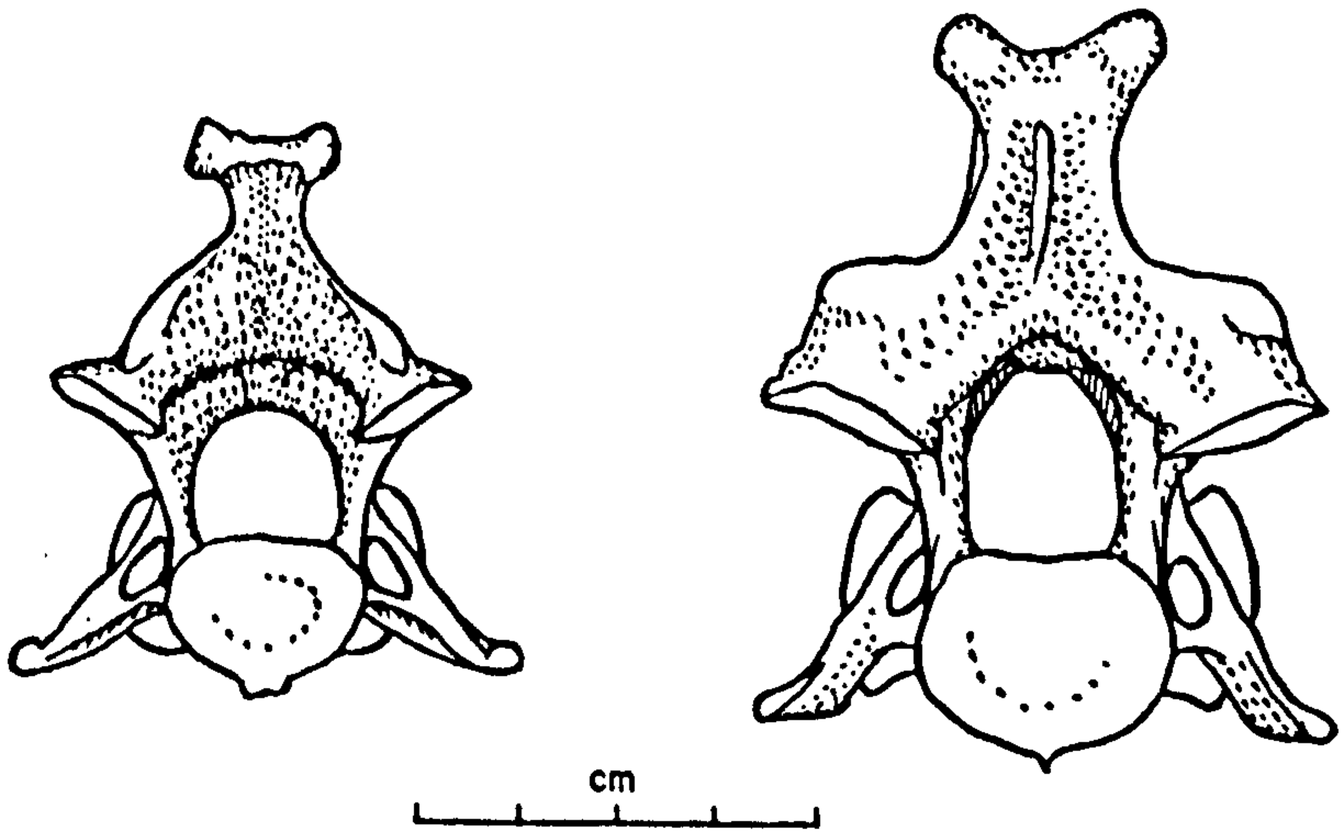

FIG. 6. Norma caudalis of the axis of *Hyaena* (left) and *Crocuta* (right).

encroaches upon the arcus ventralis atlantis almost to the midline, but is always separated from its fellow by a groove: its ventral margin is raised. In *Crocuta* the corresponding facet lacks any raised margin and encroaches upon the ventral arch to become normally contiguous to its fellow. In *Hyaena* the posterior atlantal articular facet is roughly quadrilateral in outline, in *Crocuta* triangular in outline.

The axis vertebra is relatively gracile in *Hyaena*, robust in *Crocuta*. In *Hyaena* the neurospine is long, slender and terminally bifid, in *Crocuta* short and more divaricate terminally. In *Hyaena* the laminae slope uninterruptedly into the spinal canal; the neurospine caudal border is virtually straight; the spinal canal is arch shaped with inverted base; the posterior articular surface of the centrum subtends an angle of some 69° with the venter of the centrum; the transverse processes are rounded and project caudally beyond the postzygapophyses; the odontoid process is dorsally reflected. In *Crocuta* the neurospine caudal border is sinuous (biconcave caudally); the laminae converge upon an inter-postzygapophyseal ridge; the spinal canal is of pointed arch outline anteriorly but of rounded outline posteriorly; the posterior articular surface of the centrum subtends an angle of some 56° with the centrum's ventral surface; the acuminate transverse processes do not project caudally beyond the postzygapophyses.

(c) *Myological*

Reference is herein restricted to the two groups of muscles most closely associated with the configuration of the hyaena skull, viz. the masticatory and nuchal muscles. Since a detailed description of these is not essential to understanding of their role in modifying the external characters of the skull, the differences they manifest in the two genera are alone noted.

The m. masseter is a more powerful muscle in *Crocuta* than in *Hyaena*, in conformity with the broader jugal and lower zygomatic arch.

The m. temporalis is extremely well developed in both genera, effecting rapid mouth closure in powerful biting movements. Additional strength is obtained by the formation of a thick central tendinous aponeurosis. The posterior horizontal fibres of the muscle are much more emphatically developed in *Crocuta* than in *Hyaena*; the main mass of the muscle is appreciably the larger in *Crocuta*, being particularly large in its midportion, whereas the *Hyaena* temporalis is best developed in its hind portion.

Crocuta has the relatively more massive neck, from greater relative development of certain of the nuchal muscles. Thus the m. cleido-cervicalis and m. sterno-occipitalis are the more coarsely fibred (and inferentially more powerful) in *Crocuta*, and the m. splenius is relatively broader, larger and the more compact. The m. complexus minor (m. biventer cervicis) and the m. complexus major are both more bulky muscles in *Crocuta* than in *Hyaena*. The mm. spinales dorsi et cervicis are extremely well developed in both genera, but of more extensive insertion in *Crocuta*. The m. longus capitis (rect. cap. ant. maj.) is separable from the m. rectus capitis ventralis, not as stated by Watson & Young (1879): its insertion is close to the tympanic bulla into a tuberosity in *Crocuta*, but into a fossa in *Hyaena*. In both genera the m. longus colli inserts into the anterior cervical vertebral bodies close to the midline, the most cranial insertion being into the atlantal ventral tubercle by fleshy fibres in *Crocuta*, by tendons in *Hyaena*. The m. obliquus capitis cranialis (*vel* superior) is in both genera closely associated with the more medially positioned m.

rectus capitis lateralis and the insertions of both are higher on the nuchal crest in *Crocuta* than in *Hyaena*. The m. obliquus capitis caudalis (*vel* inferior) is extremely well developed in *Crocuta*, but in *Hyaena* is a patently weaker muscle.

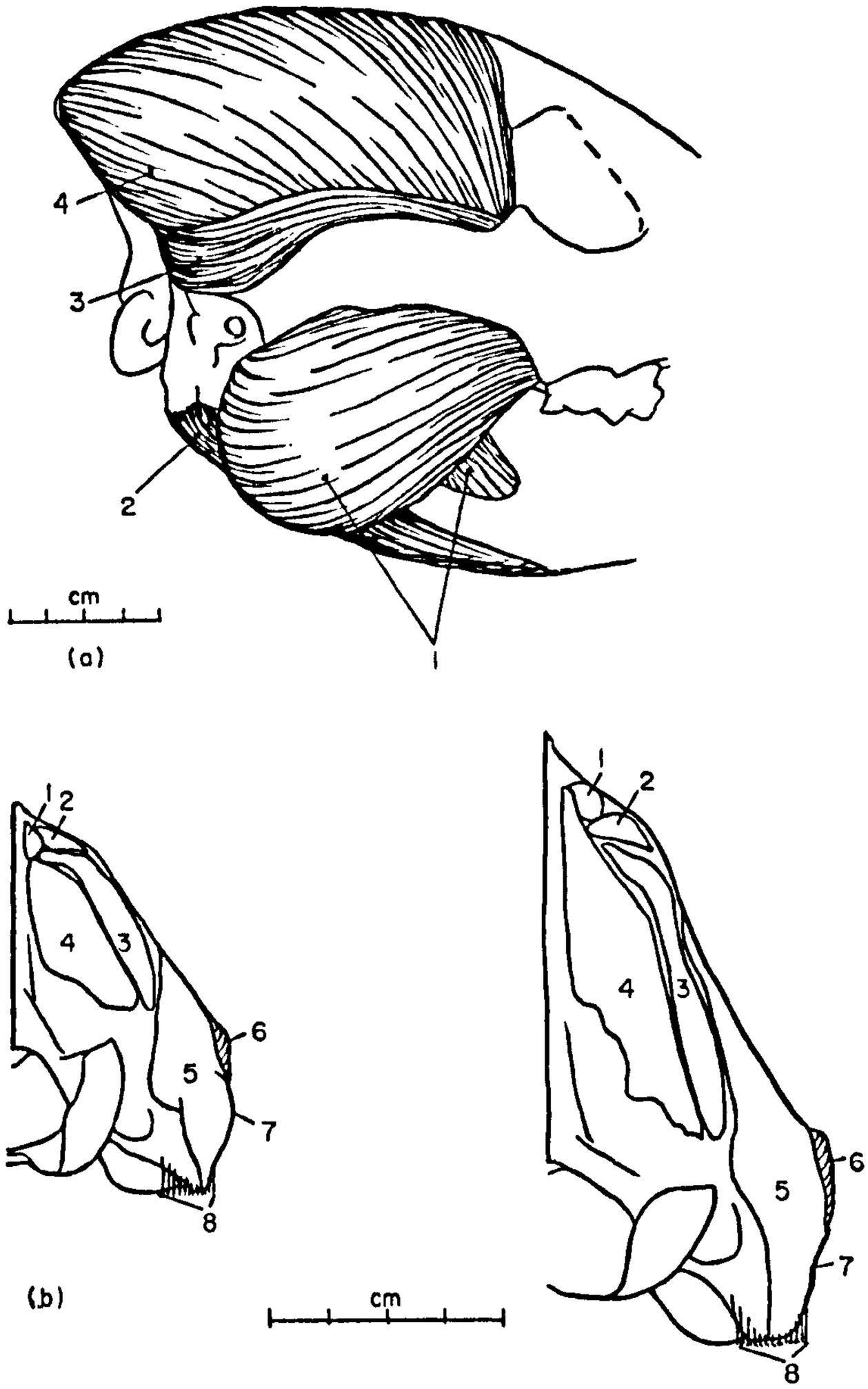

FIG. 7.—(a) Norma lateralis of *Crocuta*, showing the masticatory muscles. 1, M. masseter; 2, m. biventer mandibulae; 3, m. temporalis.

(b) Occiputs of *Hyaena* (left) and *Crocuta* (right) showing the insertions of the nuchal muscles. 1, M. complexus minor; 2, m. complexus major; 3, m. rectus capitis dorsalis major; 4, m. rectus capitis dorsalis minor; 5, m. obliquus capitis cranialis; 6, mm. splenius and longissimus capitis; 7, mm. cleidomastoideus and sternomastoideus; 8, m. biventer mandibulae.

Discussion

The most striking feature of the external morphology of the hyaena is the powerful development of the head-neck-and-shoulder region compared with the relatively weak

hindquarters. It is the dietary specialization of these animals as bone-crushers which has necessitated so considerable a functional development of the masticatory and nuchal muscles, the former to facilitate the seizing and crushing of prey, the latter to support the skull in the carrying off of heavy prey. To the relative degree of specialization of these particular muscle groups may be traced the craniological and osteological differences representative of generic distinction between *Hyaena* and *Crocuta*.

The extremely well developed temporalis muscle, larger relatively in hyaenas than in other carnivores, has necessitated the formation of a high sagittal crest and an emphatic nuchal crest. In *Crocuta* its posterior, horizontal fibres arise higher up the nuchal crest, the squamosal fossa is more pronounced, and both the zygomatic attachment and the coronoid insertion of the muscle are more extensive than in *Hyaena*. The main mass of the muscle is larger than in *Hyaena*, and is concentrated towards its mid-region, not towards its posterior region as in *Hyaena*. This is adequately illustrated by the nuchal crest in *Crocuta* lying in a more forward position. In short, the *Crocuta* m. temporalis fibres are so positioned as to exert a greater mechanical advantage than those of *Hyaena*, and to increase the functional power of the jaws. The muscle's relatively more forward siting on the lateral cranial wall has permitted the planum occipitale to broaden and thus to provide the necessary insertion area for the nuchal musculature, more powerfully developed in this genus. The increased strength of the masseter in *Crocuta* has necessitated the deepening of the jugal and the reduction in the convexity of the zygomatic arch's temporal component relative to that of *Hyaena*.

Anatomically, therefore, *Crocuta* exhibits, in comparison with the more primitive *Hyaena*, a structural specialization which confers a greater facility both for the seizing and crushing of prey and for its carrying away by mouth.

I wish to thank Dr L. S. B. Leakey for enabling me to carry out this investigation in East Africa and for his interest and encouragement throughout. Gratitude is also tendered to Professor R. R. Hofmann for assistance in the study of the musculature; to Dr C. B. Cox for his constructive criticism and to the staff of the British Museum (Natural History) and Mr M. Croydon for permission to examine material in their care. I am also very grateful to Professor A. J. E. Cave for the help he has given me in revising the manuscript of this paper.

REFERENCES

Bishop, O. N. (1966). *Statistics for biology*. London: Longman.

Ehrenberg, K. (1938). Die fuchs oder teufels lucken bei Eggenburg, Niederdau. *Abh. Zool.-bot. Ges. Wien* **17**: 27–50.

Reynolds, S. H. (1902). A monograph on the British pleistocene mammalia. (1) The cave hyaena. *Palaeont. Soc. Monogr.* **1902 2**: 1–25.

Watson, M. & Young, A. H. (1879). On the anatomy of *Hyaena crocuta* (*H. maculata*). *Proc. zool. Soc. Lond.* **1879**: 91–95.

A radiographic examination of frontal sinuses in early British populations

J. C. Buckland-Wright

Reprinted from Man vol 5 no 3 September 1970

A RADIOGRAPHIC EXAMINATION OF FRONTAL SINUSES IN EARLY BRITISH POPULATIONS

J. C. Buckland-Wright

British Museum (Natural History)

The determination of skeletal characteristics of populations by radiographic methods had been neglected until the recent work of Brothwell *et al.* (1968). In their study on the radiographic aspects of normal variation in early populations, they suggested several fields of study, two of which dealt with the cortical thickness of the femora and variations in the frontal sinuses. These two aspects were considered in some detail and have been shown to be of definite value in defining intergroup differences. This note is an attempt to extend the work of Brothwell *et al.* on the variation in the frontal sinus print between a British Bronze Age and a Saxon population, and to define, by means of indexes, the shape of the sinuses of these populations, and those of a Romano-British and a Medieval population.

The frontal sinuses in man normally appear by the third year (Libersa & Faber 1958: 454), and have completed their growth by the twentieth year. Their shape is largely determined by the interaction of three factors: 1) endocrinal (Schuller 1943; Libersa & Faber 1958); 2) mechanical; and 3) factors inherent in the mucus membranes (Libersa & Faber 1958: 457). The sinuses are generally larger in males, although in females the arcades of the scalloped upper border are smaller and more numerous (Schuller 1943: 555). With old age, the walls of the frontal sinus often become thin and the sinuses appear to be larger. Further changes in the radiographic appearance of the frontal sinuses during life are caused by inflammatory processes (e.g. sinusitis, tuberculosis, and syphilis), tumours or injuries to the forehead. Schuller has also remarked (1943: 555) that metopism accounts to a large extent for the absence or reduction in size of the frontal sinuses; this point however remains debatable (Torgerson 1950; Samuel 1952; Hodgson 1957; Marciniak & Nizankowski 1959).

Despite the number of external factors that can alter the size and shape of the sinuses, their configuration is primarily determined by genetic and mechanical factors (Libersa & Faber 1958; Schuller 1943); and accordingly it has been stated by Schuller (1921) and by Poole in 1931 (quoted Mayer 1935 and Cornwell 1956) that the frontal sinus prints of no two persons are alike. This aspect has been fairly extensively studied and has been developed as a method of identifying individuals (Culbert & Law 1927; Law 1934; Singleton 1951; Thorne & Thyberg 1953; Krogman 1962; Vlcek 1968), which Sassouni (1959) regards as 100 per cent. accurate. Within this range of individual variation Sir Logan Turner (quoted Mayer 1935: 517) attempted to determine the racial characteristics of frontal sinuses; the results of his studies proved largely negative. Recently Brothwell *et al.* (1968: 160–2) showed that the variation in height, width and surface area of frontal sinuses in the African negro, Australian aboriginal and European man were

entirely different. These results were based on direct observation, and an attempt is here made to place these results on a simple statistical foundation.

The range of material examined is set forth in table 1, and is part of the collection of the British Museum (Natural History), the number of individuals examined depended on the size of the respective populations represented in the collections. The populations studied were all adult and were divided into three groups, the first consisting of the British Bronze Age and Saxon series which had originally been examined by Metreweli (in Brothwell *et al.* 1968). The second and third groups comprised the male and female members respectively of a Romano-British and a Medieval population.

TABLE 1. Material examined.

Population	*Locality*	*Sex*	*Size of sample*
Bronze Age	East Riding, Yorkshire (7 individuals were from outside this area).	Male	31
British Saxon	Near Abingdon, Berkshire (11 of the individuals were from outside this area).	Male	28
Romano-British	Ancaster, Lincolnshire.	Male	51
		Female	28
Medieval	Wharram Percy, Yorkshire Wolds.	Male	24
		Female	15

The frontal sinus prints of all three groups were obtained from postero-anterior radiographs of the skulls. The procedure involved placing the nasal bones on the X-ray film. With the aid of plastic foam wedges, the forehead was raised a short distance above the film so that the principal rays passed through a region above the lambda. This arrangement avoided obliteration of the frontal sinus configuration by the ethmoid. The sinus depth in group two was measured from lateral radiographs of the skulls.

The lateral and superior extent of the frontal sinus development can easily be defined (fig. 1*a*), however, the inferior limit is not so clear. The lower limit has been taken as that defined by Libersa & Faber (1958: 453), and is represented by a line tangential to the superior borders of the orbits, A–F in fig. 1*a*. This was based on Terracol and Guerrier's (1958) statement that the sinuses are truly frontal when they extend above the line A–F. The sinus measurements taken on the radiographs were as follows: greatest height (A–B), greatest width (A–F); measurements were also taken on the sinus print one centimetre above the line A–F and is represented by the line D–E: height (D–B) and width (D′–C). A planimeter was used to obtain the surface area of the sinuses above the line A–F and D–E. The depth was measured (J in fig. 1*b*) from the anterior surface of the sinus, at a point level with the superior margin of the orbits, horizontally posterior to the endocranial face of the sinus. The product of half the depth times the surface area was used to calculate the volume. The measurements were used to establish simple indexes in order to express the relative shape of the frontal sinuses, and these appear in the text. The percentage of scalloping on the upper borders of the left and right moities of the sinuses and the percentage number of skulls which have a vertical extension of the frontal sinuses greater than one centimetre above the line A–F were also calculated. The mean and standard deviation were computed by the method described by Lewis (1966:

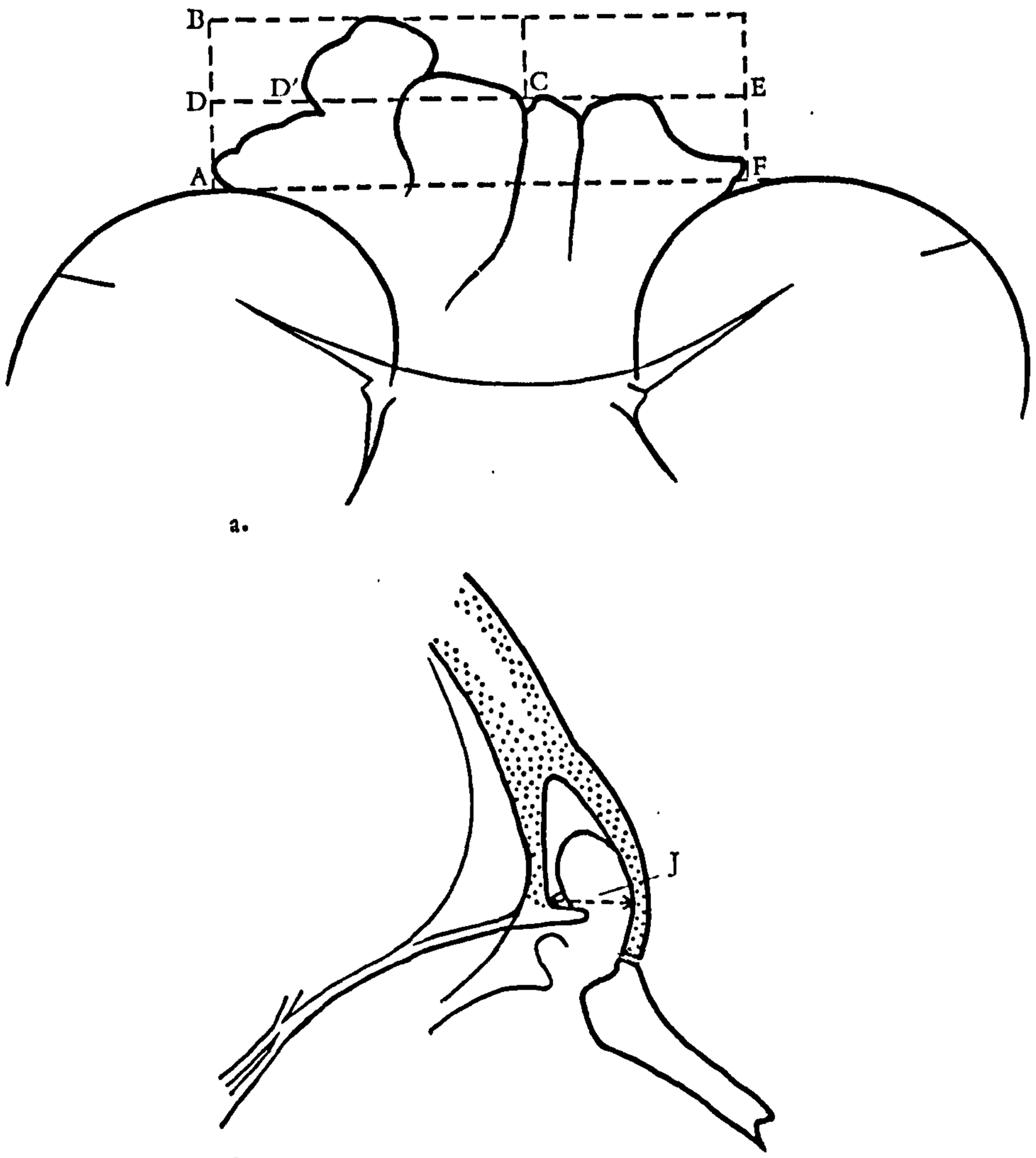

FIGURE 1. Measurements taken on a) the postero-anterior and b) the lateral radiographs of the frontal sinuses. For explanation see text.

40–1) for both measurements and indexes. In comparing the means of the populations the null hypothesis was set up in the standard way (Lewis 1966). As the wide range of individual variation in the population was expressed by the large standard deviation, a probability $P \leqslant 0{\cdot}02$ was considered significant when comparing the differences between the means and variances.

The results of the measurements on the height (A–B) and width (A–F) on the frontal sinuses of the males showed that the Romano-British had the highest values, with the Medieval, Saxon and Bronze Age populations following successively. The surface area of the sinuses above the line A–F showed that the Saxons had the largest mean area and following successively were the Romano-British, Medieval and Bronze Age populations. From the indexes (1) width (A–F) divided by height (A–B); and (2) area above the line A–F, divided by width (A–F) it was possible to separate the Bronze Age (mean (1): 3·04, and (2): 1·15) and Saxon (mean

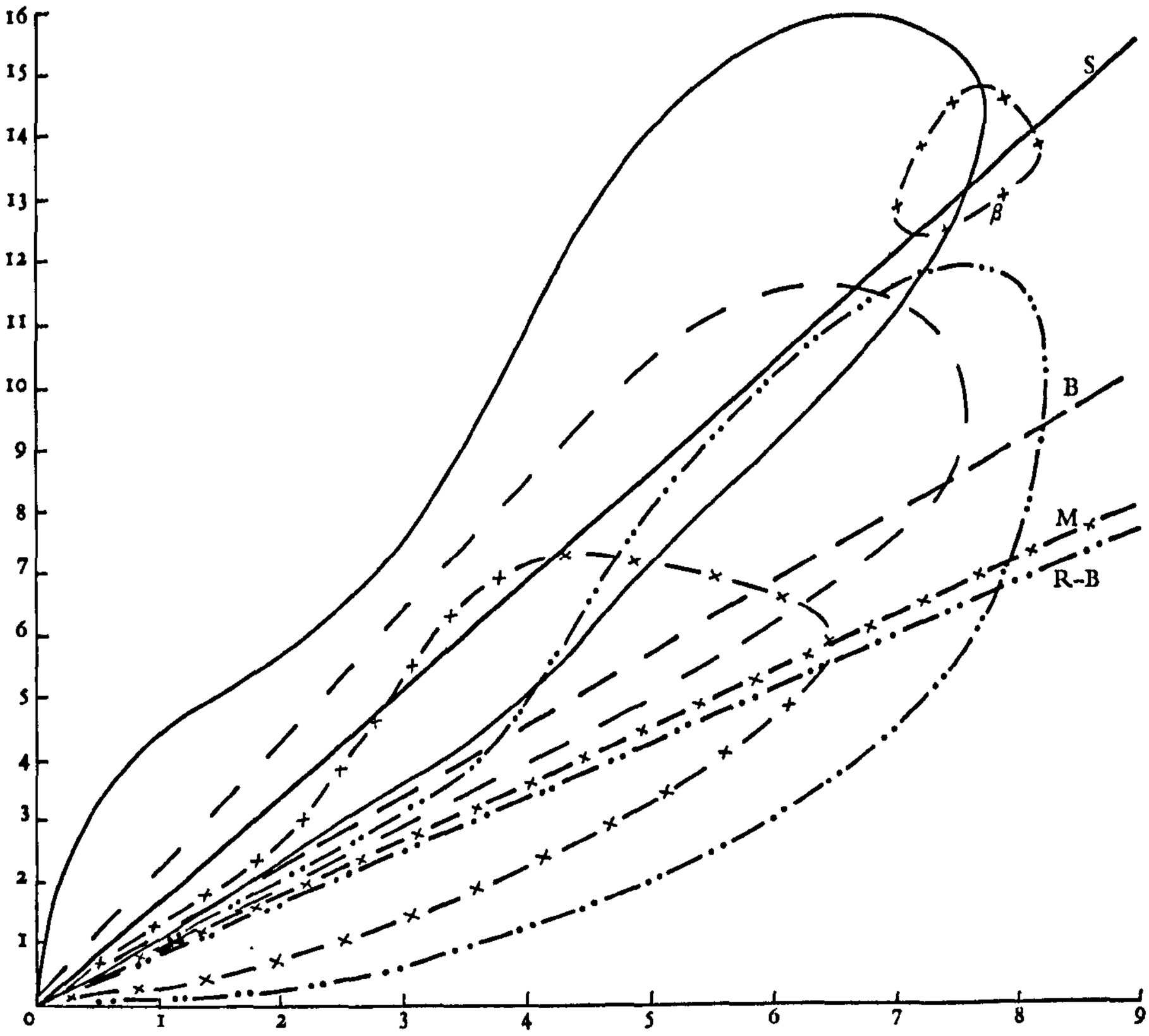

FIGURE 2. Graph showing the intergroup differences based on the ratio: surface area in square centimentres (ordinate) to greatest width in centimetres (abscissa) in (B) Bronze Age (31 males), (S) Saxon (28 males), (R–B) Romano-British (51 males), and (M) Medieval (24 males). The straight lines represent the statistical means for the above ratio (index (2) in text), the encompassing lines represent the extent of variation in the populations. In computing index (2) the skulls without sinuses had been included; this accounts for the low value and hence position on the graph of the lines representing the means relative to the trend in the populations as represented by the encompassing lines. β are the three Medieval skulls with very large sinuses.

(1): 3·60, and (2): 1·73) on their means. The Romano-British and Medieval proved statistically inseparable (fig. 2). With index (3) area above the line A–F, divided by height (A–B) the Romano-British (mean (3): 3·34) and Medieval (mean (3): 3·11) could be separated, whereas this was not possible with the Bronze Age and Saxons. The results of these indexes divided the populations into two statistically different groups, namely: 1) Bronze Age and Saxons; 2) Romano-British and Medieval. The results given above indicate that it is possible to separate the Bronze Age and Saxon populations on the area of their sinuses and indexes (1) and (2).

Although index (3) indicated that there was a slight difference between Romano-British and Medieval, the degree of separation was considered to be too small to be of any significant value. In order to find a more satisfactory index for separating these two populations, the depth (J), height (D–B), width (D′–C) and the surface area above the line D–E were then measured. The volume and the indexes (4) area above the line A–F, divided by depth (J), (5) height (A–B) divided

by depth (J) and (6) width (A–F) divided by depth (J) proved to be of no value in separating the Romano-British from the Medievals; the only observable difference was the slightly greater depth in the Romano-British population. However, it was possible to differentiate between the Romano-British and Medievals from measurements taken on the sinus one centimetre above the line A–F. The percentage number of skulls with a vertical extension greater than one centimetre was highest in the Romano-British (69 per cent.) and lowest on the Medieval (56 per cent.). The result was reflected in the indexes (7) area above the line D–E, divided by width (D′–C) and (8) area above the line D–E, divided by the height (D–B) which showed that the Romano-British (mean (7): 0·41, and (8): 1·67) had larger values than the Medievals (mean (7): 0·29 and (8): 1·49). The degree of separation between the means would have been further enhanced if it had not been for three individuals with very large frontal sinuses in the Medieval population (fig. 2). Examination of the percentage of scalloping present on the upper borders of the left and right moities of the frontal sinus in the Romano-British and Medieval populations showed no significant difference.

The measurements taken on the frontal sinuses of female Romano-British and Medieval populations clearly showed that the former had the larger sinuses, this was best illustrated by index (7) in which it was seen that the Romano-British (mean (7): 0·23) had broader sinuses than those of the Medievals (mean (7): 0·10). Comparative examination between the males and females of the two populations indicate that the males were approximately twice as large as the females.

In conclusion it can be said that the indexes of greatest value in separating the four populations are those in which the area of the sinus is divided by the width or height (indexes: (2), (3), (7) and (8)), the means of the measurements taken on the sinuses as well as a count of the number of skulls with a vertical extension of the sinus greater than one centimetre above the line A–F.

The results of the investigation suggest that apart from the mechanisms determining the individual variation of the sinus, there are either environmental or genetic factors controlling the frontal sinus configuration within each population. These factors are reflected in the overall size and shape of the sinus which remains generally constant within a population and accordingly enables intergroup differences to be established. This is shown by the frontal sinuses of the Romano-British and Medieval being larger than those of the Bronze Age and Saxon populations; in that the sinuses of the Saxons have a greater surface area with a relatively narrower sinus than those of the Bronze Age, and that the sinuses of the Romano-British above the line D–E, as seen in both males and females, are larger than those of the Medieval population. However, it should be remembered that the size of the populations studied is not large enough to allow the above separation of the populations to be considered as unequivocal. Further examination may profitably be carried out on the frontal sinuses of females. The variation in the size and shape of the sinus was not as great as in that of the males and therefore the females' sinuses may afford a more satisfactory means of separating populations.

NOTE

I wish to thank the trustees of the British Museum (Natural History) for enabling me to carry out this research during a student vacationship at the museum. My gratitude is extended to

D. R. Brothwell for his guidance and for critically reading the manuscript, and also to T. Molleson for her help at all times.

REFERENCES

Brothwell, D. R., T. Molleson & C. Metreweli 1968. Radiological aspects of normal variation in earlier skeletons: an exploratory study. In *The skeletal biology of early human populations* (ed.) D. R. Brothwell. London: Pergamon Press.

Cornwell, W. S. 1956. Radiography and photography in problems of identification: a review. *Med. Radiogr. Photogr.* **32**, 34.

Culbert, W. L. & F. M. Law 1927. Identification by comparison with roentgenograms of nasal sinuses and mastoid processes. *J. Am. med. Ass.* 88, 1634–6.

Hodgson, G. 1957. *A text-book of X-ray diagnosis.* London: Lewis.

Krogman, W. M. 1962. *The human skeleton in forensic medicine.* Illinois: Thomas.

Law, F. M. 1934. Roentgenograms as a means of identification. *Am. J. Surg.* **26**, 195–8.

Lewis, A. E. 1966. *Biostatistics.* New York: Reinhold.

Libersa, C. & M. Faber 1958. Étude anatomo-radiologique du sinus frontal chez l'enfant. *Lille méd.* **3**, 453–9.

Marciniak, R. & C. Nizankowski 1959. Metopism and its correlation with the development of the frontal sinuses. *Acta radiol.* **51**, 343–52.

Mayer, J. 1935. Identification by sinus prints. *Va. med. Mon.* **62**, 517.

Samuel, E. 1952. *Clinical radiology of the ear, nose and throat.* London: Lewis.

Sassouni, V. 1959. Cephalometric identification: a proposed method of identification of war dead by means of radiographic cephalometry. *J. forens. Sci.* 4, 1–10.

Schuller, A. 1921. Das Roentgenogram der Stirnhole: ein Hilfsmittel für die Identitätsbestimmung von Schädeln. *Mschr. Ohrenheilk. Lar.-Rhinol.* **55**, 1617–20.

——— 1943. A note on the identification of skulls by X-ray pictures of the frontal sinuses. *Med. J. Aust.* **1**, 554–6.

Singleton, A. C. 1951. The roentgenological identification of victims of the 'Noronic' disaster. *Am. J. Roentg.* **66**, 375–84.

Terracol, J. & Y. Guerrier 1958. Les sinusites de l'enfance. *Monogr. Otol. Rhinol. Lar. int.* **35**, 40–5.

Thorne, H. & H. Thyberg 1953. Identification of children (or adults) by mass miniature radiography of the cranium. *Acta odont. scand.* **2**, 129–40.

Torgerson, J. 1950. A roentgenological study of the metopic suture. *Acta radiol.* **33**, 1–11.

Vlcek, E. 1968. Nález pozustatku neandertálce v Sali na Slovensku. *Anthropozoikum* **5**, 105–20.

PRINTED IN GREAT BRITAIN BY
WILLIAM CLOWES AND SONS, LIMITED
LONDON, BECCLES AND COLCHESTER

Reprint from J. Zool., Lond. (1972) 168 : 424-426

J.C. BUCKLAND-WRIGHT

Ph.D. Thesis, 1974

Radiographic and histological examination of the femur of the fruit bat (*Rousettus aegyptiacus*)

Introduction

The primary aim of this paper is to present some observations on the structure and histology of the femur of *Rousettus aegyptiacus*. Attention had been drawn to the simplicity of its organization during an investigation of the effects of calcium/vitamin D deficiency in this fruit bat (Buckland-Wright & Pye, 1973). Comparative histology of the bones of small vertebrates (Enlow & Brown, 1956; Enlow, 1962*a*, *b*; Jowsey, 1966, 1968; Felts & Spurrell, 1967) have shown very simple patterns of vascular channels and distributions of bony tissues, the simplest being the nonhaversian or primary tissue cylinder with an avascular diaphysis. Felts & Spurrell (1967) have stated that the threshold of vascularity for the femora lay between that of a mammal the size of the Masked shrew (*Sorex cinereus*) and the mouse (male C57 black mice) (Table I). This statement is re-examined in the light of the observations herein and comparisons drawn where appropriate with the same bone of small mammals.

TABLE I

Mean greatest length of the femora in Sorex cinereus and Rousettus aegyptiacus

Sorex cinereus[1]	6·8 mm	(6·5– 7·2 mm)
Male C57 black mice[1]	14·8 mm	(14·5–15·7 mm)
Rousettus aegyptiacus[2]	29·4 mm	(28·5–30·8 mm)
Male albino rats[1]	32·0 mm	(31·7–33·0 mm)

[1]Data from Felts & Spurrell (1967).
[2]Data from Dr J. D. Pye collection.

Materials and methods

The bone histology described here is based on three adult *Rousettus aegyptiacus* from Uganda, of which one was deemed normal as it had died within a few days of capture, a summary autopsy performed on the specimen gave no indications of pathology and the bone was considered normal by macroscopic and histological criteria. The remaining specimens had been kept in captivity for over a year and showed physiological disturbances, however, the macroscopic and major histological features of the bones showed a similar pattern with those of the normal specimen.

After preservation in formalin solution, the left femur of the specimens were dissected out and stereopair projection radiographs were taken with the XX 90 fine focus x-ray tube (Ely, 1967, 1972) which produced magnified images 6 times natural size. A 2 mm block of the diaphysial mid-shaft was removed and embedded in "Autoplax" resin, 400 μm transverse sections were cut on a diamond wheel and the sections ground to 100 μm. Contact microradiographs were taken using the Intercol 30B/VST fine focus x-ray machine. The remaining portions of the femora were decalcified and prepared for routine histology. 7 μm transverse and longitudinal sections were cut and stained in haematoxylin and eosin, Mallory and Van Giesen.

Observations

Macroscopic and radiographic examination

The external configuration of the femur of *Rousettus* is characteristic of the Megachiroptera. The condylar head lies close to the line of the diaphysial axis with the greater and lesser trochanters almost diametrically opposite each other (Plate I(a)). The diaphysis in the mature bone is cylindrical, without a linea aspera and the shaft becomes slightly ovoid (long axis in the medio-lateral plane) close to the distal metaphysis. The projection radiographs revealed the channels for the nutrient vessels passing into the marrow cavity; which are present as a single foramen at the dorso-lateral wall of the proximal end of the diaphysis and as several foramina at the mid-ventral aspect of the distal metaphysis.

The compact cortical bone of the diaphysis has a maximum thickness of 24 μm which diminishes abruptly to a thin cortex over most of the epiphyses (6–4 μm). The spongiosa is relatively sparse and indicates that the femur of *Rousettus* is not a primary weight bearing structure. Within the distal end of the femur the spongiosa is more dense and fine structured than in the proximal end. There are no distinct interregional tracts of bone between the diaphysis, trochanters and condylar head as described for humans by Koch (1917), Tobin (1955) and many other workers. The only representation of such a load distributing system in this fruit bat is an irregular grouping of trabeculae running from the distal articular condyles to the walls of the shaft. The largest individual trabeculae occurred at the proximal end of the diaphysis (12 μm); within the epiphyses and metaphyses the trabeculae ranged in size from 9 μm to less than 1 μm.

Microradiographic and histological examination

The periosteal and endosteal surfaces are smooth (Plate I(b)), and no vascular channels apart from those for the nutrient vessels, occurred in the diaphysis. The lacunae are relatively numerous and are arranged in random fashion approximately parallel to the axis of the shaft. The cement lines (a resting phase in the calcification process) contained circumferentially uneven concentrations of calcium salts which showed up in the microradiographs as radio-dense or radio-lucent circumferential bands. The histological study confirmed that the diaphysis consisted of a primary tissue or nonhaversian cylinder (Plate I(c)), comprising of a number of circumferential lamellae composed of a type of bone not previously described. The cannalicular system characteristic of human Haversian bone is absent, however, there are structures which suggest the presence of fine cannaliculi associated with some of the lacunae.

An osteocyte differential count (Baud & Auil, 1971) gave a percentage number of small osteocytes in steady state as 55 %±3, enlarged osteocytes with osteolytic or osteoplastic activity as 37 %±3 and empty lacunae corresponding to dead osteocytes as 8 %±1. The percentage corresponded approximately to those given for normal adult human trabecular cancellous bone (Baud & Auil, 1971).

Discussion

The histology of the femoral shaft in small rodents including the mouse (Enlow, 1962*a*; Felts & Spurrell, 1967) revealed primary vascular channels penetrating the cortex. In the rat the cortex contains a number of primary osteons. Experiments performed by Ruth (1953) demonstrated that secondary Haversian systems could be produced by artificially induced calcium deficiency (resulting in resorption) followed by a period of dietary

calcium excess (causing regenerative redeposition). The femur of *Rousettus* is, in size, slightly shorter and narrower than that of the rat and approximately twice the length of that of the mouse (Table I). Under calcium/vitamin D deficiency the diaphysis of *Rousettus* (Buckland-Wright & Pye, 1973) showed endosteal resorption by osteoclasis and osteocyte osteolysis within the shaft. Regenerative redeposition resulted in a reversal of these processes without the formation of a vascularized system.

The femur of *Rousettus aegyptiacus* probably constitutes the largest avascular cylindrical bone described for mammals. And it is suggested that the threshold of vascularity may well lie, as stated by Felts & Spurrell (1967), between that of *Sorex cinereus* and the mouse for terrestrial mammals, where the exogenous forces on the bones are large. However, the threshold may lie above that of the size of *Rousettus* for a tubular bone not continually subjected to similar forces. The bone histology of *Rousettus* is of a type hitherto not recorded and this preliminary description warrants a more comprehensive examination than is possible with the material available to the author, in particular the lack of a clear cannalicular system raises the problem of how the vitality of this bone is maintained. Furthermore investigations on the femora of alternative Megachiroptera and subsequent comparisons with other mammals and reptiles may assist in determining more precisely the threshold of vascularity in tubular bones.

I am very grateful to a number of people whose help made this investigation possible: to Dr David Pye for supplying me with the specimens of *Rousettus*; to Mr John Wells for preparing the histological sections; to Mr R. D. Reed and Mr Philip Batten for taking the photographs and to Mr Raymond Ely of the M. R. Research Trust for the use of the fine focus x-ray machines at King's College London. The research was supported by a postgraduate scholarship from the Science Research Council. Gratitude is also tendered to Dr Barry Brown and Dr Martin Hobdell for their constructive criticisms.

REFERENCES

Baud, C. A. & Auil, E. (1971). Osteocyte differential count in normal human alveolar bone. *Acta anat.* **78**: 321–327.
Buckland-Wright, J. C. & Pye, J. D. (1973). Dietary deficiency in fruit bats. *Int. Zoo Yb.* **13**: 00–00.
Ely, R. V. (1967). Micro and enlargement radiography. *X-ray Focus* **8**: 14–21.
Ely, R. V. (1972). X-ray microscopy. In *Physical methods of chemistry. Part IIIA.* Weissberg, A. & Rossiter, B. W. (Eds.). Chichester: J. Wiley.
Enlow, D. H. (1962*a*). A study of the post-natal growth and remodelling of bone. *Am. J. Anat.* **110**: 79–102.
Enlow, D. H. (1962*b*). Functions of the haversian system. *Am. J. Anat.* **110**: 269–306.
Enlow, D. H. & Brown, S. O. (1956). A comparative histological study of fossil and recent bone tissues. Part I. *Tex. J. Sci.* **8**: 405–443.
Felts, W. J. & Spurrell, F. A. (1967). Microradiographic visualization of structure in bones of the masked shrew, *Sorex cinereus*. *Am. J. Anat.* **120**: 89–112.
Jowsey, J. (1966). Studies of haversian systems in man and some animals. *J. Anat.* **100**: 857–864.
Jowsey, J. (1968). Age and species differences in bone. *Cornell Vet.* **58**: 74–94.
Koch, J. C. (1917). The laws of bone architecture. *Am. J. Anat.* **21**: 177–298.
Ruth E. B. (1953). Bone studies. II. An experimental study of the haversian-type vascular channels. *Am. J. Anat.* **93**: 429–456.
Tobin, W. J. (1955). The internal architecture of the femur and its clinical significance. *J. Bone. Jt Surg.* **37A**: 57–73.

J. C. BUCKLAND-WRIGHT
Department of Anatomy,
University of London,
King's College,
Strand, London WC2

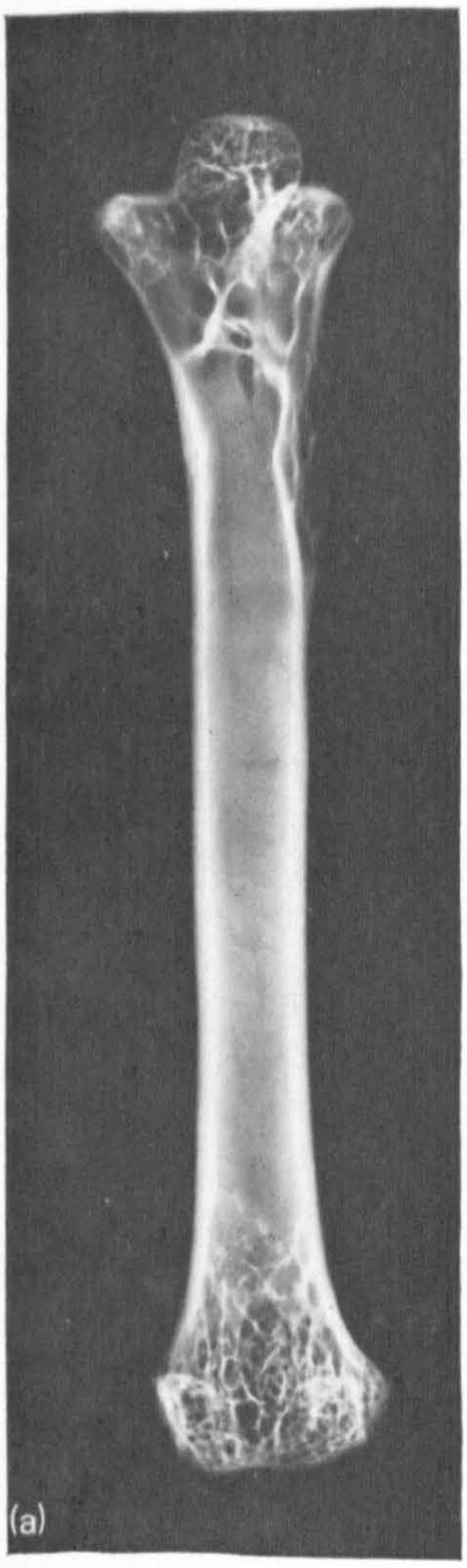

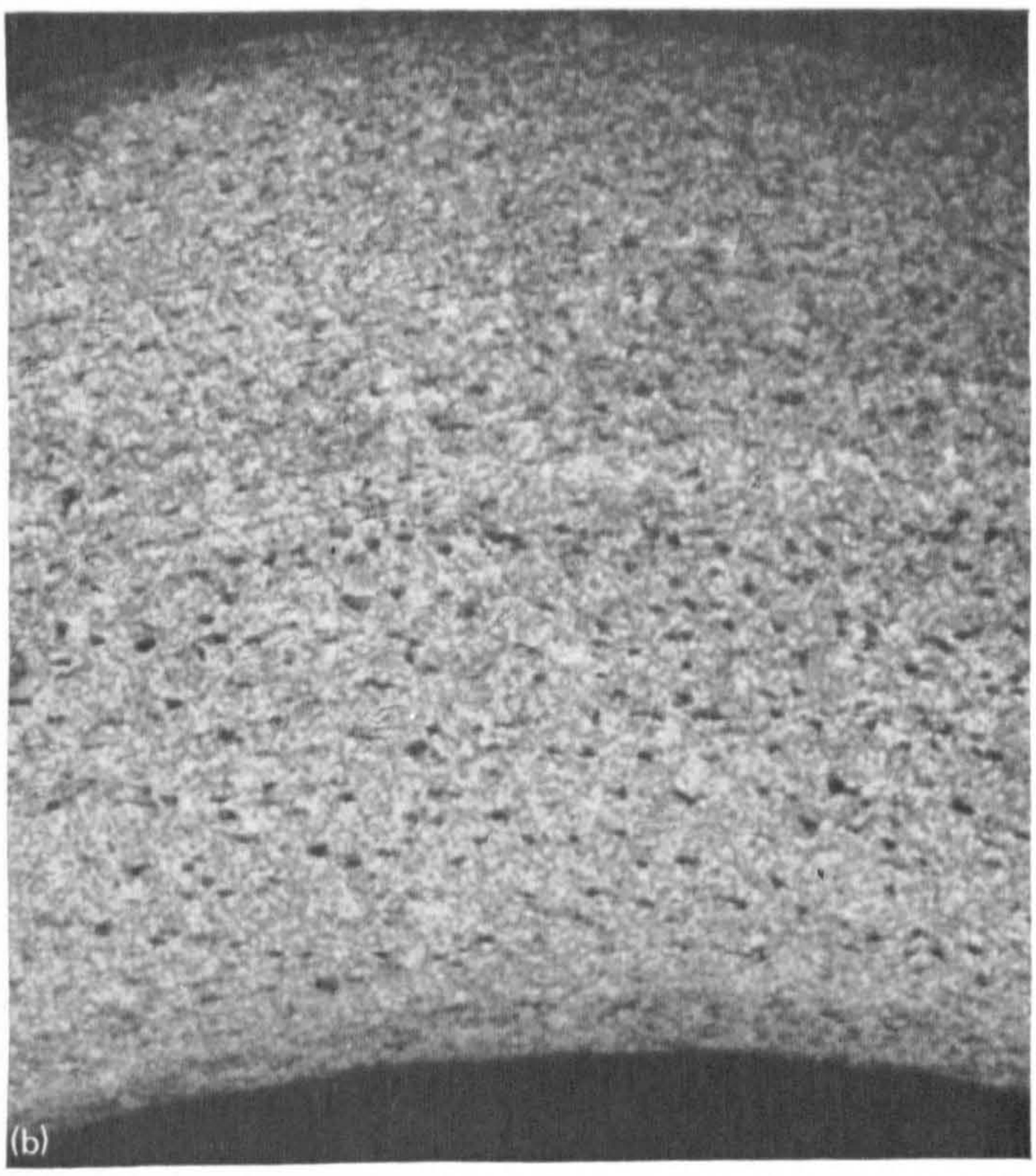

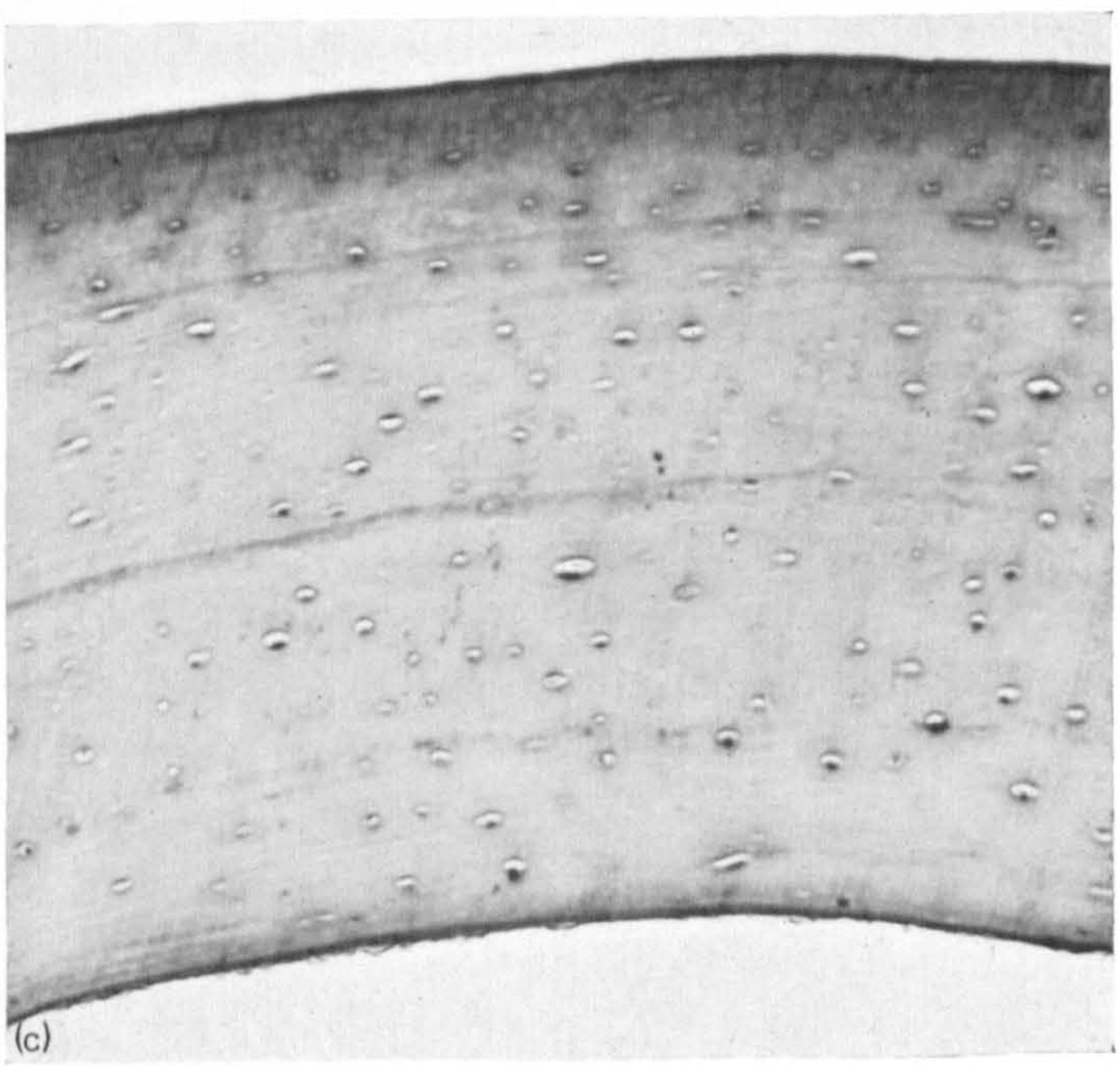

PLATE I. (a) Dorso-ventral projection radiograph of the left femur of *Rousettus aegyptiacus*. ×3·4. Transverse sections of the diaphysis of the femur: (b) microradiograph; (c) histological section stained in haematoxylin and eosin. (b), (c) ×240.

[*To face page* 426

J.C. BUCKLAND-WRIGHT

Ph.D. Thesis. 1974

Reprinted from the
INTERNATIONAL ZOO YEARBOOK
VOLUME 13 - (1973):271 – 277

Dietary deficiency in fruit bats

J. C. BUCKLAND-WRIGHT & J. D. PYE
Departments of Anatomy and Zoology, University of London King's College, Strand, London, W.C.2, Great Britain

One of us (J.D.P.) has maintained a variety of fruit bats (Megachiroptera; Pteropidae) in captivity for a number of years with superficial success. All losses followed a common pattern: hyperexcitability during handling or other disturbance giving a tetanic condition with the wings partly unfolded, leading to death within minutes of an apparently healthy animal. A way of avoiding this and the probable explanation will be described here.

The species of fruit bats kept in London were three *Pteropus giganteus*, 15 *Rousettus aegyptiacus*, one *Rousettus amplexicaudatus*, one *Myonycteris torquata*, one *Epomops franqueti*, one *Micropteropus pusillus*, and 15 *Nanonycteris veldkampi*. All lived for well over a year and the *Rousettus aegyptiacus* and *Nanonycteris veldkampi* bred freely in two seasons although the latter's young remained rather stunted. *Pteropus giganteus* accepted a variety of soft fruits, particularly apples, but sweet citrus only with reluctance. All other species would only accept bananas; this was pulped with sugar and water for the smaller species. Lord Medway (*in litt.*) pointed out that bananas have an extremely low calcium content and a high phosphorus level and recommended adding powdered milk to the diet. This is confirmed by McCance & Widdowson (*10*) as shown in Table 1. The very low calcium level is shared by canned fruit salad, black (but not white) grapes, mandarines, nectarines, passion fruit and peaches. Fruits with a high calcium level (figs, rhubarb, lemons, blackberries and black currants) are generally unacceptable to bats although this is unlikely to be true of their diet in the wild. The phosphorus level of bananas is not excessively high and Davidson & Passmore (*4*) strongly deny that, in man at least, a high phosphorus intake depresses calcium levels.

The fatal symptoms were then recognised as typical of calcium-phosphorus imbalance, parathyroid disturbance or vitamin D deficiency, all of which are related as causes of tetany (*2*). Dried milk, an extremely rich source of calcium, was immediately added to the bananas daily, but was soon replaced by Complan which is basically dried milk with additives that make it into 'a complete food' suitable for convalescents and in particular has a high level of vitamin D (Table 1). This has now been liberally sprinkled on chopped bananas at least five times a week for two years and has led to a dramatic improvement in the condition of *Rousettus aegyptiacus* (the only species now available). Two young, born soon after the change in diet was started, rapidly reached full size and the animals now accept handling or other disturbance without any sign of hyperexcitability. Dr Ann Brown (pers. comm.), who has operated on this species for recording cochear potentials, has reported a similarly marked improvement in the condition of the bone, connective tissues and blood vessels.

In order to investigate the effects in a little more detail, three selected cadavers of *Rousettus aegyptiacus* have been examined by the senior author. All were originally collected from a cave at Queen Elizabeth National Park, Uganda. One ('Normal') died within a few days of capture, while awaiting importation formalities at London Airport, one ('Deficient') died in a tetanic state after more than a year in captivity on a diet of

	CALCIUM (mg/100 g)	PHOSPHORUS (mg/100 g)	VITAMIN D (μg/100 g)
Banana pulp (1) (excluding skins)	6·8	28·1	0
Dried milk (1) skimmed	1265	1050	trace
whole	960	760	0·3
Glaxo 'Complan' (2)	825	780	5·5

(1) Data from McCance & Widdowson (*10*).
(2) Data from the manufacturers' packet.

Table 1. The comparative amounts of calcium, phosphorus and vitamin D found in banana pulp, dried milk and Complan.

bananas only and one ('Recovered') survived for more than a year on bananas only and was then given the Complan additive for a few months before being sacrificed by Dr Brown for cochlear studies.

The study of the material began sometime after the bats had died. The 'Deficient' specimen had been decapitated and all three had had their abdominal walls opened to permit the infusion of formalin solution into the viscera. Measurements were made of the length of the left forearms and of the left femora which had been dissected out. (Table 2).

Histology of the 'Normal' femur: Radiographic and histological examinations showed that the compact bone of the shaft diminished abruptly to a thin cortex over most of the metaphysis and epiphysis, and the spongiosa was seen as an aggregation of trabeculae in these regions. The diaphysis can be regarded as a primary tissue cylinder, as it consists of a number of concentric lamellae composed of a type of bone not previously described, in which the formative bone cells were arranged in random fashion approximately parallel to the axis of the shaft. The cannalicular system characteristic of human Haversian bone is absent. However, there are structures which suggest the presence of fine cannaliculi associated with some of the lacunae. Microradiographs showed that the cementing lines (a resting phase in the calcification process) contained a concentric uneven concentration of calcium salts. The femur is lined by vascularised periosteal and endosteal layers; the diaphysis itself is avascular except for the channels for the nutrient vessels supplying the marrow. A more detailed histological account of the normal femur is in press (*3*).

Comparative radiographic examination: Dorso-ventral (i.e. at right angles to the latero-medial plane) projection radiographs of the femora were taken with the XX 90 fine focus X-ray tube (*5*); the stereopair radiographs produced were six times natural size. Examination under the stereoviewer showed that the overall radiographic appearance of the 'Normal' and 'Recovered' was similar. In the 'Deficient,' the cortex of the metaphysis and epiphysis was thinner by approximately 30%, the endosteal layer along the length of the shaft was irregular and the trabeculae were narrower and reduced in number. Contact microradiographs were taken of 100μm transverse sections of the femoral midshaft with the Intercol 30B/VST fine focus X-ray machine.

Calcification in the 'Normal' appeared even. Where concentration of calcium salts occurred in the cementing lines, these showed up as thin radio-dense bands. The lacunae were generally small and the endosteal surface was smooth. In the 'Deficient' specimen active resorption (*7*) of the diaphysial bone was seen on the whole of the endosteal surface and at a number of sites on the

	'NORMAL' (mm)	'DEFICIENT' (mm)	'RECOVERED' (mm)
Overall length of the forearm	96	97	99
Femora: Head-condylar length	29·1	28·5	30·8
Dorso-ventral midshaft width	2·1	2·1	2·2

Table 2. Skeletal measurements (mm) of the three adult fruit bats *Roussettus aegyptiacus*.

periosteal layer. The cementing lines showed a loss in calcium and in some regions appeared as radiolucent lines. Numerous enlarged lacunae occurred close to the endosteum and extended to approximately half the width of the shaft. The 'Recovered' specimen showed a well-defined zone of less dense, recently deposited bone at the endosteal region. The surface of the latter and the periosteum were smooth, the lacunae and cementing lines had a similar appearance to that of the 'Deficient' specimen.

Comparative Histology: The proportions of the femora not used for micro-radiography were decalcified and prepared for routine histological examination. The transverse section of the shaft of the 'Deficient' was divisible into a larger inner or endosteal zone and an outer or periosteal zone as in Fig. 2 a, Plate 47. In the former the cementing lines were very irregular and enclosed resorption spaces of approximately lacunar size. The lacunae and the fine cannaliculi were enlarged and at a number of loci in the mid-circumferential region complete localised demineralisation had occurred around the lacunae. Howship's lacunae were numerous on the endosteal surface.

The periosteal zone demonstrated little change from the 'Normal' apart from a narrow layer of

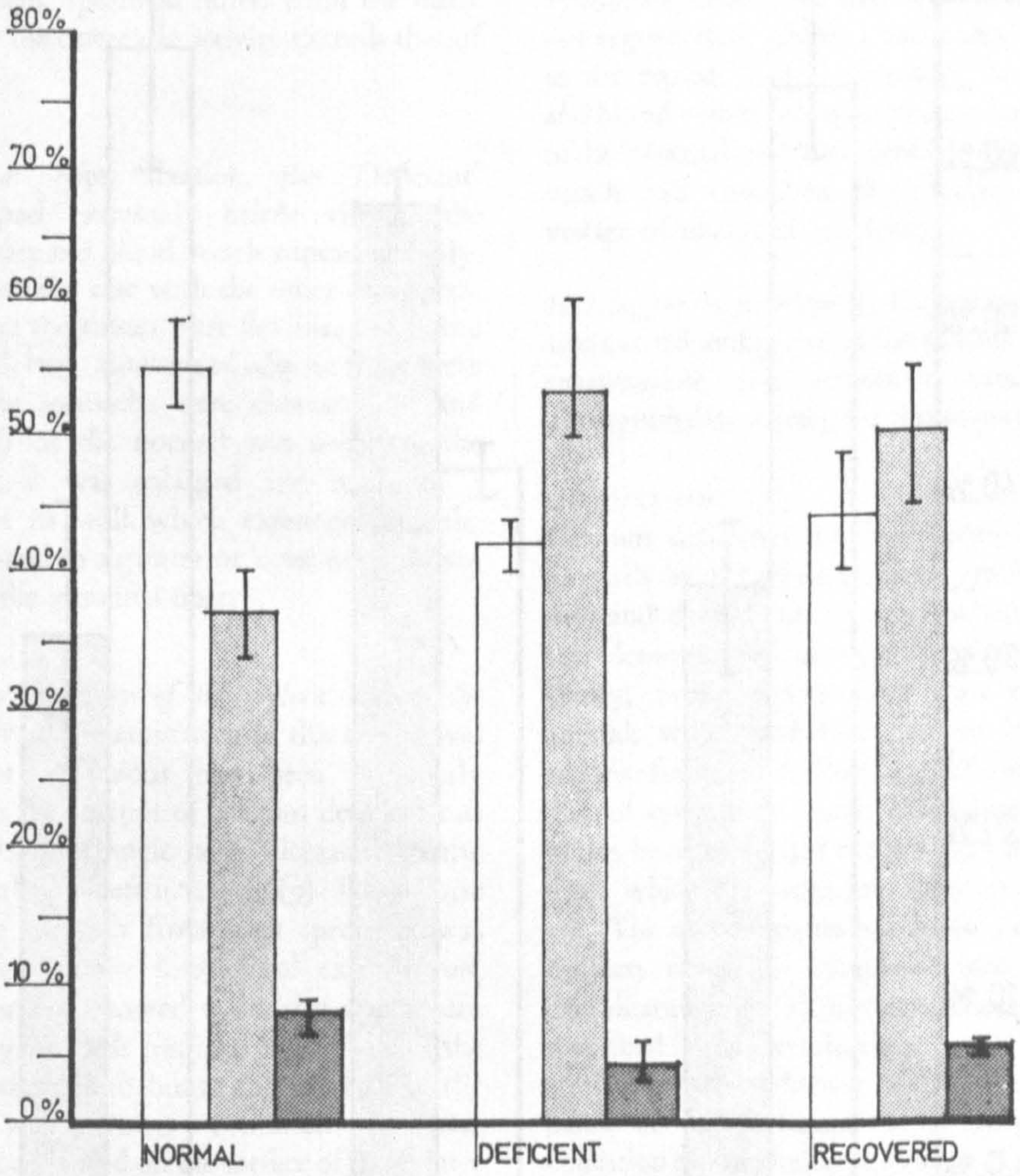

Histogram 1. Percentage of osteocytes in femora of the 'Normal', 'Deficient' and 'Recovered' specimens of the fruit bat *Rousettus aegyptiacus.*
Left: small osteocytes in steady state.
Middle: enlarged osteocytes with osteolytic or osteoplastic activity.
Right: empty lacunae corresponding to dead osteocytes.

demineralisation associated with the periosteal surface and underlying cementing lines.

The 'Recovered' specimen differed little from the 'Deficient', apart from the formation of a well-defined layer of recently deposited bone lining the endosteal surface and from which osteoclasts were absent. Within this layer of new bone was a cementing line indicating a resting phase in the process of calcification during recovery. The reversal line bordering the older bone was highly irregular and demarcated the extent of bone resorption during the phase of dietary deficiency. Bone deposition on the periosteal surface was slight except in the regions of the empty Howship's lacunae where the new bone had filled in these pits. A high proportion of the enlarged lacunae contained large basophylic cells characteristic of osteoplasis.

Osteocyte differential count: Baud & Auil (*1*) have

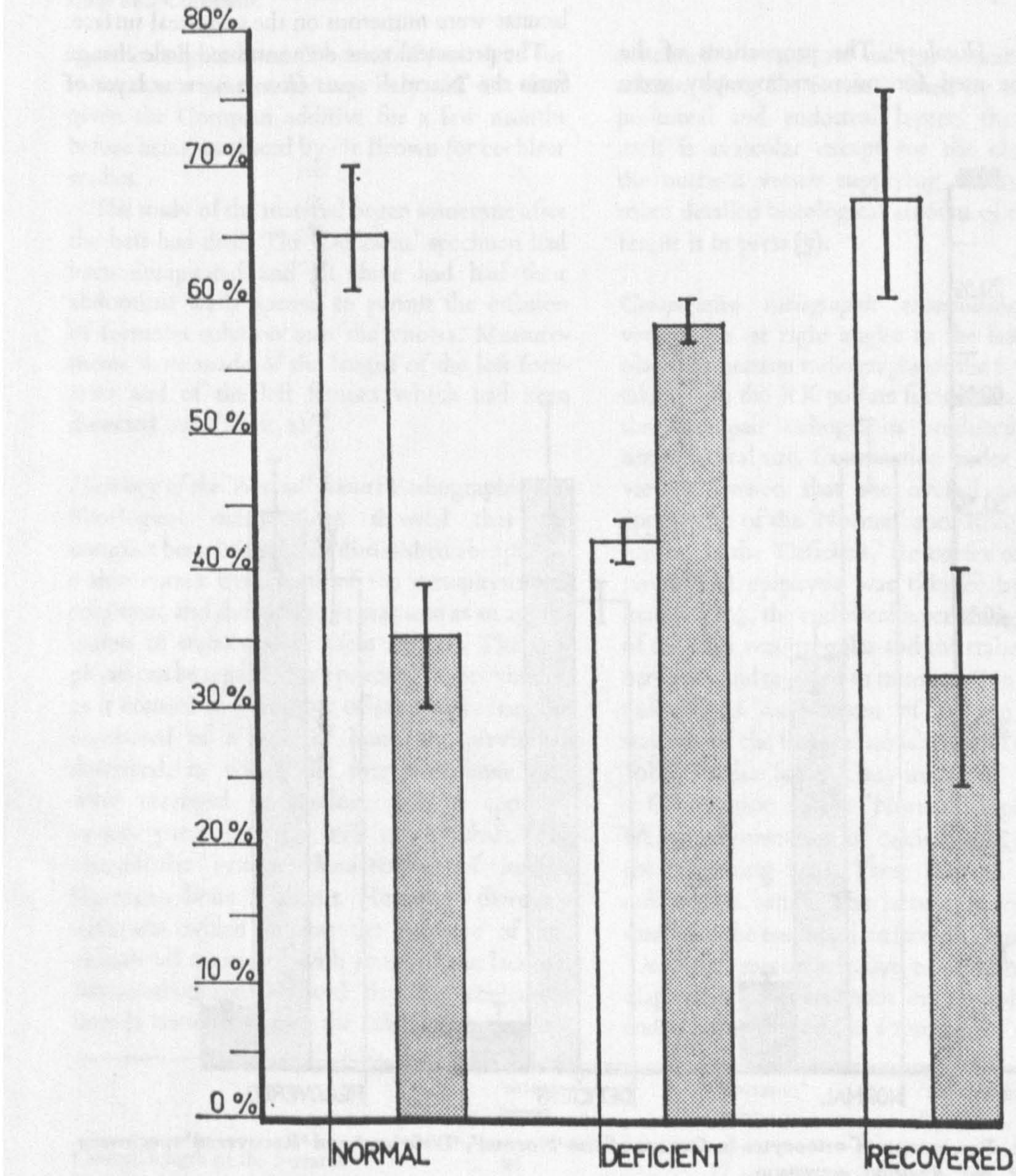

Histogram 2. Estimated percentage of large osteocytes undergoing osteolysis (right) and osteoplasis (left) in femora of 'Normal', 'Deficient' and 'Recovered' specimens of the fruit bat *Rousettus aegyptiacus.*

classified osteocytes into three groups, (a) those composed of small osteocytes in steady state, (b) enlarged osteocytes with osteolytic or osteoplastic activity, and (c) empty lacunae corresponding to dead osteocytes. The percentage of each group was determined in the three specimens in order to establish the existence of any changes in osteocyte activity.

Histogram 1 demonstrates the increased vitality of the osteocytes in the 'Deficient' and 'Recovered' specimens. An estimation of the percentage number of large osteocytes undergoing osteolysis (multinucleate acidophylic cells in irregular walled lacunae) and osteoplasis (uninucleate basophylic cells in smooth walled lacunae) was carried out and the results are presented in Histogram 2. The 'Deficient' specimen differs from the other two in that the osteolytic activity exceeds that of osteoplasis.

The viscera: After fixation, the 'Deficient' specimen had extremely brittle viscera, the intestinal tract and blood vessels rupturing easily. This was not the case with the other two specimens, where the tissues were flexible, and in the 'Recovered', large amounts of adipose tissue were present. The stomachs were dissected out and deviation from the normal was noted in the 'Deficient'; it was enlarged and exhibited a thinning of its wall which extended into the duodenum and to a greater or lesser extent along the rest of the intestinal tract.

Comparative histology of the pyloric end of the stomach body: An examination of this region was carried out as lesions had been previously recorded in the antrum of calcium deficient rats (*15*) and haemorrhagic and ulcerated gastric lesions in calcium-deficient dogs (*9*). The pyloric end of the stomach from each specimen was prepared for routine histological examination.

The 'Normal' showed a healthy appearance with mucogenic cells confined to the base of the pits and surface epithelium. The stomach of the 'Deficient' was necrotic, a condition which was particularly advanced on the surface of the greater curvature. The rugae were almost entirely absent and the submucosa was confined to a narrow band. The cellular organisation showed advanced karyolysis. Mucus was almost completely absent from the surface epthelium and the cells of the stomach wall showed desquamation into the lumen. Associated with the extensive necrosis was the destruction of blood vessels with resulting haemorrhages; the remaining blood vessels were either empty or contained ghost cells of haemolysed blood corpuscles, possibly the result of conditions induced by complex dietary deficiency. The darker staining particles in Fig. 2a, Plate 48 associated with the lining of the stomach are the remains of food debris.

The 'Recovered' specimen had regained its normal configuration and the remains of a meal were still visible in the lumen. Regeneration of the cells at the isthmus of the submucosa had replaced the surface epithelium and parietal cells. The zymogenic cells at the base were absent and had not regenerated, giving a vacuolated appearance to this region. The condition of the submucosa and blood vessels was intermediate between those of the 'Normal' and 'Deficient.' Some of the blood vessels still contained ghost cells, a probable vestige of advanced deficiency.

Histology of the parathyroid: The parathyroid gland was excised and prepared for routine histological examination. No structural alterations were distinguishable among the three specimens.

DISCUSSION

Calcium deficiency has been produced experimentally by dietary means in rats, rabbits, guinea-pigs and dogs. Prior to 1937, when Martin (*9*) first demonstrated uncomplicated calcium deficiency, many reports had been recorded of animals which had been fed on low calcium rations; for example Voit (*13*) gave young dogs a diet of only horse meat. More recently, cereal grains have been used as the main constituents of diets which produced low calcium rickets (*11*; *12*). The above studies produced a complicated calcium deficiency syndrome into which this examination must fall, in view of the circumstances described in the introduction.

The apparent absence of parathyroid disturbance in the 'Deficient' is not surprising in a condition of this kind as an absence of pathological condition of the parathyroid under calcium/vitamin D deficiency has been reported (*2*; *6*). The death of this specimen therefore appears to be the result of gross calcium deficiency and/or the absence

of vitamin D and almost certainly further dietary deficiencies resulting from the induced pathological condition of the gastro-intestinal tract.

The calcium/vitamin D deficiency resulted in the resorption of calcium salts into the highly vascular marrow cavity of the femur from its endosteal region by the combined effect of osteocyte osteolysis and osteoclastic activity. Osteolysis may possibly have been the result of enzyme action (*8*) altering the organisation of the bone and causing the demineralisation of the circumlacunar areas and cementing lines. The relative reduction in resorption from the periosteal region may be associated with the necessity for diaphysial rigidity connected with exogenous forces. A similar pattern of osteolytic activity occurs in the femur of *Myotis lucifugus* during hibernation (*14*).

Lesions and haemorrhages of the pyloric end of the stomach body described here have been previously recorded in the antrum of calcium deficient animals. However, it is suggested that the advanced state of necrosis in the gastro-intestinal tract and the haemolysis are associated with further deficiencies set in train by the initial dietary condition.

The effectiveness of the 'Complan' additive in offsetting the dietary deficiencies is seen by the extent of recovery of the tissues in the 'Recovered' specimen. The rate of deposition of bone on the endosteal surface had been very rapid in re-establishing its original configuration, although the changes in the old bone had not been as great and its condition indicated a more advanced state of calcium deficiency than was shown by the 'Deficient' specimen. The remarkable state of recovery of the stomach, however, would suggest that it had not reached the degree of deterioration seen in the 'Deficient'.

From the rate of repair demonstrated in the 'Recovered' specimen it is probable that a normal physiological and biochemical condition would have been attained had the bat not been sacrificed for cochlear studies.

It is clear, therefore, that the deficient condition was primarily due to lack of calcium probably aggravated by lack of vitamin D. Our observations strongly suggest that bananas alone do not form a suitable diet for fruit bats in captivity, although the addition of a dried milk preparation such as 'Complan' appears to be entirely adequate.

ACKNOWLEDGEMENTS

We are grateful to a number of people whose help has made this investigation possible: to Dr S. K. Eltringham, NUTAE (now the Uganda Institute of Ecology) for taking J.D.P. to the *Rousettus* cave and for subsequently shipping live bats by air to London; to Lord Medway for originally pointing out the calcium deficiency of bananas and to Mrs Mary Jones for advice in dietetics; to Mr John Wells for preparing the histological specimens and to Mrs Sylvia Hunt and Mrs Claire Howe for preparing the microradiographic sections; to Mr R. D. Reed and Mr Alan Howard for taking the photographs. J.C.B.-W. holds a post-graduate scholarship from the Science Research Council under the supervision of Dr Martin Hobdell, and took the projection and microradiographs with the equipment at King's College made available by Mr Raymond Ely of the M.R. Research Trust.

PRODUCT MENTIONED IN TEXT

Complan: manufactured by Glaxo Laboratories Ltd., Greenford, Middlesex, England. For similar products compare manufacturers' data with Table 1.

REFERENCES

1. BAUD, C. A. & AUIL, E. (1971): Osteocyte differential count in normal human alveolar bone. *Acta anat.* **78**: 321.

2. BELL, G. H., DAVIDSON, J. N. & SCARBOROUGH, H. (1965): *Textbook of physiology and biochemistry.* 6th edition. Livingstone.

3. BUCKLAND-WRIGHT, J. C. (1972): Radiographic and histological examination of the femur of the fruit bat *Rousettus aegyptiacus. J. Zool., Lond.* **168**.

4. DAVIDSON, S. & PASSMORE, R. (1966): *Human nutrition and dietetics.* 3rd edition. Livingstone.

5. ELY, R. V. (1967): Micro and enlargement radiography. *X-ray Focus* **8**: 14.

6. FOLLIS, R. H. (1958): *Deficiency disease.* Springfield; Thomas.

7. JOWSEY, J., KELLY P. J., RIGGS, B. L., BIANCO, A. J., SCHOLZ, D. A. & GERSHON-COHEN, J. (1965): Quantitative micro-radiographic studies of normal and osteoporotic bone. *J. Bone Jt. Surg.* **47A**: 785.

8. KEITZMAN, S. N., FRITZ, M. E. & SAFFER, A. J. (1970): Enzymatic destruction of bone *in vitro. Nature, Lond.* **228**: 575.

9. MARTIN, G. J. (1937): Calcium deficiency syndrome produced in growing animals. *Growth* **1**: 175.

10. MCCANCE, R. A. & WIDDOWSON, E. M. (1960): *The composition of foods. Amended impression* 1967. London: Her Majesty's Stationery Office.

11. MCCULLUM, E. V., SIMMONS, N., PARSONS, H. T., SHIPLEY, P. G. & PARK, E. A. (1921): Studies on experimental rickets. I. The production of rachitis and similar diseases in the rat by deficient diets. *J. biol. Chem.* **45**: 333.

12. MCCULLUM, E. V., SIMMONS, N., SHIPLEY, P. G. & PARK, E. A. (1921): Studies on experimental rickets. VI. The effects on growing rats of diets deficient in calcium. *Am. J. Hyg.* **1**: 492.

13. VOIT, C. (1878): Uber den Einfluss kalkarmen Futters auf die Knochen. *Z. Tiermed.* **4:** 128.
14. WHALEN, J. P., KROOK, L. & NUNEX, E. A. (1972): A radiographic and histologic study of bone in the active and hibernating bat (*Myotis lucifugus*). *Anat. Rec.* **172:** 97.
15. ZUCKER, T. F., BERG, B. N. & ZUCKER, L. M. (1945): Nutritional effects on the gastric mucosa of the rat. I. Lesions of the antrum. *J. Nutr.* **30:** 301.

Manuscript received 18 April 1972

47. Transverse section of the femur of African fruit bat *Rousettus aegyptiacus*.
1. "normal";
2. "deficient";
3. "recovered".
(a) histological sections stained in haematoxylin and eosin;
(b) microradiographs.
All × 217.

Transverse sections
ıe pyloric end of the
nach of African fruit
Rousettus aegyptiacus
ned in haematoxylin
eosin.
normal";
deficient";
recovered".
whole sections, × 8;
enlargement of the
mucosa, × 200.

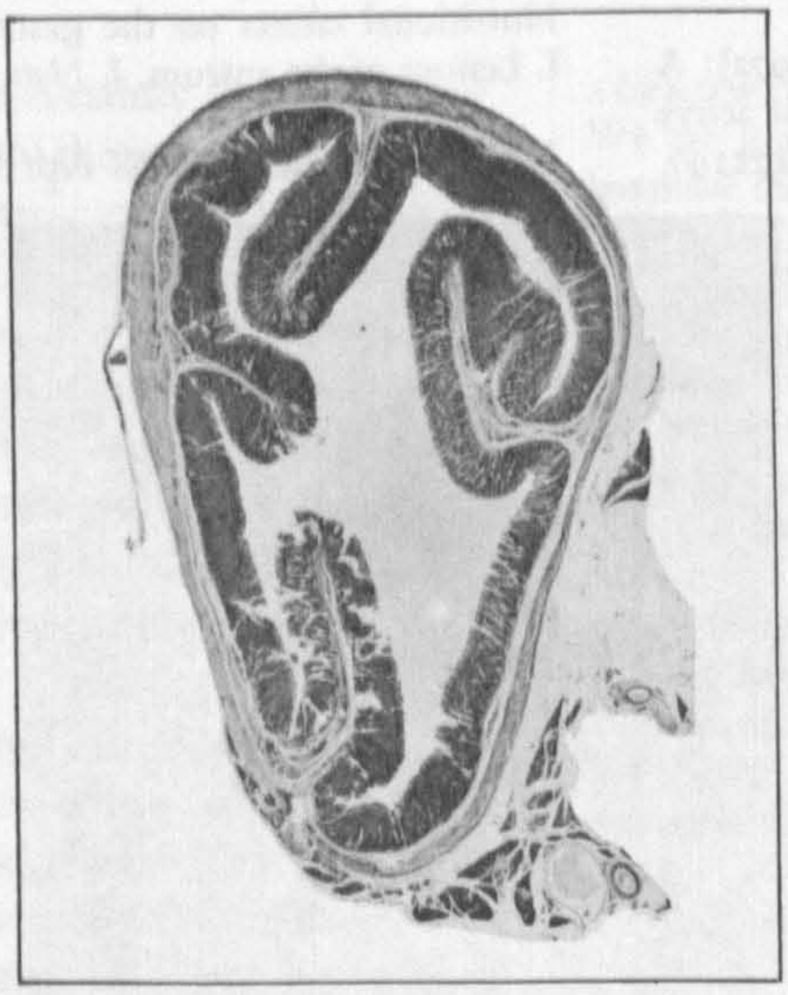

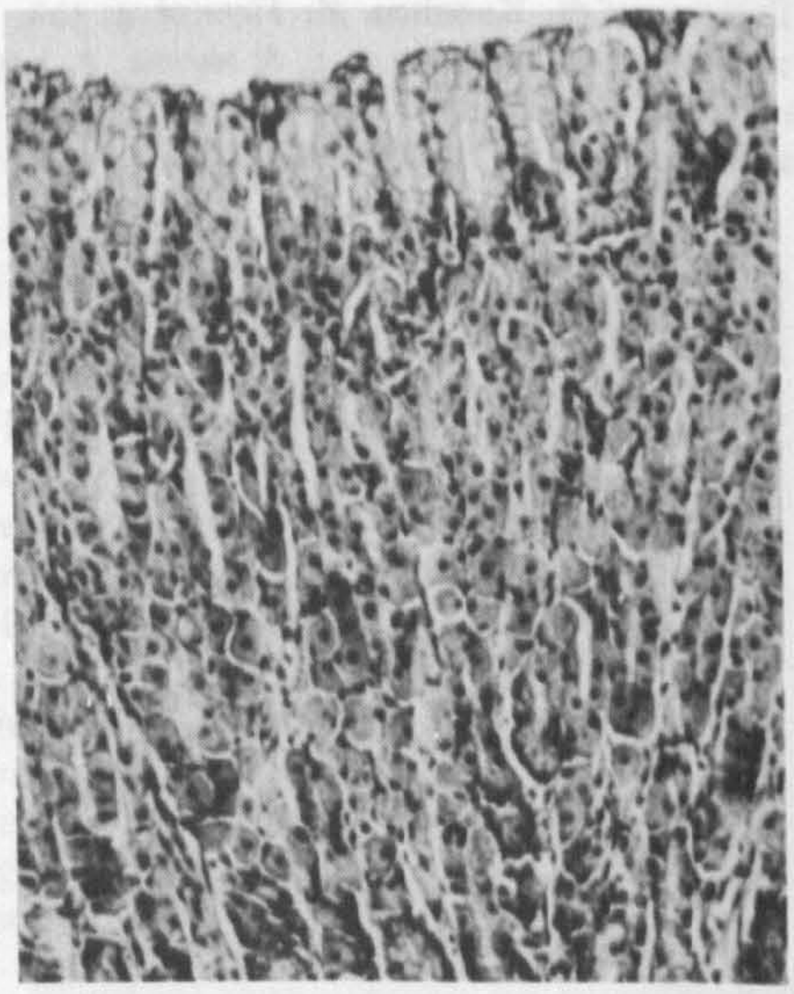

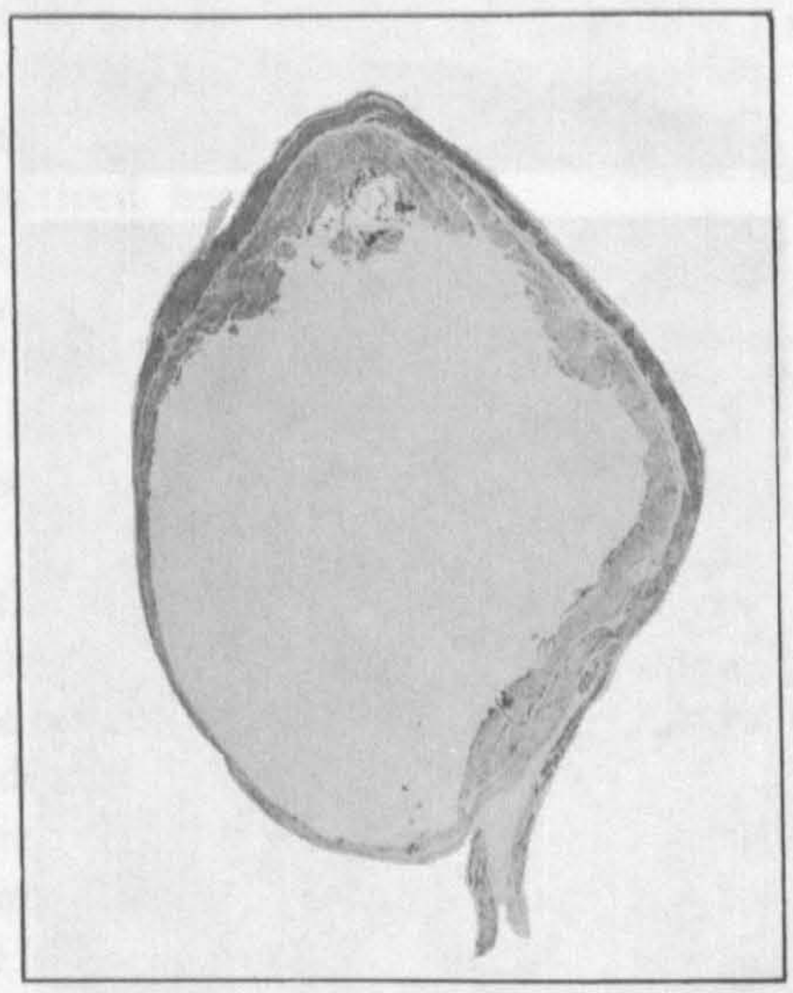

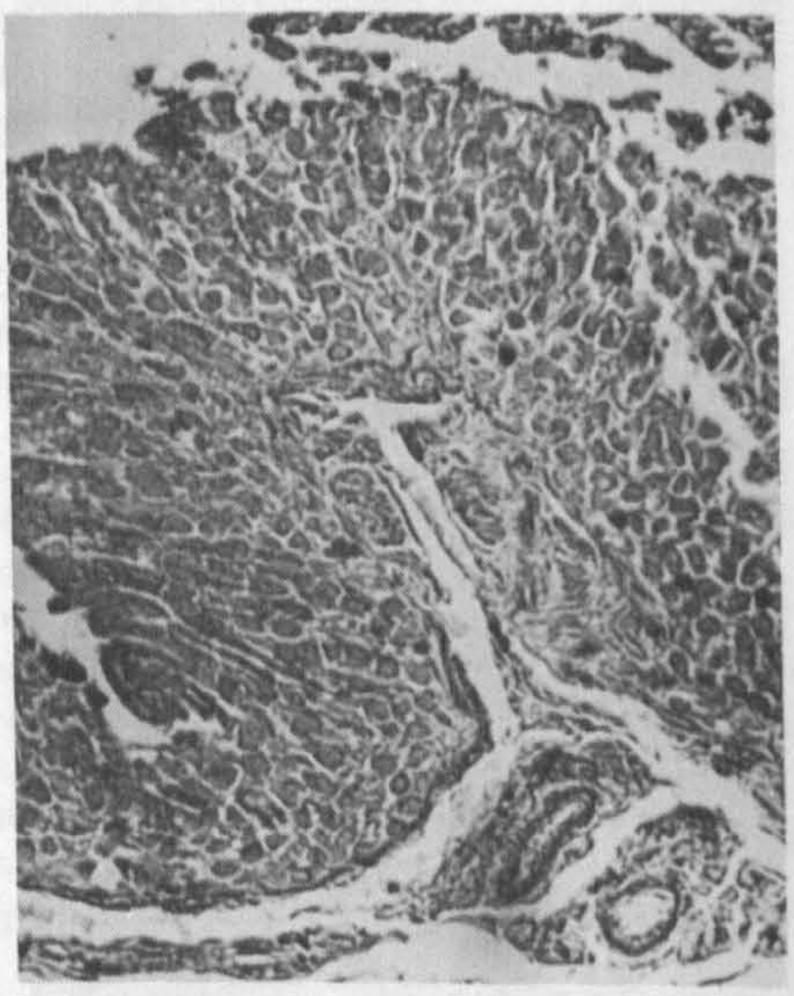

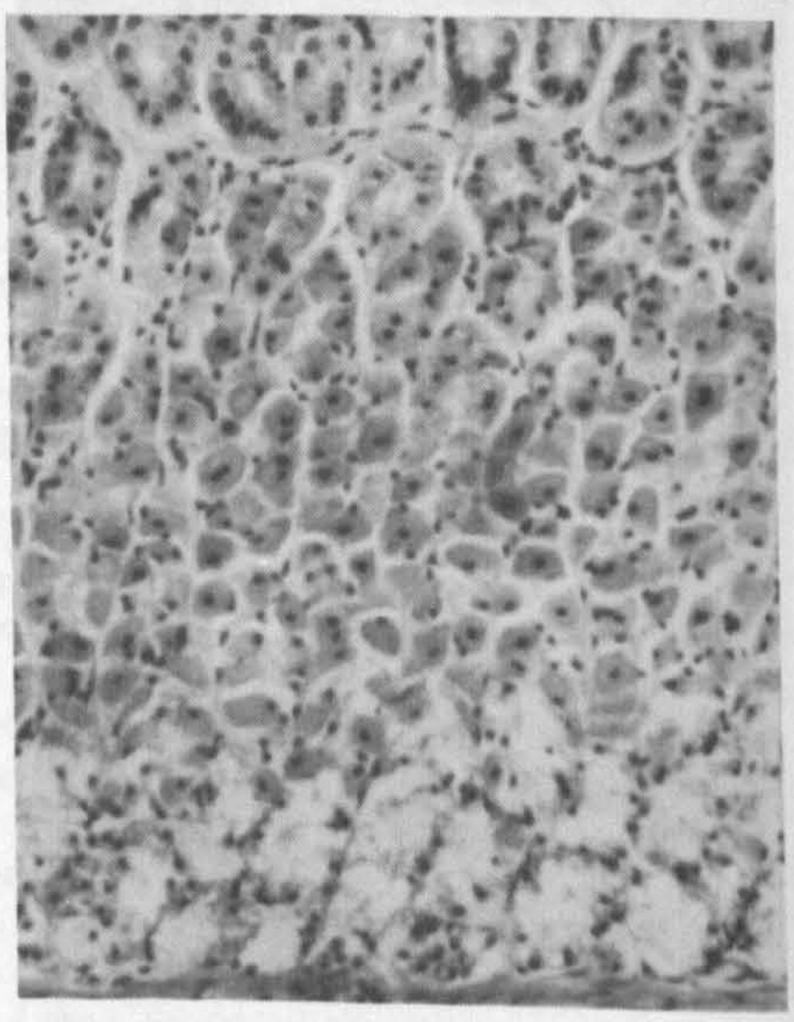

The greater convexity of the supraoccipital in *Hyaena* is reflected by the angle subtended between the nuchal crest and the paramastoid ridge, estimated in norma lateralis (Fig. 3): the mean for *Hyaena* is 121° (variance 12°), for *Crocuta* 130° (variance 7·3°). The difference shows the lambda to be relatively more superiorly situate in *Crocuta* and

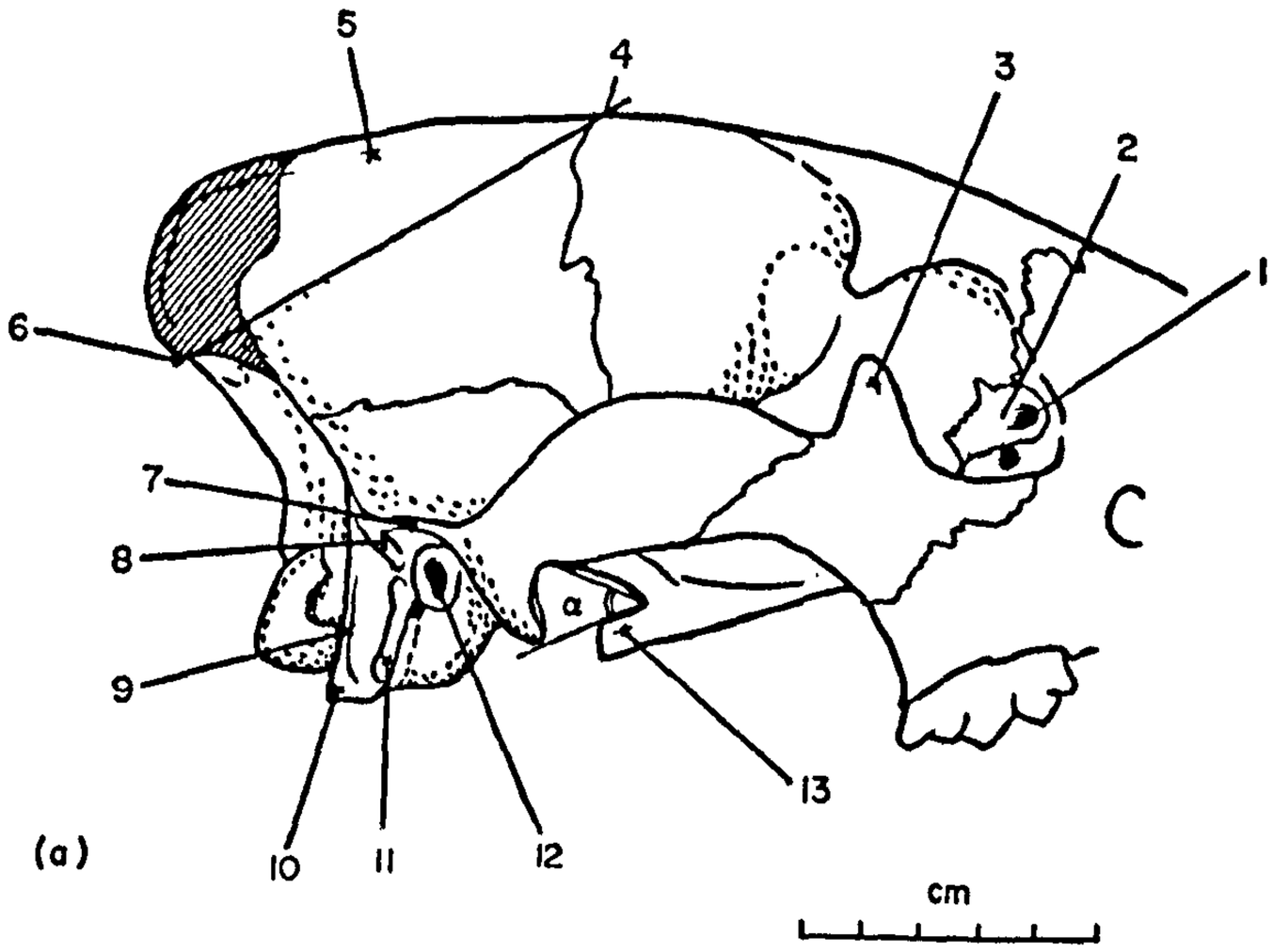

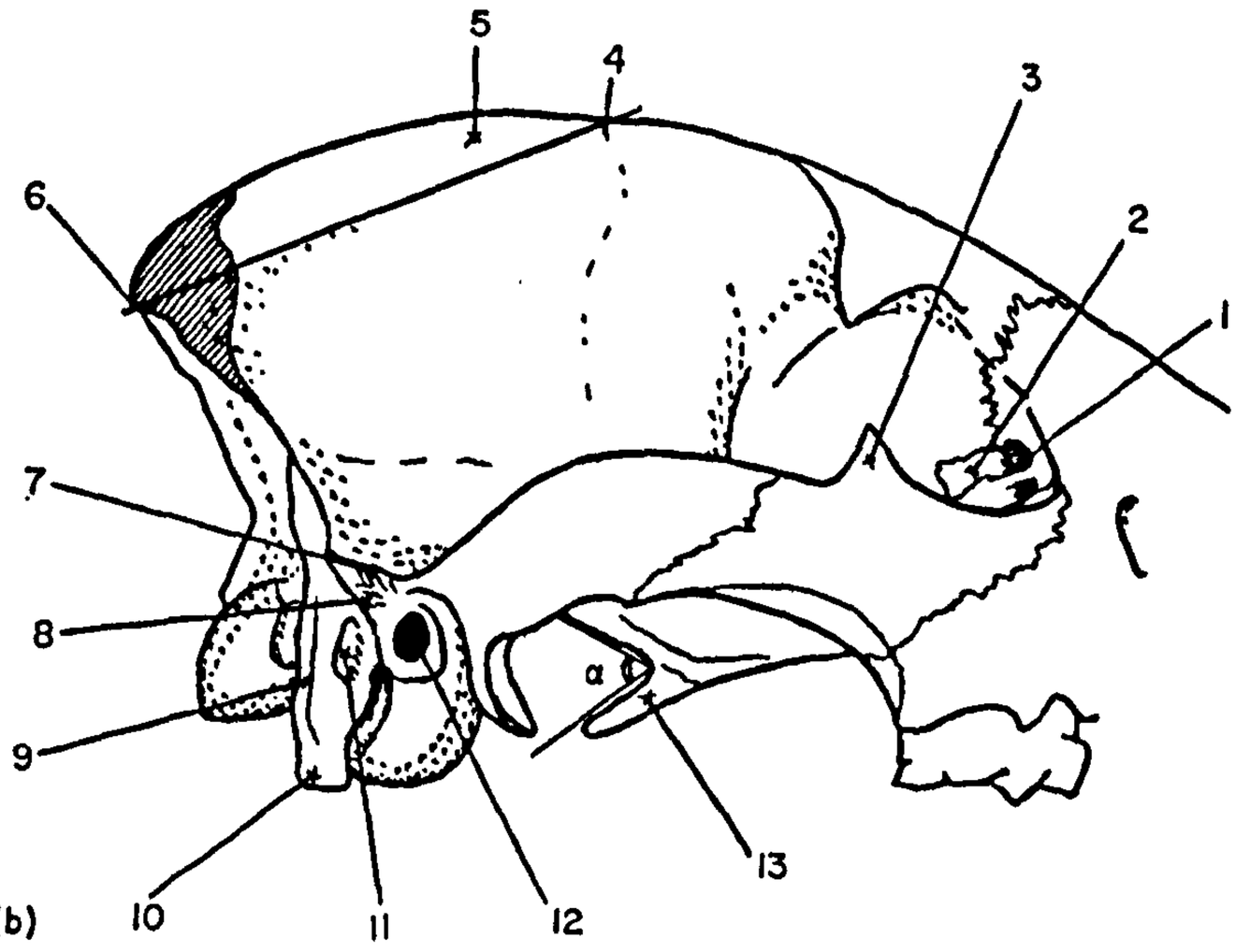

FIG. 1. (a) Norma lateralis of *Hyaena* and (b) of *Crocuta*. The shaded area is the region of the supraoccipital which forms the posterior part of the sagittal crest. The area above the line from the bregma to the lambda was calculated in order to find the relative size of the posterior part of the sagittal crest in *Hyaena* and *Crocuta*, α shows the angle measured between the basis cranii and the dorsal border of the medial pterygoid lamina.

1, Lachrymal foramen; 2, lachrymal bone; 3, frontal process of the jugal; 4, bregma; 5, sagittal crest; 6, lambda; 7, supramastoid crest; 8, mastoid crest; 9, paramastoid ridge; 10, paramastoid process; 11, mastoid process; 12, external auditory meatus; 13, medial pterygoid lamina.